University of Trento
University of Bergamo
University of Brescia
University of Padova
University of Trieste
University of Udine
University IUAV of Venezia

Simone Rossi

SEISMIC BEHAVIOUR AND DUCTILITY EVALUATION OF MULTI-STOREY LIGHT TIMBER-FRAME BUILDINGS BY MEANS OF ANALYTICAL FORMULATIONS AND NUMERICAL MODELLING

Prof. Maurizio Piazza
Prof. Roberto Tomasi

December, 2015

UNIVERSITY OF TRENTO
Doctoral School in Engineering of Civil and Mechanical Structural Systems - XXVIII Cycle

Ph. D. Head's: Prof. Paolo Scardi

Final Examination: 17 / 12 / 2015

Board of Examiners:
Prof. Nicola Pugno (University of Trento)
Prof. Maria Adelaide Parisi (Politecnico di Milano)
Prof. Giuseppe Zurlo (University of Galway)

Sommario

Il presente lavoro di tesi è parte di un ampio ed articolato progetto di ricerca finalizzato alla determinazione del comportamento sismico degli edifici in legno eseguito dal *Timber Research Group* dell'Università degli Studi di Trento nel corso negli ultimi anni.

Nello specifico, il documento presenta lo studio del comportamento sismico di edifici in legno a pareti intelaiate (detti *Platform Frame*), sia in campo elastico che in campo post-elastico; risulta pertanto diviso in due parti principali: nella prima parte viene presentato lo studio del comportamento elastico, la seconda invece è dedicata alla definizione del comportamento non lineare.

Dopo una breve introduzione che presenta lo stato dell'arte, sia dal punto di vista costruttivo che normativo, in merito agli edifici in legno, la prima parte del documento tratta lo studio del comportamento elastico di una singola parete intelaiata. Tale studio è finalizzato alla determinazione di una formulazione analitica e di un macro-modello semplificato in grado di caratterizzare una singola parete sia in termini di capacità di spostamento che, aspetto più importante per il presente lavoro, in termini di rigidezza. Infatti, la corretta identificazione della rigidezza della singola parete di taglio è fondamentale nell'interpretazione sismica del comportamento degli edifici in esame. Nella sezione successiva, sulla base di quanto sviluppato relativamente alla singola parete, lo studio viene esteso a sistemi di più pareti accoppiate ad un piano e poi a sistemi di singole pareti multi piano. Tale studio ha permesso di evidenziare l'influenza che il carico verticale esercita sulla redistribuzione

di una forza esterna tra le varie pareti, nonché sulla variazione di rigidezza che subisce il sistema al variare dello stato degli hold-down. L'identificazione di tali aspetti ha permesso di sviluppare delle formulazioni analitiche mediante le quali è stata definita la matrice di rigidezza di un intero edificio e sono stati messi a punto dei metodi iterativi per l'applicazione dell'analisi dinamica modale con spettro di risposta. La differenza tra i vari metodi, sia dal punto di vista computazionale che da quello analitico, viene discussa mediante la presentazione di un caso studio.

La seconda parte della tesi illustra lo studio non lineare di una singola parete svolto al fine di identificare in modo sia quantitativo che qualitativo l'influenza dei componenti di base sul comportamento globale della singola parete in termini di duttilità; il macro-modello di una singola parete viene in tal modo esteso al campo non lineare. Viene inoltre dimostrato come il contributo della chiodatura dei pannelli di rivestimento delle pareti risulti essere indipendente dalla spaziatura dei chiodi essendo unicamente influenzato dal rapporto di forma dei pannelli medesimi. Tale aspetto individuato analiticamente, viene dimostrato sia dal punto di vista numerico che sperimentale, madianite la realizzazione di alcuni modelli non lineari e attraverso la presentazione dei risultati sperimentali di quattro test di laboratorio eseguiti con un set-up specificamente sviluppato. Sulla base di quanto illustrato, nel capitolo successivo, viene presentato lo studio non lineare di edifici in scala reale, mono e multipiano, al fine di individuare il livello di duttilità atteso al variare delle caratteristiche dei componenti di base e dei meccanismi di rottura. Con lo scopo di generalizzare i risultati ottenuti e fornire dei valori di duttilità attendibili per la tipologia costruttiva analizzata, è stato condotto un numero considerevole di analisi non lineari mediante l'utilizzo di un codice in ambiente Matlab appositamente sviluppato. In tal modo è stato possibile identificare la duttilità esplicabile dagli edifici al variare della caratteristiche geometriche e meccaniche degli stessi, per poi giungere alla proposta di un nuovo set di valori del fattore di comportamento (q) da adottare nella progettazione sismica di questo tipo di edifici.

Summary

The present thesis is part of a wide and structured research project aimed to the determination of the seismic behaviour of timber buildings, performed by the *Timber Research Group* of the University of Trento during the last years.

Specifically, this document presents the study of both the linear and non-linear behaviour of light timber-frame shear-walls buildings (called *Platform Frame*); in the first, part the analysis of the linear-elastic behaviour is presented, whereas in the second part the non-linear behaviour is considered.

After a short introduction on the state of the art of timber buildings both from the constructive and from the legislative point of view, the linear-elastic behaviour of a single timber shear-wall is presented. The analysis of a single timber shear-wall allows to develop an analytical equation and a simplified numerical macro-model (called UniTn-Model) which are able to represent the behaviour of a wall both in terms of displacement capacity and, much more important, in terms of stiffness. In fact, the evaluation of the correct walls stiffness constitutes a fundamental step in the seismic analysis of the timber buildings.

The later section is based on what stated about the single-wall and it deals firstly with the elastic behaviour of systems composed by single-storey coupled walls and then it analyses systems of multi-storey single-walls. These analyses highlighted the influence of the vertical loads on the external force distribution within the shear walls, as well as the changing of the system stiffness caused by the hold-downs state variation. Both these aspects allow to

develop some analytical formulations through which the stiffness matrix of the full-scale buildings can be determined. Three iterative methods for the application of the Modal Response Spectrum Analysis are also presented: the differences between the methods, from the computational point of view as well as from the analytical one, are emphasized by means of a case study.

The second part illustrates the non-linear analysis of a single shear-wall in order to identify the influence of the base components features on the wall ductility, both from the qualitative and the quantitative point of view; the UniTn-Model is hence extended to the non-linear range. It is also determined that the contribution of the nails deformation is not dependent on the nails spacing but it is only dependent on the geometry ratio of the sheathing-panels themselves. This aspect, analytically determined, is demonstrated on the basis of numerical and experimental analyses, by means of some non-linear F.E.M. analysis and some ad-hoc laboratory tests respectively.

In the following section, using what developed for the single shear-wall, the non-linear analysis of single and multi-storey full-scale buildings is performed. The analyses are performed in order to assess the ductility level achievable by the buildings varying the ductility of the base components as well as the failure mechanisms. In order to get generalized results and provide reliable values of ductility for the constructive system analysed, a large set of non-linear analysis has been performed through the use of a Matlab code specifically developed. This allowed to determine the ductility level that light timber-frame buildings can reach and to propose a new set of values for the behaviour factor (q) to be used in the seismic design.

Ringraziamenti

Desidero ringraziare il Prof. Maurizio Piazza ed il Prof. Roberto Tomasi che mi hanno pazientemente aiutato durante questi tre anni.

Un sentito ringraziamento va all'amico e collega Ing. Flavio Vinante.

Ringrazio tutti i membri del Timber Research Group dell'Università degli Studi di Trento: Paolo Grossi, Daniele Casagrande, Ivan Giongo, Tiziano Sartori e Gianni Schiro.

Un doveroso ringraziamento va inoltre allo staff tecnico del Laboratorio Prove Materiali e Stutture dell'Università degli Studi di Trento per il supporto e la preziosa collaborazione durante l'esecuzione delle prove sperimentali.

Si ringrazia con gratitudine il consorzio ReLUIS (Rete dei Laboratori Universitari di Ingegneria Sismica), che con il progetto ReLUIS-DPC 2015 ha parzialmente finanziato le prove di laboratorio riportate nel presente documento.

Acknowledgments

I would like to thank my supervisors Prof. Maurizio Piazza e Prof. Roberto Tomasi for helping me patiently during these three years.

A particular acknowledgment goes to my friend and colleague Eng. Flavio Vinante.

I am really grateful to all the members of the Timber Research Group of the University of Trento: Paolo Grossi, Daniele Casagrande, Ivan Giongo, Tiziano Sartori and Gianni Schiro.

A particular thank goes to the technical staff of the Material and Structural testing Laboratory of the University of Trento for the help giving me during the execution of the laboratory tests.

I gratefully acknowledge the financial support of the ReLUIS Network (Laboratories University Network of seismic engineering) which with the ReLUIS-DPC 2015 project has partially financed the laboratory tests reported in the

present document.

Contents

Chapter 1

Introduction

With the aim of bringing up the subject of the thesis, but also to define some general concepts, the present chapter gives a brief overview on timber buildings with particular focus on the Light Timber-Frame system. An essential introduction about the seismic design practice according to European seismic code and the general assumptions used by designers are also presented. In the last part of the chapter the objectives of the thesis as well as its layout are discussed.

1.1 Background

Light timber-frame buildings are traditionally widely spread in North America and also in Scandinavian countries but nowadays they represent the construction type most used in the field of timber buildings even in the European seismic prone regions. This diffusion is mainly due to two reasons: on one side, their environmental sustainability both during the erection phase and lifetimes; the other, their intrinsic lightness and strength that make these buildings an excellent solution even for earthquake zones.

In the last decades also in Italy light timber-frame constructions have assumed a considerable importance thanks to the renewed attention given to wood as a building material with excellent physical and mechanical properties (highlighted by numerous experimental campaigns) making it an advantageous alternative compared to other materials typically used for building such as reinforced-concrete and steel.

Figure 1.1: *Some examples of light timber-frame low and mid-rise buildings (images taken from legnocase.com).*

Light timber-frame buildings represent an excellent example of exploitation of the benefits of wood in the structural design; in fact, they are characterized by a favorable ratio between mass and strength compared to buildings of other traditional materials, as well as of a relative flexibility with respect both to the global response and to the subsystem level.

Another fundamental aspect, that characterizes these buildings, is the natural redundancy in terms of walls and connections, which make such type of buildings an highly hyperstatic system capable of developing alternative load paths and consequently able to stop the propagation of the damage.

Beside all these properties, these buildings have the capacity to dissipate energy associated with inertial forces as well as a reasonable damping due to friction that ensure them a quite good ductile behaviour.

1.2 Buildings Production

The superstructure of a light timber-frame building is typically placed over a concrete foundation or a basement that can have indifferently the upper floor made of timber, concrete or other material (see Fig. 1.2).

Figure 1.2: *Timber buildings generally have concrete foundations or basements.*

The walls are usually prefabricated and are delivered to the construction site with windows and doors already installed, see Fig. 1.3.

The frame is made by means of timber plates (top and bottom plates) and studs placed side-by-side 62.5 mm apart; studs are typically 60-80 mm width and 140-160 mm depth, whereas the top and bottom plates are 60-80 mm thick. The frame, which can be regarded as a mechanism, is braced by one or two sides sheathing layers made by OSB and/or gypsum-fiber panels from 12.5 to 20 mm thick, see Fig. 1.4. The sheathing panels are connected to the timber-frame by means of threaded nails, screws or staples depending on the material of the sheathing panels. The nails (screws or staples) spacing can vary from 50 to maximum 150 mm, on the central-studs it is allowed to have a double spacing.

The sheathing panels inside the building are usually made of non-structural gypsum unless structural needs require two structural panels. The outer side of the walls is generally covered by water and wind-proof membranes, the fa-

Figure 1.3: *Prefabrication of the walls.*

cade of the building is also usually completed by an exterior insulation and finishing system.

Walls with windows and doors openings have specific framing: each opening has a *header* which collects the weight that would otherwise be carried by the wall studs and distributes it downward through a *trimmer* and a *king stud*. A *king stud* is a full length stud whereas a *trimmer stud* supports the *header* which defines the rough opening height. For windows additional *sill* which defines the bottom of the rough opening for the window are needed, see Fig. 1.5.

The walls of the first-storey are directly fastened to the foundation by means of angle-brackets and hold-downs; over the walls is placed the floor. Differently from U.S.A. and Canada, where studs run from the bottom to the top of the buildings, in Europe a *Platform Frame* system is adopted. Specifically each

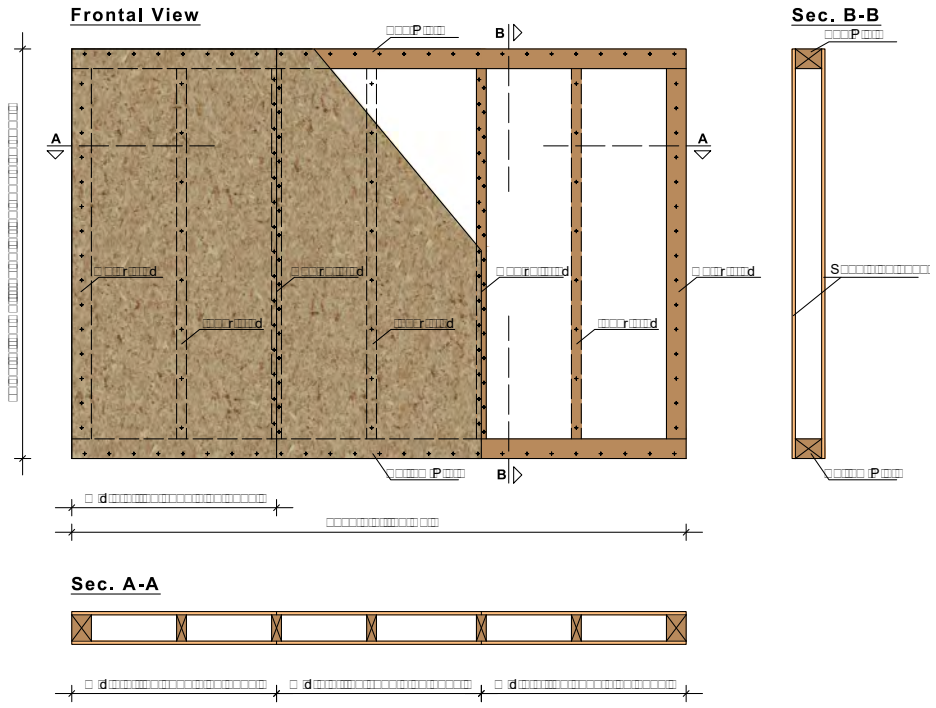

Figure 1.4: *Geometry and components of a light timber-frame wall.*

storey constitutes an independent portion and the upper storey is connected to the one below by means of specific connection devices that ensure the system continuity and the passage of bending-moments, shear and tensile forces.

1.3 Seismic behaviour and load path

The shear-walls carry both vertical loads and horizontal forces bring to them by floors, roof and orthogonal walls, see Fig. 1.6. The vertical loads are transmitted to the foundation by the studs whereas the horizontal forces are taken by the sheathing-panels; the sheathing panels are also needed to avoid the buckling phenomenon of the studs which in turns avoid the plate-buckling of the panels themselves.

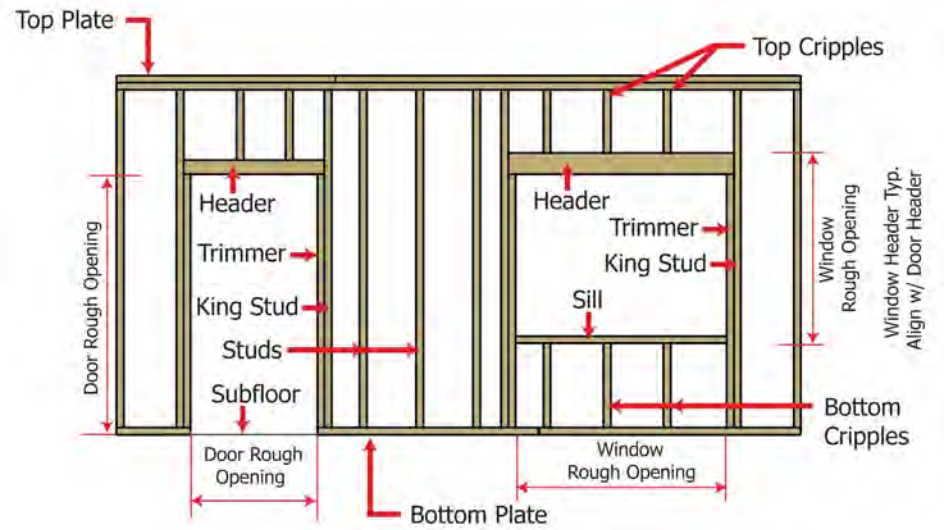

Figure 1.5: *Frame for wall with window and door openings.*

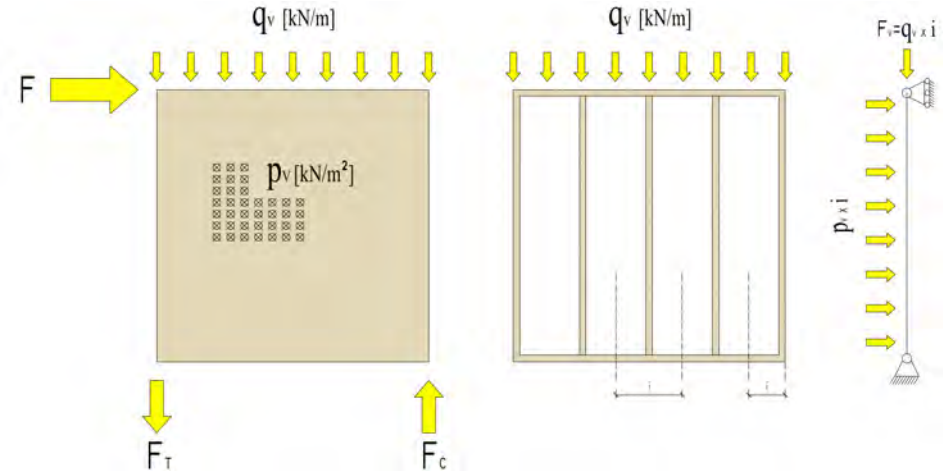

Figure 1.6: *Static systems for vertical load(q_v), horizontal force (**F**) and out-of-plane force (p_v).*

The failure mechanism of the wall can involves the connection devices as well as the sheathing-to-framing connection, see Fig. 1.7. Therefore the strength of a wall is strictly related to the strength of these base components. The shear-resistance is equal to the minimum strength between that of the

angle-brackets and that of the sheathing-to framing connections, whereas the bending resistance is provided by the tensile strength of the hold-downs.

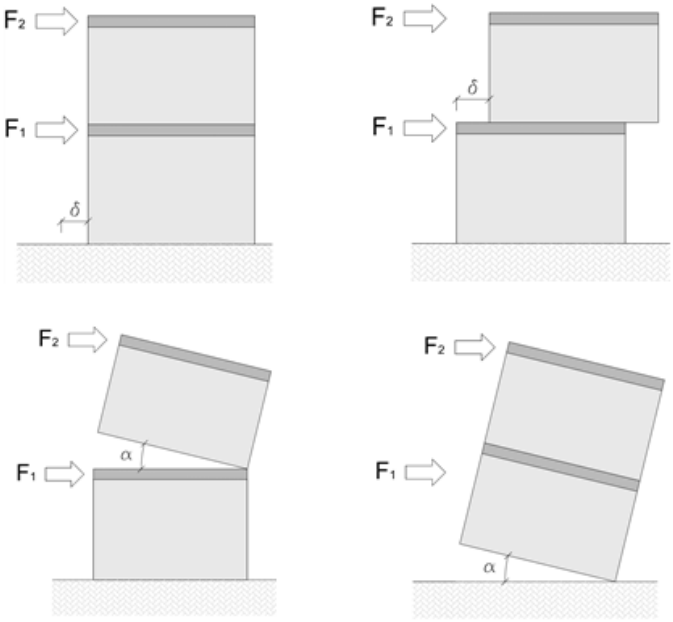

Figure 1.7: *Possible failure mechanisms for a Platform Frame Building.*

Due to the presence of several shear-walls as well as because of the large number of connection devices, light timber-frame buildings are generally characterized by a ductile behaviour. For this reason Eurocode 8, the Italian national standards and also other Standards (National Building Code of Canada, New Zeland Building Standard, etc.) allow to adopt a quite high value for the behaviour factor (q) (also known as seismic reduction factor (R)) to be used in the seismic design of these buildings.

In order to allow walls to deform and to absorb energy it is recommended to have rigid floors that behave as rigid diaphragms. In fact, in the hypothesis to provide the structure with rigid floors and roofs, the seismic forces and horizontal forces in general are distributed to the shear-walls in a proportional

manner to the walls stiffness and the buildings display a box-behaviour.

It has to be remarked that all the connection devices shall expose a bi-directional resistance, namely they must provide the same strength in two directions because seismic forces are cyclic. This develop an effective and redundant connection between all the structural component and give to the structure the capacity to develop alternative load paths and stop the propagation of the damage as previously stated.

1.4 Materials

As a conclusion to the brief introduction of light timber-frame buildings, the materials and the main connection devices used are presented.

1.4.1 Timber

The framing is typically made by means of solid wood or KVH (finger-jointed timber beams), sometime also glulam is used, see Fig. 1.8.

Figure 1.8: *Timber studs and plates (image taken from damianiholz.com)*

1.4.2 Threaded and ring shank nails.

Threaded shank nails are used for the sheathing-to-framing connection, typically these nails are 2.8 mm of diameter and 60-70 mm length. Ring shank nails are instead used to connect angle-brackets as well as hold-downs; see Fig. 1.9.

Figure 1.9: *Threaded nails and Ring nails respectively.*

1.4.3 Angle-brackets and hold-downs

Fig. 1.10 shows some angle-brackets which are used to anchor the wall against the rigid-body translation; Fig. 1.11 shows some hold-downs which are needed to avoid the rigid-body rotation.

Figure 1.10: *Typical angle-brackets (image taken from rothoblas.com).*

Figure 1.11: *Typical hold-down (image taken from rothoblas.com).*

1.4.4 OSB and gypsum-fiber panels

The walls are typically sheathed by means of OSB (Oriented Strand Board) panels, see Fig. 1.12, or gypsum fiber panels, see 1.13.

1.5 Seismic design

Seismic design, regardless of the material used, can be performed by means of two different families of analysis: the linear-elastic approaches, which take into account the dissipative capacity of structures in a simplified manner by means of the use of the behaviour factor (q) and the non-linear elastic methods that directly account for the post-elastic behaviour of buildings.

The non-linear analysis can be carried out by means of the *non-linear static analysis (push-over)* or by the *non-linear dynamic analysis (time-history)*.

Figure 1.12: *OSB panels.*

Figure 1.13: *Gypsum fiber panels.*

These methods are not often used in the seismic design but are preferred by researchers or designers to assess the behaviour of existing buildings. Non linear methods are not common because of their computational expensiveness and also because, in order to obtain reliable results, it is crucial to know in detail the geometric and mechanical characteristics of the structural elements.

Linear analysis can instead be done by means the *lateral force method of analysis*, which may be applied to buildings whose response is not significantly

affected by contributions from modes of vibration higher than the fundamental mode, or by the *modal response spectrum analysis*, which is the reference method for the seismic analysis of buildings because it can be applied to each type of building (also non regular buildings) due to the fact that it takes into account all modes of vibration contributing significantly to the global seismic response.

Despite timber buildings are nowadays widely used in many countries to build also mid-rise buildings, it has to be remarked that analytical procedure of analysis are often missing in standards and are still purely developed. Moreover, because of in literature a direct relation between the base-components properties and the behaviour of the structure is still missing, the behaviour factors given by Standards (such as Italian National building code, Eurocode 8) do not match the real dissipative capacity of timber buildings.

1.6 Objectives and scope of the thesis

This thesis work aims to study and define the seismic behavior of timber light-frame buildings both from linear and non-linear point of view.

The objectives of this work can be conveniently summarized in a list corresponding to the various topics considered:

- develop of an analytical procedure and a numerical simplified model to analyse buildings in the elastic range;
- propose a definitive iterative procedure to apply the response spectrum analysis that takes into account the real stiffness of the buildings;
- determine the relation between the mechanical properties of the base components and the ductility of the whole building;
- assess the displacement capacity of buildings and propose a new set of behaviour factors to be used in the seismic design.

1.7 Dissertation overview

This thesis is composed by five main chapters, in each of which is attached a scientific paper related to its topic.

Chapter 2 presents the study of the elastic behaviour of a single timber-shear wall. Specifically, an analytical formulation suitable to evaluate the displacement caused by a horizontal force is presented. This equation, which can be used both for light Timber-Frame walls [TF] and for Cross Laminated Timber walls [CLT], takes into consideration the main deformation contributions and it is developed on the basis of a large research campaign made in these years by the Timber Research Group. The displacement formulation is also used to determine the stiffness of the wall and it allows to assess that the stiffness is proportional to the squared length of the wall and not, as was previously supposed, linearly proportional to it. The study of the stiffness of the shear-walls highlight that the hold-down gives to the wall a non-linear behaviour even in the elastic range. On the basis of the analytical formulations presented, a simplified numerical model called UniTn-Model (Unified Trento Model) to reproduce the elastic behaviour of timber shear-walls is developed. The UniTn model is called simplified because it reproduces the wall by means of only three springs and it is developed with the aim to provide a powerful tool for the seismic analysis of timber buildings.

In Chapter 3 the study of the elastic behaviour of light timber-frame buildings is extended to coupled walls. In the first part, systems of coupled single-walls modeling one-story buildings are considered; in the second part, the elastic behaviour of multi-story shear-walls is analysed by paying particular attention on the determination of an analytical equation suitable for the evaluation of the displacement of each storey. This is a key aspect because the hold-down deformation contribution increases with the increase of the number of storey, as well as because timber buildings can be considered shear-wall buildings. In fact, the seismic behaviour of these buildings is determined by the

collaboration of all the multi-storey shear-walls which are connected together by floors (that can be considered as rigid diaphragms) and which can be considered as a set of springs placed in parallel. Thanks to the analysis of both one-storey and multi-storey systems a procedure to determine the stiffness matrix of a full-scale building is presented. The use of the stiffness matrix allows to develop an iterative procedure suitable both for the assessment of the shear-stress in the wall and the field of displacements of the building caused by a pattern of external forces. The last part of the chapter deals with the dynamic analysis of shear-wall buildings; three iterative procedure suitable for the application of the Response Spectrum Analysis are proposed. The presented methods differ in the way in which both the vertical load effects and the ON-OFF behaviour of the hold-down are considered; in order to better explain all these iterative procedures some numerical examples are shown.

In the Chapter 4 the UniTn-model is extended in the post-elastic range. With the aim of limiting the degrees of freedom necessary for the modeling and, at the same time, in order to contain the computational effort required, the behaviour of each base component is reproduced by means of an elasto-perfectly plastic force-vs-displacement curve. Due to the adoption of a bi-linear curve for each base component, the global force-vs-displacement curve of a wall becomes typically three-linear. Despite the relations between the mechanical properties of both the hold-downs and the angle-brackets with the plastic displacement of the wall are easy to assess, the definition of an analytical relation between the ductility of the nails and the ductility of the sheathing-to-framing connection requires a more complex analysis, particularly an non-linear incremental static analysis was adopted. The study of the results obtained by this analysis allows to state that the ductility expressed by a light timber-frame wall is not related to the nails spacing, but it is only dependent on the ductility of the nails themselves as well as on the shape ratio of the sheathing layers. This significant concept is then demonstrated by means of the comparison of the analytical results with the result of a set of

specifically performed laboratory tests; it is also validated through some finite element staged non-linear analyses performed with SAP2000.

In Chapter 5 the non-linear analysis of light timber-frame constructions is extended to one-storey and multi-storey buildings. Firstly, the analysis of two coupled one-storey walls is presented; this analysis is needed to determine the various failure-mechanisms that characterize light timber buildings and to evaluate the influences of the stiffness and the strength of the base components on them. Three real one-storey building are then analysed with the purpose of evaluating the ductility achievable by one-storey systems. The results highlight that by varying the strength of the hold-down used, the failure mechanism of the building changes significantly. It has also be noted that failure-mechanisms involving the hold-down do not ensure a sufficient level of ductility and therefore can be considered as brittle failures. In order to assess the influence of the plant-geometry on the ductility expressed, a large set of randomly-generated buildings are analysed. This study allows to state that the traditional seismic design of timber buildings does not assure the attainment of the ductility level hypothesized; therefore, the need of the adoption of a capacity design approach is evident. By the use of the capacity design, which considers the hold-down the weak element as well as the sheathing-to-framing connection the ductile element, it is possible to show that the ductility of one-storey buildings is linearly related to the ductility of the nails. In the second part, the non-linear analysis is extended to multi-storey buildings; thanks to the study of the non-linear behaviour of multi-storey shear walls, with the aim to contain the loss of ductility with the increase of the number of storey, the need of yielding several storey is remarked. The study of a large set of multi-storey buildings, by varying the main parameters that influence the seismic behaviour of a building, is presented. It is shown that both the behaviour factor (q) used in the design as well as the seismic level considered (pga) do not influence the displacement capacity of the buildings. It is noted instead that the ductility is strongly influenced by the number of storey and by

the mechanical properties of the base components; it can also be noted that the over-strength displayed is less scattered compared to the ductility. Finally, all the ductility values collected are used to evaluate and propose a new set of values for the behaviour factor q to be used in the seismic design of light timber-frame buildings.

The conclusions of the research as well as some ideas for the future work are exposed in the Chapter 6.

Chapter 2

Elastic response of single-storey timber shear-walls

2.1 Introduction

The analysis and the design both of Cross Laminated [CLT] and light frame [TF] timber buildings require the knowledge of the force vs. displacement curve of each shear-wall. In fact, the value of the seismic force, as well as how the force is distributed within the walls, are dependent on both the building and the wall stiffness. Moreover, because of timber buildings are generally composed by several shear-walls and many connections, their analysis is increasingly carried-out by means of F.E.M. models.

With the goal of developing useful methods and tools for the analysis of this building, in the following Section, an analytical expression to determine the horizontal displacement (Eq. 2.1) and an expression to evaluate the stiffness

of a timber shear-wall are proposed.

$$\Delta = \begin{cases} \frac{\lambda \cdot F \cdot s_c}{l \cdot n_{bs} \cdot k_c} + \left[\frac{h}{\tau \cdot l \cdot k_h} \cdot \left(\frac{F \cdot h}{\tau \cdot l} - \frac{q \cdot l}{2} \right) \right] + \frac{F \cdot i_a}{k_a \cdot l} + \frac{F \cdot h}{l \cdot G_p \cdot n_{bs} \cdot t_p} & \text{for} \quad TF \\ \left[\frac{h}{\tau \cdot l \cdot k_h} \cdot \left(\frac{F \cdot h}{\tau \cdot l} - \frac{q \cdot l}{2} \right) \right] + \frac{F \cdot i_a}{k_a \cdot l} + \frac{F \cdot h}{l \cdot G_{CLT} \cdot t_{CLT}} & \text{for} \quad CLT \end{cases} \tag{2.1}$$

The displacement expression is based on a wide experimental campaign, performed by the *Timber Research Group* of the University of Trento, and taking into account different approaches in the literature. This equation allows to evaluate the elastic displacement of a wall (both CLT and TF) by adding the main deformation contributions. Specifically, in the case of TF shear-walls, four contribution are considered: the sheathing-to-framing connection, the rigid body rotation, the rigid-body translation as well as the shear deformation of the panels; in the case of CLT shear-walls the contribution of the sheathing-to-framing connection is obviously absent.

In order to develop a simplified but reliable tool, only the main deformation contributions are considered; instead, the contributions which produce a really small displacement, for shear-walls typically used in seismic-areas, are not taken into account. The innovative aspect of this expression is the fact that the displacement is determined analytically knowing only the mechanical and geometric features of the base components. In fact, laboratory tests for calibration are not required.

The study of the displacement shows that timber shear-walls are characterized by two stiffness regimes. In fact, considering the Force-vs-Displacement curve of a wall, it is possible to note that the elastic stiffness has two different values related to the two regimes, Fig. 2.1. The first regime occurs when the hold-down is in compression, therefore it does not undergo any deformation; whereas, the second regime occurs when the hold-down is in tension, therefore its deformation produces a rigid-rotation of the wall. The transition between the regimes happens when the overturning moment, produced by the external horizontal force, exceeds the stabilizing moment, produced by

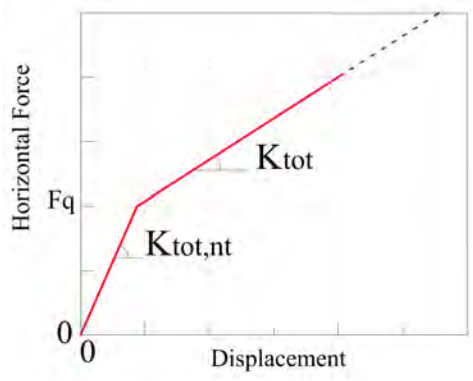

Figure 2.1: *A wall is characterized by two stiffness regimes.*

the vertical load; namely when he horizontal force (F) exceeds the activation force (F_q):

$$F_q = \frac{q \cdot l^2}{2 \cdot h} \tag{2.2}$$

Another key aspect is the reduction of the horizontal displacement caused by the vertical load; in fact by imposing the rotation equilibrium, it is possible to evaluate an equivalent force F_N produced by the vertical load, which counteracts the horizontal external force.

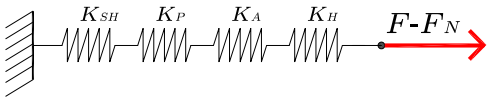

Figure 2.2: *Wall rheological model for the second regime.*

The stiffness of the wall can be determined rearranging the equation of the displacement. Due to the fact that a wall can be considered from the rheological point of view as a system of elastic springs placed in series (Fig.2.2), the stiffness is produced by the contribution of each base component. By means of a parametric study it is possible to show that the wall stiffness is propor-

tional to the squared length, due to the deformation contribution related to the hold-down elongation. This is a relevant aspect to be taken into account in the seismic design of timber buildings, as the force distribution within the walls is done proportionally to the ratio between the stiffness of the walls themselves.

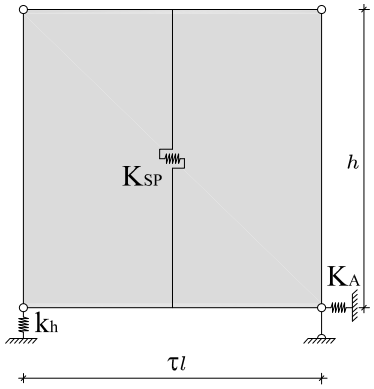

Figure 2.3: *Simplified UniTn Model.*

A simplified numerical model called UniTn-Model (Fig. 2.3), based on the expressions of displacement and stiffness, is also presented. The model can be used to efficiently reproduce the elastic behaviour of a timber shear-wall: it is composed by a frame regarded as a mechanism, which is braced by means of three springs representing the behaviour of the hold-down, the angle-brackets and the sheathing panels with its connections respectively. It has to be remarked that the spring modelling the sheating panel and its connections is placed horizontally and is connected to the frame by means of two rigid-elements.

The UniTn-Model has been developed after two other models. The first model has a diagonal spring, whereas the second-one is braced by four rotational springs (Fig. 2.4). Both these models need some geometric transformation to evaluate the springs stiffness and it is not possible to directly determine the shear-force carried by the wall; therefore they both are less useful than the UniTn-Model.

The use of the presented model may be iterative. Indeed, due to the fact

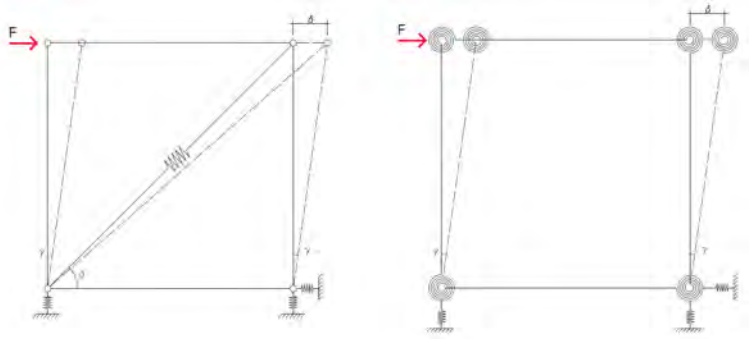

Figure 2.4: *Other models considered.*

that the wall can express two regimes (namely the wall can have two different values of stiffness), as well as the need to place the hold-down spring in the tension corner, the UniTn-Model is an iterative approach. The iterations are required in order to comply the boundary conditions hypothesized at the start of the analysis.

2.2 Appended Paper I

Proposal of an analytical procedure and a simplified numerical model for the elastic response of single-storey timber shear-walls

Daniele Casagrande, Simone Rossi, Tiziano Sartori, Roberto Tomasi

Construction and Building Materials, Elsevier (2014);
doi:10.1016/j.conbuildmat.2014.12.114

Proposal of an analytical procedure and a simplified numerical model for elastic response of single-storey timber shear-walls.

Daniele Casagrande[1], Simone Rossi[2,*], Tiziano Sartori[3], Roberto Tomasi[4]

Department of Civil, Environmental and Mechanical Engineering, University of Trento, Italy, Tel. +39 0461 282529

Abstract

A simplified and reliable tool for the elastic analysis of one-storey timber shear-walls under simultaneous horizontal and vertical loads is presented. This approach is suitable for the analysis both of light timber-frame walls and CLT walls. The analytical expressions to determine the horizontal displacement and the elastic stiffness of a single wall are provided, these expressions are then extended to walls placed in series. A simplified numerical model suitable for F.E. analysis is also developed. In the last part of the paper a comparison between an analytical example and the results of a laboratory test is shown.

Keywords:
Timber shear-wall, Light timber-frame wall, CLT wall, elastic analysis, seismic analysis, horizontal force, horizontal displacement, numerical modelling, horizontally aligned walls, UNITN model

*Corresponding Author
Email address: simone.rossi1@unitn.it (Simone Rossi)
[1]Civil Engineer, Ph.D., Assistant Researcher, daniele.casagrande@unitn.it
[2]Civil Engineer, Ph.D. Candidate
[3]Civil Engineer, Ph.D., Assistant Researcher
[4]Civil Engineer, Ph.D., Assistant Professor

1. Introduction

The structural analysis of timber buildings subjected to horizontal forces (wind, earthquakes, etc.) may require the use of Finite Element Models with the aim of evaluating the design actions of the structural members and mechanical connections. These models should well describe the structural behaviour of the timber buildings, but their complexity should be related to the design purposes as well. Simplified models, in most cases, can ensure suitable and reliable results with the added benefits of being less time-consuming and much more manageable.

This paper is the first stage of a research work concerning the seismic study of the timber buildings from the analytical point of view. It supplies a numerical process, called UNITN model, with the goal to provide designers and researchers a simplified but powerful tool to evaluate the elastic response of light timber frame (TF) shear-walls and cross laminated timber (CLT) shear-walls.

In Europe TF and CLT constructive systems are preferred, see Figure 1; respectively TF walls are made by a pinned-frame, which is a mechanism, braced by OSB (Oriented Strand Board) or GFP (Gypsum Fiber Panel) sheathing panels whereas CLT walls are solid-timber walls composed by layers of timber planks glued together. Following the increase in the use of this type of buildings, a great amount of research has been conducted on timber shear walls, with a particular focus on their behaviour when subjected to a horizontal load. Numerous experimental tests have been performed in order to characterize this type of wall [1], [2] and [3]. Push out tests and cyclic tests on the singles components of the walls have been also carried out [4], [5]. Several closed-form models have been proposed in standard or in literature, often based on energy methods or strain-displacement relationship. A quite wide review of some of these models was presented in [6]. In Conte et. al. [7] the approaches proposed in the Commentary (Erläuterung) of DIN 1052 [8], in New Zealand Standard NZS 3603:1993 [9], in Canadian Standard CSA 086-01:2005 [10], and by Källsner and Girhammar [11] have been analysed.

Most of these models neglect some elastic components (like deformation of angle brackets), and give more importance to other elastic components which could be neglected (like compression deformation and deformation of timber frame). In all proposals analysed the main deformation contribution, according to UNITN model, is attributed to the nail slip, on the contrary the effect of the vertical load is generally disregarded (not in the UNITN model).

The UNITN model (UNified Iterative TreNto model) has been developed to provide a simplified equation to describe the elastic behaviour of timber shear-walls through the use of a equivalent stiffness for each shear-walls. Four deformation contributions are taken into account as well as the role of the vertical load (this key concept has no investigated before). The Model arises from the large campaign research (See [12], [4], [13], [14]) made by the Timber Research Group of University of Trento.

The Model is characterized by generality because the same approach can be adopted for TF and CLT shear-walls, and by the fact that it takes into account the variation of the wall stiffness when the hold-down is activated, entails inevitably an iterative procedure to find out the real force distribution between multiple shear-walls. A parametric study of the hold-down stiffness contribution demonstrates that the wall elastic stiffness cannot be considered linearly proportional to the wall length as is usually assumed nowadays by designers. The use of the UNITN model is presented in this paper only to analyze single-storey buildings, whereas, its use for multi-storey timber buildings is already under investigation by the authors and it will be presented in a future paper.

2. Elastic horizontal displacement of a timber shear-wall

The elastic horizontal displacement (Point C, Figure 1) of a light timber frame wall subjected to a horizontal force can be obtained by adding the contributions of deformation from various sources, viz. the sheathing-to-framing connection (Δ_{sh}), the rigid-body rotation (Δ_h), the rigid-body translation (Δ_a)

and the sheathing-panels (Δ_p), as stated by the following equation:

$$\Delta = \Delta_{sh} + \Delta_h + \Delta_a + \Delta_p \tag{1}$$

Some other contributions (such as compression perpendicular to the grain between studs and bottom rails, bending deflection etc.) could be taken into account. However, according to [7] for the wall typologies tested (See [13] and [14]), and considering the authors' intention to develop a simplified approach, these contributions can be neglected.

These contributions are considerably smaller compared to the others, therefore according to the intention of the author to develop a simplified approach, they are neglected according to [7]. The final expression of the horizontal displacement of a light timber frame wall, which components will be illustrated in the following subsections, is:

$$\Delta = \frac{\lambda \cdot F \cdot s_c}{l \cdot n_{bs} \cdot k_c} + \left[\frac{h}{\tau \cdot l \cdot k_h} \cdot \left(\frac{F \cdot h}{\tau \cdot l} - \frac{q \cdot l}{2}\right)\right] + \frac{F \cdot i_a}{k_a \cdot l} + \frac{F \cdot h}{l \cdot G_p \cdot n_{bs} \cdot t_p} \tag{2}$$

Equation 2 has been developed by considering also the presence of a uniformly distributed vertical load q.

The length and the height of the wall are respectively assumed equal to l and h. Each deformation contribution is obtained by means of the mathematical calculations reported from Section 2.1 to 2.4. In the case of a CLT wall, Equation 2 can be modified by substituting the sheathing panel contribution with the CLT panel contribution and removing the term for the sheathing-to-framing connection, to obtain:

$$\Delta = \left[\frac{h}{\tau \cdot l \cdot k_h} \cdot \left(\frac{F \cdot h}{\tau \cdot l} - \frac{q \cdot l}{2}\right)\right] + \frac{F \cdot i_a}{k_a \cdot l} + \frac{F \cdot h}{l \cdot G_{CLT} \cdot t_{CLT}} \tag{3}$$

In Equations 2 and 3, as shown in Section 2.2, the term Δ_h concerning the wall rigid-body rotation must be taken into account only if it is positive or equal to zero, i.e. hold-down in tension, otherwise it must to be removed.

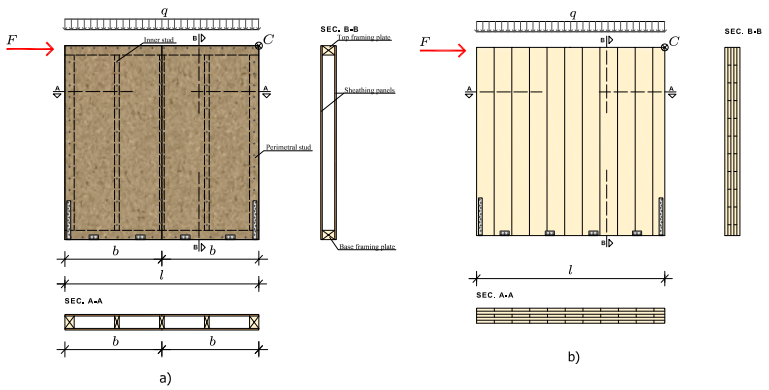

Figure 1: a) TF (timber framed wall) ; b) CLT (Cross laminated timber wall)

There is the uncommon chance to have vertical concentrated force instead of vertical distributed load or even in addition to it. In this event, Equations 2 and 3 are not valid; a specific equation will be developed by authors. The equations can be anyway use replacing the vertical concentrated force with an equivalent distributed load losing precision in proportion to the eccentricity of the vertical force with respect to the center of the wall.

It is important to note that, according with Figure 1, hold-downs are placed onto the external studs and angle-brackets are considered uniformly spaced along the base plate. For different configurations, Equations 2 and 3, could be anyway used considered an equivalent hold-down action.

2.1. Sheathing-to-framing connection deformation

A timber frame wall consists of a wood frame made with wood studs and a top and bottom wood plate. The frame is braced by sheathing panels which are connected to the frame by means of fasteners (nails or staples). According to [11] the deformation contribution of the sheathing to framing connection Δ_{sh}, can be evaluated for a wall with a single sheating panel ($l = b$) as follows:

$$\Delta_{sh} = \frac{F \cdot h^2}{k_c} \cdot \left[\frac{1}{\sum_{i=1}^{n} x_i^2} + \frac{1}{\sum_{i=1}^{n} y_i^2} \right] \tag{4}$$

where:

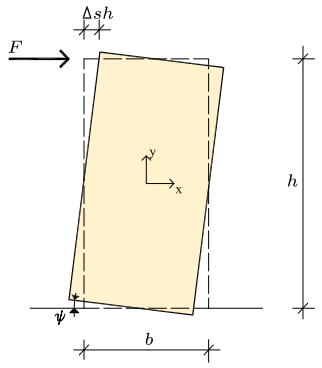

Figure 2: Sheathing-to-framing connection deformation

- F: is the applied horizontal force;
- h: is the height of the panel; it is also the height of the wall. In this article only walls with panels of the same height are considered;
- k_c: is the fastener stiffness;
- x_i, y_i: are the fasteners coordinates with respect to a reference system with its origin in the middle of the panel, see [11];
- n: is the number of fasteners.

The ratio between panel height h and panel breadth b, can be conveniently defined as the panel geometrical parameter α.

$$\alpha = \frac{h}{b} \tag{5}$$

For rigid framing members (this assumption is valid for the wall typologies tested by authors), assuming a constant spacing of fasteners along the plates s_p, on the perimeter studs s_{ps} on the inner studs s_{is}, we obtain:

$$\sum_{i=1}^{n} x_i^2 \cong \frac{1}{6} \cdot \left(1 + 3 \cdot \frac{s_p}{s_{ps}} \cdot \frac{h}{b}\right) \cdot \frac{b}{s_p} \cdot b^2 \tag{6}$$

$$\sum_{i=1}^{n} y_i^2 \cong \frac{1}{12} \cdot \left(6 + 2 \cdot \frac{s_p}{s_{ps}} \cdot \frac{h}{b} + \frac{s_p}{s_{is}} \cdot \frac{h}{b}\right) \cdot \frac{b}{s_p} \cdot h^2 \tag{7}$$

Assuming that the inner stud fastener spacing s_{is} is usually double that of s_p and s_{ps}, a reference fastener spacing s_c is defined as:

$$s_c = s_{ps} = s_p = \frac{s_{is}}{2} \tag{8}$$

The parameters η and ξ can be introduced:

$$\eta = \frac{1}{6} \cdot \left(1 + 3 \cdot \alpha\right) \tag{9}$$

$$\xi = \frac{\alpha^2}{12} \cdot \left(6 + \frac{5}{2} \cdot \alpha\right) \tag{10}$$

Equations 6 and 7 become:

$$\sum_{i=1}^{n} x_i^2 \cong \eta \cdot \frac{b^3}{s_c} \tag{11}$$

$$\sum_{i=1}^{n} y_i^2 \cong \xi \cdot \frac{b^3}{s_c} \tag{12}$$

Therefore, the displacement Δ_{sh} is:

$$\Delta_{sh} = \frac{F \cdot b^2}{k_c} \cdot \alpha^2 \cdot \left[\frac{1}{\eta} + \frac{1}{\xi}\right] \cdot \frac{s_c}{b^3} \tag{13}$$

In Kallsner et. al. [11], for standard bracing panels with h=2b, Equation 13 becomes:

$$\Delta_{sh} = 4.52 \cdot \frac{F}{k_c} \cdot \frac{s_c}{b} \tag{14}$$

To analyze wall braced with panels different from standard (i.e. $h \neq 2b$), it is useful to define a new parameter λ depending on the panel shape function α:

$$\lambda = \alpha^2 \cdot \left[\frac{1}{\eta(\alpha)} + \frac{1}{\xi(\alpha)}\right] = \lambda(\alpha) \tag{15}$$

The displacement Δ_{sh} becomes:

$$\Delta_{sh} = \frac{F}{k_c} \cdot \lambda(\alpha) \cdot \frac{s_c}{b} \tag{16}$$

Equation 14 represents the horizontal displacement due to the sheathing-to-framing connection deformation of a wall with a length equal to b, i.e. a wall with a single sheathing panel. In the general case of a wall with more than one sheating panel, namely a wall with $l > b$, Equation 14 becomes:

$$\Delta_{sh} = F \cdot \left(\sum_{j=1}^{n_{p,side1}} \frac{s_{c,j} \cdot \lambda_j(\alpha)}{k_{c,j} \cdot b_j} + \sum_{j=1}^{n_{p,side2}} \frac{s_{c,j} \cdot \lambda_j(\alpha)}{k_{c,j} \cdot b_j} \right) \tag{17}$$

where $n_{p,side1}$ and $n_{p,side2}$ are the number of sheathing panels placed on side 1 and side 2 of the wall respectively.
When the wall is braced by several sheating panels with the same width b (as usual in practice) and assuming the use of the same type of nails along the wall with the same spacing, Equation 17 can be rewritten as:

$$\Delta_{sh} = \frac{F \cdot \lambda(\alpha) \cdot s_c}{k_c \cdot l \cdot n_{bs}} \tag{18}$$

where $n_{bs} \in [1; 2]$ is the number of braced sides of the wall.

The shape function λ, depending on α, is plotted in Figure 3. For values of $1 < \alpha < 5$, a possible approximation of λ can be expressed by the linear regression Equation 19.

$$\lambda(\alpha) = 0.81 + 1.85 \cdot \alpha \tag{19}$$

For the value of $\alpha = 2$, λ is equal to 4.52 as developed by [11].

For cross-laminated-timber walls, according to Equation 3, the sheathing-to-framing deformation contribution Δ_{sh} is obviously not considered.

2.2. Rigid-body rotation

The rigid-body rotation contribution accounts for the tensile deformation of the hold-downs used at each corner of the wall to prevent the wall rotation caused by the acting overturning moment $M = F \cdot h$. From the equilibrium around the right-bottom corner (point O in Figure 4), the force acting on the hold-down $T$is :

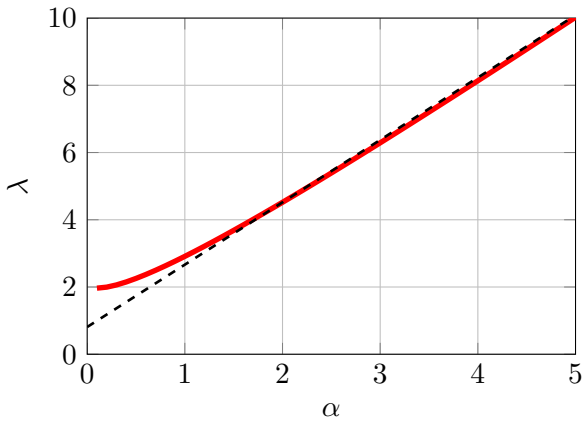

Figure 3: Shape function vs sheathing panel dimensions ratio

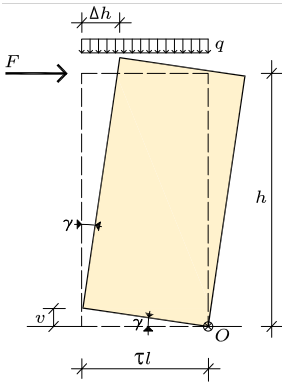

Figure 4: Rigid-body rotation

$$T = \frac{F \cdot h}{\tau \cdot l} \tag{20}$$

where $\tau \cdot l$ is the internal lever arm (effective length of rotation, see Figure 4). According to [15] for CLT walls typical values of τ range from 0.90 to 0.95, while for timber frame can be expected values closer to 1.

Considering also the presence of the vertical load the force on the hold-down becomes:

$$T = (\frac{F \cdot h}{\tau \cdot l} - \frac{q \cdot l}{2}) \tag{21}$$

The rigid-body deformation contribution (see also Figure 4), differently from the other contributions, is influenced by the vertical load. Indeed, the hold-down elongation v can be evaluated by:

$$v = \left(\frac{F \cdot h}{\tau \cdot l} - \frac{q \cdot l}{2}\right) \cdot \frac{1}{k_h} \tag{22}$$

where k_h is the hold-down stiffness.

The rigid rotation angle γ is equal to:

$$\gamma = \frac{v}{\tau \cdot l} = \left(\frac{F \cdot h}{\tau^2 \cdot l^2} - \frac{q}{\tau \cdot 2}\right) \cdot \frac{1}{k_h} \tag{23}$$

Thus, the rigid-body rocking deformation Δ_h becomes:

$$\Delta_h = \gamma \cdot h = \left(\frac{F \cdot h}{\tau \cdot l} - \frac{q \cdot l}{2}\right) \cdot \frac{h}{k_h \cdot \tau \cdot l} \tag{24}$$

However, when the vertical load is large enough to prevent the wall rotation $F > F_q = \frac{\tau \cdot q \cdot l^2}{2 \cdot h}$, i.e the overturning moment is less than the stabilizing moment due to the vertical load, the hold-down elongation v is equal to zero. Consequently, Equation 24 can be rewritten as:

$$\Delta_h = \begin{cases} 0 & \text{when} \quad F \leq F_q \\ \frac{h}{\tau \cdot l \cdot k_h} \cdot \left(\frac{F \cdot h}{\tau \cdot l} - \frac{q \cdot l}{2}\right) & \text{when} \quad F > F_q \end{cases} \tag{25}$$

2.3. Rigid-body translation

The wall is usually connected to the foundation by means of angle-brackets or screws in order to prevent a rigid-body translation, see Figure 5.

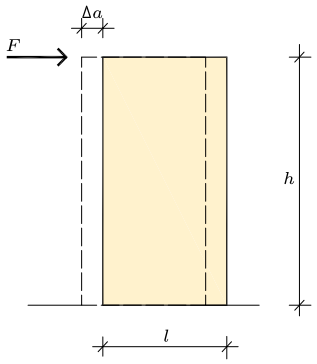

Figure 5: Rigid-body translation

Neglecting the friction, the deformation contribution due to the rigid-body translation Δ_a, is not dependent on the vertical load and it is given by:

$$\Delta_a = \frac{F}{k_a \cdot n_a} \tag{26}$$

where:

- k_a: is the stiffness of the angle-bracket or screw;

- n_a: is the number of angle-brackets or screws.

When the spacing between the angle-brackets or screws i_a is constant, Equation 26 can be rearranged as:

$$\Delta_a = \frac{F \cdot i_a}{k_a \cdot l} \tag{27}$$

2.4. Sheathing-panel shear deformation

The sheathing panel shear deformation contribution Δ_p is not dependent on vertical load and can be evaluated in the following way. Referring to Figure 6 the shear strain ζ is equal to:

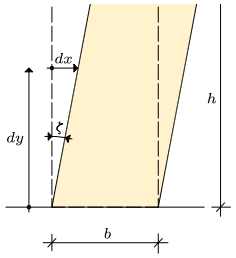

Figure 6: Sheathing-panel deformation

$$\zeta = \frac{dx}{dy} = \chi \cdot \frac{F}{G_p \cdot A_p} = \chi \cdot \frac{F}{G_p \cdot t_p \cdot b} \tag{28}$$

Where:

- A_p is the shear area of the sheathing panels;
- G_p is the shear modulus of the sheathing panels;
- t_p is the sheathing panel thickness.
- χ is the panel shear factor.

The displacement Δ_p can be evaluated as the product between ζ and the wall height h, where the shear factor χ is assumed equal to one.

$$\Delta_p = \zeta \cdot h = \frac{F \cdot h}{G_p \cdot t_p \cdot b} \tag{29}$$

In case of multi-panel wall, the displacement Δ_p results:

$$\Delta_p = F \cdot h \cdot \left(\sum_{j=1}^{n_{p,side1}} \frac{1}{G_{p,j} \cdot t_{p,j} \cdot b_j} + \sum_{j=1}^{n_{p,side2}} \frac{1}{G_{p,j} \cdot t_{p,j} \cdot b_j} \right) \tag{30}$$

When the wall is braced by the same type of panels characterized by the same width b, Equation 30 can be rewritten as:

$$\Delta_p = \frac{F \cdot h}{G_p \cdot t_p \cdot l \cdot n_{bs}} \tag{31}$$

For CLT walls the equation 29 should be rewritten with account taken of the thickness t_{CLT} and the equivalent shear modulus G_{CLT} [16]:

$$\Delta_p = \zeta \cdot h = \frac{F \cdot h}{G_{CLT} \cdot t_{CLT} \cdot l} \tag{32}$$

2.5. Single component contribution

The average percentage of deformation due to each single contribution, with regards to a typical wall configuration, is shown in Figure 7 for both a timber frame wall and a CLT wall. These values are obtained considering the most typical range of mechanical and geometrical properties of the shear wall structural components, according to what reported in [7], in [12] and in[17]. The hold-down in tension case is considered.

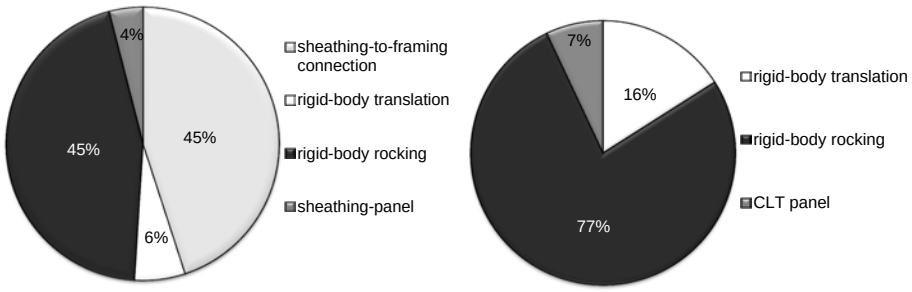

Figure 7: Percentage of deformation due to each single contribution

It is shown that for timber frame walls the main contribution is mostly made by the sheathing-to-framing connection and the hold-down connection. For CLT walls it is mainly made by the rigid body rotation contribution.

3. Horizontal stiffness of a timber shear-wall

Plotting the force vs displacement relationship (see Equation 2) and taking into account that the term concerning the wall rigid body rotation is to be considered only if it is positive, a bi-linear curve is obtained: see Figure 8. Two regimes are to be considered. The first is when the hold-down is not in tension

($F < F_q$) because the stabilizing moment is greater than the overturning one. The related wall stiffness is called $K_{tot,nt}$. The second regime occurs when the hold-down is in tension ($F > F_q$). The related wall stiffness is defined as K_{tot}. If the wall is vertically non-loaded (q=0), only the second regime occurs.

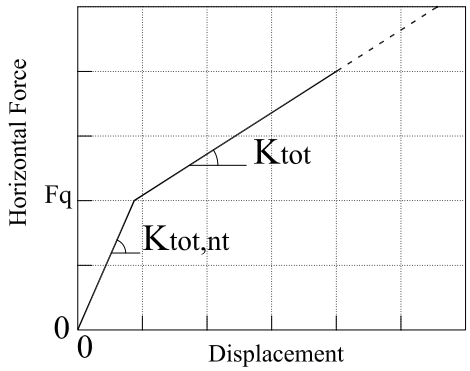

Figure 8: Two stiffness regimes. The force F_q is the force that activates the hold-down.

In the second regime, the total horizontal displacement can be rewritten to highlight the contribution of the external force F, as shown by Equation 33.

$$\Delta = \frac{F}{K_{SH}} + \frac{F}{K_P} + \frac{F}{K_A} + \frac{F}{K_H} - \frac{N \cdot h}{\tau l \cdot k_h} \tag{33}$$

where:

- $K_{SH} = \frac{n_{bs} \cdot k_c \cdot l}{\lambda \cdot s_c}$ is the sheathing-to-framing connection stiffness;
- $K_P = \frac{G_p \cdot n_{bs} \cdot t_p \cdot l}{h}$ is the sheathing panel shear stiffness;
- $K_A = \frac{k_a \cdot l}{i_a} = k_a \cdot n_a$ is the rigid body translation stiffness;
- $K_H = \frac{k_h \cdot \tau^2 \cdot l^2}{h^2}$ is the rigid body rotation stiffness;
- $N = \frac{q \cdot l}{2}$ is the half part of the vertical load.

Defining the global stiffness of the wall K_{tot} as:

$$\frac{1}{K_{tot}} = \frac{1}{K_{SH}} + \frac{1}{K_P} + \frac{1}{K_A} + \frac{1}{K_H} \tag{34}$$

and the horizontal wall displacement due to the vertical load Δ_N:

$$\Delta_N = \frac{N \cdot h}{\tau \cdot l \cdot k_h} \tag{35}$$

the total horizontal displacement of Equation 33 can be expressed as:

$$\Delta = \frac{F}{K_{tot}} - \Delta_N \tag{36}$$

The external force F can be expressed as:

$$F = K_{tot} \cdot \Delta + K_{tot} \cdot \Delta_N = F_{el} + F_N \tag{37}$$

where F_{el} is the horizontal elastic force and F_N is the equivalent horizontal force due to the vertical load.

Equation 37 can be represented by four elastic springs in series subjected to a total force equal to $F_{el} = (F - F_N)$: see Figure 9 and 10.

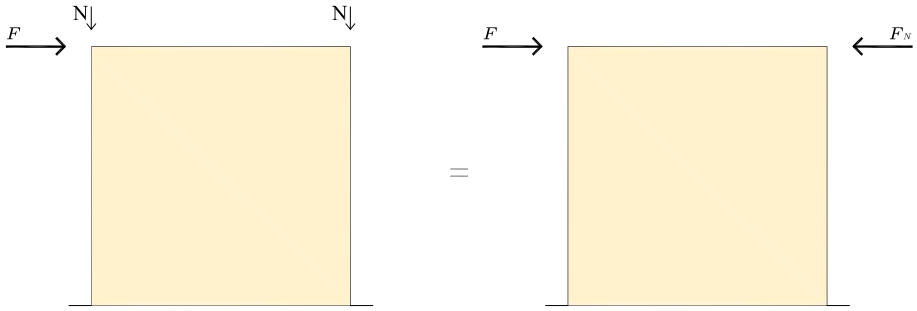

Figure 9: Equivalent force distribution for the second regime rheological model

Equations 36 and 37 prompt the following two considerations (see Figure 11):

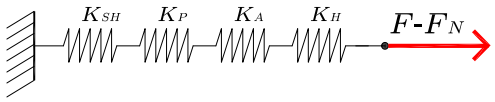

Figure 10: Wall rheological model for the second regime

1. the horizontal displacement produced by the horizontal force F is decreased at a rate caused by the vertical load equal to Δ_N, which is constant;
2. the force F required to warp the wall is the sum of two different quantities: the elastic force F_{el} and the force to counteract the vertical load F_N.

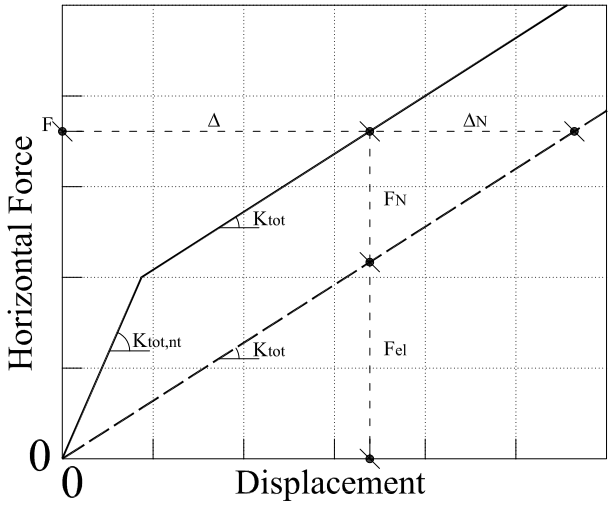

Figure 11: Horizontal force vs displacement

The first regime, i.e. when the hold-down is not in tension, may be considered a sub-case of the second regime, setting the hold-down stiffness k_h equal to infinity. Hence the global stiffness $K_{tot,nt}$ of Equation 34, becomes:

$$\frac{1}{K_{tot,nt}} = \lim_{k_h \to \infty} \frac{1}{K_{tot}} = \frac{1}{K_{SH}} + \frac{1}{K_P} + \frac{1}{K_A} \tag{38}$$

The horizontal displacement due to the vertical load Δ_N becames 0. Hence, the global displacement is given by:

$$\Delta = \frac{F}{K_{tot,nt}} \tag{39}$$

Equation 39 can be represented by three elastic springs in series subjected to a total force equal to F, see Figure 12

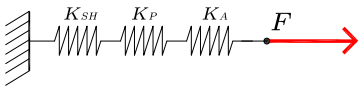

Figure 12: Wall rheological model for the first regime

3.1. Parametric study of wall stiffness

The stiffness of a timber shear-wall is commonly considered to be linearly proportional to the wall length. In order to show that this assumption cannot be considered correct for all cases a dimensionless parametric study is performed. In regard to the second regime, i.e. the hold-down is in tension (assuming a wall braced by sheating panels with the same width $b_j = b$) the wall stiffness is rewritten as follows:

$$\frac{1}{K_{tot}} = \frac{h}{l} \cdot \frac{1}{G_p \cdot n_{bs} \cdot t_p} + \frac{\lambda \cdot s_c}{l \cdot n_{bs} \cdot k_c} + \frac{i_a}{k_a \cdot l} + \frac{h^2}{\tau^2 \cdot l^2 \cdot k_h} \tag{40}$$

Four parameters are defined, as follows:

$$\frac{1}{\vartheta} = \frac{h}{G_p \cdot n_{bs} \cdot t_p} = \frac{l}{K_P} \tag{41}$$

$$\frac{1}{\beta} = \frac{s_c}{n_{bs} \cdot k_c} \cdot \lambda = \frac{l}{K_{SH}} \tag{42}$$

$$\frac{1}{\varphi} = \frac{i_a}{k_a} = \frac{l}{K_A} \tag{43}$$

$$\frac{1}{\delta} = \frac{h^2}{\tau^2 \cdot k_h} = \frac{l^2}{K_H} \tag{44}$$

Using the four previous parameters, Equation 40 becomes:

$$\frac{1}{K_{tot}} = \frac{1}{\vartheta \cdot l} + \frac{1}{\beta \cdot l} + \frac{1}{\varphi \cdot l} + \frac{1}{\delta \cdot l^2} \tag{45}$$

This acts as a useful check on the equation. Thus, the wall stiffness is:

$$K_{tot} = \frac{\vartheta \cdot \beta \cdot \varphi \cdot \delta \cdot \mathbf{l}^2}{(\vartheta \cdot \varphi \cdot \delta + \beta \cdot \varphi \cdot \delta + \vartheta \cdot \beta \cdot \delta) \cdot \mathbf{l} + \vartheta \cdot \beta \cdot \varphi} \tag{46}$$

Equation 46 shows that the stiffness of the wall is not linearly proportional to the wall length. Indeed the contribution related to the rigid-body rotation is proportional to the square of the length.
If the hold-down is not in tension, i.e. the first regime is considered, the parameter $\delta \longrightarrow \infty$. The wall stiffness is hence given by:

$$K_{tot,nt} = \lim_{\delta \to \infty} K_{tot} = \frac{\vartheta \cdot \beta \cdot \varphi \cdot \mathbf{l}}{\vartheta \cdot \beta + \vartheta \cdot \varphi + \beta \cdot \varphi} = \omega \cdot \mathbf{l} \tag{47}$$

Equation 47 shows how the assumption that the wall stiffness is proportional to the wall length is correct only if the first regime is considered, i.e. the rigid body rotation contribution is absent.
In order to assess the influence of the rigid body rotation contribution a dimensionless parametric study of the wall stiffness K_{tot} is performed. Defining the parameter Φ given in Equation 48 and using $\alpha = \frac{h}{b}$, the charts shown in Figures 13 and 14 can be plotted. The x-axis is referred to the dimensionless length $\tilde{l} = \frac{l}{b}$, whereas on the y-axis the wall dimensionless horizontal stiffness $\tilde{K_{tot}} = \frac{K_{tot}}{K_{tot,b}}$ is reported, where $K_{tot,b}$ is the horizontal stiffness of a wall with a length l equal to b.

$$\Phi = \frac{s_c \cdot k_h}{b \cdot k_c} \tag{48}$$

Parameters Φ and α are chosen because they represent the ratio between the stiffness of the rigid body rotation spring and the stiffness of the sheathing-to-framing spring, as apparent in Equation 49. The parameter Φ represents the mechanical properties of the hold-down and the sheathing-to-framing connections, whereas α represent the geometrical dimensions of the panel.

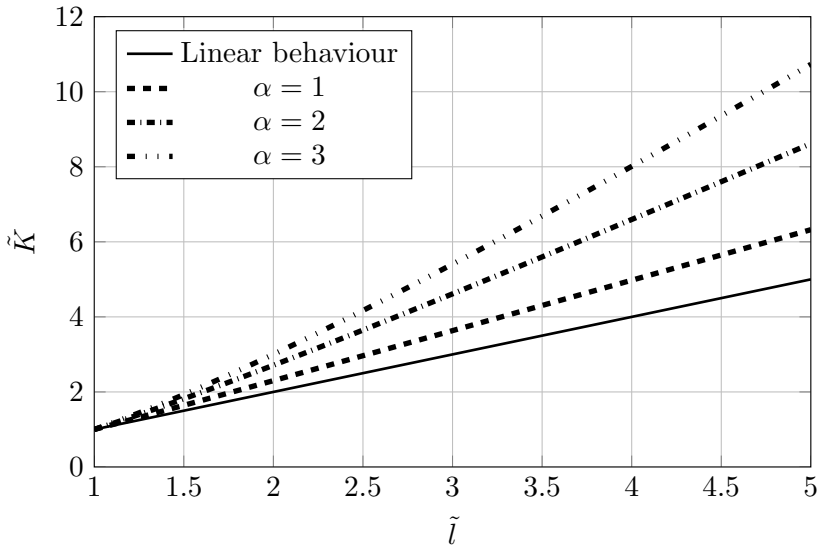

Figure 13: Stiffness dimensionless behavior for $\Phi = 0,72$

$$\frac{K_H}{K_{SH}}(\Phi, \alpha) = \Phi \cdot \frac{\lambda(\alpha)}{\alpha^2} \cdot \tilde{l} \tag{49}$$

The value of Φ increases when hold-down stiffness k_h becomes larger. Conversely, the value of Φ decreases when the fastener sheathing-to-framing connection stiffness k_c becomes larger.

The following properties of the walls are chosen to plot the chart in Figure 13 and Figure 14:

- sheathing panels: OSB/3, t_p=15 mm, n_{bs}=2; G_p=1080 MPa;
- angle brackets: i_a=625 mm; k_a= 3746 kN/mm;

In Figures 13 and 14 the linear behaviour is represented by the solid lines, where the wall stiffness is directly dependent on the wall length. The dashed - dashed-dotted lines move away from the solid lines, i.e. the walls stiffness is more than linear with the length when the α increases or when the parameter Φ decreases. Hence, the wall horizontal stiffness becomes significantly non-linear for slender walls or for more flexible hold-downs. Consequently, the wall stiffness

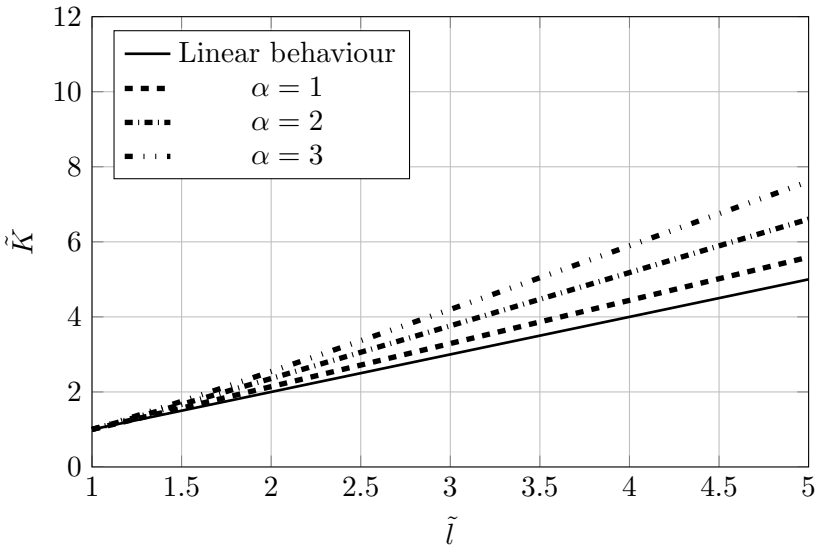

Figure 14: Stiffness dimensionless behavior for $\Phi = 2,87$

cannot be considered a priori as linearly proportional to the wall length. For instance, when $\alpha = 3$ and $\Phi = 0,72$ a wall of length $l = 4b$ is *eight* times stiffer than a wall of length $l = b$. In the common design practice, instead, a wall of length $l = 4b$ is usually considered *four* times stiffer than a wall of length $l = b$. For CLT walls $\Phi = 0$, because the sheathing-to-framing connection are not present. The rigid body rotation contribution, as can be seen in Figure 7, is the most important one if the hold-down is in tension. For this reason the non-proportionality between wall stiffness and wall length is more evident than in the case of timber frame wall.

4. Simplified finite element model of a timber shear-walls

The elastic behavior of a timber shear-wall can be reproduced by complex finite element models which have a fine resolution and several details. However, a complete model is characterized by a large number of degrees of freedom, especially if each fastener is represented by springs. For this reason a complete and complex finite element model requires a lot of time to be set-up and to be

run (especially for seismic analysis of multi-story buildings). Therefore, the use of a less complicated procedure shall be preferable.
Following, a simplified model, called UNITN model, is presented. This model is based on Equation 34 and it is suitable to be inserted in a commercial software for timber buildings. It reproduces the wall by means of four infinite rigid pinned beams, which has to be regarded as a mechanism, with height h and length $\tau \cdot l$. In addition, three equivalent springs are used to brace the frame and to connect it to the ground, see Figure 15. Each spring is defined according to the analytical expressions reported in Section 3.

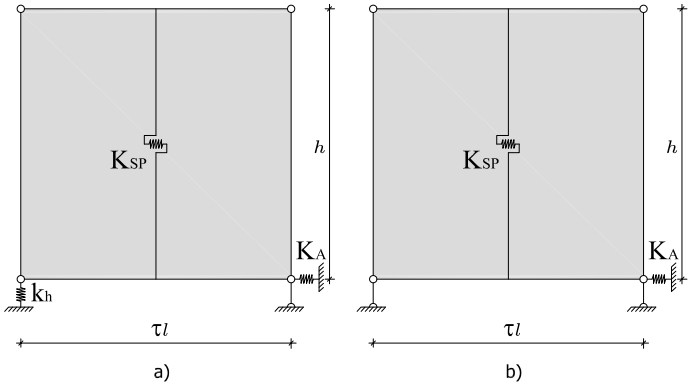

Figure 15: a) Simplified model for in-tension hold-down; b) simplified model for not in-tension hold-down

The uplifting corner is vertically connected to the ground by means of a spring with stiffness equal to k_h which models the hold-down behaviour, whereas a pinned axially rigid beam is placed on the other corner. The horizontal spring with stiffness K_A, see Equation 33, models the rigid body translation contribution. The sheathing-to-framing and sheathing-panel deformation contributions are modeled by means of an equivalent horizontal linear spring of stiffness K_{SP} which is evaluated as:

$$\frac{1}{K_{SP}} = \frac{1}{K_{SH}} + \frac{1}{K_P} \tag{50}$$

or rearranging:

$$K_{SP} = \frac{K_P \cdot K_{SH}}{K_P + K_{SH}} \tag{51}$$

For CLT shear-walls K_{SH} results equal to 0, getting $K_{SP} = K_P$,

The stiffness of the model frame elements must be taken as infinite to prevent its bending deformation.

According to the analysis in Section 2.2, when the hold-down is not in-tension the spring with stiffness equal to k_h must be removed and substitute with another vertical rigid-pinned beam: see Figure 15 b).

An iterative analysis must be performed in order to obtain a consistent model which takes account of the correct condition (in-tension or not in-tension) of the hold-down. First, the spring must be included in the model and the hold down force must be evaluated. If the hold-down is in tension the model is consistent. If the hold-down is not in-tension then it should be substitute by the pinned-beam in order to re-run the analysis to obtain the correct result.

The UNITN model reproduces a TF shear-wall or a CLT shear-wall by means of three springs. Usually, a timber wall has two hold-downs (one in each corner), but only one hold-down at a time is in tension, whereas the other one does not work because it is placed in the compression side of the wall. According to Figure 16, the hold-down spring shall be placed in the UNITN Model on the tension corner of the wall.

4.1. Experimental validation of the model

An extended validation of the numerical model is reported in [13] and [14] where a deep experimental investigation carried out at the University of Trento is described. The accuracy of the model is also demonstrated by the authors in [18]. It should be highlighted that the analytical expression is not developed with the aim to fit the entire experimental horizontal force vs displacement curve, but to predict an equivalent elastic stiffness of the wall.

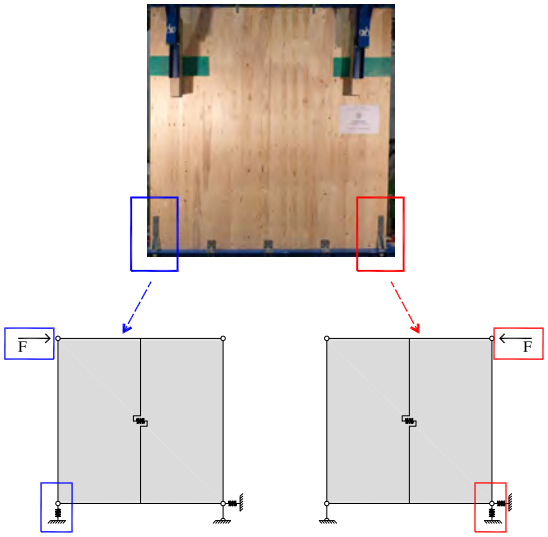

Figure 16: Simplified model for left or right horizontal force

5. Model for n horizontally-aligned walls

The study of the horizontal displacement of a timber shear-wall (analytical procedure and simplified model) can be exploited to assess the behaviour of horizontally aligned walls subjected to a horizontal force.
A system of n horizontally-aligned walls, see Figure 17, is obtained by connecting each wall to the next one by means of a pinned-beam with infinite axial stiffness. The pinned-beams simulate the behaviour of the upper floor, which imposes the same horizontal displacement on the walls. This means that the walls work together to support the horizontal force acting at that storey, thus the walls can be regarded as a system of springs in parallel.

The current design approach distribute a horizontal force F acting on a system of horizontally-aligned walls only with regard to the ratio $\frac{l_i}{\sum_{i=1}^{n} l_i}$, where l_i is the length of a certain wall and $\sum_{i=1}^{n} l_i$ is the total length of all the walls. In fact as reported in Section 3.1, wall stiffness is assumed to be directly proportional to wall length. Thanks to the equations given in Section 3, it is known that the stiffness of a wall is not linearly proportional to the wall's

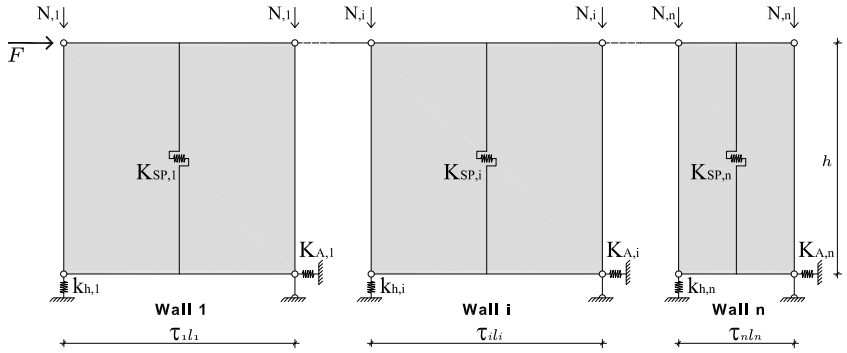

Figure 17: System of n horizontally-aligned walls

length. Therefore, the method currently used is not completely correct. The force F_i which each wall $i-th$ supports must be determined using the three following equations:

- Equation 37 makes it possible to write the constitutive law: $F_i = K_{tot,i} \cdot (\Delta_i + \Delta_{N,i}),\ for\ i \in [1, n]$;
- owing to the presence of the pinned-frames connecting the walls to each other, is possible to write the compatibility law: $\Delta_i = \Delta,\ for\ i = 1..n$;
- the equilibrium law is: $\sum_{i=1}^{n} F_i = F$.

The force F_i of each wall and the total horizontal displacement Δ can be obtained as:

$$\Delta = \frac{F - \sum_{i=1}^{n} (K_{tot,i} \cdot \Delta_{N,i})}{\sum_{i=1}^{n} K_{tot,i}} \tag{52}$$

$$F_i = \frac{K_{tot,i}}{\sum_{j=1}^{n} K_{tot,j}} \cdot \left[F - \sum_{j=1}^{n} [K_{tot,j} \cdot (\Delta_{N,j} - \Delta_{N,i})] \right] \tag{53}$$

Two important consideration can be done from Equations 52 and 53 :

- the horizontal force F_i which is taken from the wall $i-th$ is proportional to the ratio $\frac{K_{tot,i}}{\sum_{i=1}^{n} K_{tot,i}}$. Hence F_i is not linearly proportional to the wall

length (K_{tot} is not linearly proportional to the wall length, as illustrated in section 3.1;

- the presence and the magnitude of the vertical load q_j acting on the $j-th$ wall modifies the distribution of the horizontal load.

The tensile force of each hold-down T_i can be obtained from:

$$T_i = \frac{F_i \cdot h}{\tau \cdot l_i} - \frac{q_i \cdot l_i}{2} \tag{54}$$

If a hold-down is not in tension ($T_i < 0$) the wall stiffness becomes $K_{tot,nt,i}$ and the horizontal displacement $\Delta_{N,i}$ is equal to zero. The analysis must be performed again according to the new consistent model. The method is still iterative. In order to clarify the method proposed, a numerical application is described in Section 5.1.

5.1. A numerical example of the load distribution in a system of two horizontally-aligned walls

This section presents a numerical example to show how the method presented in Section 5 should be applied. Consider the system of two horizontally aligned timber frame walls ($\tau = 1$) in Figure 18. Their geometrical and mechanical properties are shown in Table 1. The horizontal force applied F is 15 kN.

The stiffness of each equivalent spring of the simplified model is:

- $K_{P,1} = \frac{G_{p,1} \cdot n_{bs,1} \cdot t_{p,1} \cdot l_1}{h} = 30000 \frac{N}{mm}$
- $K_{P,2} = \frac{G_{p,2} \cdot n_{bs,2} \cdot t_{p,2} \cdot l_2}{h} = 15000 \frac{N}{mm}$
- $K_{SH,1} = \frac{n_{bs,1} \cdot k_{c,1} \cdot l_1}{\lambda_1 \cdot s_{c,1}} = 5531 \frac{N}{mm}$
- $K_{SH,2} = \frac{n_{bs,2} \cdot k_{c,2} \cdot l_2}{\lambda_2 \cdot s_{c,2}} = 2765 \frac{N}{mm}$
- $K_{A,1} = k_{a,1} \cdot n_{a,1} = 12000 \frac{N}{mm}$
- $K_{A,2} = k_{a,2} \cdot n_{a,2} = 6000 \frac{N}{mm}$
- $K_{H,1} = \frac{k_{h,1} \cdot \tau^2 \cdot l_1^2}{h_1^2} = 5000 \frac{N}{mm}$

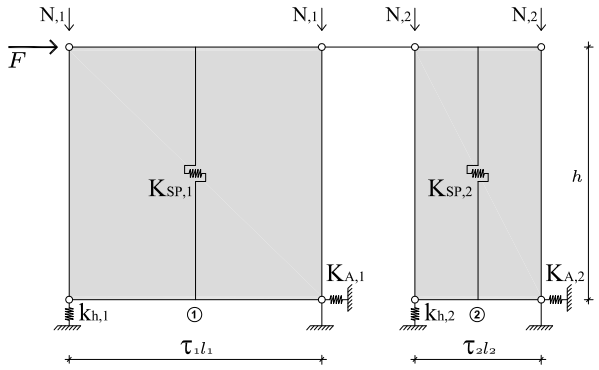

Figure 18: System of 2 horizontally-aligned walls

- $K_{H,2} = \frac{k_{h,2} \cdot \tau^2 \cdot l_2^2}{h_2^2} = 1250 \frac{N}{mm}$

The first iteration is carried-out considering that both the hold-downs of the two walls are in tension. Hence, the total stiffness of the walls are:

$$K_{tot,1} = \frac{1}{\frac{1}{K_{SH,1}} + \frac{1}{K_{P,1}} + \frac{1}{K_{A,1}} + \frac{1}{K_{H,1}}} = 2010 \frac{N}{mm} \tag{55}$$

$$K_{tot,2} = \frac{1}{\frac{1}{K_{SH,2}} + \frac{1}{K_{P,2}} + \frac{1}{K_{A,2}} + \frac{1}{K_{H,2}}} = 717 \frac{N}{mm} \tag{56}$$

Using Equation 35, the displacement contributions due to the vertical load are:

$$\Delta_{N,1} = \frac{(q_1 \cdot l_1/2) \cdot h}{l_1 \cdot k_{h,1}} = 5.0 \; mm \tag{57}$$

$$\Delta_{N,2} = \frac{(q_2 \cdot l_1/2) \cdot h}{l_2 \cdot k_{h,2}} = 0 \; mm \tag{58}$$

From the equation 53 the forces which act on each wall are:

$$F_1 = \frac{K_{tot,1} \cdot (F - \Delta_{N,2} \cdot K_{tot,2} + \Delta_{N,1} \cdot K_{tot,2})}{K_{tot,1} + K_{tot,2}} = 13.70 \; kN \tag{59}$$

$$F_2 = \frac{K_{tot,2} \cdot (F - \Delta_{N,1} \cdot K_{tot,1} + \Delta_{N,2} \cdot K_{tot,1})}{K_{tot,1} + K_{tot,2}} = 1.30 \; kN \tag{60}$$

	Wall n.1	**Wall n.2**
length l $[mm]$	2500	1250
height h $[mm]$	2500	2500
vertical load q $[kN/m]$	20	0
number of braced sides n_{bs}	2	2
sheathing panel shear modulus G_p $[N/mm^2]$	1000	1000
sheathing panel thickness t_p $[mm]$	15	15
sheathing panel length b $[mm]$	1250	1250
fastener stiffness k_c $[N/mm]$	500	500
fastener spacing s_c $[mm]$	100	100
hold down stiffness k_h $[N/mm]$	5000	5000
angle bracket stiffness k_a $[N/mm]$	3000	3000
number of angle brackets n_a	4	2

Table 1: Properties of the walls

Moreover, the total displacement is:

$$\Delta = \frac{F - \Delta_{N,1} \cdot K_{tot,1} - \Delta_{N,2} \cdot K_{tot,2}}{K_{tot,1} + K_{tot,2}} = 1.81\ mm \tag{61}$$

The forces in the hold-downs are therefore:

$$T_1 = \frac{F_1 \cdot h_1}{\tau \cdot l_1} - \frac{q_1 \cdot l_1}{2} = -11.30\ kN \tag{62}$$

$$T_2 = \frac{F_2 \cdot h_2}{\tau \cdot l_2} - \frac{q_2 \cdot l_2}{2} = 2.60\ kN \tag{63}$$

The hold-down of Wall 1 is not in tension. It must therefore be removed from the model ($k_{h,1} \longrightarrow \infty$) and the procedure has to be iterated. The new values of the stiffness are:

$$K_{tot,nt,1} = \frac{1}{\frac{1}{K_{SH,1}} + \frac{1}{K_{P,1}} + \frac{1}{K_{A,1}}} = 3362\frac{N}{mm} \tag{64}$$

$$K_{tot,2} = \frac{1}{\frac{1}{K_{SH,2}} + \frac{1}{K_{P,2}} + \frac{1}{K_{A,2}} + \frac{1}{K_{H,2}}} = 717\frac{N}{mm} \tag{65}$$

The displacement contributions due to the vertical load for Wall 1 is:

$$\Delta_{N,1} = \frac{(q_1 \cdot l_1/2) \cdot h}{l_1 \cdot k_{h,1}} = 0\ mm \tag{66}$$

The forces become:

$$F_1 = \frac{K_{tot,nt,1} \cdot (F - \Delta_{N,2} \cdot K_{tot,2} + \Delta_{N,1} \cdot K_{tot,2})}{K_{tot,nt,1} + K_{tot,2}} = 12.36\,kN \tag{67}$$

$$F_2 = \frac{K_{tot,2} \cdot (F - \Delta_{N,1} \cdot K_{tot,nt,1} + \Delta_{N,2} \cdot K_{tot,nt,1})}{K_{tot,nt,1} + K_{tot,2}} = 2.64\,kN \tag{68}$$

The hold-down tensile force are given by:

$$T_1 = \frac{F_1 \cdot h_1}{\tau \cdot l_1} - \frac{q_1 \cdot l_1}{2} = -12.64\ kN \tag{69}$$

$$T_2 = \frac{F_2 \cdot h_2}{\tau \cdot l_2} - \frac{q_2 \cdot l_2}{2} = 5.27\ kN \tag{70}$$

Moreover, the total displacement is:

$$\Delta = 3,68\ mm \tag{71}$$

The results are consistent and the iterative method has come to convergence. If the common force distribution had been used, Wall 1 would have supported $\frac{2}{3} \cdot F = 10\,kN$ and Wall 2 would have supported $\frac{1}{3} \cdot F = 5\,kN$. This means that the method commonly used would have committed an error of 19% for Wall 1 and of 89% for Wall 2.

5.2. Full scale test

In order to demonstrate that the UNITN model is a tool suitable for predicting the force distribution in a series of horizontally aligned walls, an ad-hoc preliminary-test was carried out at the Materials and Structural Testing Laboratory of the University of Trento. This is the first test of a campaign research, which is still in progress. Two horizontally aligned walls with the characteristics shown in Table 2 were tested, See also Figure 20.

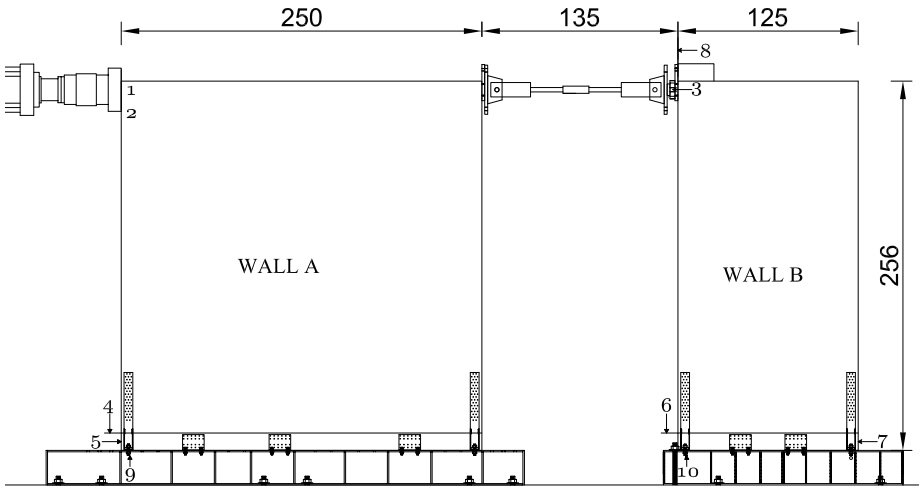

Figure 19: Test instrumentation setup (all dimensions in cm)

The setup used had been specific developed to test timber shear-walls subjected to monotonic and static load according to [19]. Details and properties of the setup used are reported in [13], in [14] and in [20].

The longer wall (wall A, see Figure 21) was anchored to the bottom steel base of the setup. The second wall was anchored to a new steel base, with the same cross-section as the first one and placed at a distance of 0,95 [m] from it. Moreover, to prevent the out-of-plane buckling of the wall an additional lateral support was added. A pinned-beam, made of a steel tube, connected the two walls in order to reproduce the effect of the upper floor: see Figure 21.

Ten instruments were placed as shown by Figure 19: LVDT 4 and LVDT 6 measured the uplift of the wall when the load was applied. LVDT 5 and LVDT 7 measured the relative horizontal displacement between the ground and the bottom surface of the panel. LC 1 was the load cell (LC) of the hydraulic jack and it measured the force applied; another transducer LVDT 2 incorporated in the actuator measured the displacement at the same point. LC 9 and LC10

Figure 20: Global view of the setup adopted for the full scale test

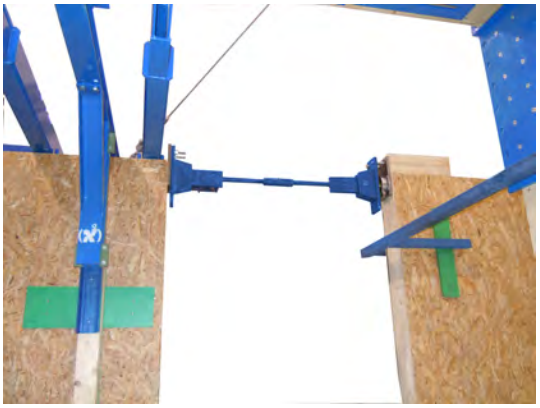

Figure 21: Pinned-beam connecting the two walls

were load cells incorporated into the hold-down bolts to measure the vertical reactions under the walls. LVDT 2 measured the absolute horizontal translation of the upper part of wall B. LC 3 was a load cell that measured the force acting in the pinned-beam.

	Wall A	**Wall B**
length l $[mm]$	2500	1250
height h $[mm]$	2500	2500
vertical load q $[kN/m]$	20	0
number of braced sides n_{bs}	2	2
type of sheathing panel	OSB3	OSB3
sheathing panel thickness t_p $[mm]$	15	15
sheathing panel base b $[mm]$	1250	1250
type of fasteners	Ring nails $2.8 \cdot 60$	Ring nails $2.8 \cdot 60$
fasteners spacing s_c $[mm]$	100	100
type of hold down	WHT340	WHT340
type of angle brackets	TTF200	TTF200
number of angle brackets n_a	3	2

Table 2: Properties of the two walls tested. For more details see [14]

Figure 22 reports the test results, in terms of load versus horizontal displacement. The solid line represents the global force acting on the two walls, the dashed line the force on the wall B, the dashed-dotted line the force on the Wall A.

The practical rules used by the designer distributes the horizontal force proportional to the walls length. According to this assumption, the wall A (250 cm long) should be loaded by 2/3 of the force (66.6%) whereas wall B (125 cm long) should be loaded by 1/3 of the force (33.3%). Due to the vertical force action, according to UNITN Model, the test results show the real force distribution, which is different from the common practice. A comparison between the test results and the prediction of the UNITN model is reported in Table 3. The comparisons are generally good, except for Wall A at 10mm, where the UNITN model is 20 % out from the test. The difference between the Wall A curves and the Model may have been due to the friction between concrete

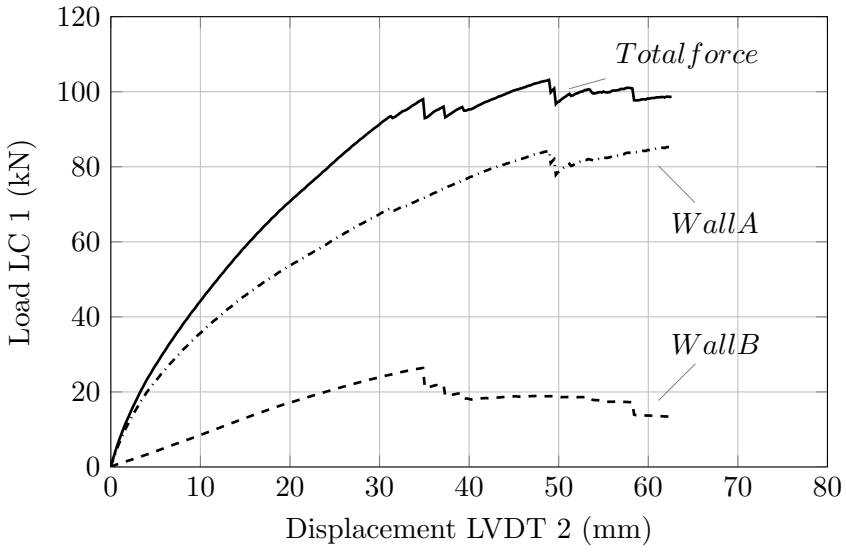

Figure 22: Test results

foundation and sill-beam, which increases the horizontal stiffness of the walls (Wall B friction is almost absent, only Wall A was loaded by a vertical load of 20kN/m). This friction, according to the Eurocode Standard requirements, should not be included in the model, especially with reference to seismic action, where friction must not be considered as a resistance mechanism.

	Experimental		UNITN Model		Percentage of Error	
Displacement	Wall A	Wall B	Wall A	Wall B	Wall A	Wall B
$[mm]$	$[kN]$	$[kN]$	$[kN]$	$[kN]$	[%]	[%]
10	35,67	8,52	28,15	8,42	21	1
20	53,65	17,15	49,09	16,85	8	2
30	67,44	23,94	70,05	25,26	3	5

Table 3: Comparison between test results and prediction of UNITN Model

6. Conclusions

This paper has presented an equation suitable to describe the elastic behavior of a single storey timber shear-wall. The total displacement was obtained by adding four different deformation contributions: those of the sheathing-to-framing, the rigid body rotation, the rigid-body translation and the sheathing-panels. In the case of CLT walls, sheathing-to-framing connections are absent, so that the sheathing-to-framing connection deformation is zero.

The analysis of the timber wall stiffness highlighted that two different regimes can occur. The first is when the hold-down is not in tension, since the stabilizing moment is greater than the overturning one. The related wall stiffness is called $K_{tot,nt}$. The second regime occurs when the hold-down is in tension. The related wall stiffness is defined as K_{tot}. If the wall is vertically non loaded (q=0), only the second regime occurs. Moreover, a parametric study was performed. It demonstrates that wall stiffness is linearly proportional to wall length only if the first regime occurs. The assumption commonly made in practice is therefore not correct in all cases.
Thirdly, a numerical simplified model, called UNITN Model, was proposed. The model is composed of only three elastic springs whose stiffness is evaluated according to the expressions related to the wall deformation contribution. The use of only three springs is the main feature of the Model because of it reduces the time needed to create and to run the analysis without loosing precision. Lastly, analysis was conducted for horizontally-aligned walls. The reported expressions proved that the force distribution is proportional to the wall stiffness and it also depends on the vertical load. This behaviour was experimentally observed by means a full scale test. The use of the UNITN Model for building with more than one-storey is under investigation by the authors and it will be presented in a future paper.

Acknowledgment

The presented research has been carried out in the framework of the ReLUIS-DPC 2015 project. Support from the ReLUIS-DPC network, the Italian University Network of Seismic Engineering Laboratories and Italian Civil Protection Agency, is gratefully acknowledged. Authors would also to thanks Prof. M. Piazza for his precious technical suggestions.

Nomenclature

α	Geometrical parameter of sheathing panel for Timber-Frame walls
β	Stiffness parameter related to the sheathing to framing connection deformation
χ	Panel shear factor
Δ	Elastic horizontal displacement
δ	Stiffness parameter related to the rigid body rotation
Δ_N	Horizontal wall displacement due to the vertical load
Δ_a	Rigid-body translation horizontal displacement
Δ_h	Rigid-body rotation horizontal displacement
Δ_p	Sheathing-panel horizontal displacement
Δ_{sh}	Sheathing-to-framing connection horizontal displacement
η	Dimensionless parameter needed for the determination of λ
γ	Angle of rigid rotation
λ	Shape function related to the wall horizontal displacement do to the sheathing-to-framing connection deformation
ω	Ratio between the wall stiffness of the second regime $K_{tot,nt}$ and the wall length l
Φ	Dimensionless parameter related to hold-down and sheathing-to-framing connections
τ	Hold-downs dimensionless internal lever arm
$\tilde{K_{tot}}$	Dimensionless horizontal stiffness of the wall

$\tilde{l}$	Dimensionless length of the wall
φ	Stiffness parameter related to the rigid body translation
ϑ	Stiffness parameter related to the sheathing panel shear deformation
ξ	Dimensionless parameter needed for the determination of λ
ζ	Panel shear strain
A_p	Shear area of the sheathing panel
b	Sheathing panel width
CLT	Cross Laminated timber wall
F	Horizontal force applied on the shear-wall
F_N	Equivalent horizontal force due to the vertical load
F_q	Minimum horizontal force which activates the hold-downs
F_{el}	Horizontal elastic force
G_p	Sheathing panel Shear modulus
G_{CLT}	CLT panel shear modulus
h	Height of the shear-wall
i_a	Angle brackets or screws spacing
k_a	Angle bracket stiffness
k_c	Sheathing-to-framing fastener stiffness
k_h	Hold-down stiffness
K_A	Rigid body translation stiffness
K_H	Rigid body rotation stiffness

K_P Sheathing panel shear stiffness

K_{SH} Sheathing-to-framing connection stiffness

K_{SP} Stiffness of the internal horizontal spring in the simplified model of the wall

$K_{tot,nt}$ Wall stiffness for the first regime

K_{tot} Wall stiffness for the second regime

l Length of the shear-wall

N Half part of the resulting vertical load

n number of sheathing-to-framing fasteners

n_a Angle-brackets or screws number

n_{bs} Number of braced sides of the wall (1 or 2)

q Vertical distributed load

s_c Sheathing-to-framing fastener spacing

s_p Spacing of fastener along the top and bottom plates of Timber-Frame walls

s_{is} Spacing of timber-frame fasteners along the inner studs

s_{ps} Spacing of timber-frame fasteners along the perimeter stud

T_i Hold-down tensile force

t_p Sheathing panel thickness

t_{CLT} CLT panel thickness

TF Timber-frame wall

v Hold-down elongation

x_i Horizontal coordinate of timber-frame fasteners

y_i Vertical coordinate of timber-frame fasteners

7. References

[1] Sartori, T., Piazza, M., Tomasi, R., Grossi, P.. Characterization of the mechanical behaviour of light-frame timber shear walls through full-scale tests. In: World Conference on Timber Engineering 2012, WCTE 2012; vol. 3. 2012, p. 180–188.

[2] Pardoen, G.C.. Testing and analysis of one-story and two-story shear walls under cyclic loading. Consortium of Universities for Research in Earthquake Engineering; 2003.

[3] Vogt, T., Hummel, J., Seim, W.. Timber framed wall elements under cyclic loading. World 2012;15:19.

[4] Tomasi, R., Sartori, T.. Mechanical behaviour of connections between wood framed shear walls and foundations under monotonic and cyclic load. Construction and Building Materials 2013;44:682–690.

[5] Fonseca, F.S., Rose, S.K., Campbell, S.H.. Nail, Wood Screw, and Staple Fastener Connections W-16. 2002.

[6] Salenikovich, A.J.. The racking performance of lightframe shear walls. Ph.D. thesis; Wood Science and Forest Products, Virginia Polytechnic Institute and State University, VA; 2000.

[7] Conte, A., Piazza, M., Sartori, T., Tomasi, R.. Influence of sheathing to framing connections on mechanical properties of wood framed shear walls. In: Congresso Ingegneria Sismica Anidis. 2011,.

[8] Ehlbeck, J., Kreuzinger, H., Steck, G., Blaß, H.J.. DIN 1052 Erläuterungen. Bruderverlag; 2005. ISBN 9783871041464.

[9] NZS 3603, . Timber Structures Standard. 1993. NZS, Wellington, New Zealand.

[10] CSA 086-01:2005, . Engineering design in wood. 2005. CSA, Canadian Standard Association, Toronto, Canada.

[11] Källsner, B., Girhammar, U.. Analysis of fully anchored light-frame timber shear walls-elastic model. Materials and Structures 2009;42:301–320. doi:10.1617/s11527-008-9463-x. URL http://dx.doi.org/10.1617/s11527-008-9463-x.

[12] Sartori, T., Tomasi, R.. Experimental investigation on sheathing-to-framing connections in wood shear walls. Engineering Structures 2013;56:21972205.

[13] Grossi, P., Sartori, T., Tomasi, R.. Tests on timber frame walls under in-plane forces: Part 1. Proceedings of the Institution of Civil Engineers-Structures and Buildings 2014;Special Issue on Seismic Test on Timber Buildings:xx.

[14] Grossi, P., Sartori, T., Tomasi, R.. Tests on timber frame walls under in-plane forces: Part 2. Proceedings of the Institution of Civil Engineers-Structures and Buildings 2014;Special Issue on Seismic Test on Timber Buildings:xx.

[15] Sustersic, I., Dujic, B.. Simplified cross-laminated timber wall modelling for linear-elastic seismic analysis. In: CIB-W18 Timber Structures. August 2012,.

[16] Joebstl, R., Bogensperger, T., Schickhofer, G.. In-plane shear strength of cross laminated timber. In: 41st CIB-Meeting, St. Andrews, Canada (August 2008). 2008,.

[17] Tomasi, R.. Seismic behavior of connections for buildings in clt. In: Proceeding CLT conference Graz. 2013,.

[18] Casagrande, D., Rossi, S., Sartori, T., Tomasi, R.. Analytical and

numerical analysis of timber framed shear walls. In: World Conference on Timber Engineering 2012, WCTE 2012; vol. 5. 2012, p. 497–503.

[19] EN 594:2011, . EN 594:2011 Timber structures - Test methods - Racking strength and stiffness of timber frame wall panels. 2011. CEN, European Committee for Standardization, Brussel, Belgium.

[20] Andreolli, M., Grossi, P., Sartori, T., Tomasi, R.. Design and production of an heavy timber reaction frame for a laboratory test set-up. In: ICSA 2013. 2013,.

Chapter 3

Iterative approaches for the seismic elastic analysis of light timber-frame multi-storey buildings

3.1 Introduction

The *Response Spectrum Analysis* [RSA], according to Eurocode 8, shall be used to design non regular buildings in elevation. It also should be considered the reference design method for the seismic design of buildings because it can be adopted to each type of buildings without any limitation. The results got by using this method can be considered more reliable compared to those given by the *Linear Force Method* [LFM]; in fact, they are determined considering all the significant modes of vibration. Anyway, despite the use of timber buildings is nowadays more and more frequent, the diffuse-application of the RSA to these building is still missing mainly because a definitive and dependable procedure to analyze them has not been developed yet.

With the purpose of developing a reliable analytical procedure to apply the RSA to light timber-frame buildings, in the following Section an iterative method to properly distribute a horizontal load to the shear-walls, taking into consideration of both the vertical load effects and the stiffness of the building, is presented. Three different procedures to apply the RSA are also proposed; the procedures are iterative and allow to properly consider the hold-down ON-OFF behaviour.

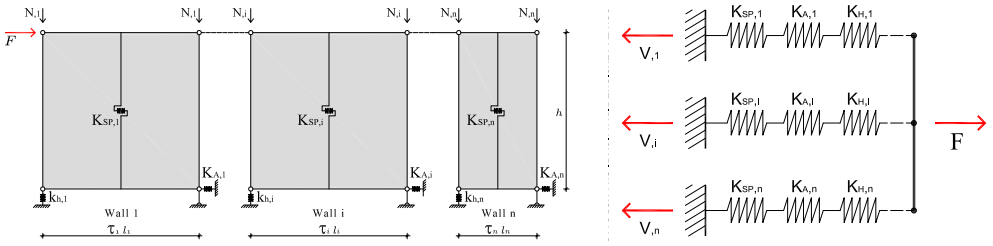

(a) Numerical $1 \times n$ model, (b) Rheological model,

Figure 3.1: *System of* $1 \times n$ *walls modelling a one-storey building.*

All the methods presented are based on the use of the UniTN-Model, previously introduced (see Ch. 2), which is here extended to coupled walls and more complex systems. In detail, the analysis of several horizontally-aligned walls, modeling one-storey buildings, is initially considered. From the rheological point of view, a system of horizontally-aligned walls can be regarded as a system of springs placed in parallel. In fact, the presence of the upper floor, which performs a rigid-diaphragm behaviour, imposes to the walls the same horizontal-displacement.

From the analytical point of view, this kind of systems can be analised by imposing the equilibrium, the compatibility and the constitutive lows. The equilibrium is given by:

$$F = \sum_{i=1}^{n} F_i \tag{3.1}$$

the constitutive law is represented by the following equations:

$$F_i = K_{tot,i} \cdot (\Delta_i + \Delta_{N,i}) \tag{3.2}$$

whereas the compatibility is provided by:

$$\Delta = \Delta_i \rightarrow for\ 1 \in [1; n] \tag{3.3}$$

By substituting Eq. 3.2 in Eq. 3.1 it is possible to get:

$$F = \sum_{i=1}^{n} K_{tot,i} \cdot (\Delta_i + \Delta_{N,i}) \tag{3.4}$$

which can be rearranged in:

$$F = \sum_{i=1}^{n} K_{tot,i} \cdot \Delta_i + \sum_{i=1}^{n} K_{tot,i} \cdot \Delta_{N,i} \tag{3.5}$$

from which it is possible to determine the horizontal displacement of the system Δ using Eq. 3.3:

$$\Delta = \frac{F - \sum_{i=1}^{n} K_{tot,i} \cdot \Delta_{N,i}}{\sum_{i=1}^{n} K_{tot,i}} \tag{3.6}$$

Using Eq.3.6 to rewriting Eq.3.2, it is possible to determine the shear-force carried by each wall:

$$F_i = K_{tot,i} \cdot \left(\frac{F - \sum_{i=1}^{n} K_{tot,i} \cdot \Delta_{N,i}}{\sum_{i=1}^{n} K_{tot,i}} + \Delta_{N,i} \right) \tag{3.7}$$

The analysis of these equations highlights the fact that a horizontal force F is distributed to the walls of the system proportionally the their stiffness, which in turns is proportional to its squared length. It is also worth noting that the vertical load affects this force-distribution through the quantity $\Delta_{N,i}$, which is the equivalent horizontal displacement produced by the vertical load itself.

It is therefore possible to state that the common procedure to distribute the vertical load in a linearly-proportional manner to the wall-length (see Eq.3.8) is not correct nor safe and it could lead to significant design errors.

$$F_i = \frac{F \cdot l_i}{\sum_{i=1}^{n} l_i} \tag{3.8}$$

The analysis is then extended to multi-storey walls. This part of the research represents a fundamental step for the study of the behaviour of these timber-building. In fact, light frame buildings can be be considered as shear-walls buildings (see Fig. 3.2).

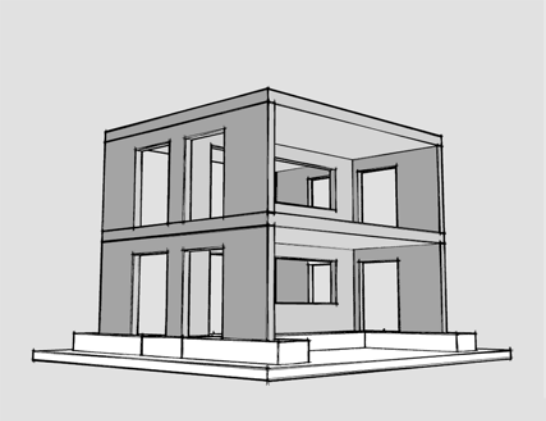

Figure 3.2: *Shear walls building.*

From the rheological point of view a m-storey shear-wall can be considered as a system of m-springs placed in series, and therefore it can be modeled by means of the superimposition of m-UniTn models (see Fig. 3.3) connected each other thanks to a spring of stiffness $k_{h,i}$ representing the hold-down, a spring of stiffness $K_{A,i}$ modeling the shear connections (angle-brackets or screws) and also a pinned rigid beam placed in the compression corner of the wall. The use of a pinned rigid beam allows to consider the action of the lower floor which offers a compression support avoiding the lowering but allowing the mutual horizontal displacement between the walls.

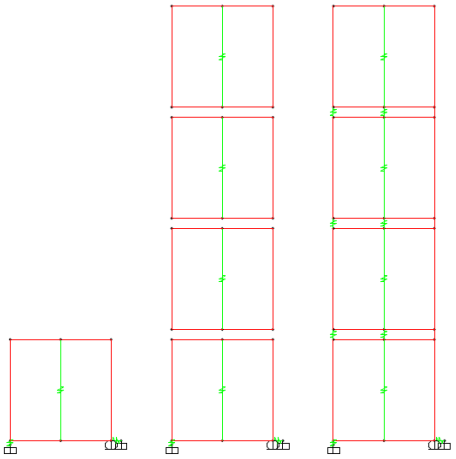

Figure 3.3: *System of $m \times 1$ walls modelling a multi-storey wall.*

It can be immediately noted that it is not possible to know in advance the regime of the j-th hold-down, namely it is not possible to know if it will be in tension or in compression. In the same way, the position of the tension corner (in which the hold-down spring shall be placed) can not be known a priori. The need of an iterative approach is therefore evident.

The horizontal displacement of the j-th storey, as for the single wall, can be determined by adding the main deformation contributions. Anyway, in the case of multi-storey walls it is necessary to consider the sum of all the deformation contributions of each wall. In fact, all the base components placed below the horizontal force undergo deformation:

$$\Delta_{j,\xi} = \sum_{r=1}^{min(j,\xi)} F_\xi \cdot \left[\frac{1}{K_{SP,r}} + \frac{1}{K_{A,r}}\right] + \sum_{r=1}^{min(j,\xi)} \left[\left(F_\xi \cdot \frac{z_\xi - z_{r-1}}{\tau \cdot l} - \frac{M_r}{|M_r|} \sum_{y=r}^{m} N_y\right) \cdot \frac{z_j - z_{r-1}}{k_{h,r} \cdot \tau \cdot l}\right] \tag{3.9}$$

Eq. 3.9 has two main parts: the first-one accounts for the sheathing-to-framing and angle-brackets contributions, which produce a constant displacement at each storey; the second part instead accounts for the hold-down deformation contribution which produces an increasingly large displacement at each storey. In the second part of Eq.3.9 there is also a dimensionless quantity $\frac{M_r}{|M_r|}$

needed to take into account of the vertical load effects, which corresponds to correctly place the hold-downs in the tension corners.

The convention used in the analyses (see Fig. 3.4) is to consider the hold-down contribution as positive when the tension corner is the left-corner (in this case the vertical load produces a negative displacement), whereas the contribution is negative when the tension corner is the right-one (in this case the vertical load produces a positive displacement).

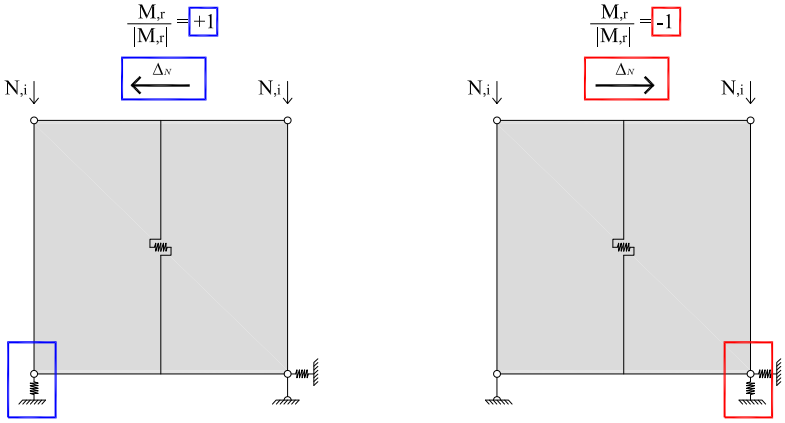

Figure 3.4: *Effect of the dimensionless quantity* $\frac{M_r}{|M_r|}$

An other fundamental aspect to be considered is the deformation contribution of the hold-downs; in fact, for multi-storey walls it becomes more and more important with the increase of the storey number. Considering a multi-storey wall, loaded by a horizontal force at the top floor, it is easy to note that the rigid-rotation of the walls (produced by the hold-downs elongation) increases at each storey due to the fact that the rotation of the j-th storey is added to the rotation of lower wall, see Fig. 3.5.

In order to better explain this aspect, let's consider a three-storey shear-wall, which mechanical and geometric features are shown in Tab. 3.1.

Due to the fact that the force pattern is composed by a force placed at

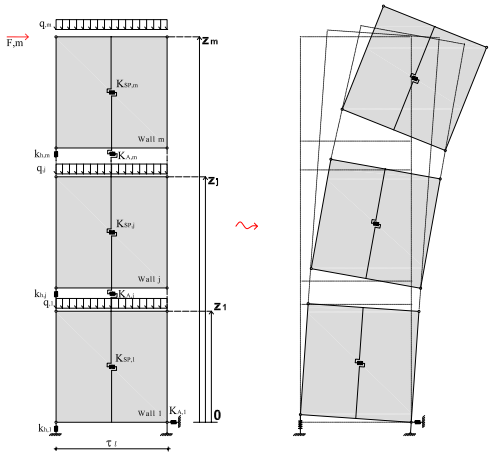

Figure 3.5: *Horizontal displacement for a system of* $m \times 1$ *walls.*

	Storey 1	Storey 2	Storey 3
length l $[mm]$	2500	2500	2500
height h $[mm]$	2500	2500	2500
storey heights z $[mm]$	2500	5000	7500
vertical load q $[kN/m]$	7.5	7.5	5
horizontal applied force F $[kN]$	10	12	15
number of braced sides n_{bs}	2	2	2
sheathing panel shear modulus G_p $[N/mm]$	1000	1000	1000
sheathing panel thickness t_p $[mm]$	15	15	15
sheathing panel breadth b $[mm]$	1250	1250	1250
fasteners stiffness k_c $[N/mm]$	500	500	500
fasteners spacing s_c $[mm]$	100	125	150
hold-downs stiffness k_h $[N/mm]$	7000	3500	3500
angle-brackets stiffness k_a $[N/mm]$	3000	3000	3000
angle-brackets number n_a	4	3	2

Table 3.1: *Example* 3×1*, Geometrical and mechanical properties of the walls.*

each storey, the Eq. 3.9 has to be used three-times to assess the deformation produced by all the forces.

The displacements produced by the horizontal force applied at the first-

storey F_1 are:

$$\begin{cases} \Delta_{1,1}[mm] = 2.14 + 0.83 + 1.43 \\ \Delta_{2,1}[mm] = 2.14 + 0.83 + 2.86 \\ \Delta_{3,1}[mm] = 2.14 + 0.83 + 4.92 \end{cases} \tag{3.10}$$

The displacements produced by the horizontal force applied at the second-storey F_2 are:

$$\begin{cases} \Delta_{1,2}[mm] = 2.57 + 0.83 + 3.43 \\ \Delta_{2,2}[mm] = 5.76 + 2.33 + 10.29 \\ \Delta_{3,2}[mm] = 5.76 + 2.33 + 17.14 \end{cases} \tag{3.11}$$

The displacements produced by the horizontal force applied at the third-storey F_3 are:

$$\begin{cases} \Delta_{1,3}[mm] = 3.21 + 1.25 + 6.43 \\ \Delta_{2,3}[mm] = 7.10 + 2.92 + 21.43 \\ \Delta_{3,3}[mm] = 11.67 + 5.42 + 40.71 \end{cases} \tag{3.12}$$

In the Equations 3.10, 3.11, 3.12, the three terms represent the sheathing-to-framing, the rigid-body translation and the rigid-body ration deformation contributions respectively. The total horizontal displacement at each storey (reduced by the effects of the vertical load) and the axial force in the hold-down are resumed in Tab. 3.2.

	Storey 1	**Storey 2**	**Storey 3**
Horizontal displacement Δ_j $[mm]$	18.7	44.0	68.8
Hold-down tensile force $T_{HD,j}$ $[kN]$	54	26.38	8.75

Table 3.2: *Results obtained from the model.*

The percentage of deformation due to each deformation contribution is reported in the chart of Fig. 3.6. The rigid body translation remains almost constant, the same consideration is valid for the sheathing board deforma-

tion whereas the sheathing-to-framing percentage of deformation decreases storey by storey. On the contrary, it is clear how the rigid body rotation contribution increases with each story up to over the 60% on the top floor, confirming what exposed previously.

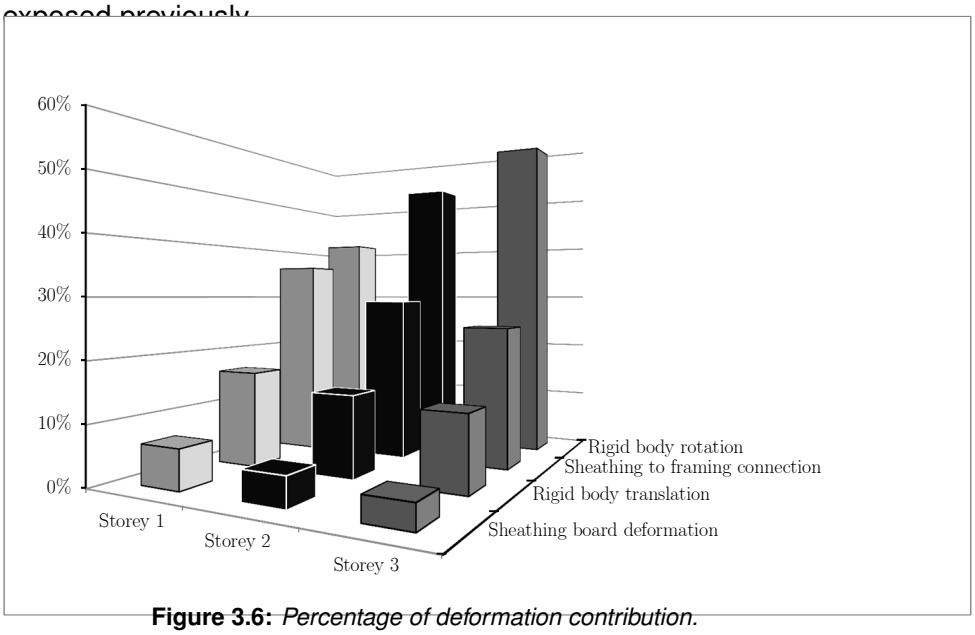

Figure 3.6: *Percentage of deformation contribution.*

It is worth noting that the computational effort required in order to apply the procedure increases with the dimensions of the system considered, the use of a matrix formulation is preferable:

$$\boldsymbol{\Delta} = \tilde{\boldsymbol{U}}\, \boldsymbol{F} - \boldsymbol{\Delta_N} \tag{3.13}$$

The displacement expression of Eq. 3.9 can be conveniently used to evaluate the elements of the flexibility matrix of a multi-storey shear-wall:

$$\tilde{U}_{j,\xi} = \sum_{r=1}^{min(j,\xi)} \frac{1}{K_{SP,r}} + \frac{1}{K_{A,r}} + \frac{(z_\xi - z_{r-1}) \cdot (z_j - z_{r-1})}{k_{h,r} \cdot (\tau \cdot l)^2} \tag{3.14}$$

Known the flexibility matrix, the stiffness matrix can be immediately deter-

mined by inverting it:.

$$\boldsymbol{K} = \boldsymbol{U}^{-1} \tag{3.15}$$

The stiffness matrix allows to develop an iterative procedure suitable to apply the LFM to timber shear-wall buildings. This procedure (see Fig.3.7) is composed by two different levels of iteration: the first-one is needed to check the correct position of the hold-downs (which have to be placed in the tension corner), whereas the second level of iteration is required to check the consistency of the results of the procedure with the boundary conditions adopted.

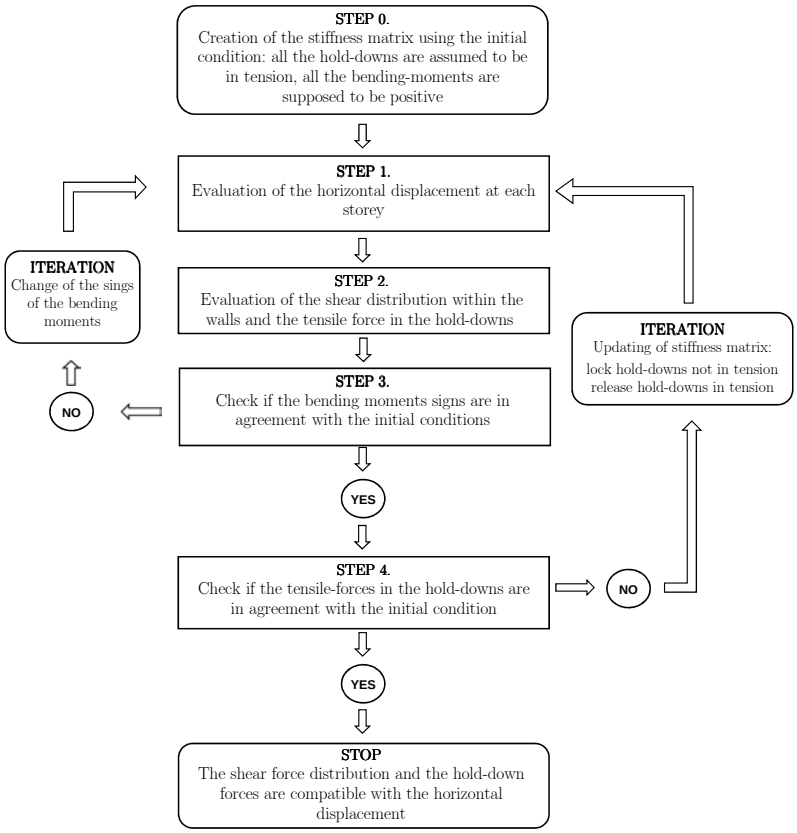

Figure 3.7: *Flow-chart for the iteration.*

This iterative method can be used to analyse both two-dimensional and three-dimensional buildings, see Fig. 3.8. Analysis of several three-dimensional buildings have been already performed in order to validate and to check the convergence of the method. Because of 3-Dimension buildings are much more complex from the geometric point of view compared to two-dimensional systems, a higher number of iterations is required to get the results. It has to be remarked that the number of iterations changes by changing the boundary conditions assumed in the first step of the analysis.

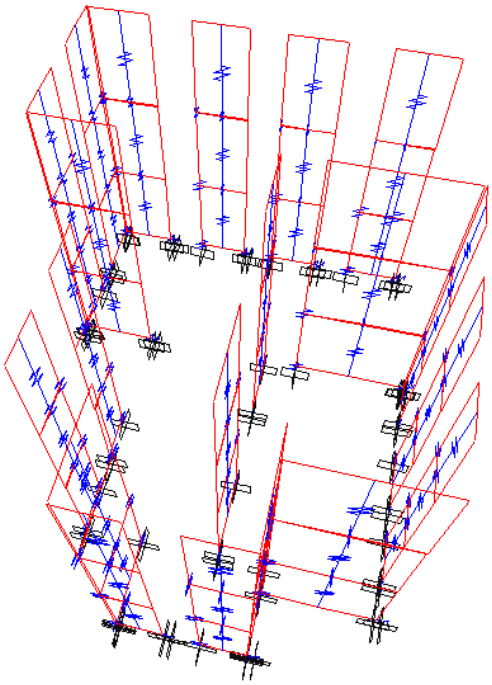

Figure 3.8: *3-D model of a building.*

According to the Eurocode 8, buildings not regular in elevation shall designed taking into consideration all the significant modes of vibration and not only the first-one as performed by LFM; this means that these buildings must be designed using the RSA.

The use of the RSA method to design timber buildings is not however easy

to apply. In fact, the magnitude of the seismic force to be used in the design is dependent on the vibration period of the structure, which in turns is dependent on the stiffness of the building. However, light timber-frame buildings, as stated before, display a variable stiffness depending on the regime of the hold-downs, which can be in tension or not depending on the magnitude of the seismic force. The recursive nature of the RSA for these building is therefore clear and it is effectively represented by Fig.3.9.

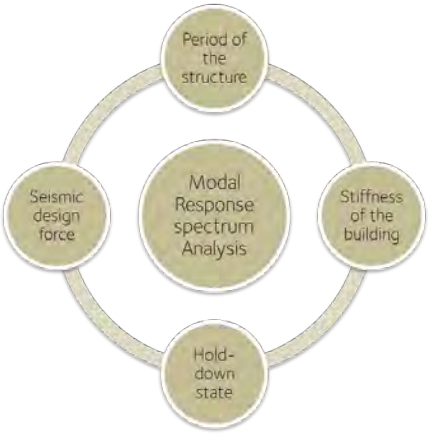

Figure 3.9: *Recursive nature of the RSA for timber buildings*

With the purpose of developing a suitable and reliable analytical procedure for the correct application of the RSA to timber buildings, namely taking into consideration both the changing of the stiffness due to the hold-downs state and vertical load effects, three iterative methods are proposed:

- VNA: Vertical Load Not Applied;
- VTM: Vertical Load to Main mode;
- CAN: Complete Numerical Analytical.

The methods differ in the way in which the vertical loads is considered. The VNA is the fasted method but at the same time it is the less accurate, in fact it considers the effects of the vertical load only as reduction of the tensile

force acting in the hold-down. The VTM method considers instead the vertical load both during the modal analysis and as reduction of the tensile force; the CNA-method can be considered the most rigorous-one but it requires an high computational effort.

The three methods give comparable results in terms of bending-moments, shear forces and tensile forces in the hold-down; the differences between the values increase with the increasing of the building dimensions and with the changing of the vertical load magnitude.

3.2 Appended Paper II

Seismic elastic analysis of light timber-frame multi-storey buildings: proposal of an iterative approach

Simone Rossi, Daniele Casagrande, Roberto Tomasi, Maurizio Piazza

Construction and Building Materials, Elsevier (2015);

doi:10.1016/j.conbuildmat.2015.09.037

Seismic elastic analysis of light timber-frame multi-storey buildings: proposal of an iterative approach

Simone Rossi[1,*], Daniele Casagrande[2], Roberto Tomasi[3], Maurizio Piazza[4]

Department of Civil, Environmental and Mechanical Engineering, University of Trento, Italy, Tel. +39 0461 282529

Abstract

This paper deals with the static and dynamic seismic analysis of light timber-frame buildings. Through the use of the UNITN-model proposed in a previous work, the study is here extended to full-scale buildings. An iterative procedure to properly distribute a horizontal load to the shear-walls, considering the coupled action of the vertical-load and the hold-downs state, is developed; three methods for the application of the response spectrum analysis are proposed as well. These methods may be used to predict the seismic-behaviour and to design non-regular timber shear-walls buildings. A numerical example illustrates the application of the procedures.

Keywords:
Light timber-frame buildings, Seismic analysis, Horizontal displacement, Response spectrum analysis, UNITN model

*Corresponding Author
Email address: simone.rossi1@unitn.it (Simone Rossi)
[1]Civil Engineer, Ph.D. Candidate
[2]Civil Engineer, Ph.D., Assistant Researcher
[3]Civil Engineer, Ph.D., Assistant Professor
[4]Civil Engineer, Professor

1. Introduction

In Europe, timber buildings are traditionally more widespread in northern countries (e.g. Sweden, Norway, Finland etc.) as well as in Germany and Austria. The fact that the seismic activity in these areas is not particularly intense has led to a not fully-developed awareness about the potentialities of timber wall buildings in terms of seismic response. Research undertaken in last decades have highlighted these potentialities ([1], [2], [3], [4]-[5] and [6]), so that timber building are becoming widespread even in south Europe and in Central America, where earthquakes are more frequent and damaging. For this reason it is necessary to deepen the knowledge of the dynamic behaviour of timber buildings; in fact, both standard requirements and method of analysis are still poorly developed. Some useful researches have been done, see [7], [8] and [9], but they are mainly focused on case-study buildings and based on the use of finite-element analysis, therefore analytical models as well as numerical procedures and practical tools for designer are needed.

This paper is based on a previous work [10] focused on the elastic analysis of one-storey timber shear-walls, both Light-Timber frame walls (TF) and Cross Laminated Timber walls (CLT). In that work an analytical procedure and a simplified numerical model (called UNITN model) were proposed to asses the elastic-horizontal behaviour of single-storey buildings.

The objective of the paper is to develop a correct procedure to apply the *linear lateral force method* (LFM) and a suitable procedure in order to give an answer to the open technical problem of the application of the *response spectrum analysis* (RSA) for multi-storey light-timber frame buildings. In fact, nowadays, LFM is mainly used by designers because a definitive procedure to extend the analytical modal analysis to timber wall building is still missing. The implementation of the common LFM could lead to analysis errors because it is suitable for buildings which behaviour can be mainly attributed to the first modal shape (i.e. regular buildings in elevation, [11]).

In the first part of the paper, a procedure to evaluate the horizontal de-

formation of one timber shear-wall composed by m storeys (system of $m \times 1$ walls) is presented. The analysis is then extended to a more complex system composed of n timber shear-walls of m storeys (system of $m \times n$ walls), which reproduces a full-scale building. Both the procedures are iterative due to the presence of the hold-downs (i.e. the connection devices which prevent the uplift of the wall), which is responsible of a geometrical and mechanical non-linear behaviour. The hold-down action in fact, should be taken into account only when the overturning moment produced by a horizontal force exceeds the stabilizing moment due to the vertical load [12].

In the second part of the paper, the system of $m \times n$ walls is further developed; a procedure to asses the dynamic properties of a timber building (e.g. natural frequencies, mode-shapes, participating masses) is presented. Three methods to apply the RSA are also proposed. The procedures, better explained in section 4.2, differ in the way they consider the vertical load effects; in fact, the vertical load affects both the stiffness-matrix of the building and the shear-force distribution between the walls.

2. Mechanical behaviour of a single-storey timber shear-wall

This section gives a brief overview of [10] about the seismic elastic behaviour of a single storey timber shear-wall; reference is made thereto for a detailed discussion.

2.1. Analytical formula

The elastic displacement Δ_C of a TF shear-wall subjected to a horizontal external force F, see Fig. 1 (a), can be evaluated using the equation 1, which considers the four main deformation contributions, namely the sheeting to framing connection, the rigid body rotation, the rigid-body translation and the sheathing-boards respectively.

$$\Delta_C = \begin{cases} \frac{\lambda \cdot F \cdot s_c}{l \cdot n_{bs} \cdot k_c} + \frac{F \cdot i_a}{k_a \cdot l} + \frac{F \cdot h}{l \cdot G_p \cdot n_{bs} \cdot t_p} & \text{when} \quad F \cdot h \leq \frac{q \cdot l^2}{2} \\ \frac{\lambda \cdot F \cdot s_c}{l \cdot n_{bs} \cdot k_c} + \left[\frac{h}{\tau \cdot l \cdot k_h} \cdot \left(\frac{F \cdot h}{\tau \cdot l} - \frac{q \cdot l}{2} \right) \right] + \frac{F \cdot i_a}{k_a \cdot l} + \frac{F \cdot h}{l \cdot G_p \cdot n_{bs} \cdot t_p} & \text{when} \quad F \cdot h > \frac{q \cdot l^2}{2} \end{cases} \tag{1}$$

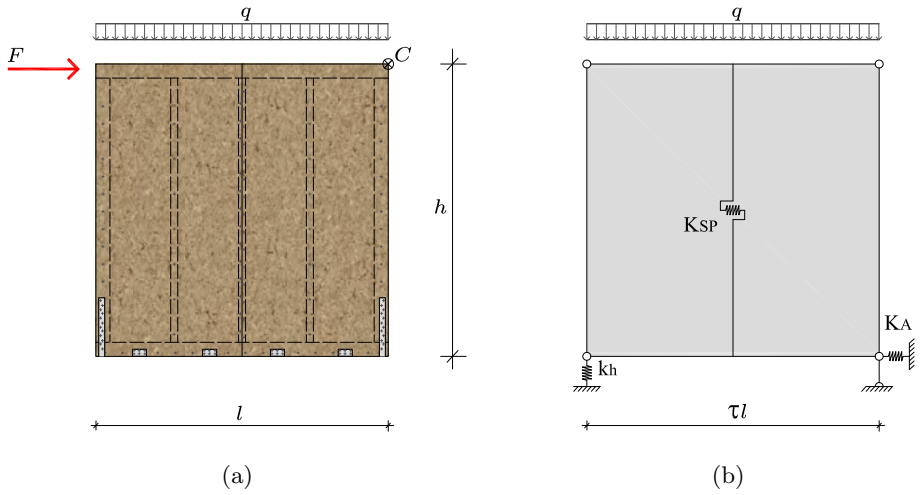

Fig. 1: Timber shear-wall: (a) configuration and load pattern; (b) UNITN simplified model

where:

- F: is the applied horizontal force;
- s_c: is the fasteners spacing;
- l: is the wall length;
- b: is the breadth of the sheathing-panel;
- λ: is a parameter related to the sheathing-panel dimensions;
- k_h: is the hold-down stiffness;
- q: is the vertical distributed load;
- k_a: is the angle-brackets (or screws) stiffness;
- i_a: is the angle-brackets (or screws) spacing;
- G_p: is the shear modulus of the sheathing panels;
- t_p: is the sheathing panel thickness.
- h: is the height of the panel;
- k_c: is the fasteners stiffness;
- n_{bs}: is the number of braced sides of the wall;
- τ: is a number accounting for the distance between the hold-downs, typically $\in [0.9; 1]$;

Other contributions (as frame deformation, bending deflection, ect.) could be taken into account, but for the wall typologies most used in south Europe, these contributions are negligible compared to the other. For more details see [10], [13] and [14].

2.2. Simplified numerical model

The behaviour of a timber wall can be faithfully reproduced by means of complex finite element models (see [15], [2] and [16]). These models are mainly useful for researchers but, requiring a high-number of parameters as well a high processing time, they are rarely used by engineers in common practice.

These models are developed by researchers because in order to reproduce properly the behaviour of a single wall, they require a high-number of parameters as well a high processing time. This leads to the consequence that complex finite element models are rarely used by engineers in common practice.

For this reason, a simplified numerical model, called UNITN model, was developed in [10], see Fig. 1 (b). The UNITN model is simplified because it reproduces the behaviour of a timber wall by means of three linear-elastic springs placed in series; each spring has a stiffness related to the corresponding deformation contribution, namely the hold-down, the angle brackets and the coupled action of the sheathing-panels with the fasteners:

$$\frac{1}{K_{SP}} = \frac{1}{K_P} + \frac{1}{K_{SH}} = \frac{h}{G_p \cdot n_{bs} \cdot t_p \cdot l} + \frac{s_c \cdot \lambda}{n_{bs} \cdot k_c \cdot l} \tag{2}$$

$$\frac{1}{K_A} = \frac{i_a}{k_a \cdot l} \tag{3}$$

$$\frac{1}{K_H} = \frac{h^2}{k_h \cdot (\tau \cdot l)^2} \tag{4}$$

Considering equation 4, it is evident that when the hold-down is in tension the behaviour of the wall is not linearly-proportional to the wall length, indeed the wall stiffness depends on the squared length. Furthermore, it is important to remark that when the hold-down is in tension, the horizontal displacement of a timber wall is reduced by the vertical load:

$$\Delta = \frac{F}{K_{tot}} - \Delta_N \tag{5}$$

where K_{tot} is the global stiffness of a TF wall:

$$K_{tot} = \left(\frac{1}{K_{SP}} + \frac{1}{K_A} + \frac{1}{K_H} \right)^{-1} \tag{6}$$

and Δ_N is the equivalent horizontal force produced by the vertical load (which counteracts the horizontal external force):

$$\Delta_N = \frac{q \cdot l/2 \cdot h}{\tau \cdot l \cdot k_h} = \frac{N \cdot h}{\tau \cdot l \cdot k_h} \tag{7}$$

3. Elastic linear behaviour of a of $m \times n$ walls

This section illustrates the behaviour of a system of $m \times n$ walls, namely the model of a full-scale building (see Fig. 2). Firstly, a series of horizontally-aligned walls (system of $1 \times n$ walls) is analyzed and then a system of vertically-aligned walls (system of $m \times 1$ walls) is studied. These two cases allow to develop a method suitable to analyze a full-scale building subjected to the simultaneous action of a horizontal and a vertical load.

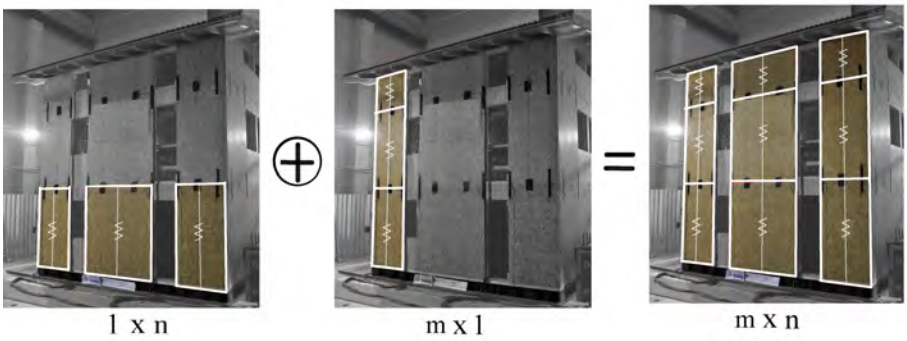

Fig. 2: Timber shear-walls building modelled by-means of a system of $m \times n$ elements

3.1. Modelling of horizontally-aligned walls (system of $1 \times n$ walls)

As deeply explained in [10], a system of several horizontally-aligned walls, i.e. a system of $1 \times n$ walls modelling a single-storey building (see Fig. 3 (a)), is obtained by connecting each wall-model to the next one by means of

a infinite rigid pinned-beam. This pinned-beam simulates the effects of the upper floor/roof (diaphragms are assumed to be rigid, namely they do not undergo any deformation during earthquake), which imposes to the walls the same horizontal displacement. Therefore, the horizontal force acting on the building is supported by all the walls, which can be regarded as a system of springs in parallel (see Fig. 3 (b)).

The horizontal displacement Δ of the system of $1 \times n$, as well as the horizontal force carried-out by each wall F_i, can be assessed by the two following equations (equations 8 and 9 were determined using the compatibility as well as the constitutive and equilibrium laws):

$$\Delta = \frac{F - \sum_{i=1}^{n} (K_{tot,i} \cdot \Delta_{N,i})}{\sum_{i=1}^{n} K_{tot,i}} \tag{8}$$

$$F_i = V_i = \frac{K_{tot,i}}{\sum_{j=1}^{n} K_{tot,j}} \cdot \left[F - \sum_{j=1}^{n} [K_{tot,j} \cdot (\Delta_{N,j} - \Delta_{N,i})] \right] \tag{9}$$

it is important to note that for a one-storey building, the horizontal force carried-out by each wall is equal to the shear-force acting on it.

Equations 8 and 9 demonstrate that both the displacement and the shear-force distribution are influenced by the presence and the magnitude of the vertical load. Moreover, the presence of the vertical load leads to the need of adopting an iterative procedure. In fact, the stiffness of a wall depends on the hold-down state (i.e. hold-down in tension= active or hold-down in compression= not active) which, in turn, depends on the shear-force distribution.

3.2. Modelling of vertically-aligned walls (system of $m \times 1$ walls)

A system of vertically-aligned walls, modelling a timber shear-wall of m storey, can be obtained by means the superimposition of m single walls, see Fig. 4 (a). Each wall model is characterized by three springs which stiffness can be determined through the equations 2, 3 and 4. The wall uplifting corner is vertically connected to the lower wall by means of a spring with stiffness

equal to $k_{h,j}$, which models the j-th hold-down behaviour. In the other corner, instead, a pinned-axially-rigid beam is placed. This pinned beam is used to avoid the corner lowering but, at the same time, to allow a mutual translation between the walls connected by it. Moreover, a horizontal spring with a stiffness equal to $K_{A,j}$ reproduces the behaviour of the shear connection to the lower support (i.e. angle brackets or screws, as well as steel plates).

The rigid-rotation deformation becomes extremely relevant for a multi-storey shear-wall; in fact, the elongation of a hold-down produces an increasing horizontal displacement at each upper floor, because a multi-storey shear-wall

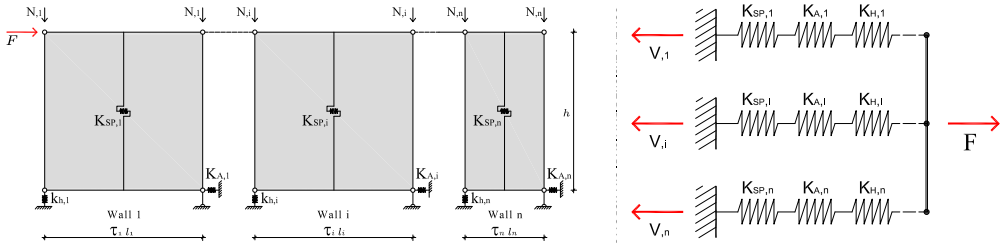

(a) Numerical $1 \times n$ model (b) Rheological model

Fig. 3: System of $1 \times n$ walls modelling a one-storey building

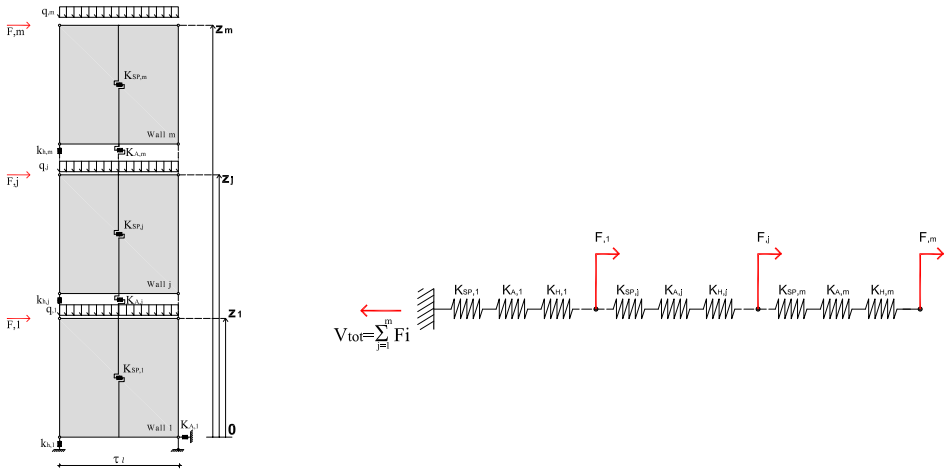

(a) Numerical $m \times 1$ model (b) Rheological model

Fig. 4: System of $m \times 1$ walls modelling a single-shear wall of m-storey

can be considered as a system of several springs placed in series, see Fig. 4 (b). Moreover, the non linear relationship between the wall length and its stiffness, as reported in equation 4, is directly related to the rigid-body rotation, which increases significantly for multi-storey walls.

Let's consider a system of $m \times 1$ walls loaded by a force F_1 placed at the first floor, see Fig. 5 (a), where, in order to properly asses the effect of the hold-downs deformation, the other deformation contributions can be neglected. It is evident that, because of the horizontal force is placed at the first floor, only the first hold-down undergoes deformation; this deformation corresponds to the hold-down spring $k_{h,1}$ elongation, which causes a rigid rotation γ of the whole system, that produces different horizontal displacements at the $j-th$ storey, see equation 10:

$$\Delta_{HD,j,1} = \gamma \cdot z_j = \frac{v}{\tau \cdot l} \cdot z_j = \frac{T_{h,1}}{k_{h,1}} \cdot \frac{z_j}{\tau \cdot l} = \frac{F_1 \cdot z_1}{k_{h,1} \cdot \tau \cdot l} \cdot \frac{z_j}{\tau \cdot l} \tag{10}$$

where:

- $\Delta_{HD,j,1}$: is the horizontal displacement at the $j-th$ storey, produced by the elongation of the hold-down of the first storey;
- z_j: is the height of the j-th storey;
- $T_{h,1}$: is the tensile force in the hold-down of the first storey;
- F_1: is the horizontal force placed at the first floor;
- v: elongation of the hold-down of the first floor.

The horizontal displacement of equation 10 is linearly proportional with the height of the floor, in fact, only the hold-down of the first floor produces a rotation. In the case of a system of $m \times 1$ walls loaded by a force F_ξ placed at the ξ_{th} floor (see Fig. 5 (b), where the force is placed at the top floor, i.e. $\xi = m$), all the hold-downs placed below the force undergo deformation and the horizontal displacement of the j-th floor ($\Delta_{HD,j}$) can be obtained as:

$$\Delta_{HD,j,\xi} = \sum_{r=1}^{min(j,\xi)} F_\xi \cdot \frac{(z_\xi - z_{r-1}) \cdot (z_j - z_{r-1})}{k_{h,r} \cdot (\tau \cdot l)^2} \tag{11}$$

where the displacement at a certain storey is produced by the deformation of all the hold-down placed at the underlying storeys.

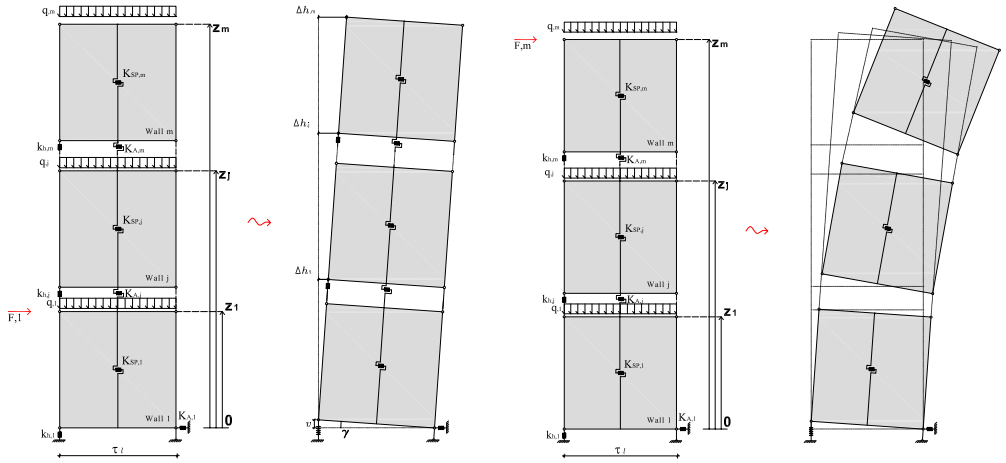

(a) Horizontal force at the 1-st floor (b) Horizontal force at the ξ-th floor

Fig. 5: Horizontal displacement for a system of $m \times 1$ walls

In the general case of a system of $m \times 1$ walls, considering all the deformation contributions and the vertical load, equation 11 can be developed to determine $\Delta_{j,\xi}$, which is the horizontal displacement of the j-th storey caused by a force placed at the ξ-th storey:

Equation 11 can be developed to determine $\Delta_{j,\xi}$, which is the horizontal displacement at the j-th storey of a system of $m \times 1$ walls loaded by force placed at the ξ-th storey considering all the deformation contributions as well as the vertical load:

$$\Delta_{j,\xi} = \sum_{r=1}^{min(j,\xi)} F_\xi \cdot \left[\frac{1}{K_{SP,r}} + \frac{1}{K_{A,r}}\right] + \sum_{r=1}^{min(j,\xi)} \left[\left(F_\xi \cdot \frac{z_\xi - z_{r-1}}{\tau \cdot l} - \frac{M_r}{|M_r|} \sum_{y=r}^{m} N_y\right) \cdot \frac{z_j - z_{r-1}}{k_{h,r} \cdot \tau \cdot l}\right] \tag{12}$$

Where N_y is the vertical concentrated load at the y-th floor:

$$N_y = \frac{q_y \cdot l}{2} \tag{13}$$

and where M_r is the bending moment acting at the r-th storey and the quantity $\frac{M_r}{|M_r|}$ is needed to give the correct sign to the equivalent displacement $\Delta_{N,j}$.

It is important to remark that when the vertical load at a certain storey exceeds the tensile force produced by the horizontal loads, the hold-down contribution at that level has to be removed from equation 12; in fact, when a hold-down is in compression, it does not undergo any deformation and it does not produce any horizontal displacement. In order to asses the magnitude of the tensile force in the hold-down the following equation can be used:

$$T_{HD,j} = \left| \sum_{r=j}^{m} \left[\frac{F_r \cdot (z_r - z_{j-1})}{\tau \cdot l} \right] \right| - N_j \tag{14}$$

where $T_{HD,j}$ is the tensile force in the hold-down of the $j-th$ storey. A positive value means tension whereas a negative value means compression. This allows to define two states: hold-down active when it is in tension, hold-down not active when it is in compression. Because a not-in-tension hold-down does not produce any deformation, its stiffness can be considered infinite.

The number of degrees of freedom increases with the building storey, and so a matrix formulation is needed. The equation 12 can be written in the following matrix form:

$$\boldsymbol{\Delta} = \tilde{\boldsymbol{U}}\ \boldsymbol{F} - \boldsymbol{\Delta_N} \tag{15}$$

where $\tilde{\boldsymbol{U}}$ is the flexibility matrix and $\boldsymbol{\Delta_N}$ is the displacement array due to the vertical load.

The j,ξ-element of the flexibility matrix can be obtained from:

$$\tilde{U}_{j,\xi} = \sum_{r=1}^{min(j,\xi)} \frac{1}{K_{SP,r}} + \frac{1}{K_{A,r}} + \frac{(z_\xi - z_{r-1}) \cdot (z_j - z_{r-1})}{k_{h,r} \cdot (\tau \cdot l)^2} \tag{16}$$

The j-element of the displacement array $\boldsymbol{\Delta_N}$ can be determined from:

$$\Delta_{N,j} = \sum_{r=1}^{j} \frac{M_r}{|M_r|} \left(\sum_{y=r}^{m} N_y \right) \cdot \frac{z_j - z_{r-1}}{k_{h,r} \cdot \tau \cdot l} \tag{17}$$

The bending moment M_r can be evaluated by means of the following equation:

$$M_r = \sum_{p=r}^{m} F_p \cdot (z_p - z_{r-1}) \tag{18}$$

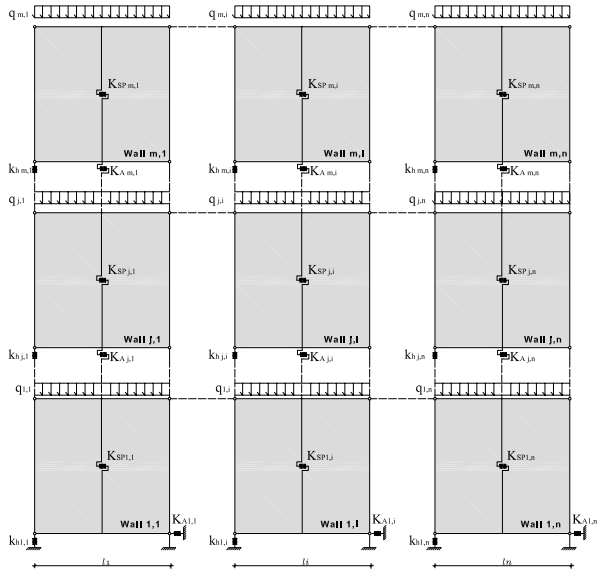

Fig. 6: System of $m \times n$ walls modelling a full-scale building

The equation 15 can be rearranged as:

$$\boldsymbol{F} = \tilde{\boldsymbol{U}}^{-1} \ (\boldsymbol{\Delta} + \boldsymbol{\Delta_N}) = \boldsymbol{K}\ \boldsymbol{\Delta} + \boldsymbol{K}\ \boldsymbol{\Delta_N} = \boldsymbol{K}\ \boldsymbol{\Delta} + \boldsymbol{F_N} \tag{19}$$

where the inverse of the flexibility matrix represents the stiffness matrix of one timber shear-wall of $m - storey$:

$$\boldsymbol{K} = \tilde{\boldsymbol{U}}^{-1} \tag{20}$$

and $\boldsymbol{F_N}$ is the array of the equivalent force due to the vertical load.

3.3. Modelling of a full scale building (system of $m \times n$ walls)

The two models $1 \times n$ and $m \times 1$ presented in sections 3.1 and 3.2 respectively, can be combined to modelling a system of $m \times n$ walls, representing a full scale building, see Fig. 6. According to the UNITN model, each wall is represented by means of three springs, $K_{SP,ji}$, $K_{A,ji}$ and $k_{h,ji}$, and each wall is properly connected to the upper, lower and side wall. Moreover, the load pattern is composed by the vertical loads $q_{j,i}$ and the horizontal force distribution F_j.

The constitutive law of a system of $m \times n$ walls, can be derived from 19 ad it is:

$$\boldsymbol{F} = \boldsymbol{K_{sys}}\ \boldsymbol{\Delta} + \boldsymbol{F_{N,sys}} \tag{21}$$

where K_{sys} is the stiffness matrix of the model of $m \times n$, and it is given by the sum of the stiffness matrices K_i (see equation 20) of each multi-story wall $m \times 1$:

$$\boldsymbol{K_{sys}} = \sum_{i=1}^{n} \boldsymbol{K_i} \tag{22}$$

and the array of the equivalent forces $F_{N,sys}$ due to the vertical load is equal to:

$$\boldsymbol{F_{N,sys}} = \sum_{i=1}^{n} \boldsymbol{K_i \Delta_{N,i}} \tag{23}$$

Generally, known the applied external force distribution $\boldsymbol{F}$ (e.g. wind or seismic loads), the horizontal displacement vector $\boldsymbol{\Delta}$ is given by:

$$\boldsymbol{\Delta} = \boldsymbol{K_{sys}^{-1}} \left(\boldsymbol{F} - \boldsymbol{F_{N,sys}}\right) \tag{24}$$

The external force array acting on the a multi-storey shear-wall $m \times 1$ can be determined by the following equation:

$$\boldsymbol{F_i} = \boldsymbol{K_i} \left(\boldsymbol{\Delta} + \boldsymbol{\Delta_{N,i}}\right) \tag{25}$$

the shear-force distributions, the bending-moments as well as the hold-down forces of the j, i-th shear-wall can be determined as:

$$V_{j,i} = \sum_{r=j}^{m} F_{r,i} \tag{26}$$

$$M_{j,i} = \sum_{r=j}^{m} F_{r,i} \cdot (z_r - z_{j-1}) \tag{27}$$

$$T_{HD,j,i} = \frac{|M_{j,i}|}{\tau \cdot l_i} - N_{j,i} \tag{28}$$

Anyway, the complexity of the analysis is not seated in the matrix formulation, but it is due to the non-linearity introduced by the binary behaviour of

the hold-downs. In fact, the state of the hold-downs (i.e. activation or not) depends on the shear-distribution; but this depends on the stiffness of the walls which depends in turn on the state of the hold-downs and so on. Moreover, for the evaluation of the equivalent horizontal displacement of each wall (see eq 17) the bending moment sign should be predetermined but this depends in turn on the force distribution.

Therefore, the problem shows a recursive nature and it requires an iterative procedure of solution. In detail, as shown in the flow-chart of Fig. 7, it is necessary to assume the model initial condition (i.e. state of the hold-downs), which allows to evaluate a first-attempt solution in terms of displacement, shear-distribution, bending moment sign and hold-downs stress. This solution is correct if the state of the hold-downs is consistent with the initial condition as well as with the calculation of equivalent horizontal displacement due to the vertical load; otherwise, it has to be rejected, the model has to be updated and the procedure has to be iterated up-to the achievement of the correct solution.

3.3.1. Practical example of a building composed by 3×2 *walls*

In order to explain the iteration procedure presented in section 3.3, it is applied here to a system of 3×2 walls, which mechanical and geometrical properties as well as the vertical loads are shown in Tab. 1. Despite the procedure can be used to analyze real three-dimensional buildings, a simplified bi-dimensional building is analyzed. In fact, the study of a 3D building would not have added any benefit; on the contrary, the seismic force distribution within the walls would be more complex due to the eccentricity between stiffness-center and center of mass.

The system is assumed to be loaded by the following set of external horizontal forces:

$$\mathbf{F} = \begin{bmatrix} 10 \\ 20 \\ -5 \end{bmatrix} [kN] \tag{29}$$

Diagramma per singola parete di taglio multipiano

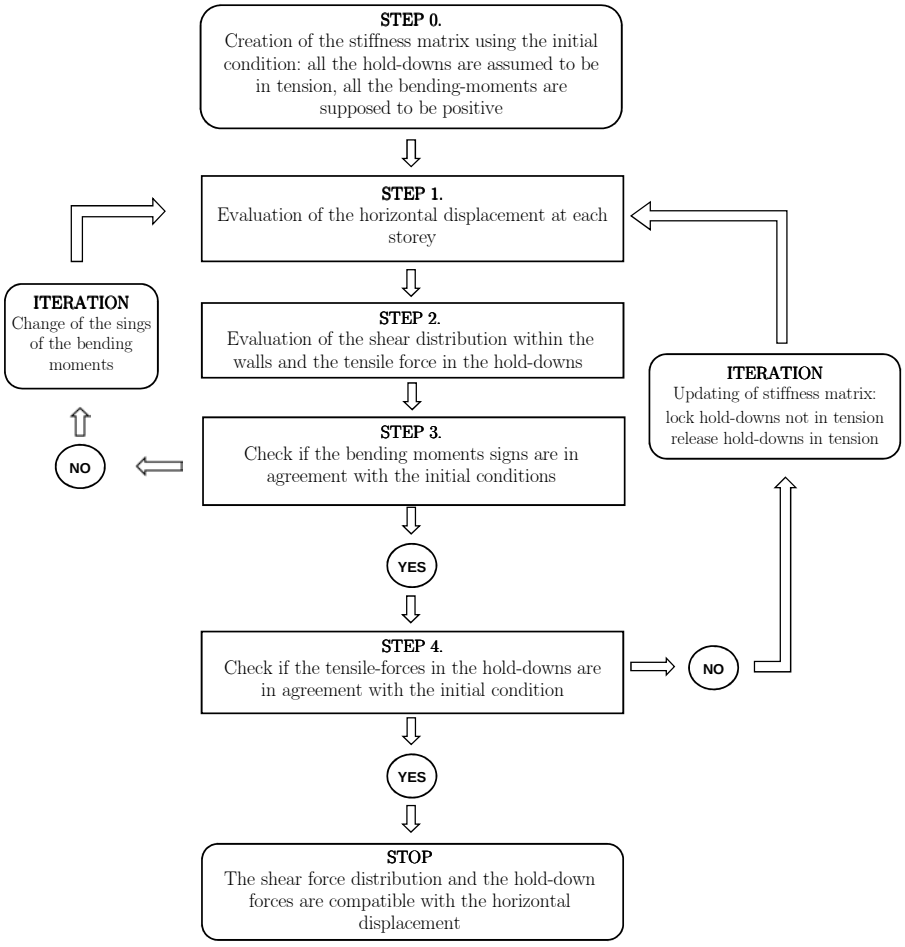

Fig. 7: Flow-chart for the iteration

Assuming all the hold-downs active as initial conditions, see Fig. 7 (a), the flexibility matrices of the two 3-storey can be evaluated by means of equation 16 (the values are given in mm/kN):

$$\tilde{\boldsymbol{U}}_1 = \begin{bmatrix} 0.4976 & 0.6976 & 0.8976 \\ & 1.8369 & 2.6369 \\ Sym & & 4.7761 \end{bmatrix}; \quad \tilde{\boldsymbol{U}}_2 = \begin{bmatrix} 1.3949 & 2.1949 & 2.9949 \\ & 6.0732 & 9.2732 \\ Sym & & 17.1515 \end{bmatrix} \tag{30}$$

known the flexibility matrices, using equation 20, the initial stiffness matrices

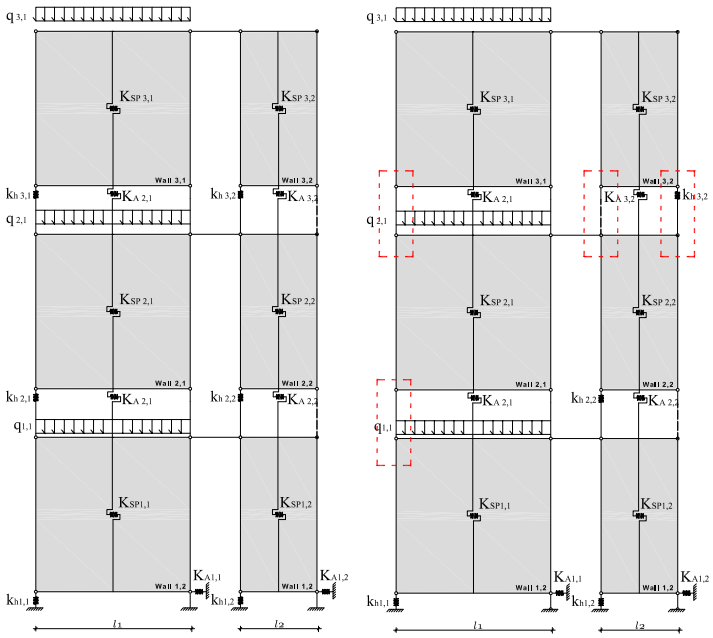

(a) *Initial state* (b) *Final state*

Fig. 8: System of $3 \cdot 2$ walls

Wall index	**1,1**	**2,1**	**3,1**	**1,2**	**2,2**	**3,2**
Length: l $[mm]$	2500	2500	2500	1250	1250	1250
Height: h $[mm]$	2500	2500	2500	2500	2500	2500
Vertical distributed load: q $[kN/m]$	5	5	5	0	0	0
Braced sides: n_{bs}	2	2	2	2	2	2
Shear Modulus: G_p $[N/mm]$	1000	1000	1000	1000	1000	1000
Sheathing pan. thickness: t_p $[mm]$	15	15	15	15	15	15
Sheathing pan. breadth: b $[mm]$	1250	1250	1250	1250	1250	1250
Fasteners stiffness: k_c $[N/mm]$	500	500	500	500	500	500
Fasteners spacing: s_c $[mm]$	100	100	100	100	100	100
HD stiffness: k_h $[N/mm]$	5000	2500	2500	5000	2500	2500
Angle-brackets stiffness: k_a $[N/mm]$	3000	2000	2000	3000	2000	2000
Angle-brackets number: n_a	4	4	4	2	2	2

Tab. 1: Example 3×2, geometrical and mechanical properties of the walls

become (the values are given in kN/mm):

$$\boldsymbol{K}_1 = \begin{bmatrix} 4.51 & -2.39 & 0.47 \\ & 3.89 & -1.70 \\ Sym & & 1.06 \end{bmatrix}; \quad \boldsymbol{K}_2 = \begin{bmatrix} 1.79 & -0.97 & 0.21 \\ & 1.47 & -0.63 \\ Sym & & 0.36 \end{bmatrix} \tag{31}$$

the global stiffness matrix of the system of 3×2 walls $\boldsymbol{K_{sys}}$, can be determined through equation 22:

$$\boldsymbol{K}_{sys} = \begin{bmatrix} 6.30 & -3.36 & 0.68 \\ & 5.36 & -2.32 \\ Sym & & 1.42 \end{bmatrix} \tag{32}$$

the arrays of the equivalent horizontal displacement produced by the vertical load $\boldsymbol{\Delta_{N,i}}$ are calculated by means of equation 17 assuming all the bending-moments positive, whereas the array of the equivalent force $\boldsymbol{F_{N,sys}}$ produced by the vertical load is determined by means of equation 23 (values are given in kN):

$$\boldsymbol{\Delta_{N,1}} = \begin{bmatrix} 3.75 \\ 12.50 \\ 23.75 \end{bmatrix}; \quad \boldsymbol{\Delta_{N,2}} = \begin{bmatrix} 0 \\ 0 \\ 0 \end{bmatrix}; \boldsymbol{F_{N,sys}} = \begin{bmatrix} -1.75 \\ -0.68 \\ 5.68 \end{bmatrix} \tag{33}$$

the total displacement at each storey (at the end of the first iteration) can be

determined by means of equation 24 (values are given in mm):

$$\boldsymbol{\Delta}^{1st} = \begin{bmatrix} 7.86 \\ 13.38 \\ 10.62 \end{bmatrix} \tag{34}$$

The arrays of external force carried out by each multi-storey wall can be determined by the equation 25 (values are shown in kN):

$$\boldsymbol{F_1} = \begin{bmatrix} 6.70 \\ 14.58 \\ -2.11 \end{bmatrix}; \quad \boldsymbol{F_2} = \begin{bmatrix} 3.30 \\ 5.42 \\ -2.89 \end{bmatrix} \tag{35}$$

the bending moments are determined from equation 27

$$\boldsymbol{M_1} = \begin{bmatrix} 73.8 \\ 25.9 \\ -5.28 \end{bmatrix}; \quad \boldsymbol{M_2} = \begin{bmatrix} 13.7 \\ -0.89 \\ -7.22 \end{bmatrix} \tag{36}$$

The signs of the bending-moments are not in agreement with the initial condition, hence the $\boldsymbol{\Delta_{N,j}}$ have to be recalculated using the values of equation 36. The updated arrays are:

$$\boldsymbol{\Delta_{N,1}} = \begin{bmatrix} 3.75 \\ 12.50 \\ 18.75 \end{bmatrix}; \quad \boldsymbol{\Delta_{N,2}} = \begin{bmatrix} 0 \\ 0 \\ 0 \end{bmatrix}; \boldsymbol{F_{N,sys}} = \begin{bmatrix} -4.12 \\ 7.82 \\ 0.38 \end{bmatrix} \tag{37}$$

the new displacement array becomes:

$$\boldsymbol{\Delta}^{2nd} = \begin{bmatrix} 7.88 \\ 13.54 \\ 14.59 \end{bmatrix} \tag{38}$$

the updated values of bendig moments are:

$$\boldsymbol{M_1} = \begin{bmatrix} 73.3 \\ 24.9 \\ -8.6 \end{bmatrix}; \quad \boldsymbol{M_2} = \begin{bmatrix} 14.2 \\ 0.1 \\ -3.9 \end{bmatrix} \tag{39}$$

Comparing the signs of the bending moments of equations 39 and 36 it can be noted that the value of the $wall_{2,2}$ is not consistent, hence, the procedure has to be iterated once-again. The necessity to iterate the procedure depends on the fact that the array of the equivalent force $\boldsymbol{F_{N_s ys}}$ as well as the displacement arrays due to the vertical load $\boldsymbol{\Delta_N}$ have been determined with a not correct signs-distribution of moments.

Using the values of equation 39, the $\boldsymbol{\Delta_{N,j}}$ have to be recalculated. The updated values are:

$$\boldsymbol{\Delta_{N,1}} = \begin{bmatrix} 3.75 \\ 12.50 \\ 18.75 \end{bmatrix}; \quad \boldsymbol{\Delta_{N,2}} = \begin{bmatrix} 0 \\ 0 \\ 0 \end{bmatrix} \; ; \boldsymbol{F_{N,sys}} = \begin{bmatrix} -4.12 \\ 7.82 \\ 0.38 \end{bmatrix} \tag{40}$$

the new displacement array becomes:

$$\boldsymbol{\Delta}^{3rd} = \begin{bmatrix} 7.88 \\ 13.54 \\ 14.59 \end{bmatrix} \tag{41}$$

the updated values of bending moments are:

$$\boldsymbol{M_1} = \begin{bmatrix} 73.3 \\ 24.9 \\ -8.6 \end{bmatrix}; \quad \boldsymbol{M_2} = \begin{bmatrix} 14.2 \\ 0.1 \\ -3.9 \end{bmatrix} \tag{42}$$

It is important to note that in this case the new iteration does not produce any change because the equivalent horizontal displacement $\boldsymbol{\Delta_{N,2}}$ is zero since no vertical load is applied, hence it is independent by the bending-moments sings.

The sings of the bending-moments of equations 42 are in agreement with the values of equation 39, therefore according to STEP 3 of the flow-chart of Fig. 7, the force in the hold-downs can be assessed by means of equation 14:

$$\boldsymbol{T_{HD,1}} = \begin{bmatrix} 10.59 \\ -2.53 \\ -2.8 \end{bmatrix}; \quad \boldsymbol{T_{HD,2}} = \begin{bmatrix} 11.33 \\ 0.07 \\ 3.10 \end{bmatrix} \tag{43}$$

According to STEP 4 of the flow-chart of Fig. 7, the force in the hold-downs is not in agreement with the initial condition of STEP 0 (all hold-down were supposed to be in tension), therefore the procedure goes back to STEP 1 after updating the stiffness matrices, namely all the hold-down in compression has a infinite stiffness. The new stiffness matrices are:

$$\boldsymbol{K}_1 = \begin{bmatrix} 6.30 & -2.94 & -0.08 \\ & 5.89 & -2.95 \\ Sym & & 2.34 \end{bmatrix}; \quad \boldsymbol{K}_2 = \begin{bmatrix} 1.79 & -0.97 & 0.21 \\ & 1.47 & -0.63 \\ Sym & & 0.36 \end{bmatrix}; \tag{44}$$

$$\boldsymbol{K}_{sys} = \begin{bmatrix} 8.08 & -3.91 & 0.13 \\ & 7.37 & -3.57 \\ Sym & & 2.70 \end{bmatrix} \tag{45}$$

Using the values of the new stiffness matrix of equation 44 and the sing of the bending-moments of equation 42, the $\boldsymbol{\Delta_{N,j}}$ and the $\boldsymbol{F_{N,sys}}$ becomes:

$$\boldsymbol{\Delta_{N,1}} = \begin{bmatrix} 3.75 \\ 7.5 \\ 11.25 \end{bmatrix}; \quad \boldsymbol{\Delta_{N,2}} = \begin{bmatrix} 0 \\ 0 \\ 0 \end{bmatrix}; \boldsymbol{F_{N,sys}} = \begin{bmatrix} 0.54 \\ 0 \\ 3.87 \end{bmatrix} \tag{46}$$

the new displacement array results:

$$\boldsymbol{\Delta}^{4rd} = \begin{bmatrix} 7.90 \\ 14.38 \\ 15.38 \end{bmatrix} \tag{47}$$

The force distribution within the wall is:

$$\boldsymbol{F_1} = \begin{bmatrix} 6.57 \\ 16.14 \\ -3.21 \end{bmatrix}; \quad \boldsymbol{F_2} = \begin{bmatrix} 3.43 \\ 3.86 \\ -1.79 \end{bmatrix} \tag{48}$$

the updated values of bending moments becomes:

$$\boldsymbol{M_1} = \begin{bmatrix} 73.0 \\ 24.3 \\ -8.0 \end{bmatrix}; \quad \boldsymbol{M_2} = \begin{bmatrix} 14.4 \\ 0.7 \\ -4.5 \end{bmatrix} \tag{49}$$

The sings of the bending-moments of equation 49 are in agreement with the sings adopted (see equation 42), therefore no iteration is needed and according to STEP 3 of the flow-chart of Fig. 7, the force in the hold-downs can be assessed by means of equation 14:

$$\boldsymbol{T_{HD,1}} = \begin{bmatrix} 10.47 \\ -2.78 \\ -3.04 \end{bmatrix}; \quad \boldsymbol{T_{HD,2}} = \begin{bmatrix} 11.56 \\ 0.56 \\ 3.57 \end{bmatrix} \tag{50}$$

The hold-down forces obtained at the end of the second iteration are in agreement with the boundary condition, the procedure therefore can be considered completed. The obtained results comply the equilibrium, the compatibility and the constitutive law.

4. Linear Seismic Analysis of timber shear-walls buildings

In Section 3.3 an approach for the linear-static analysis was presented; the horizontal external forces may represent the seismic action and therefore the presented method could be used to perform linear seismic analysis of light timber-frame walls buildings.

Two types of linear analysis are suggested by [11]: the Lateral Force Method (LFM) and the Response Spectrum Analysis (RSA). The former should be used only if the structure can be considered regular in elevation, the latter is applicable to all types of building.

4.1. Lateral Force Method - LFM

LFM can be considered as a particular case of the method introduced in Section 3.3. The LFM, indeed, assumes the seismic action as an equivalent static horizontal forces distribution. The use of the LFM has been already presented in the previous section, and the applied horizontal forces can be determined according to simplified expressions reported in several national standards, which assumes that the building response is not significantly affected by the contribution of the higher modes of vibration. For these reason, the LFM of analysis

shall be applied if the fundamental period of structure is smaller than a given value and the building meets the criteria for regularity in elevation.

Differently from the common practice, the method presented (see 3.3) considers the influence of the hold-downs even in the elastic response. Usually, designers prefer to neglect the hold-down presence because it introduces a non-linear behaviour since from the elastic-analysis, which significantly increases the difficulty and the time of analysis becoming iterative. The need to compute the hold-down contribution is however clear, both the shear-distribution and the tensile force in the hold-downs change magnitude compared with the actual-common approach. Therefore, in order to correctly asses the seismic action in a timber shear-walls building, the iterative approach is required.

4.2. Response Spectrum Analysis - RSA

RSA is usually applied to buildings which cannot be defined regular in elevation and it should be considered the reference method for determining the seismic effects because it can be applied to any type of building without any geometric limitation. Moreover, its results could be considered more reliable (compared to LFM) because the analysis takes into account all the significant modes of vibration participating to the seismic response of the structure. The effects of the analysis E^{ζ} are then combined to asses the design actions; the effects can be combined using a modal superimposition techniques such as the *Complete Quadratic Combination* [CQC] or the *Square Root Sum of Square* [$SRSS$], see [17].

Two key aspects have to be investigated to apply the RSA to timber wall buildings: the hold-downs non-linear behaviour (hold-downs can have two states) and the presence of the vertical load.

4.2.1. Modal analysis for a single-story timber shear-walls building

In order to apply the RSA to a building, the dynamic properties of the building have to be assessed through a modal analysis. Namely, the natural

periods, the mode shapes and the participating masses have to be determined using a modal analysis.

In order to perform the modal analysis of a timber shear-wall (see Fig. 9) a concentrated-mass m is added on the top-plate of the wall.

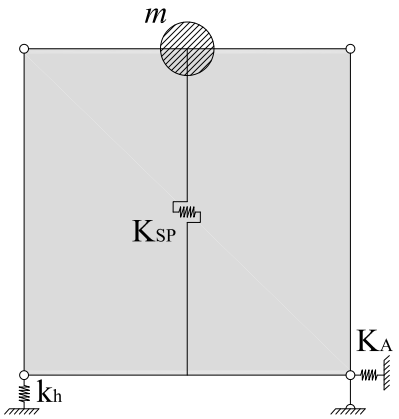

Fig. 9: UNITN model with a concentrated mass

The equation of motion can be written regarding to the equilibrium of the concentrated mass subjected to its inertial force F_{in} and the wall elastic force F_{el}:

$$F_{in} + F_{el} = 0 \tag{51}$$

The inertial force can be expressed as:

$$F_{in} = m \cdot \ddot{\Delta} \tag{52}$$

where $\ddot{\Delta}$ is the mass acceleration. The wall elastic force F_{el}, according to 5, is obtained by:

$$F_{el} = K_{tot} \cdot (\Delta + \Delta_N) \tag{53}$$

where K_{tot} is the wall stiffness accounting for all the deformation contributions. Therefore, Δ can be regarded as the horizontal displacement of the

concentrated-mass and Δ_N is the wall horizontal displacement due to the vertical load. Equation 51 can be rewritten as:

$$m \cdot \ddot{\Delta} + K_{tot} \cdot (\Delta + \Delta_N) = 0 \tag{54}$$

Equation 54 can be rearranged as follows:

$$m \cdot \ddot{\Delta} + K_{tot} \cdot \Delta = -K_{tot} \cdot \Delta_N \tag{55}$$

Equation 55 is a second order linear differential equation; each term can be divided by the mass m to get:

$$\ddot{\Delta} + \omega^2 \cdot \Delta = -\omega^2 \cdot \Delta_N \tag{56}$$

where $\omega = \sqrt{\frac{K_{tot}}{m}}$ is the circular frequency.
The solution of Equation 56 can be obtained easily considering the homogeneous and the particular terms as:

$$\Delta\,(t) = A \cdot e^{i \cdot \omega \cdot t + \theta} + \Delta_N \tag{57}$$

where: A and θ are the amplitude end the phase of the motion respectively; they are constant and can be calculated using the initial conditions. If the rigid body rotation contribution is not considered the wall stiffness can be expressed by $K_{tot,nt}$ and the term Δ_N becomes zero. The period and the natural frequency of the wall can be obtained directly from the circular frequency as:

$$T = \frac{\omega}{2\pi} \tag{58}$$

$$f = \frac{2\pi}{\omega} \tag{59}$$

4.2.2. Modal analysis for a system of $m \times n$ walls modelling a multi-story timber shear-walls building

The modal analysis of a system of $m \times n$ walls can be performed not in a much different way from the previous case. In order to consider the mass-distribution along the height, an equivalent concentrated-mass is added at each

storey and not to each wall; this assumption can be considered valid until the floor of the building can be regarded as a rigid-diaphragm. The mass-distribution hence becomes a diagonal matrix and it is defined as follows:

$$\mathbf{M} = \begin{bmatrix} m_1 & 0 & 0 & 0 \\ 0 & m_j & 0 & 0 \\ 0 & 0 & \ddots & 0 \\ 0 & 0 & 0 & m_m \end{bmatrix} \tag{60}$$

For a system of $m \times n$ walls , the modal analysis allows to evaluate the ζ *Natural Periods* $\mathbf{T}^{\zeta}$ and the relative *mode-shapes* $\boldsymbol{\phi}^{\zeta}$. Where ζ is equal to the degrees of freedom, i.e. the number of storeys.

Due to the fact that the mode-shapes can be determined using the following equation:

$$\left(\mathbf{K} - \omega_{\zeta}^2 \cdot \mathbf{M}\right) \cdot \boldsymbol{\phi}^{\zeta} = 0 \tag{61}$$

it is clear that both the *Natural Periods* and the relative *mode-shapes* strictly depend on the stiffness $\mathbf{K}$ of the structure, hence, they strongly depend on the hold-downs state. It is therefore clear once again that an iterative procedure is needed to solve the problem.

5. Proposal of three methods to apply the RSA to timber wall buildings

Three different methods for applying the RSA are presented. The three methods differ in the way in which they consider the effect of the vertical load on the hold-down forces and how it modifies the shear-distribution within the walls. All the procedures are iterative in order to determine a shear-distribution and a hold-downs force consistent with the model of the building.

5.1. Method 1: VTM

The first method presented is called VTM (*Vertical load To Main mode*) and it is suggested to be used when a prevailing mode-shape exists. The method consists of five steps as shown in Fig. 10.

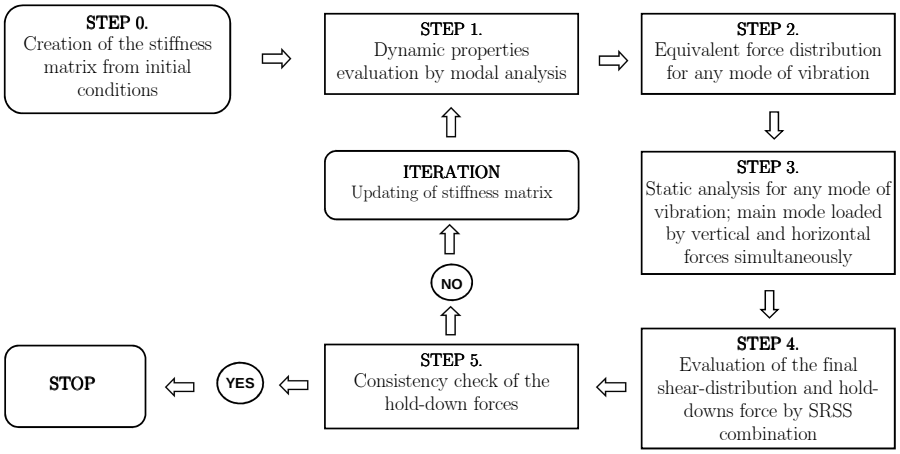

Fig. 10: Flow chart of the VTM method

In the first phase the modal analysis is performed in order to determine the dynamic properties of the model, namely the natural periods T^{ζ}, the mode-shapes ϕ^{ζ} and the modal participation factor Γ^{ζ}, which is used to identify the most important mode-shape and determined as follow:

$$\Gamma^{\zeta} = \frac{(\phi^{\zeta})^T \cdot \mathbf{M} \cdot \boldsymbol{R}}{(\phi^{\zeta})^T \cdot \mathbf{M} \cdot \phi^{\zeta}} \tag{62}$$

where $\boldsymbol{R}$ is a ones-array.

In the second step of the procedure, ζ-static analyses are performed; for any shape-mode the model of the structure is loaded by an equivalent static horizontal force distribution related to the shape-mode itself. For the analysis associated to the main shape-mode (i.e. the mode with the higher participation factor), the simultaneous presence of the vertical load is taken into account in order to consider its influence on the shear-distribution.

The static force distribution related to the ζ-th mode-shape (see Fig. 11) can be evaluated as:

$$\mathbf{F}^{\zeta} = S_d\left(T^{\zeta}\right) \cdot \Gamma^{\zeta} \cdot \mathbf{M} \cdot \mathbf{\Phi}^{\zeta} \tag{63}$$

The values of shear-force and bending-moment (given by the ζ-static analyses) acting on each wall are combined by the SRSS procedure in the fourth step.

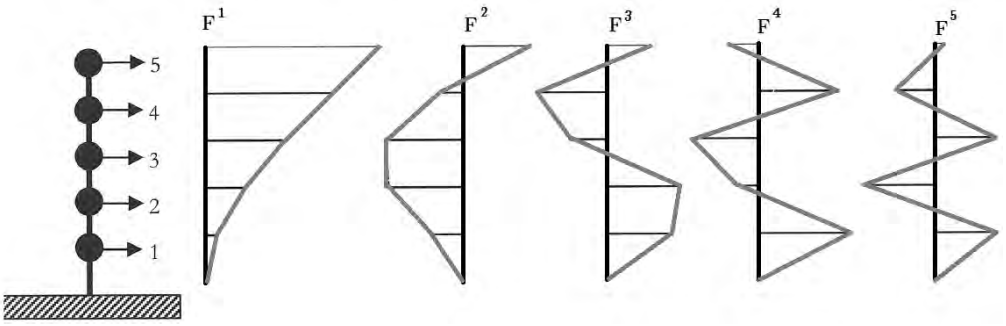

Fig. 11: Schematic equivalent force distributions related to the 5 mode-shapes of the structure, rearranged from [18]

This modal superimposition technique allows to estimate the actual response of the structure. The net force acting in the hold-downs is determined from the bending moment and the vertical load:

$$T_{HD-j,i} = \frac{M_{j,i}^{SRSS}}{\tau_i \cdot l_i} - N_{j,i} \tag{64}$$

The last step requires to verify that the values of hold-downs forces are in agreement with the state set in the initial conditions (i.e. STEP 0, see Fig. 10). If the forces are consistent, the procedure can be stopped; otherwise, the model and its stiffness matrix have to be updated changing the state of the hold-downs not compatible and the procedure has to be iterated.

5.2. Method 2: VNA

The method called VNA (*Vertical load Not Applied*) is similar to the previous one; it differs from the VTM method by the fact that the vertical load is not considered during the analysis phase (STEP 3), but it is taken into account only at the end of the analysis for the evaluation of the tensile force in the hold-downs (in the same way as equation 64).

Synthetically, the VNA method consists of the following steps (see Fig. 12): in the STEP 0, the structure is modelled and the stiffness matrix is evaluated; in the STEP 1 the modal analysis is performed to determine the dynamic

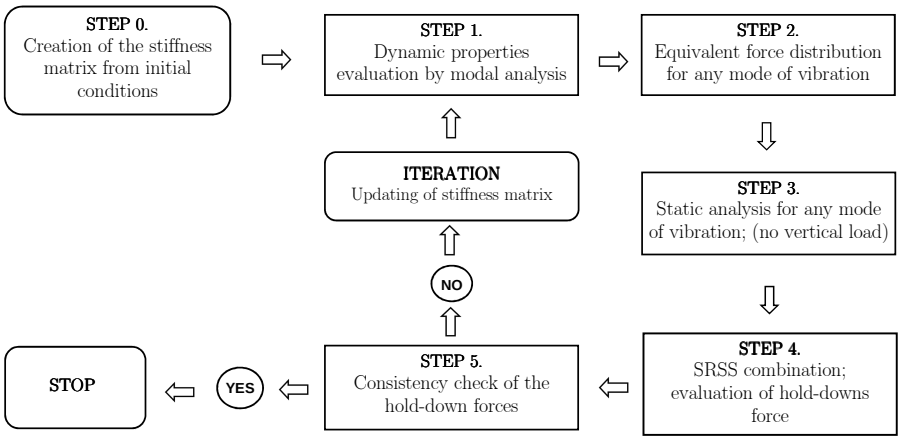

Fig. 12: Flow chart of the VNA method

properties and the modal participation factor: T^{ζ}, $\mathbf{\Phi}^{\zeta}$, $\mathbf{\Gamma}^{\zeta}$; then in the STEP 2, ζ-static equivalent force distributions are determined using equation 63, which are used in the STEP 3 to statically analyse the structure ζ-times, applying each time one of the static equivalent force distributions, the vertical load is not considered. In the STEP 4, the shear-forces and the bending moments values are combined by the SRSS and the net forces in the hold-downs are assessed by equation 64; in the last STEP the consistency of the result is checked in terms of compatibility between hold-downs forces and hold-downs state; if the compatibility is not satisfied the procedure has to be iterated.

It is important to remark that the vertical load is considered by the method only as a reduction of the tensile forces of the hold-downs and therefore its influence on the shear-force distribution is not taken into account. This approach leads to more approximated results but, on the other hand, it is faster and easier compared to the other ones.

5.3. Method 3: CNA

The method of analysis called CNA (*Complete Numerical Analytical*) was developed with the aim to estimate as correctly as possible the influence of the

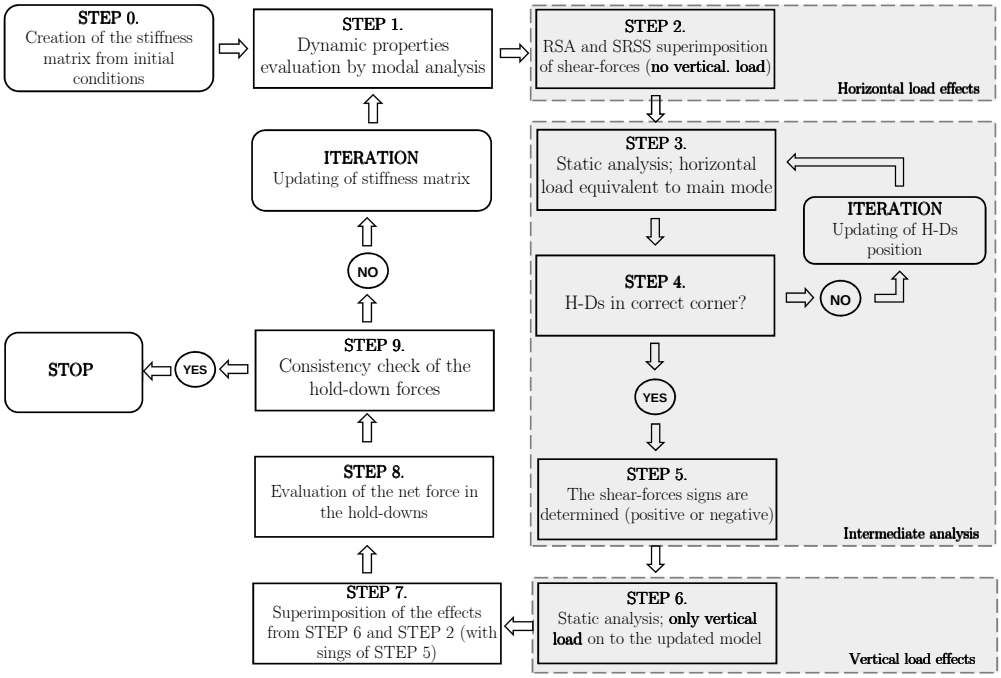

Fig. 13: Flow chart of the CNA method

vertical load on the shear-distribution. The key point of the method is the evaluation of the horizontal load and of the vertical load effects separately.

According to the flow-chart of Fig. 13, both the modal analysis and the RSA (without the vertical load) are firstly performed in order to obtain the dynamic properties and modal shear-force distribution respectively. Then, the model of the structure is analysed only applying the vertical load, which causes an auto-balanced shear-distribution.

The RSA allows to evaluate only the modulus of the shear-forces but not their sign, moreover it is not influenced by the hold-downs position (the result of the RSA is not depended on the corner where the hold-downs are placed, left-right). On the contrary, the shear-forces produced by the vertical-load can change magnitude and orientation with the hold-down position. Hence, the superimposition of the shear-forces due to the RSA and the vertical-load static analysis can not be automatically performed since only the modulus of the

shear-forces is determined by means of RSA .

In other words, both the RSA shear-forces sign and the orientation of shear-forces produced by vertical-load have to be previously determined. Therefore, an intermediate analysis is needed for the evaluation of the correct position of the hold-downs (left or right) and for the evaluation of a sign-pattern, which has to be assigned to the RSA shear-distribution. This intermediate analysis is carried-out loading the structure only with a horizontal force distribution related to the main shape mode (which allows to evaluate the correct position of the hold-down).

After evaluating the final shear-force distribution by the superimposition of the RSA effects with the vertical-load effects, the net forces in the hold-downs as well as the consistency as to be determined. In the case that the results are not in accordance with the initial conditions, the procedure are to be iterated.

6. Numerical example for the application of the RSA proposed methods

With the aim to make readers understand correctly the three methods proposed and to provide a comparison of the results, the system of 3×2 walls of Section 3.3.1 (see Fig. 8) is analysed.

The mass matrix adopted is (the masses are given in tons):

$$\mathbf{M} = \begin{bmatrix} 2 & 0 & 0 \\ 0 & 2 & 0 \\ 0 & 0 & 2 \end{bmatrix} \tag{65}$$

For the initial condition all the hold-downs are considered active in accordance with Fig. 8 (a).

6.1. Modal analysis

All the three proposed methods require, as STEP 1, the modal analysis of the structure-model in order to assess its dynamic properties as well as the mass participating factor.

From the mass matrix of equation 65 and the global stiffness matrix of equation 32, according to Equation 61, the periods result:

$$T^1 = 0.63\,sec; \quad T^2 = 0.16\,sec; \quad T^3 = 0.09\,sec \tag{66}$$

and the related shape-modes are :

$$\mathbf{\Phi}^1 = \begin{bmatrix} 0.21 \\ 0.59 \\ 1.00 \end{bmatrix}; \qquad \mathbf{\Phi}^2 = \begin{bmatrix} 1.00 \\ 0.80 \\ -0.68 \end{bmatrix}; \qquad \mathbf{\Phi}^3 = \begin{bmatrix} -1.00 \\ 0.95 \\ -0.35 \end{bmatrix} \tag{67}$$

The participation factors, evaluated using the equation 62, are the following:

$$\Gamma^1 = 1.29; \qquad \Gamma^2 = 0.53; \qquad \Gamma^3 = -0.19 \tag{68}$$

It is clear that the main mode of vibration is the first one, This can be more emphasized evaluating the participation masses:

$$\tilde{M}^1 = 4.66\,ton; \qquad \tilde{M}^2 = 1.19\,ton; \qquad \tilde{M}^3 = 0.15\,ton \tag{69}$$

In order to evaluate the equivalent force distributions related to the mode-shapes, the reduced response spectrum (called design spectrum) of Fig. 14 is considered. For each period, the spectral values are:

$$S_d\,(T_1) = 0.42g; \quad S_d\,(T_2) = 0.56g; \qquad S_d\,(T_3) = 0,64g \tag{70}$$

the equivalent static force distributions are determined by-means of 63 (the forces are given in kN):

$$\mathbf{F}^1 = \begin{bmatrix} 2.26 \\ 6.27 \\ 10.67 \end{bmatrix}; \qquad \mathbf{F}^2 = \begin{bmatrix} 5.84 \\ 4.67 \\ -3.98 \end{bmatrix}; \qquad \mathbf{F}^3 = \begin{bmatrix} 2.45 \\ -2.33 \\ 0.85 \end{bmatrix} \tag{71}$$

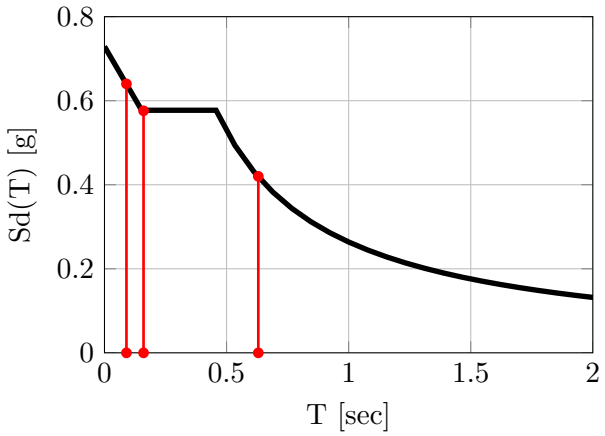

Fig. 14: Design spectrum adopted

6.1.1. VTM method

According to the Step 3 of the VTM method, three static analyses of the model are performed, namely one for each static force distributions. It has to be reminded that the analysis related to the main mode-shape considers the simultaneous presence of the equivalent horizontal and the vertical loads. Conversely, the analyses related to the other mode-shapes consider only the equivalent horizontal loads.

The shear-force distributions and the bending-moments for each mode-shape are shown in Tab. 2; for each equivalent static analysis, the initial-condition assumed considers all the bending-moments to be positive. According to the procedure of Section 3.3, the states of the hold-down were checked at every step; for the first mode-shape no iteration has been required; conversely, the other two methods needed two iterations each.

The Step 4 of the VTM method consists in the modal superimposition of the shear-forces and the bending moments, the SRSS procedure gives the values shown in Tab. 3.

The net vertical-force acting in the hold-downs and the related compatibility verification are shown in Tab. 4.

Shape-mode 1							
$V_{11}^1 =$	15.07	$V_{12}^1 =$	4.13	$M_{11}^1 =$	97.93	$M_{12}^1 =$	19.09
$V_{21}^1 =$	14.23	$V_{22}^1 =$	2.71	$M_{21}^1 =$	60.26	$M_{12}^1 =$	8.76
$V_{31}^1 =$	9.89	$V_{32}^1 =$	0.79	$M_{31}^1 =$	24.69	$M_{12}^1 =$	1.98
Shape-mode 2							
$V_{11}^2 =$	4.73	$V_{12}^2 =$	1.79	$M_{11}^2 =$	5.63	$M_{12}^2 =$	2.47
$V_{21}^2 =$	0.50	$V_{22}^2 =$	0.18	$M_{21}^2 =$	-6.21	$M_{12}^2 =$	-2.01
$V_{31}^2 =$	-2.99	$V_{32}^2 =$	-0.99	$M_{31}^2 =$	-7.47	$M_{12}^2 =$	-2.47
Shape-mode 3							
$V_{11}^3 =$	0.68	$V_{12}^3 =$	0.28	$M_{11}^3 =$	0.59	$M_{12}^3 =$	0.26
$V_{21}^3 =$	-1.06	$V_{22}^3 =$	-0.41	$M_{21}^3 =$	-1.12	$M_{12}^3 =$	-0.45
$V_{31}^3 =$	0.62	$V_{32}^3 =$	0.23	$M_{31}^3 =$	1.54	$M_{12}^3 =$	0.59

Tab. 2: VTM, shear-force distributions and bending moments for the 1^{st} iteration

Shear-forces V_{ij} $[kN]$				**Bending-moments** M_{ij} $[kNm]$			
$V_{11} =$	15.80	$V_{12} =$	4.51	$M_{11} =$	98.1	$M_{12} =$	19.2
$V_{21} =$	14.27	$V_{22} =$	2.75	$M_{21} =$	60.6	$M_{12} =$	9.00
$V_{31} =$	10.33	$V_{32} =$	1.29	$M_{31} =$	25.8	$M_{12} =$	3.22

Tab. 3: SRSS values of shear-forces and bending-moments, 1^{st} iteration VTM

Tensile force T_{ij} $[kN]$			
$T_{HD,11} =$	20.47	$T_{HD,12} =$	7.7
$T_{HD,21} =$	11.73	$T_{HD,22} =$	3.6
$T_{HD,31} =$	4.1	$T_{HD,32} =$	1.3
Compatibility verification			
verified		verified	
verified		verified	
verified		verified	

Tab. 4: Hold-downs force and compatibility verification, 1^{st} iteration VTM

The final result of the first iteration are in agreement with the initial condition adopted, therefore the results are consistent with the boundary condition used and no more iteration are needed. It is important to remark that if the

hold-down forces would have not been compatible with the hypothesized hold-down state, the procedure would have been iterated after the updating of the boundary condition, hence the updating of the stiffness matrix.

6.1.2. VNA method

As for the previous method, in the first phase, the VNA method consists in the evaluation of the dynamic properties, which are determined through modal analysis. Periods of the structure, mode-shapes and modal participation factors are needed to evaluate the equivalent force distributions related to the mode-shapes, see section 6.1. The static equivalent distributions (which values are determined in equation 71) are used to statically-analyse the structure, conversely from the other methods the VNA method considers (at this stage) only the effect of the horizontal load, namely the vertical load is not applied. The results of the three equivalent static analyses are reported in Tab. 5.

Shape-mode 1							
$V_{11}^1 =$	14.29	$V_{12}^1 =$	4.90	$M_{11}^1 =$	90.28	$M_{12}^1 =$	26.75
$V_{21}^1 =$	13.13	$V_{22}^1 =$	3.80	$M_{21}^1 =$	54.54	$M_{12}^1 =$	14.48
$V_{31}^1 =$	8.68	$V_{32}^1 =$	1.99	$M_{31}^1 =$	21.70	$M_{12}^1 =$	4.98
Shape-mode 2							
$V_{11}^2 =$	4.73	$V_{12}^2 =$	1.79	$M_{11}^2 =$	5.63	$M_{12}^2 =$	2.47
$V_{21}^2 =$	0.50	$V_{22}^2 =$	0.18	$M_{21}^2 =$	-6.21	$M_{12}^2 =$	-2.01
$V_{31}^2 =$	-2.99	$V_{32}^2 =$	-0.99	$M_{31}^2 =$	-7.47	$M_{12}^2 =$	-2.47
Shape-mode 3							
$V_{11}^3 =$	0.68	$V_{12}^3 =$	0.28	$M_{11}^3 =$	0.59	$M_{12}^3 =$	0.26
$V_{21}^3 =$	-1.06	$V_{22}^3 =$	-0.41	$M_{21}^3 =$	-1.12	$M_{12}^3 =$	-0.45
$V_{31}^3 =$	0.62	$V_{32}^3 =$	0.23	$M_{31}^3 =$	1.54	$M_{12}^3 =$	0.59

Tab. 5: VTM, shear-force distributions and bending moments for the 1^{st} iteration

The values of shear-forces and the bending moments determined with the three static analyses have to be combined by the SRSS modal-superimposition. The values are shown in Tab. 6; the values are different from the VTM case because the vertical load was not taken into account.

Shear-forces V_{ij} $[kN]$				**Bending-moments** M_{ij} $[kNm]$			
$V_{11} =$	15.07	$V_{12} =$	5.23	$M_{11} =$	90.46	$M_{12} =$	26.86
$V_{21} =$	13.19	$V_{22} =$	3.83	$M_{21} =$	54.91	$M_{12} =$	14.63
$V_{31} =$	9.20	$V_{32} =$	2.24	$M_{31} =$	23.00	$M_{12} =$	5.59

Tab. 6: SRSS values of shear-forces and bending-moments, 1^{st} iteration VNA

The net vertical-load acting in the hold-downs and the related compatibility verification are shown in Tab. 7.

Tensile force $T_{HD,ij}$ $[kN]$			
$T_{HD,11} =$	17.43	$T_{HD,12} =$	10.74
$T_{HD,21} =$	9.46	$T_{HD,22} =$	5.85
$T_{HD,31} =$	2.95	$T_{HD,32} =$	2.24
Compatibility verification			
verified		verified	
verified		verified	
verified		verified	

Tab. 7: Hold-downs force and compatibility verification, 1^{st} iteration VNA

Even for the VNA-method only one iteration is required to solve the structure and to obtain compatible results with the initial condition.

6.1.3. CNA method

The CNA method initially performs a modal analysis for the determination of the dynamic properties of the model (see section 6.1) and a RSA for the determination of the modal values of shear-forces and bending-moments, which are the same as for the VNA method, see Tab. 6. However, the shear-forces and bending-moments given by the SRSS modal-superimposition, are absolute values, and therefore the direction of action of the forces are not known.

The direction of action of the forces represents a key aspect for the timber-wall buildings, because it is fundamental to know which hold-down can be in tension. To correctly evaluate the effects of the modal forces, the third step CNA method proposes to perform a further equivalent static analysis related

to the main shape-mode. Therefore the structure initially has to be loaded by only the equivalent static horizontal load force distribution and in a second phase only with the vertical load.

The first analysis is exclusively done to determine the direction of shear and hold-downs forces; the forces direction for the analysed example is shown in Tab. 8. It is important to note that forces are assumed positive (*Posit.*) if oriented from left to right and bending-moments are assumed positive if acting clockwise.

Shear-forces V_{ij}				**Hold-downs force** $T_{HD,ij}$			
$V_{11} =$	Posit. -	$V_{12} =$	Posit.	$T_{HD,11} =$	Tension -	$T_{HD,12} =$	Tension
$V_{21} =$	Posit. -	$V_{22} =$	Posit.	$T_{HD,21} =$	Tension -	$T_{HD,22} =$	Tension
$V_{31} =$	Posit. -	$V_{32} =$	Posit.	$T_{HD,31} =$	Tension -	$T_{HD,32} =$	Tension

Tab. 8: Shear and hold-down force directions, 1^{st} iteration CNA

A second-level of iteration is not needed (see Fig. 13) because all the hold-down are in tension, namely the hold-downs forces are in agreement with the initial condition hypothesized.

The model is then loaded by only the vertical load which produces the shear-forces and bending-moment shown in Tab. 9.

Shear-forces V_{ij} $[kN]$				**Bending-moments** M_{ij} $[kNm]$			
$V_{11} =$	0.77	$V_{12} =$	-0.77	$M_{11} =$	7.65	$M_{12} =$	-7.65
$V_{21} =$	1.09	$V_{22} =$	-1.09	$M_{21} =$	5.72	$M_{12} =$	-5.72
$V_{31} =$	1.20	$V_{32} =$	-1.20	$M_{31} =$	2.99	$M_{12} =$	-2.99

Tab. 9: Shear-forces and bending-moments produced by the vertical load, 1^{st} iteration CNA

At the end of the first-level of iteration of the CNA method, the final values of shear and hold-down forces (see Tab. 10) are determined summing the actions produced by the vertical load (values of Tab. 9) with the actions given by the SRSS-procedure of the RSA (values of Tab. 6) to which are assigned the direction of Tab. 8.

The analysis procedure leads to consistent results with only one iteration, the final shear and hold-down forces (compatible with the initial condition

Shear-forces V_{ji} $[kN]$	
$V_{11} = (+)\,\lvert 15.07\rvert + 0.77 = 15.84$	$V_{12} = (+)\,\lvert 5.23\rvert - 0.77 = 4.46$
$V_{21} = (+)\,\lvert 13.19\rvert + 1.09 = 14.28$	$V_{22} = (+)\,\lvert 3.83\rvert - 1.09 = 2.74$
$V_{31} = (+)\,\lvert 9.20\rvert + 1.2 = 10.40$	$V_{32} = (+)\,\lvert 2.24\rvert - 1.2 = 1.04$
Bending moments M_{ji} $[kNm]$	
$M_{11} = (+)\,\lvert 90.46\rvert + 7.65 = 98.10$	$M_{12} = (+)\,\lvert 26.86\rvert - 7.65 = 19.21$
$M_{21} = (+)\,\lvert 54.91\rvert + 5.72 = 60.63$	$M_{22} = (+)\,\lvert 14.63\rvert - 5.72 = 8.91$
$M_{31} = (+)\,\lvert 23.00\rvert + 2.99 = 25.99$	$M_{32} = (+)\,\lvert 5.59\rvert - 2.99 = 2.60$

Tab. 10: Final values of shear-forces and bending-moments, 1^{nd} iteration CNA

adopted for the model) are shown in Tab. 11.

Tensile force $T_{HD,ij}$ $[kN]$			
$T_{HD,11} =$	20.49	$T_{HD,12} =$	7.68
$T_{HD,21} =$	11.75	$T_{HD,22} =$	3.56
$T_{HD,31} =$	4.15	$T_{HD,32} =$	1.04
Compatibility verification			
verified		verified	
verified		verified	
verified		verified	

Tab. 11: Hold-downs force and compatibility verification, 1^{st} iteration CNA

6.1.4. Results comparison

The three methods give comparable results in terms of magnitude of shear, bending-moments and tensile forces in the hold-down, see Tab. 12.

The CNA method is the most rigorous one from the mathematical point of view, because it considers the vertical load effects both in terms of magnitude and sign; in fact the auto-balanced shear-forces and the bending-moments due-to the vertical load are added to the forces and moments obtained by the SRSS combination, to which a signs-distribution determined from an ad-hoc analysis is applied. However, the CNA is more complex than the other two methods because two further analyses to establish the vertical load influence are required.

The VTM method is less complex than the CNA one; indeed it takes into

VTM Method					
Shear-forces V_{ij} $[kN]$		**Bending-moments** M_{ij} $[kNm]$		**HDs Force** $T_{HD,ij}$ $[kN]$	
$V_{11} = 15.80$	$V_{12} = 4.51$	$M_{11} = 98.06$	$M_{12} = 19.24$	$T_{HD,11} = 20.47$	$T_{HD,12} = 7.70$
$V_{21} = 14.27$	$V_{22} = 2.75$	$M_{21} = 60.57$	$M_{12} = 9.00$	$T_{HD,11} = 11.73$	$T_{HD,12} = 3.60$
$V_{31} = 10.33$	$V_{32} = 1.29$	$M_{31} = 25.83$	$M_{12} = 3.23$	$T_{HD,11} = 4.08$	$T_{HD,12} = 1.29$
VNA Method					
Shear-forces V_{ij} $[kN]$		**Bending-moments** M_{ij} $[kNm]$		**HDs Force** $T_{HD,ij}$ $[kN]$	
$V_{11} = 15.07$	$V_{12} = 5.23$	$M_{11} = 90.46$	$M_{12} = 26.86$	$T_{HD,11} = 17.43$	$T_{HD,12} = 10.74$
$V_{21} = 13.19$	$V_{22} = 3.83$	$M_{21} = 54.91$	$M_{12} = 14.63$	$T_{HD,11} = 9.46$	$T_{HD,12} = 5.85$
$V_{31} = 9.20$	$V_{32} = 2.24$	$M_{31} = 23.00$	$M_{12} = 5.59$	$T_{HD,11} = 2.95$	$T_{HD,12} = 2.24$
CNA Method					
Shear-forces V_{ij} $[kN]$		**Bending-moments** M_{ij} $[kNm]$		**HDs Force** $T_{HD,ij}$ $[kN]$	
$V_{11} = 15.85$	$V_{12} = 4.46$	$M_{11} = 98.11$	$M_{12} = 19.21$	$T_{HD,11} = 20.49$	$T_{HD,12} = 7.68$
$V_{21} = 14.28$	$V_{22} = 2.74$	$M_{21} = 60.63$	$M_{12} = 8.91$	$T_{HD,11} = 11.75$	$T_{HD,12} = 3.56$
$V_{31} = 10.40$	$V_{32} = 1.04$	$M_{31} = 25.99$	$M_{12} = 2.60$	$T_{HD,11} = 4.15$	$T_{HD,12} = 1.04$

Tab. 12: Results Comparison

account the vertical load effect directly in the equivalent-static analysis of the shape-mode with the highest participating factor. It is not so accurate as the CNA method, but the results are anyway reliable and comparable with those of the CNA method, see Tab. 12.

The fastest procedure is the VNA, but it is the less accurate because it considers the vertical load only in the post-process phase as reduction of the tensile force acting in the hold-downs.

7. Concluding remarks

This paper has dealt with the static and dynamic seismic elastic analysis of light timber-frame multi-storey buildings by-meas of the UNITN model (presented in a previews work), assuming a cantilever-behaviour for the shear-walls.

In the first part of the paper an iterative procedure for the static analysis has been developed. This procedure is necessary to determine the horizontal-forces distribution proportionally to the walls stiffness and it can be conveniently used for applying the seismic lateral force method. The procedure involves two level of iteration; the first iteration-level is required to evaluate which of the two hold-downs of each wall is working and the auto-balanced shear forces due to the vertical load. The second level of iteration is necessary to update the stiffness matrix of the system in the case that some hold-downs are in compression.

The second part of the paper is focused on the modal analysis of the timber

light-frame buildings; in particular three approaches for the application of the RSA are proposed. The modal analysis can not be directly applied to these type of timber building due to the non-linearity introduced by the hold-down and the vertical load. In fact, the seismic force depends on the stiffness of the structure which depends on the state of the hold-downs; but the hold-downs state is in turn influenced by the magnitude of the seismic force. Therefore three iterative methods with varying levels of accuracy have been developed. The CNA method is the most correct from the mathematical point of view, but the its complexity makes it the most expensive in terms of time of analysis. The VNA method is less accurate because it accounts for the vertical load effect only in the post-process phase, but at the same time it results faster than the other ones. The VTM method represents a compromise between computational expensiveness and accuracy; for this reason the VTM should be the reference method.

The three procedures may be expensive from the computational point of view because, generally, they require several steps of iteration to achieve the solution. However, they allow to get a balanced and compatible solution (allowing their use even in the S.L.S). In particular, through the iteration process, a stiffness matrix modelling properly the building, can be determined which enables to get reliable values of the periods of vibration. Other methods, on the contrary, solve directly the problem without any iteration, neglecting the behaviour of the hold-downs (active: tension; not active: compression) and assuming them active. This leads to high values of period of vibration as well as to an underestimation of the seismic force (which produces a dangerous under-design of the building).

Acknowledgments

The presented research has been carried out in the framework of the ReLUIS-DPC 2015 project. Support from the ReLUIS-DPC network, the Italian University Network of Seismic Engineering Laboratories and Italian Civil Protection

Agency, is gratefully acknowledged. Authors would also to thanks Eng. F. Vinante and Eng. A. Di Paolo for their help.

Nomenclature

α is the shape parameter of the sheathing-panel;

$\mathbf{\Delta_N}$ is the array of the equivalent horizontal displacements of due to the vertical loads;

$\mathbf{\Delta}$ is the array of the displacement provoked by the external force;

$\mathbf{\Phi}$ is the array of the mode-shapes;

$\tilde{\mathbf{U}}$ is the flexibility matrix of the multi-storey shear-wall;

$\mathbf{F_N}$ is the array of equivalent horizontal force due to the vertical load;

$\mathbf{F}$ is the array of the external horizontal force;

$\mathbf{K_{sys}}$ is the stiffness matrix of the building;

$\mathbf{K}$ is the stiffness matrix of a multi-storey shear wall;

$\mathbf{M}$ is the mass matrix of the building;

$\mathbf{R}$ is a ones-array;

Δ is the horizontal displacement of the wall;

Δ_{HD} is the horizontal displacement of the wall provoked by the elongation of the hold-down;

Δ_N is the equivalent horizontal displacement of due to the vertical load;

Γ^{ζ} is the ζ-th modal participation factor;

λ Shape function related to the wall horizontal displacement do to the sheathing-to-framing connection deformation

λ is the shape function related to the wall horizontal displacement do to the sheathing-to-framing connection deformation;

ω is the circular frequency of a single-wall;

Φ^{ζ} is the ζ-th mode-shape;

τ Hold-downs dimensionless internal lever arm

τ is the hold-downs dimensionless internal lever arm;

τ is the internal level arm ratio of the hold-downs;

$\tilde{U}_{j,\xi}$ is j, ξ-th element of the flexibility matrix of the multi-storey shear-wall;

ξ is the ratio between the force activating the friction block and the strength of the wall;

b is the width of the sheathing-panels;

CLT Cross Laminated timber wall

F Horizontal force applied on the shear-wall

F is the horizontal external force applied to a wall;

f is the natural frequency of a single wall;

F_q is the magnitude of the horizontal force which activates the friction block;

F_N is the equivalent horizontal force due to the vertical load;

G_p Sheathing panel Shear modulus

G_p is the sheathing panel Shear modulus;

h Height of the shear-wall

h is the height of the shear-wall;

i_a Angle brackets or screws spacing

i_a is the angle-brackets or screws spacing;

K_A is the stiffness of the equivalent horizontal spring related to the angle-brackets;

k_a Angle bracket stiffness

k_a is the stiffness of the angle-brackets;

k_c Sheathing-to-framing fastener stiffness

k_c is the sheathing-to-framing fastener stiffness;

k_c is the stiffness of the nails;

K_H is the stiffness of the equivalent horizontal spring related to the hold-downs;

k_h Hold-down stiffness

k_h is the hold-down stiffness;

k_h is the stiffness of the hold-downs;

K_P is the sheathing panel shear stiffness;

K_{SH} is the stiffness of the equivalent horizontal spring related to the sheathing-to-framing connection;

$K_{tot,nt}$ is the stiffness of the wall when the rigid rotation contribution is not considered;

K_{tot} is the stiffness of the wall when the rigid rotation contribution is considered;

K_W is the stiffness of the wall;

l Length of the shear-wall

l is the length of the shear-wall;

l is the length of the wall;

n_h is the number of hold-downs;

n_{bs} Number of braced sides of the wall (1 or 2)

n_{bs} is the number of braced sides of the wall (1 or 2);

OSR is the Over Strength Ratio;

q Vertical distributed load

q is the vertical distributed load;

s_c Sheathing-to-framing fastener spacing

s_c is the sheathing-to-framing fastener spacing;

T is the period of vibration of a single-wall;

t_p Sheathing panel thickness

t_p is the sheathing panel thickness;

T_{HD} is the tensile force acting in the Hold-down;

TF Timber-frame wall

$V_{j,i}$ is the shear force acting in the j, i-th shear-wall;

8. References

[1] Tomasi, R., Sartori, T., Casagrande, D., Piazza, M.. Shaking table testing of a full scale prefabricated three-story timber framed building. Journal of Earthquake Engineering 2014;.

[2] Pozza, L., Scotta, R., Trutalli, D., Ceccotti, A., Polastri, A.. Analytical formulation based on extensive numerical simulations of behavior factor q for clt buildings. In: Proceedings of the 46th meeting of the working commission W18-timber structures, CIB, Vancouver, Canada, paper CIB-W18/46-15-5. 2013,.

[3] van de Lindt, J.W., Pei, S., Pang, W., Shirazi, S.M.H.. Collapse testing and analysis of a light-frame wood garage wall. Journal of Structural Engineering 2012;138(4):492–501. doi:10.1061/(ASCE)ST.1943-541X.0000472. URL http://link.aip.org/link/?QST/138/492/1.

[4] Folz, B., Filiatrault, A.. Seismic analysis of woodframe structures. i: Model formulation. Journal of Structural Engineering 2004;130(9):1353–1360.

[5] Folz, B., Filiatrault, A.. Seismic analysis of woodframe structures. ii: Model implementation and verification. Journal of Structural Engineering 2004;130(9):1361–1370.

[6] Christovasilis, I.P.. Numerical and experimental investigations of the seismic response of light-frame wood structures. State University of New York at Buffalo; 2011.

[7] Leung, T., Asiz, A., Chui, Y.H., Hu, L., Mohammad, M.. Predicting lateral deflection and fundamental natural period of multi-storey wood frame buildings. In: Proceedings of World conference timber engineering. 2010,.

[8] Polastri, A., Pozza, L., Trutalli, D., Scotta, R., Smith, I.. Structural characterization of multi-storey buildings with clt cores. 2014,.

[9] Reynolds, T., Bolmsvik, ., Vessby, J., Chang, W.S., Harris, R., Bawcombe, J., et al. Ambient vibration testing and modal analysis of multi-storey cross-laminated timber buildings. 2014,.

[10] Casagrande, D., Rossi, S., Sartori, T., Tomasi, R.. Proposal of an analytical procedure and a simplified numerical model for elastic response of single-storey timber shear-walls. Construction and Building Materials 2015;DOI:10.1016/j.conbuildmat.2014.12.114.

[11] UNI EN 1998-1:2013, . Eurocode 8: Design of structures for earthquake resistance part 1: General rules, seismic actions and rules for buildings. 2013. Brussels, Belgium: CEN, European Committee for Standardization.

[12] Casagrande, D., Rossi, S., Tomasi, R., Mischi, G.. Apredictive analytical model for the elasto-plastic behaviour of a light timber-frame shear-wall. Construction and Building Materials -IN PRESS- 2015;.

[13] Grossi, P., Sartori, T., Tomasi, R.. Tests on timber frame walls under in-plane forces: Part 1. Proceedings of the Institution of Civil Engineers-Structures and Buildings 2014;Special Issue on Seismic Test on Timber Buildings:xx.

[14] Grossi, P., Sartori, T., Tomasi, R.. Tests on timber frame walls under in-plane forces: Part 2. Proceedings of the Institution of Civil Engineers-Structures and Buildings 2014;Special Issue on Seismic Test on Timber Buildings:xx.

[15] Doudak, G., Smith, I., McClure, G., Mohammad, M., Lepper, P.. Tests and finite element models of wood light-frame shear walls with openings. Progress in Structural Engineering and Materials 2006;8(4):165–174.

[16] Conte, A., Piazza, M., Sartori, T., Tomasi, R.. Influence of sheathing to framing connections on mechanical properties of wood framed shear walls. Proceedings of Italian National Association of Earthquake Engineering, ANIDIS 2011;.

[17] Pauley, T., Priestley, M.. Seismic design of reinforced concrete and masonry structures, j. J Wiley & Sons, INC USA 1992;.

[18] Petrini, L., Pinho, R., Calvi, G.M.. Criteri di progettazione antisismica degli edifici. IUSS Press; 2004.

Chapter 4

Elasto-plastic behaviour of single-storey light timber-frame shear-walls

4.1 Introduction

The modern seismic design of buildings, regardless the structural type and the structural material, permits the structure to exceed the elastic range. In other words, it allows the structure to be seriously damaged both in the non-structural elements and in the structural-ones after a seismic event. This type of design approach may seem conceptually wrong: design a structure admitting damage such as to make convenient the demolition and reconstruction rather than the rehabilitation of the building seems indeed a nonsense. Actually, in view of the intensity and the rarity of earthquakes, economically speaking, a more traditional design could be unsustainable and therefore not competitive.

The admitted level of damage, as well as the verification of the residual vertical resistance that the building shall have in order to ensure the safeguard

of the people inside the building itself, is however the responsibility of the designer. This design philosophy, updated and improved, is commonly known as *Performance based design* and it therefore is a *limit state approach* based on the displacement demand and displacement capacity of the structures.

It is evident that this type of design implies a deep and strong knowledge of the behaviour of the buildings: from one-side, in order to force the activation of a determined failure mechanism; on the other-side, in order to ensure the attainment of a specific level of ductility. In other word, the knowledge of the correlation between the mechanical properties of the base-components and the overall behavior of the structure is required .

With the purpose to establish the relationship between the three principal base-components of a light timber-frame shear-wall (namely the sheathing-to-framing connection, the hold-down and the angle-brackets) with the displacement capacity as well as the ductility level, in the following Section, the study of the post-elastic behaviour of single timber shear-wall is presented. This study represents a key aspect in the analysis of the seismic design of light timber-frame buildings because it aims to develop an analytical relation between the ductility of a wall and the ductility of the yielded base component.

This analysis is performed by extending the UniTn-Model (see Ch. 2) in the post-elastic range by modeling the base-components through three non-linear springs which have a bi-linear elasto-perfectly plastic force-vs-displacement curves (see Fig. 4.1). The use of an elasto-perfectly plastic behaviour has been chosen with the aim of developing a simplified but reliable approach which allows to modeling a shear-wall by means of only three curves, without the need to perform laboratory tests for the definition of the typical parameters needed to calibrate the various nonlinear models available in the literature. This type of simplified approach may be less accurate in terms of curve-fitting than other models, especially talking about strength, but it provides quite good results in terms of displacement capacity and therefore in terms of ductility. It also has the advantage to be useful to model full-scale building, even large

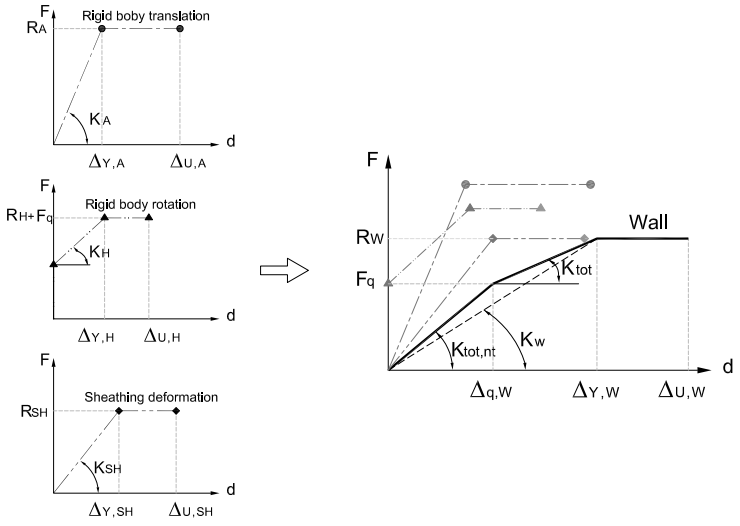

Figure 4.1: *Tri-linear mechanical curve wood-framed wall.*

buildings, without a high computational efforts.

The use of an elasto-perfectly plastic behaviour for the base components led to describe the behaviour of the whole wall typically by means of a three-linear curve (see Fig. 4.1). It is worth noting that a single-wall, even if extended to the post-elastic range, can still be defined as a system of springs placed in series and therefore remains an isostatic system. This aspect implies that the post-elastic behaviour is strongly influenced by the features of the spring which models the weakest base-component. On the basis of the constitutive law adopted, it has to be remarked that the strength of the wall is equal to the yielding force of the weakest component.

Taking into consideration one deformation contribution at a time, namely hypothesizing that the other deformation contributions can be considered infinite rigid, through some mathematical manipulations it is possible to determine the strength, the yielding and ultimate displacement, as well as the ductility of the wall, on the basis of the features of the deformation contribution considered.

Considering the angle-brackets it is possible to evaluate the following expressions:

$$R_A = \frac{r_a \cdot l}{i_a} = r_a \cdot n_a \tag{4.1}$$

$$K_A = \frac{k_a \cdot l}{i_a} = k_a \cdot n_a \tag{4.2}$$

$$\Delta_{Y,A} = \delta_{y,a} \tag{4.3}$$

$$\Delta_{U,A} = \delta_{u,a} \tag{4.4}$$

$$\mu_A = \frac{\delta_{u,a}}{\delta_{y,a}} = \mu_a = \frac{\Delta_{U,A}}{\Delta_{Y,A}} \tag{4.5}$$

Considering the hold-down it is possible to evaluate the following expressions:

$$R_H = n_h \cdot \frac{r_h \cdot \tau \cdot l}{h} \tag{4.6}$$

$$K_H = \frac{R_H}{\Delta_{Y,H}} = n_h \cdot k_h \cdot \left(\frac{\tau \cdot l}{h}\right)^2 \tag{4.7}$$

(4.8) $$\Delta_{Y,H} = \frac{\delta_{y,h}}{\tau \cdot l} \cdot h$$

(4.9) $$\Delta_{U,H} = \frac{\delta_{u,h}}{\tau \cdot l} \cdot h$$

(4.10) $$\mu_H = \frac{\Delta_{U,H}}{\Delta_{Y,H}} = \frac{\delta_{u,h}}{\delta_{y,h}} = \mu_h$$

Considering the angle-brackets it is possible to evaluate the following expressions:

(4.11) $$R_{SH} = n_{bs} \cdot r_c \cdot \frac{\sum b_i \cdot c_i}{s}$$

(4.12) $$K_{SH} = \frac{n_{bs} \cdot k_c}{s \cdot \sum \frac{\lambda_i(\alpha_i)}{b_i}}$$

(4.13) $$\Delta_{Y,SH} = \frac{R_{SH}}{K_{SH}}$$

(4.14) $$\Delta_{U,SH} = \mu_{SH} \cdot \Delta_{Y,SH}$$

$$\mu_{SH} = \rho(\alpha) \cdot \mu_c + \nu(\alpha) \tag{4.15}$$

The equations related to the sheathing-to-framing deformation have been determined through a incremental static analysis by considering for the nails a circular yielding surface in according with the specification of the Eurocode 8. In fact, the strength and the stiffness of a nail is not dependent on the angle between the wood grain and the force direction.

The relationship between the ductility of the nails and that of the wall is linear and it depends only on the shape of the sheathing panels and therefore it is not related to the nails spacing. This is a fundamental aspect for the non-linear analysis of timber buildings; in fact, thanks to this, it is possible to evaluate the ductility of a building independently from the nails spacing, which is often variable at different storey.

In order to prove and validate that the ductility of a light timber-frame wall is not dependent on the nails spacing, a set of four specifically developed laboratory tests has been performed. The specimens tested were four light timber shear wall of 1.25 x 2.5 m geometrically equal, braced by one sheathing layer of OSB/3, see Fig. 4.2.

Four monotonic tests were performed; each test has been done under displacement control, the applied displacement velocity was of 0.1 mm/sec. The displacement was imposed to the specimens by a MTS-244 hydraulic-actuator; the tests were carried out in the The Materials and Structural Testing Laboratory of the Dpt. of Civil, Environmental and Mechanical Engineering of the University of Trento. The test set-up was composed by a heavy timber reaction frame on which a system of four lever-arms were connected and by a steel sole-plate, which is used to anchor the walls to the ground.

In order to reproduce the fully-anchoring conditions, namely with the aim to avoid both the rigid-body rotation and the rigid-body translation, the spec-

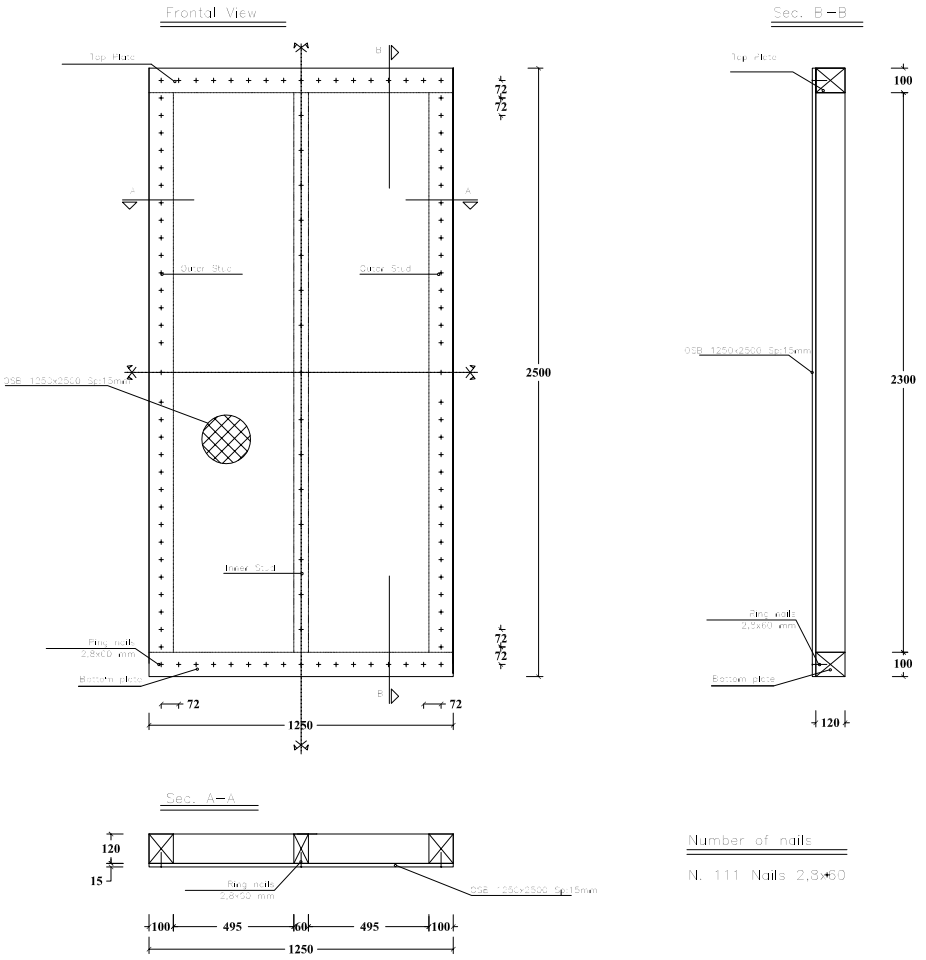

Figure 4.2: *M-D-B8 Specimen, nails spacing =144mm.*

(a) LockPlate; (b) Hold-Down;

Figure 4.3: *Connecting-devices: hold-down and locking rectangular tube.*

imens were connected to the ground by means of two specifically developed connection devices see Fig. 4.3. In detail, the horizontal translation was prevented thanks to a rectangular tube made of steel of grade S355, anchored to the sole-plate of the set-up. The uplifting was instead prevented using a hold-down made of steel of grade S355 bolted to the sole-plate of the setup. The hold-down was built specifically for the tests and it is designed to withstand a tensile force of 350 kN.

It is worth noting that the hold-down (see Fig. 4.4) is composed by two parts connected each-other by means of a cylindrical hinge, made by a steel dowel of grade S355 with a diameter of 25 mm. In other words, the hold-down allows the specimens to rotate and deform without its vertical flange giving the system a flexural stiffness which could affect the result of the tests.

Each test was monitored by-means of five instruments:

- the load-cell of the actuator to measure the applied-horizontal-force;
- a LVDT transducer incorporated in the actuator to control the applied-horizontal displacement;
- a wire potentiometer to measure the horizontal displacement of the top rail of the walls;

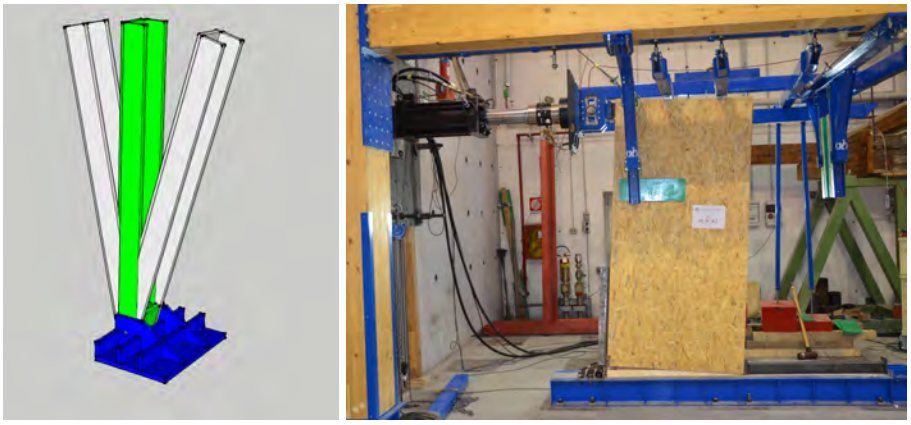

(a) 3D-Sketch; (b) Test picture;

Figure 4.4: *The Hold-down can rotate to allow the shear deformation of the sheathing-to-framing connection.*

- two LDVT to measure the uplifting and the rigid-body translation.

The properties of the load-cell incorporated in the actuator (see Fig. 4.5) are shown in in Tab. 4.1;

Properties of MTS 661.31F-01			
Force Capacity $[kN]$	**Spring Rate** $10^6\,[N/mm]$	**Diameter** $[mm]$	**Lenght** $[mm]$
1000	10	222	305

Table 4.1: *MTS actuator data.*

The displacement transducers were LVDT HBM WA-T 100 (see 4.6), their properties are show in Tab. 4.2.

The wire potentiometer was a $\mu\epsilon$ WDS-100-P60-CR-P, its features are shown in Tab. 4.3.

The tests results confirm that the ductility of a wall is not related to the nails spacing; in fact considering the chart of Fig. 4.8, it is clear that the yielding points as well as the ultimate displacements can be considered constant for all nails spacing.

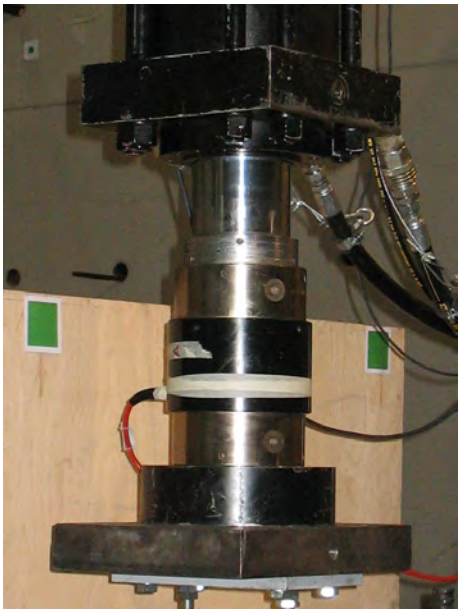

Figure 4.5: *Load cell on the hydraulic jack.*

Version	probe
Type of ceonnection	half and full bridge
Sensitivity	+ 80 $[mV/V]$
Linear deviation	$\pm 0,2$ to $\pm 0,1$
Degree of protection	IP 67 (IP 54)
Nominal displacement	100 mm
Nominal Temperature range	$-20 \div 80$ ÂřC
Carrier frequancy	$4,8 \pm 1\%$ $[kHz]$

Table 4.2: *HBM WA-T 100 Technical data.*

Linear deviation	$\pm 0.5\%$
Degree of protection	IP 65
Nominal displacement	100 mm
Nominal Temperature range	$-20 \div 80$ ÂřC

Table 4.3: *WDS-100-P60-CR-P Technical data.*

Anyway, it is not possible to directly apply the Eq. 4.15 to the specimens in order to assess their ductility and to compare the analytical values with the

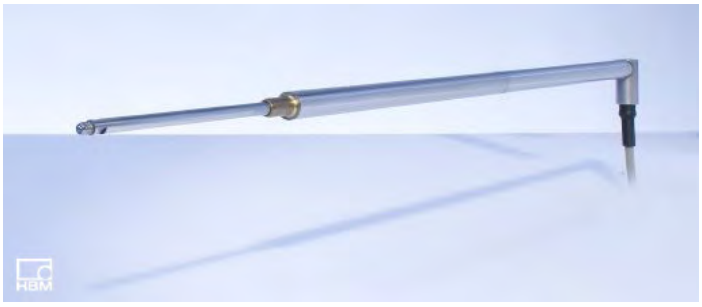

Figure 4.6: *Inductive displacement transducer HBM WA-T 100.*

Figure 4.7: *Wire potentiometer WDS-100-P60-CR-P.*

laboratory-test values of the ductility because of the variability that characterizes the wood and which does not allow to determine in an unequivocal and final manner the ductility of the nails.

Therefore, in order to further validate the proposed theory, some non-linear staged analysis on a set F.E. Models made on SAP 2000 (see Fig. 4.9) were performed. The aim of the analyses is assess the ductility of the wall by varying the ductility of the nails.

The wall modeling and it analysis require a quite high computational effort and need a special attention in the definitions of the nails link because of the nails yielding surface and the force directions. In fact, as stated before, the

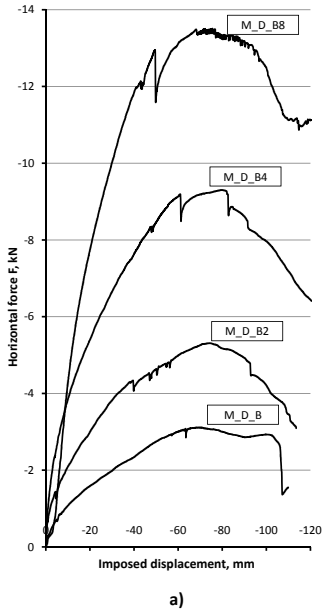

Figure 4.8: *Test results: Force-vs-Displacement curves.*

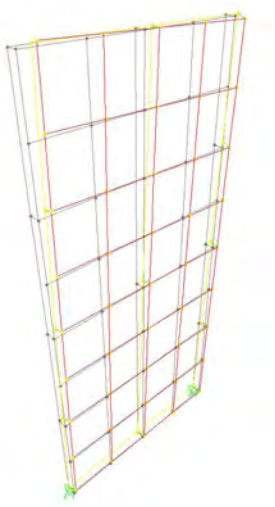

Figure 4.9: *SAP200 Non-linear model.*

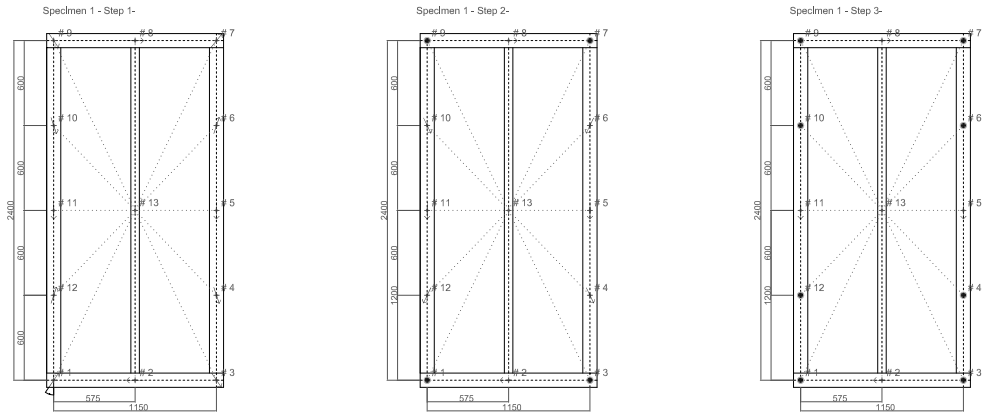

Figure 4.10: *Force rotation during the analysis.*

yielding surface of the nails is circular, namely it does not have a principal axis and the nails behave in a isotropic manner (see Fig. 4.11) and the force acting on the nails changes directions during the analysis.

Specifically, the force direction is dependent on both the position and number of the nails used for the sheathing-to-framing connection and on their stress. In fact, as shown in Fig. 4.10, the force direction rotates when some nails reach the yielding conditions. This aspect involves the need of the rotation of the axes of the links used to model the nails.

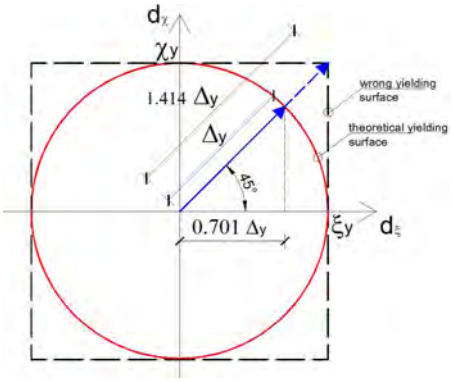

Figure 4.11: *Yielding surface of the nails.*

The rotation of the links axes is a fundamental aspect and it is needed to

provide nails with a circular yielding surface; it has to be remarked that the use of a rectangular surface would provide a wrong estimation of the strength of the system and also a not correct value of ductility, see Fig. 4.11.

In the chart of Fig. 4.12, as an example, are shown the capacity curve of two models: the higher and wrong curve is determined adopting for the nails a rectangular yielding-surface whereas the lower curve is determined using the correct circular yielding-surface.

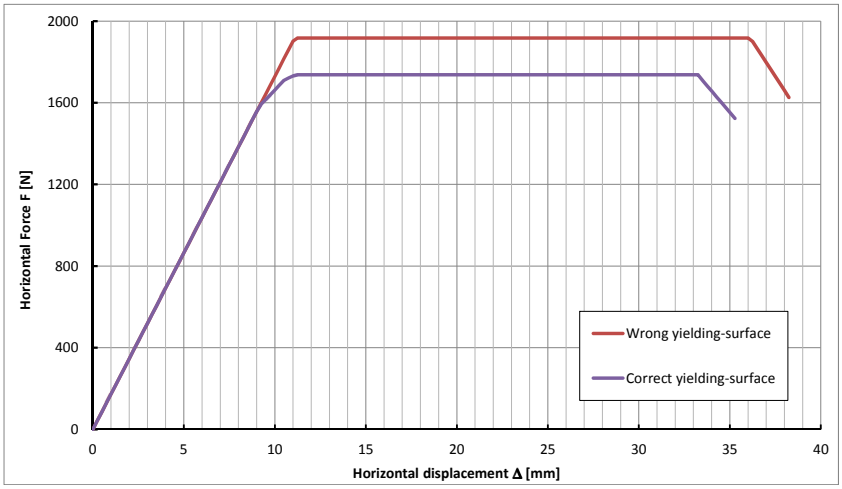

Figure 4.12: *Push-over curves of the walls.*

These analyses confirm the fact that the ductility of the wall is not dependent on the nails spacing and provide the same results of the analytical formulation proposed. The ductility of the wall of Fig. 4.12, using nails with a ductility equal to 4, is equal to: $\mu_{SH,SAP} = \frac{33.1}{9.7} = 3.41$; it can be noted that this value is very close to that determined by Eq. 4.15, in fact:

$$
\begin{cases}
\rho = -0.054 \cdot \alpha^2 + 0.350 \cdot \alpha + 0.305 \\
\quad -0.054 \cdot \left(\dfrac{2400}{1150}\right)^2 + 0.350 \cdot \dfrac{2400}{1150} + 0.305 = 0.800 \\
\nu = 0.068 \cdot \alpha^2 - 0.415 \cdot \alpha + 0.753 \\
\quad 0.068 \cdot \left(\dfrac{2400}{1150}\right)^2 - 0.415 \cdot \left(\dfrac{2400}{1150}\right) + 0.753 = 0.183
\end{cases} \tag{4.16}
$$

$$
\mu_{SH} = \rho(\alpha) \cdot \mu_c + \nu(\alpha) = 0.800 \cdot 4 + 0.183 = 3.38 \tag{4.17}
$$

4.2 Appended Paper III

A predictive analytical model for the elasto-plastic behaviour of a light timber-frame shear-wall

Daniele Casagrande, Simone Rossi, Roberto Tomasi, Gianluca Mischi

Construction and Building Materials, Elsevier (2015);
doi:10.1016/j.conbuildmat.2015.06.025

A predictive analytical model for the elasto-plastic behaviour of a light timber-frame shear-wall ☆

Daniele Casagrande[1], Simone Rossi[2,*], Roberto Tomasi[3], Gianluca Mischi[4]

Department of Civil, Environmental and Mechanical Engineering, University of Trento, Italy, Tel. +39 0461 282529

Abstract

This paper presents a predictive analytical model for the elasto-plastic behaviour of a light timber-frame wall under horizontal loading. The possibility to represent the total force carried by all fasteners (allowing for their sequential yielding) in one nonlinear spring is shown to be a key benefit. The development of this spring was investigated via a parametric study in which the variables were the sheathing panel aspect ratio and the fastener spacing. By developing equivalent springs for the other components, a rheological model for elasto-plastic behaviour of a sheathed timber-frame as function of the mechanical properties of connections was also defined.

Keywords:
Light timber-frame wall, Elasto-plastic behaviour, Analytical model, Ductility, Seismic capacity, Experimental tests

☆This document is a collaborative effort.

*Corresponding Author
Email address: simone.rossi1@unitn.it (Simone Rossi)
[1]Civil Engineer, Ph.D., Assistant Researcher, daniele.casagrande@unitn.it
[2]Civil Engineer, Ph.D. Candidate
[3]Civil Engineer, Ph.D., Assistant Professor
[4]M.Sc Civil Engineer

1. Introduction

A fundamental step in the investigation of the seismic capacity of light timber-frame shear-walls structure is the study of the non linear behaviour of a single shear wall. The most common strategies in seismic analysis and design consider in fact that the structure global capacity strongly depends on the local ductility of the structural elements. Structures are hence designed so that the seismic energy dissipation is located in some structural components which should be designed to yield during a seismic event (ductile elements). On the contrary, the other components must be designed to remain in the elastic range (brittle components) according to the capacity design approach [1], [2] & [3].

Several seismic analysis methods are suggested by Standards, but linear elastic analyses are mostly performed in practice. The nonlinear response of the structure to the seismic event is then considered by modification of the elastic seismic forces via the behaviour factor of the structure. This depends on the global over-strength of the structure and on the global ductility, which, in turn, is related to the ductility of the local components. For this reason, in order to define accurately the q value of a timber structure (see [4] and [5]), the relationship between the ductility of the components (e.g. fasteners, hold-downs, angle-brackets, etc.) and the global ductility should be pre-determined. In several international Standards for seismic design of light timber-frame buildings, values of q are suggested. However, a specific relationship between the local and the global ductility of the structure, differently from other structural types, e.g. concrete or steel, is not provided. Local components, where the yielding is expected, should in fact be designed by reference to the ductility demand of the entire structure: the greater the q value, the higher the ductility demand of the local components. An analytical relationship is hence necessary to determine the local demand.

For this purpose a predictive analytical model for the elasto-plastic behaviour of a light timber-frame shear wall under horizontal loading is presented in this paper. In particular, the main goal of this model is to link the local

properties, i.e. ductility, of each component to the global properties of a single wall. This does not fully define the required relationship, but it represents the first fundamental step. One of the key parts of the work presented in the next sections is in fact the representation of the mechanical behaviour of all sheathing-to-frame fasteners in one nonlinear horizontal spring. This approach reduces considerably the complexity of the wall model and for this reason it may be very suitable to analyse the non-linear behaviour of an entire building. The number of degrees-of-freedom and hence the run-time of the model are in fact significantly lower than those of a model where all fasteners are represented as non linear elements. The employment of the non linear static analysis method on several timber-frame structures represents in fact one of the future possible developments of the work presented in this paper, correlating the ductility of each wall to the global structure ductility.

2. Analytical models for the behaviour of light timber-frame shear-walls under horizontal loading

The elastic behaviour of a light timber-frame shear-wall subjected to a horizontal load can be obtained by means of several analytical expressions proposed in literature or in Standards, considering different contributions to deflection from structural components. In [6] four contributions are taken into account, due to sheathing-to-framing connection, the shear deformation of panel, the wood-frame and the rigid-body rotation of the wall caused by the compression perpendicular to the grain of the compressed stud respectively. The same deformation contributions are reported in the [7] considering in the rigid-body rotation of the wall also the deformation of anchor devices subjected to a tensile force. On the contrary, in [8] the rigid-body rotation contribution is calculated only from the total vertical elongation of the wall anchorage system. A similar approach was proposed in [9] and [10] defining an equivalent single degree of freedom model. In the model proposed in [11] four contribution are considered too, neglecting the wood-frame contribution and the compression perpendicular

to the grain, but adding the rigid-body translation of the wall due to anchorage system and taking into account the stabilizing effect of the vertical load acting on the wall.

Regarding the non-linear behaviour, many studies were conducted to investigate the capacity of timber shear-walls under horizontal loads simulating seismic actions, see [12], [13], [14], [15] and [16]. However, most of them were focused on experimental tests or advanced numerical modeling rather than on the proposal of an analytical expression to predict the non-linear behaviour.

In [17] a plastic model is proposed for the analysis of fully anchored light frame-timber shear-walls applying the upper and lower bound methods and evaluating the plastic strength of a fully anchored wall. The expressions proposed in [10], characterized by linear relationship to the sheathing-to-fastener deformation e_n and to the anchorage connection deformation d_a, might be used also in the non-linear range since the displacement of the wall due to these two contributions was obtained by geometrical considerations on the deformation of the wall.

In the paper an alternative approach is proposed to predict analytically the elasto-plastic behaviour of a timber shear-wall by means of the definition of a rheological model. The deformation contributions taken into account refer to the elastic model suggested in [11] which includes the mathematical model proposed in [18] for the sheathing-to-framing fastener deformation. However, as reported in next sections, more deformation contributions can be added to the rheological model if these cannot be neglected.

3. Rheological model for the elasto-plastic behaviour of a light timber-frame shear wall

According to [11] the elastic behaviour of a light timber-frame shear wall under a horizontal force F and a uniform distributed vertical load q, can be represented by a simple pinned frame, braced by a horizontal spring of stiffness equal to K_{SH} representing the sheathing-to-framing connection see Figure 1.

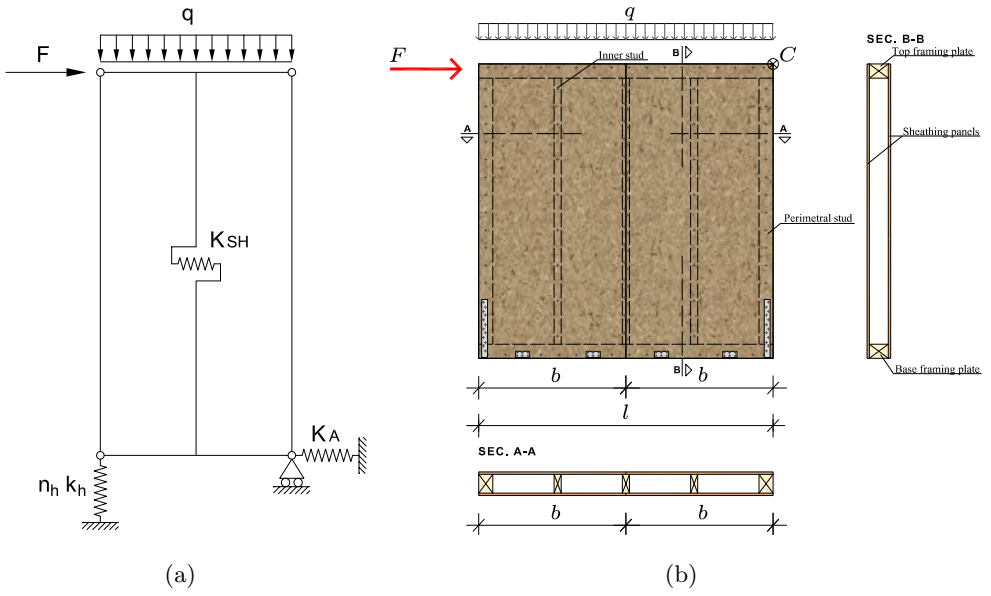

Figure 1: Light timber-frame wall: a) simplified numerical model, b) configuration

The contribution given by the devices, which prevents the horizontal translation of the wall, is represented by horizontal spring of stiffness K_A connected to the ground, whereas the rigid-body rotation, arising from the hold-down device, is taken into account by means of a vertical spring of stiffness equal to k_h. The replacement of the sheathing-to-framing connection fasteners with a single horizontal spring (K_{SH}) allows in fact a considerable reduction of the degrees of freedom of the model.

In [11] the frame internal equivalent spring is characterized by a stiffness equal to K_{SP}, which accounts for the sheathing-to-framing connection stiffness K_{SH} and the sheathing shear deformation K_P. Because K_P is usually much greater than K_{SH} we get: $\frac{1}{K_{SP}} = \frac{1}{K_P} + \frac{1}{K_{SH}} \cong \frac{1}{K_{SH}}$. Is important to note that to consider even the stiffness contribution of the sheathing panel K_P, K_{SH} has to be replaced in the following sections by K_{SP} .

The implementation of the wall model in the non-linear range is quite simple and straightforward: each spring is described in general by a non-linear curve. In order to obtain a simple analytical expression relating the behaviour of each

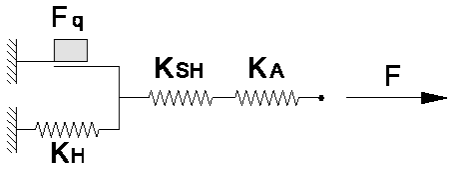

Figure 2: Rheological model

individual connection and of the wall, the non-linear behaviour of each spring is assumed to be described by an elasto-perfectly plastic idealized force vs displacement curve, characterized by stiffness, strength and ductility.

Assuming an elasto perfectly plastic behaviour of each model spring, the non-linear mechanical behaviour of the wall is therefore described by a bi-linear or tree-linear curve, as showed hereinafter, depending on the magnitude of the vertical distributed q.

In order to obtain a simple analytical relationship between the parameters (stiffness, strength and ductility) of each non-linear spring and the mechanical parameters of the wall, the model has been substituted by a rheological model characterized by means of two in-series non-linear horizontal springs (sheathing-to-framing K_{SH} and rigid translation K_A) and a third element, placed in series with the described horizontal springs, made up by a non-linear horizontal spring K_H (representing the rigid-body rotation) placed in parallel to a friction block (F_q) standing for the vertical load contribution, see Figure 2.

The main goal of the paper is to propose a general approach to relate the local mechanical properties to the wall ones in a general way. However, the rheological model can be updated adding other elasto-plastic springs if other deformation contributions were to be considered. The same approach reported in next sections (developed considering only the contributions due to hold-down, angle brackets and fasteners) can be adopted. The analytical expressions can be in fact easily modified.

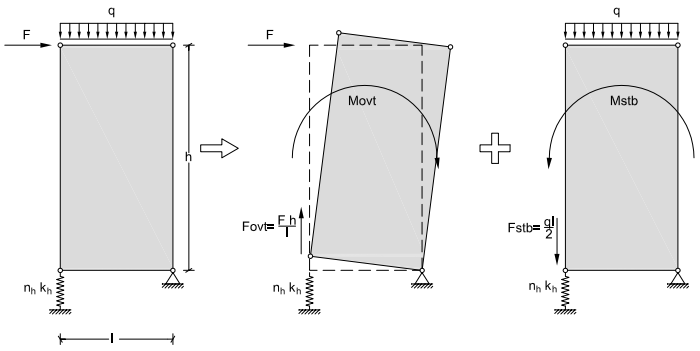

Figure 3: Overturning and stabilizing moment

3.1. Rigid-body rotation connection

The parameters, describing the mechanical behaviour of the rigid-body rotation connection, can be obtained by geometrical and mechanical observations of the simplified numerical model of the wall [11], depending on the vertical load q, on the geometry of the wall (height h and length l) and on the mechanical parameters that characterize the hold-down (stiffness k_h, strength R_H and ductility μ_h), Figure 5.

The hold-down device, used to prevent the wall from the rigid rotation, is loaded by a tensile force only in the event that the overturning moment M_{ovt}, caused by the horizontal force F, is greater than the stabilizing moment M_{stb}, resulting from vertical load q, see Figure 3. This condition occurs when:

$$M_{ovt} = F \cdot h \geq M_{stb} = \frac{q \cdot l^2}{2} \tag{1}$$

Hence the value F_q of the horizontal force which characterizes the friction block (Figure 4) is given by:

$$F_q = \frac{q \cdot l^2}{2 \cdot h} \tag{2}$$

If the horizontal force F is lower than F_q, the hold-down device is not in tension and the wall undergoes no rotation. On the contrary, if F is greater

than F_q , the hold-down device is in tension and the wall deformation is also characterized by the rigid-body rotation contribution.

The mechanical behaviour of the hold-down horizontal spring, see Figure 4, can be obtained from the hold-down elasto-perfectly plastic curve, see Figure 5, by-means of some simple analytical expressions. The hold-down horizontal elasto-perfectly plastic curve is characterized by the stiffness K_H, the strength R_H and the ductility μ_H, whereas the hold-down connection devices curve is described by the stiffness k_h, the resistance R_H and ductility μ_h.

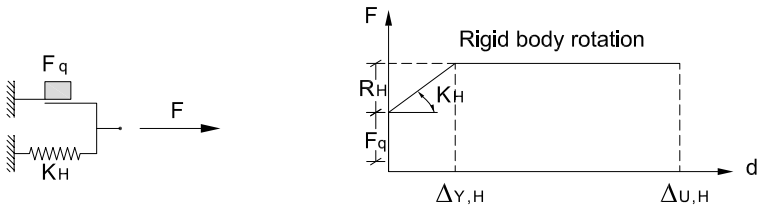

Figure 4: Rigid-rotation (horizontal) spring mechanical behaviour

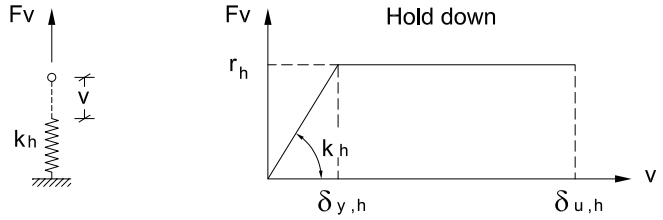

Figure 5: Hold-down mechanical behaviour

The strength R_H can be directly calculated from the hold-down strength r_h as:

$$R_H = n_h \cdot \frac{r_h \cdot \tau \cdot l}{h} \tag{3}$$

- R_H is the hold-down strength;

- l is the length of the wall;

- n_h is the number of hold-downs for each corner of the wall;

- τ represents the internal level arm ratio, usually between 0.95-1.

The yield displacement $\Delta_{Y,H}$ can be obtained by the hold-down yield displacement $\delta_{y,h}$, by means of a simple geometrical transformation:

$$\Delta_{Y,H} = \frac{\delta_{y,h}}{\tau \cdot l} \cdot h \tag{4}$$

The stiffness K_H is therefore given by:

$$K_H = \frac{R_H}{\Delta_{Y,H}} = n_h \cdot k_h \cdot \left(\frac{\tau \cdot l}{h}\right)^2 \tag{5}$$

Similarly, the ultimate displacement $\Delta_{U,H}$ can be obtained as:

$$\Delta_{U,H} = \frac{\delta_{u,h}}{\tau \cdot l} \cdot h \tag{6}$$

therefore the ductility μ_H is equal to the hold-down ductility μ_h, according to the following expression:

$$\mu_H = \frac{\Delta_{U,H}}{\Delta_{Y,H}} = \frac{\delta_{u,h}}{\delta_{y,h}} = \mu_h \tag{7}$$

3.2. Rigid-body translation connection

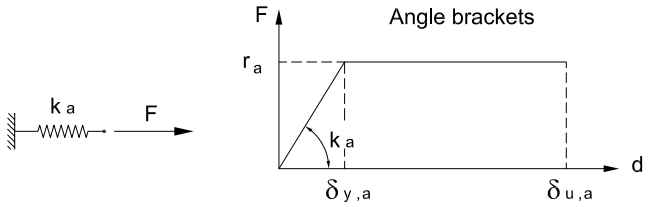

Figure 6: Angle brackets (or screws) mechanical behaviour

The rigid-body translation of the wall is usually prevented by means of metallic angle brackets (nailed or screwed to the wall) or inclined screws. If the

devices are placed along the wall length with constant spacing i_a the number of devices n_a can be obtained by:

$$n_a = \frac{l}{i_a} \tag{8}$$

The idealized elasto-perfectly plastic linear curve of each device can be obtained by a numerical model or by the bi-linearisation of the experimental curve, defining its strength r_a, its stiffness k_a and its ductility μ_a (Figure 6). The parameters, which characterize the mechanical behaviour of the horizontal non-linear spring K_A of the rheological model (Figure 7), can be obtained by isolating the contribution of the wall rigid translation :

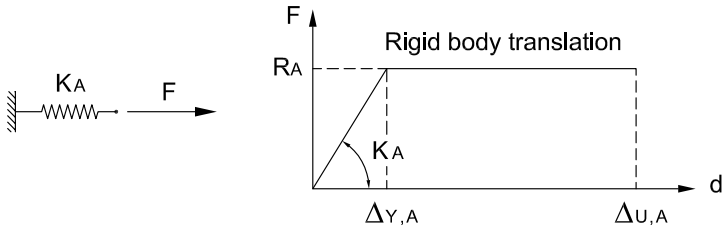

Figure 7: Rigid translation spring mechanical behaviour

$$\Delta_{Y,A} = \delta_{y,a} \tag{9}$$

$$\Delta_{U,A} = \delta_{u,a} \tag{10}$$

$$R_A = \frac{r_a \cdot l}{i_a} = r_a \cdot n_a \tag{11}$$

$$K_A = \frac{k_a \cdot l}{i_a} = k_a \cdot n_a \tag{12}$$

$$\mu_A = \frac{\delta_{u,a}}{\delta_{y,a}} = \mu_a = \frac{\Delta_{U,A}}{\Delta_{Y,A}} \tag{13}$$

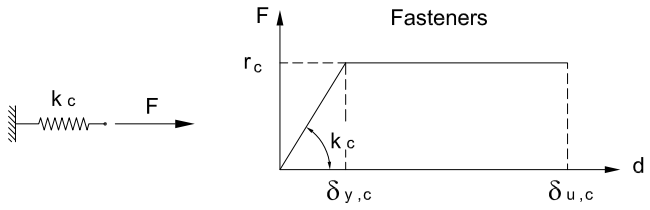

Figure 8: Fastener mechanical behaviour

3.3. Sheathing-to-framing connection

The sheathing-to-framing connection, represented by the horizontal non-linear spring indicated with K_{SH}, see Figure 9, takes into account the deformation contribution given by the fasteners (nails or staples) which connect the wood frame to the sheathing panel. However, the mechanical behaviour of the connection (and thus the strength R_{SH}, the stiffness K_{SH} and the ductility μ_{SH}) does not depend only on the mechanical behaviour of the fasteners (the strength f_c, the stiffness k_c and the ductility μ_c, see Figure 8), but it is also strongly influenced by their disposition. Since fasteners are generally placed with constant spacing along the edge of the panel, only the spacing s and the ratio between the height and the length of the panel h/b can be considered. Hence, in general, the mechanical behaviour of each fastener is not equal to the sheathing-to-framing connection one.

The fastener elasto-perfectly plastic curve can be obtained, for example, by experimental tests (monotonic or cyclic test, in the same way of angle brackets or hold-downs); performing experimental tests on full-scale walls, considering all the possible cases (varying the type of fastener, the fastener spacing s and the ratio h/b of the panel) results anyway burdensome and expensive. Consequently an analytical expression, relating the mechanical behaviour of the fasteners to the sheathing-to-framing connection one, is required.

In European Standard for timber structures [19] a relationship between the strength of fasteners f_c and the sheathing to panel connection strength R_{SH} is reported. This equation was obtained by means of the limit analysis static

theorem assuming an equal distribution of the shear stresses on the edge of the panel and hence a constant shear action on each fastener. For a light timber-frame wall braced by several panels with a width equal to b_i the expression is given by:

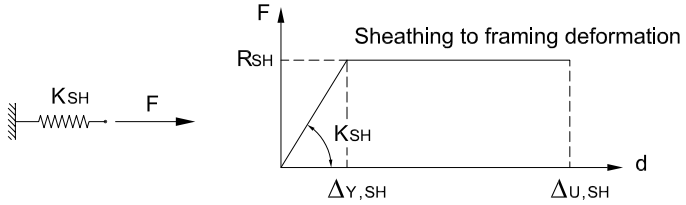

Figure 9: Sheathing-to-framing connection spring mechanical behaviour

$$R_{SH} = n_{bs} \cdot r_c \cdot \frac{\sum b_i \cdot c_i}{s} \tag{14}$$

where:

- n_{bs} is the number of the wall braced sides (1 or 2);
- $c_i = \begin{cases} 1 \; if \; \alpha < 2 \\ \frac{\alpha}{2} \; if \; 2 < \alpha < 4 \\ 0 \; if \; \alpha > 4 \end{cases}$
- $\alpha = \frac{h}{b}$ is the panel shape parameter;
- b_i is the panel width.

Moreover, the sheathing-to-framing connection strength R_{SH} can be increased by a factor equal to 1.2 according to the [19].

When the wood frame can be assumed rigid, namely the flexural deformation of studs and plats is negligible (this hypothesis can be assumed realistic in most cases, see [20]), the stiffness K_{SH} can be obtained directly by the model proposed in [18], known the stiffness k_c of fasteners, the spacing s, the panel parameter α and the wall length:

$$K_{SH} = \frac{n_{bs} \cdot k_c}{s \cdot \sum \frac{\lambda_i(\alpha_i)}{b_i}} \tag{15}$$

where $\lambda_j(\alpha_j) = 0.810 + 1.855 \cdot \alpha_j$, see [11].

According to Equations 14 and 15, the yield displacement $\Delta_{Y,SH}$ is therefore calculated as:

$$\Delta_{Y,SH} = \frac{R_{SH}}{K_{SH}} \tag{16}$$

whereas the ultimate displacement $\Delta_{U,SH}$ is given by:

$$\Delta_{U,SH} = \mu_{SH} \cdot \Delta_{Y,SH} \tag{17}$$

Concerning with the sheathing-to-framing connection ductility μ_{SH}, Standards do not specifically suggest an expression for its calculation, known the fastener ductility μ_c.

The equivalent single degree of freedom model [10], relates linearly the sheathing-to-framing connection deformation $\Delta_{SH} = \Delta_{nail}$ to the nail deformation δ_c according to linear geometrical assumptions:

$$\Delta_{nail} = \lambda_{swn} \cdot \delta_c \tag{18}$$

where λ_{swn} depends on geometrical properties of the panel. Hence it is not difficult to show that the sheathing-to-framing connection ductility μ_{SH} results equal to fastener ductility μ_c. However this model, differently from the model proposed in [18], is based on the assumption that the nails along the perimeter of the panel are equally stressed.

In section 4, an alternative analytical expression based on the model developed in [18] is proposed, evaluating the evolving stress in each nail due to the load increasing on the wall and demonstrating that in several cases the sheathing-to-framing connection ductility μ_{SH} results lower than the fastener ductility μ_c. A linear relationship is however confirmed.

3.4. Definition of the idealized elasto-perfectly plastic curve of a wood-framed wall

After defining the idealized elasto-perfectly plastic curve of each element of the rheological model (the three horizontal springs and the friction block), the elasto-plastic curve of the entire model, and hence of the wall, can be obtained. Known the mechanical behaviour of each component of the model, the mechanical properties, which define the model curve, can be calculated by means of simple mathematical expressions. As reported in Figure 10, the parameters of the curve are the friction block yield force F_q, the wall strength R_W, the wall stiffness $K_{tot,nt}$, when the rotation contribution is not considered (block friction not yielded), the wall stiffness K_{tot}, when the rotation contribution is considered, the wall secant stiffness K_W, the wall displacement $\Delta_{q,W}$ when the friction block yields, the wall yield displacement $\Delta_{Y,W}$, the wall ultimate displacement $\Delta_{U,W}$.

The friction block yield force F_q can be calculated according to Equation 2 depending on the wall geometry and the vertical load q.

The wall stiffness $K_{tot,nt}$ depends only on the sheathing-to-framing and the rigid-body translation contribution. It can be obtained by:

$$\frac{1}{K_{tot,nt}} = \frac{1}{K_{SH}} + \frac{1}{K_A} \tag{19}$$

The displacement $\Delta_{q,W}$ of the system for which the friction block yields results:

$$\Delta_{q,W} = \frac{F_q}{K_{tot,nt}} = \frac{q \cdot l^2}{2 \cdot h} \cdot \left(\frac{1}{K_{SH}} + \frac{1}{K_A} \right) \tag{20}$$

The wall strength R_W is defined as the minimum value from the strength of each connection (sheathing-to-framing, translation and rotation) according to the following expression:

$$R_W = min(R_H + F_q; R_A; R_{SH}) \tag{21}$$

The weakest connection, which firstly yields since characterized by the minimum strength, can be identified by the index i, defined as:

$$\begin{cases} if \quad R_W = R_H + F_q \rightarrow i = H \\ if \quad R_W = R_A \rightarrow i = A \\ if \quad R_W = R_{SH} \rightarrow i = SH \end{cases} \tag{22}$$

If the wall strength R_W is greater than the friction block yield force F_q, the curve of the mechanical behaviour of the wall is characterized by an additional linear elastic segment and for this reason it is described by a three-linear curve (Figure 10).

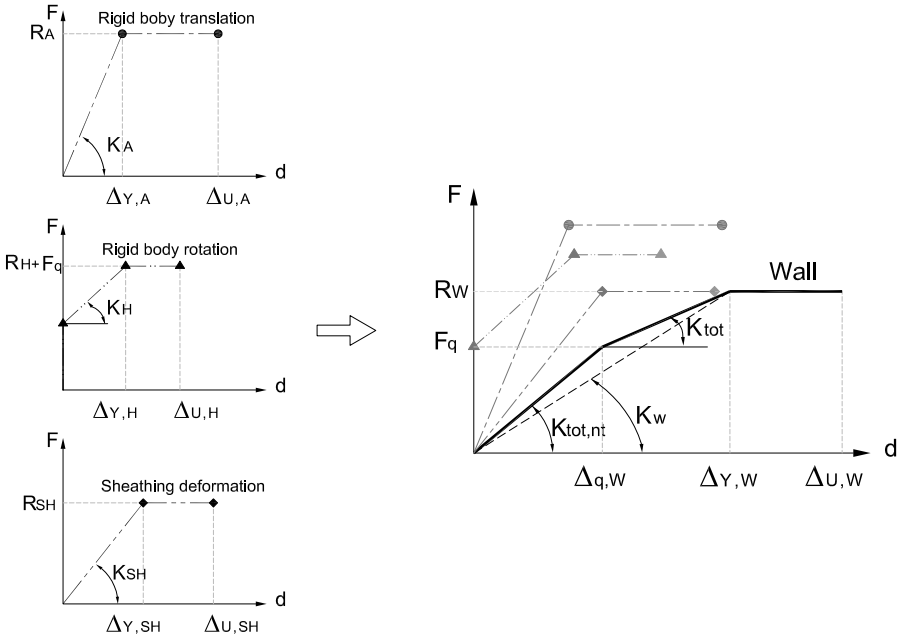

Figure 10: Trilinear mechanical curve wood-framed wall

The wall stiffness K_{tot} can be calculated taking into account the stiffness of each model component (sheathing-to-framing, translation and rotation) according to the following expression:

$$\frac{1}{K_{tot}} = \frac{1}{K_{SH}} + \frac{1}{K_A} + \frac{1}{K_H} \tag{23}$$

Therefore the wall yield displacement $\Delta_{Y,W}$ can be obtained by:

$$\Delta_{Y,W} = \frac{F_q}{K_{tot,nt}} + \frac{R_W - F_q}{K_{tot}} = \frac{R_W}{K_{tot}} - \frac{F_q}{K_H} \tag{24}$$

Hence the wall secant stiffness K_W, defined as the ratio between the wall strength R_W and the yield displacement $\Delta_{Y,W}$, is given by:

$$K_W = \frac{R_W}{\Delta_{Y,W}} = \frac{R_W}{\frac{R_W}{K_{tot}} - \frac{F_q}{K_H}} = \left(\frac{1}{K_{tot}} - \frac{F_q}{K_H \cdot R_W}\right)^{-1} \tag{25}$$

Substituting:

$$\xi = \frac{F_q}{R_W} \tag{26}$$

for $\xi < 1$ we get:

$$\frac{1}{K_W} = \frac{1}{K_{tot}} - \frac{\xi}{K_H} \tag{27}$$

When the wall strength R_W is lower than the block friction activation force F_q ($\xi > 1$) the friction block does not yield. This condition usually occurs in case of weak fasteners or a high vertical load. The mechanical curve of the wall is therefore bi-linear (Figure 11), and the secant stiffness K_W results equal to $K_{tot,nt}$.

$$\frac{1}{K_W} = \frac{1}{K_{tot,nt}} = \frac{1}{K_{SH}} + \frac{1}{K_A} \tag{28}$$

The wall yield displacement $\Delta_{Y,W}$ can be obtained by:

$$\Delta_{Y,W} = \frac{R_W}{K_{tot,nt}} = \frac{R_W}{\frac{1}{K_{SH}} + \frac{1}{K_A}} \tag{29}$$

Therefore, considering the two different cases, the wall secant stiffness K_W and the wall yield displacement can be defined by the following expressions:

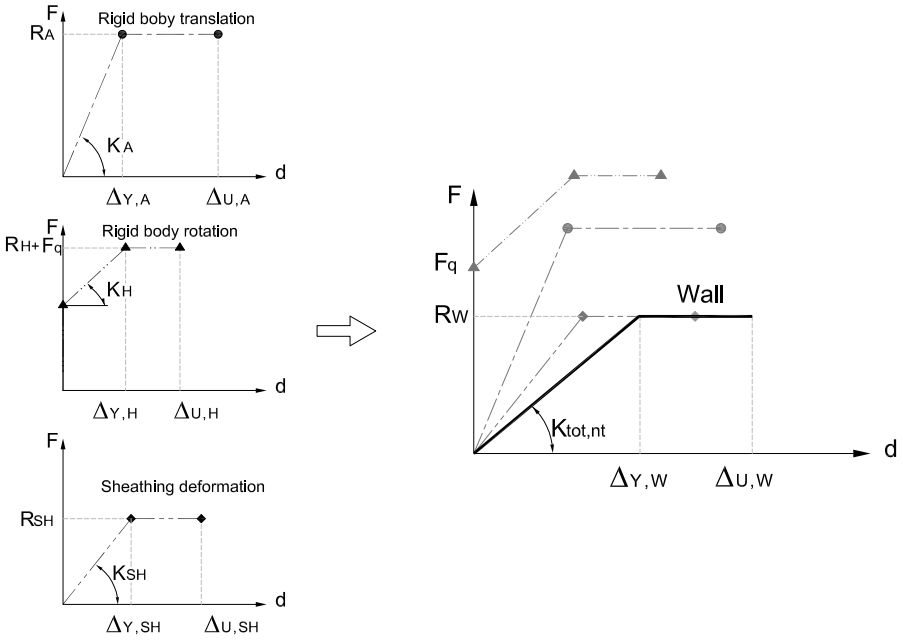

Figure 11: Bilinear mechanical curve wood-framed wall

$$\begin{cases} \xi \geq 1 \rightarrow \dfrac{1}{K_W} = \dfrac{1}{K_{tot,nt}} \\ \xi < 1 \rightarrow \dfrac{1}{K_W} = \dfrac{1}{K_{tot}} - \dfrac{K_{tot}}{K_H} \end{cases} \tag{30}$$

The wall yielding displacement $\Delta_{Y,W}$ can be calculated in both cases as:

$$\Delta_{Y,W} = \frac{R_W}{K_W} \tag{31}$$

For the evaluation of the wall ductility μ_W, the plastic displacement of the rheological model is equal to the plastic displacement of the weakest (and hence yielded) connection. For this reason, an increase of the system displacement is caused only by the stretch of the spring representing the weakest yielded connection. In fact, an increase of the stretch of the other elastic spring would require an increase of the external force F. Therefore we get:

$$\Delta_{pl,W} = \Delta_{pl,i} \tag{32}$$

The wall ductility μ_W is defined as the ratio between the wall ultimate displacement $\Delta_{U,W}$ and the wall yield displacement $\Delta_{Y,W}$. Because the ultimate displacement $\Delta_{U,W}$ is given by the sum of the yield displacement $\Delta_{Y,W}$ and the plastic displacement $\Delta_{pl,i}$ we obtain:

$$\mu_W = \frac{\Delta_{U,W}}{\Delta_{Y,W}} = \frac{\Delta_{Y,W} + \Delta_{pl,W}}{\Delta_{Y,W}} = 1 + \frac{\Delta_{pl,W}}{\Delta_{Y,W}} = 1 + \frac{\Delta_{pl,i}}{\Delta_{Y,W}} \tag{33}$$

The plastic displacement of the weakest connection $\Delta_{pl,i}$ can be correlated directly to the yield displacement of the same connection $\Delta_{Y,i}$ and to its ductility μ_i according to the following expression:

$$\Delta_{pl,i} \quad = \quad \Delta_{U,i} - \Delta_{Y,i} = \frac{R_i}{K_i} \cdot (\mu_i - 1) \tag{34}$$

Substituting Equations 31 and 34 in the Equation 33, we obtain:

$$\mu_W = 1 + \frac{\frac{R_i}{K_i} \cdot (\mu_i - 1)}{\frac{R_W}{K_W}} \tag{35}$$

If the weakest element is represented by the sheathing-to-framing connection or the rigid translation connection, the wall strength R_W is given by:

$$R_W = F_i \tag{36}$$

with:

$$i = SH \; or \; A$$

Therefore, the wall ductility can be obtained by the following simplified equation:

$$\mu_W = 1 + \frac{K_W}{K_i} \cdot (\mu_i - 1) = 1 + \kappa \cdot (\mu_i - 1) \tag{37}$$

As the κ parameter is lower than 1, the ductility of the weakest connection μ_i is always greater than the wall ductility μ_W.

If the weakest connection is represented by the sheathing-to framing or the translation connection ($i = SH\ or\ A$), in case of $\xi \geq 1$ we get:

$$\kappa = \frac{K_W}{K_i} < 1 \rightarrow \frac{1}{K_i} < \frac{1}{K_W} \rightarrow \frac{1}{K_i} < \frac{1}{K_{SH}} + \frac{1}{K_A} \tag{38}$$

whereas in case of $0 < \xi < 1$ we obtain:

$$\kappa = \frac{K_W}{K_i} < 1 \rightarrow \frac{1}{K_i} < \frac{1}{K_W} \rightarrow \frac{1}{K_i} < \frac{1}{K_{SH}} + \frac{1}{K_A} + \frac{1 - K_{tot}}{K_H} \tag{39}$$

If the weakest connection is represented by the rigid-body rotation one ($i = H$), we obtain:

$$R_W = R_H + F_q > R_H \tag{40}$$

In this case the wall ductility μ_W can be calculated by means of the following expression:

$$\mu_W = 1 + \frac{R_H}{R_H + F_q} \cdot \frac{K_W}{K_H} \cdot (\mu_i - 1) = 1 + \iota \cdot \kappa \cdot (\mu_i - 1) \tag{41}$$

Since $\kappa < 1$ and $\iota < 1$, as shown previously, the weakest connection ductility is greater than the wall ductility. For this reason, in order to maximize the wall ductility, the stiffness of the strong connections which has to remain in the elastic range, should be as great as possible so that the parameter κ tends to 1.

Known the wall ductility, the wall ultimate displacement $\Delta_{Y,W}$ can be obtained by:

$$\Delta_{U,W} = \mu_W \cdot \Delta_{Y,W} \tag{42}$$

4. Non-linear mechanical behaviour of a fully anchored light timber-frame wall

A light timber-frame wall is defined fully-anchored if the stiffness constraints, which prevent the rigid-body motion of the wall (K_A, K_H), can be

considered infinitely rigid. The wall deformation, according to the models described in the previous section, is represented only by the sheathing-to-framing connection contribution (K_{SH}).

In this section a fully anchored wall model is used to obtain an analytical relationship between the non-linear behaviour of the sheathing-to-framing connection ductility μ_{SH} and the fastener ductility μ_c. This relationship is in fact necessary, as reported in section 3.3, for the rheological model making.

The analytical expression was carried out by means of an elasto-plastic analysis, increasing step by step the external horizontal force F and assuming a redistribution of the forces of the fasteners.

The analysis was performed also defining a kinematic mechanisms of the wall as well, up to the wall failure condition related to the achievement of the acceptable ultimate displacement $\delta_{u,c}$ of one fastener at least.

The mathematical model proposed by [21] was used to perform the analysis at each step, assuming the wood-frame as rigid. According to that, the wall frame was represented by pinned beams (the frame is hence not restrained for horizontal loads) whereas the sheathing panel was assumed like a rigid-body. The fasteners were modeled by bi-directional elastic spring: the internal force of the fasteners was hence linear to their displacement, see Figure 12. The fasteners position was described considering a referring system placed in the center of gravity of the fasteners. Generally, the fastener disposition is symmetric (the fasteners are placed along the edge of the panel with an equal spacing), therefore the origin of the referring system was placed at the center of the panel. The external force F was applied at the top corner of the frame.

At each step the structure was analysed assuming its elastic behaviour (the solution was obtained by means of the method of minimum of the potential energy) after updating the stiffness matrix of the model in order to consider that some fasteners had already yielded at the previous steps.

When the stiffness matrix of the model becomes singular, further elastic steps are no more achievable: the structure is to be solved by means of the

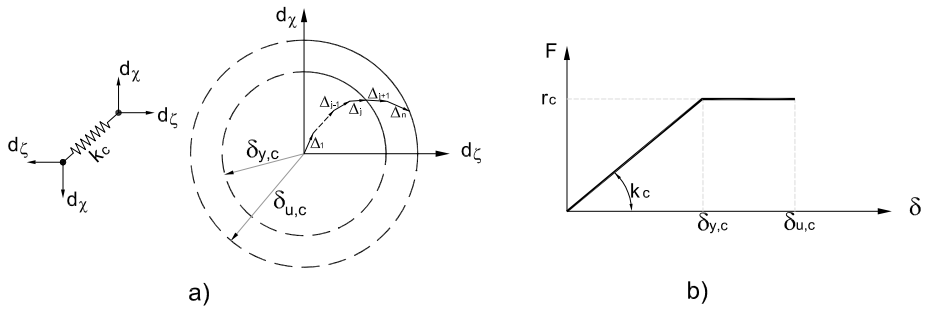

Figure 12: a) fasteners bi-directional spring and yielding surface; b) elastic-perfectly plastic behaviour of fasteners

kinematic theory.

According to [19], the yielding surface on the mathematical model of fasteners was assumed circular since fasteners have a small diameter and hence their mechanical properties are not influenced by the grain orientation. The yielding condition occurs when global displacement, obtained summing the relative displacement Δ_j, is equal to $\delta_{y,c}$. After the fastener has yielded, an internal constant force equal to r_c is assumed, independently on the direction of the fastener relative displacements in the plastic phase $\Delta_{j+1}...\Delta_n$, see Figure 12 (the ultimate displacement surface is assumed circular as well). As reported in [22], the assumption of circular surfaces to represent the internal state of the fasteners cannot be represented by two perpendicular springs, each of one is characterized by an elasto-plastic curve. In this case in fact the yielding surface is squared and the yielding condition is dependent on the direction. Assuming for example a loading direction of fastener equal to 45°, the yielding condition is reached when in both springs a displacement equal to $\delta_{y,c}$ is achieved. This corresponds to a global displacement equal to $\sqrt{2}\delta_{y,c}$, greater then $\delta_{y,c}$.

Analyzing the common cases in practice, three different types of kinematic-model for a light timber-frame wall can be defined. In each kinematic-model, the lateral stability of the wall is not longer ensured because of the progressive yielding of the fasteners. It is also important to remark that the stiffness of a yielded fastener is assumed equal to zero, according to the constitutive law

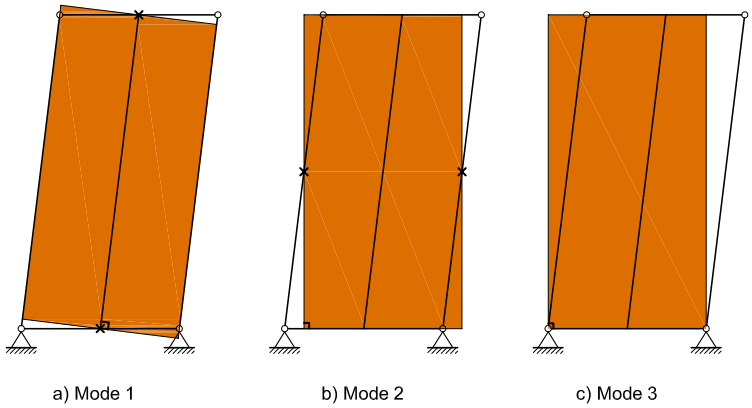

Figure 13: fully anchored wall kinematic mechanisms

used for it (see Figure 12).

The first kinematic model is defined *vertical rod*, see Mode 1 of Figure 13, because the fasteners are placed only along the intermediate vertical stud of the wall. For this reason the sheathing panel acts like a vertical rod, whose rotation is equal to the wood frame one.

The second kinematic model is defined *horizontal rod*, see Mode 2 of Figure 13. In this case the sheathing panel is connected to the frame by means of only two fasteners placed in the middle point of both perimeter studs. The sheathing panel acts like a horizontal rod characterized by a rigid-body horizontal displacement equal to half of the displacement of the top horizontal displacement of the wood frame.

The third kinematic model is defined *not restrained panel*, see Mode 3 of Figure 13, since no fastener connects the panel to the frame. The sheathing panel is in fact completely released from the wood framed.

The kinematic analysis is carried out by increasing the kinematic degree of freedom (usually represented by the top horizontal displacement of the frame) up to the failure condition, defined by the achievement of the ultimate displacement of one fastener at least.

However, the failure condition might be reached before the kinematic mecha-

nism of model occurs since one fastener might achieve its ultimate displacement when some other fasteners are not yielded yet. This condition usually occurs when the fastener spacing is little.

The force-displacement curve obtained by the elasto-plastic analysis is represented by a piecewise-linear curve. Each line segment is characterized by a gradually decreasing slope. The kinematic mechanism is represented by the last line segmented, characterized by an horizontal slope.

The analyses are based on the hypothesis that wood-frame is assumed rigid. As reported in [23], this assumption can be considered true for most of typical European walls where massive studs and plates are used. On the contrary, in case of small size of wood-frame elements (i.e. 2"x4") might be necessary to take account of the real stiffness of studs and plates in the analysis. The mathematical model proposed by [18], in case of fully flexible frame, could be adopted. In this case a lower ductility of the wall is expected because of the lower stiffness than a rigid-frame wall.

4.1. Elastic - plastic analysis of a fully anchored wall with EATW

The Matlab program EATW (Elasto-plastic Analysis of Timber-frame Walls), specifically developed by authors, allowed to analyse several light timber-frame walls with several dimensionless fastener spacings (s/b), panel geometrical parameters (α) and fastener ductilities (μ_c).

The output data are represented by all parameters characterizing the mechanical behaviour of the wall at each step of the analysis (wall displacement, external force, panel rotation, frame rotation, fastener internal forces, fastener nail-slip) and by the wall force-displacement piecewise-linear curve.

Every force-displacement piecewise-linear curve of the wall,using the elasto-plastic energy strain approach, was then bi-linearized to obtain the value of ductility of each fully-anchored wall.

In Tables 1, 2, 3, the relationship between the fully-anchored wall ductility (μ_{SH}) and the fastener one (μ_c) is reported (depending on the fastener spacing and the panel geometrical parameter).

Ductility μ_{SH} with $\alpha = 1$						
μ_c	s/b					
	1/2	1/4	1/6	1/8	1/12	1/25
1.00	1.00	1.00	1.00	1.00	1.00	1.00
1.50	1.38	1.29	1.27	1.27	1.26	1.26
2.00	1.73	1.63	1.60	1.60	1.60	1.59
2.50	2.07	1.96	1.92	1.92	1.91	1.91
3.00	2.40	2.28	2.23	2.23	2.22	2.22
3.50	2.73	2.59	2.54	2.54	2.53	2.52
4.00	3.05	2.89	2.84	2.84	2.83	2.82
4.50	3.37	3.20	3.14	3.14	3.13	3.12
5.00	3.69	3.50	3.44	3.43	3.42	3.42
5.50	4.00	3.80	3.74	3.73	3.72	3.71
6.00	4.32	4.10	4.03	4.03	4.01	4.01
6.50	4.63	4.40	4.33	4.32	4.31	4.30
7.00	4.94	4.70	4.63	4.62	4.60	4.59
7.50	5.26	5.00	4.92	4.91	4.89	4.89
8.00	5.57	5.29	5.22	5.21	5.19	5.18

Table 1: fully-anchored wall ductility $\alpha = 1$; n case which the collapse displacement occurs before the kinematic

As an example, the elasto-plastic analysis, performed by the EATW Program, of a fully anchored wall characterized by $\alpha = 2$, $s/b = 1/2$ and $\mu_c = 5$ is reported. For each step of the analysis, the wall force-displacement piecewise-linear curve is obtained, see Figure 14, Figure 15, Figure 16, Figure 17. Circular and triangular dots represent unyielded and yielded fasteners respectively. In Figure 18 the bi-linear curve of the analysed wall is shown and the fastener position scheme is substituted by the wall kinematic model.

The obtained results were plotted in order to define the relationship between

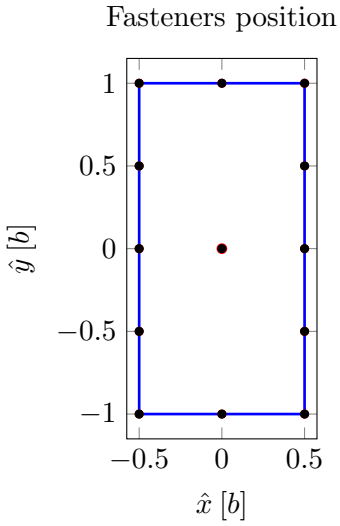

Figure 14: fasteners position on the panel

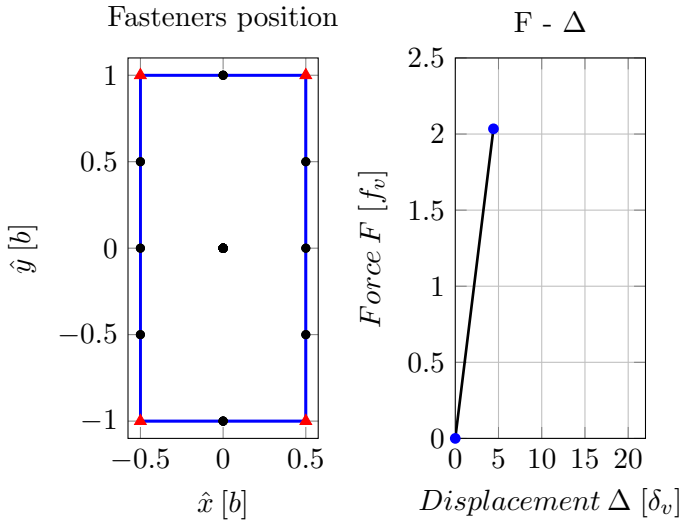

Figure 15: first step of analysis: fastener lingered in the elastic phase and graphic load-displacement

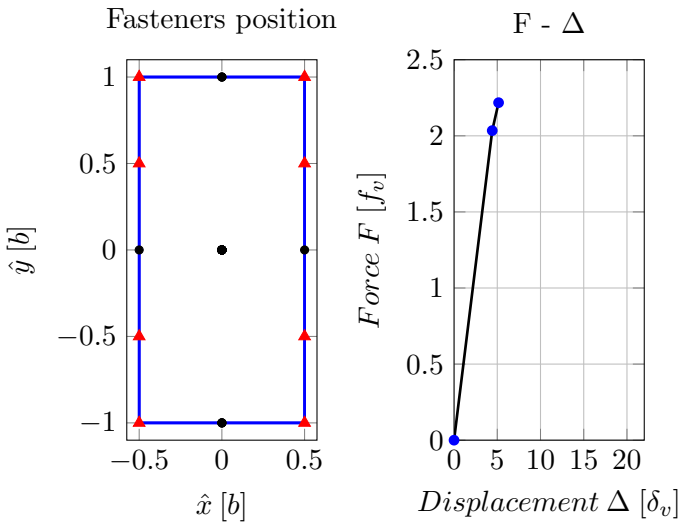

Figure 16: second step of analysis: fastener lingered in the elastic phase and graphic load-displacement

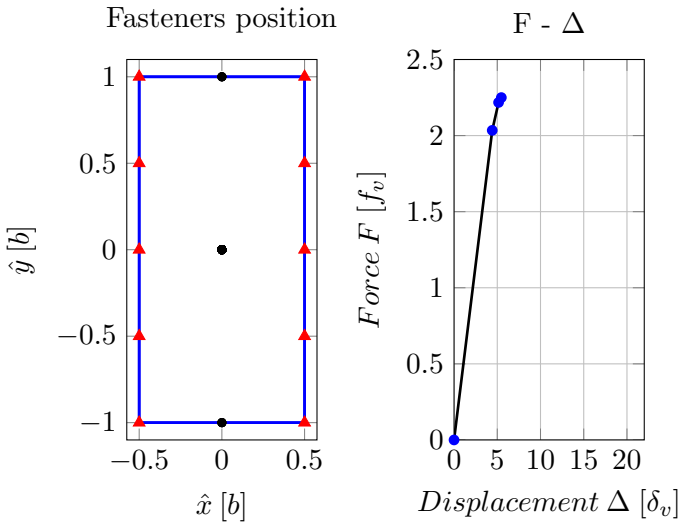

Figure 17: last step of analysis: fastener lingered in the elastic phase and graphic load-displacement

Ductility μ_{SH} with $\alpha = 2$						
μ_c	s/b					
	1/2	1/4	1/6	1/8	1/12	1/25
1.00	1.00	1.00	1.00	1.00	1.00	1.00
1.50	1.39	1.35	1.34	1.34	1.34	1.34
2.00	1.83	1.77	1.76	1.76	1.76	1.76
2.50	2.26	2.18	2.17	2.17	2.17	2.17
3.00	2.69	2.59	2.57	2.57	2.57	2.57
3.50	3.11	2.99	2.97	2.97	2.97	2.96
4.00	3.53	3.39	3.37	3.36	3.36	3.36
4.50	3.94	3.79	3.76	3.76	3.76	3.75
5.00	4.36	4.19	4.16	4.15	4.15	4.15
5.50	4.77	4.58	4.55	4.54	4.54	4.54
6.00	5.18	4.98	4.95	4.94	4.93	4.93
6.50	5.59	5.38	5.34	5.33	5.32	5.32
7.00	6.01	5.77	5.73	5.72	5.71	5.71
7.50	6.42	6.17	6.12	6.11	6.10	6.10
8.00	6.83	6.56	6.52	6.50	6.49	6.49

Table 2: fully-anchored wall ductility $\alpha = 2$; n case which the collapse displacement occurs before the kinematic

the sheathing-to-framing connection ductility μ_{SH} and the fastener ductility μ_c. As shown in Figure 19, a linear relationship can be assumed. The sheathing-to-framing connection ductility μ_{SH} is not significantly influenced by the fastener spacing s/b whereas, it increases with the panel geometrical parameter α.

Therefore, the analytical relationship between the sheathing-to-framing connection ductility μ_{SH} and the fastener ductility μ_c can be obtained by means of the following linear equation:

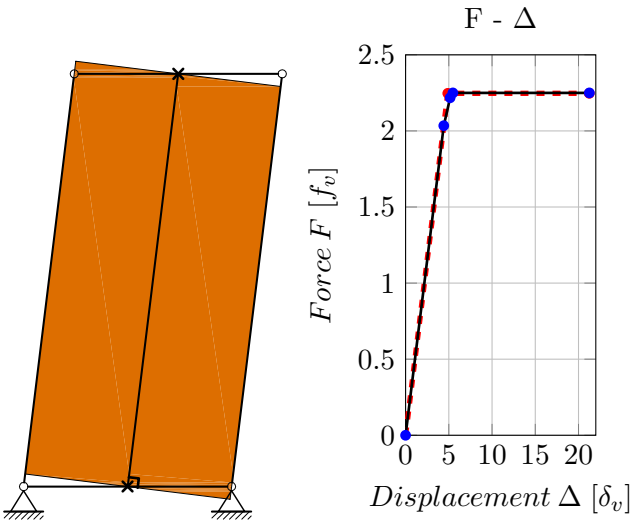

Figure 18: kinematic mechanism

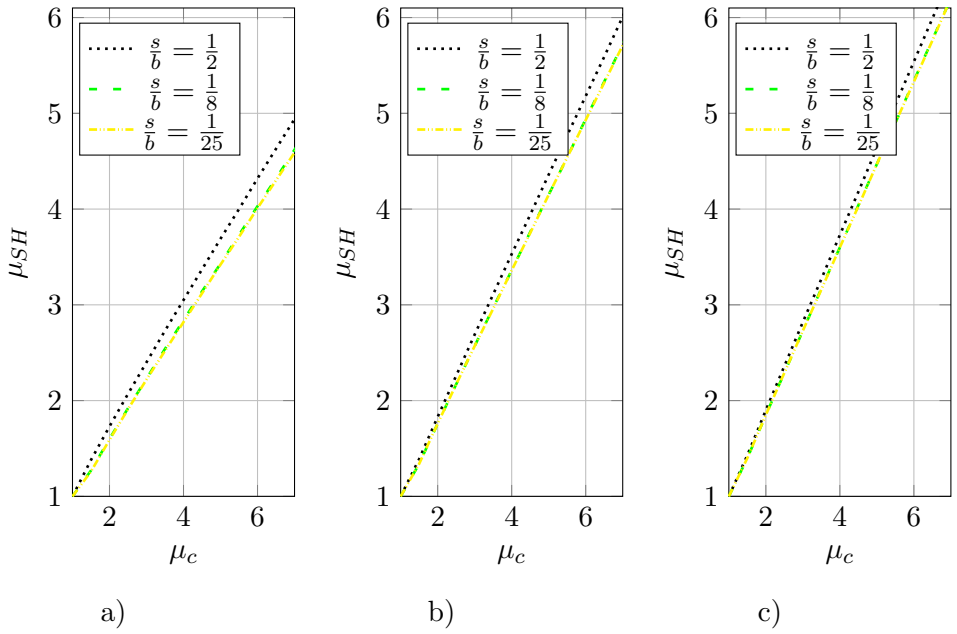

Figure 19: fully-anchored wall ductility vs fastener ductility: a) $\alpha = 1$; b) $\alpha = 2$; c) $\alpha = 3$

Ductility μ_{SH} with $\alpha = 3$						
μ_c	s/b					
	1/2	1/4	1/6	1/8	1/12	1/25
1.00	1.00	1.00	1.00	1.00	1.00	1.00
1.50	1.43	1.40	1.40	1.40	1.40	1.40
2.00	1.90	1.85	1.85	1.85	1.85	1.85
2.50	2.36	2.30	2.29	2.29	2.29	2.29
3.00	2.82	2.74	2.73	2.73	2.73	2.73
3.50	3.27	3.18	3.17	3.17	3.16	3.16
4.00	3.73	3.62	3.61	3.60	3.60	3.60
4.50	4.18	4.06	4.04	4.04	4.03	4.03
5.00	4.64	4.49	4.48	4.47	4.47	4.47
5.50	5.09	4.93	4.91	4.90	4.90	4.90
6.00	5.54	5.37	5.35	5.34	5.33	5.33
6.50	5.99	5.80	5.78	5.77	5.76	5.76
7.00	6.44	6.24	6.21	6.20	6.20	6.20
7.50	6.89	6.68	6.65	6.63	6.63	6.63
8.00	7.35	7.11	7.08	7.07	7.06	7.06

Table 3: fully-anchored wall ductility $\alpha = 3$; n case which the collapse displacement occurs before the kinematic

$$\mu_{SH} = \rho(\alpha) \cdot \mu_c + \nu(\alpha) \tag{43}$$

where α is equal to h/b.

The parameters ρ and ν, which depend on the panel geometric parameter α, can be obtained by means of an interpolation of the curves wall ductility vs fastener ductility, getting the following expressions:

$$\begin{cases} \rho = -0.054 \cdot \alpha^2 + 0.350 \cdot \alpha + 0.305 \\ \nu = 0.068 \cdot \alpha^2 - 0.415 \cdot \alpha + 0.753 \end{cases} \tag{44}$$

Known the ductility of the sheathing-to-framing connection μ_{SH}, the ultimate displacement $\Delta_{U,SH}$ can be calculated as:

$$\Delta_{U,SH} = \mu_{SH} \cdot \Delta_{Y,SH} = \mu_{SH} \cdot \frac{R_{SH}}{K_{SH}} \tag{45}$$

The mechanical behaviour of the sheathing-to-framing connection is hence completely defined.

5. Experimental investigation

5.1. Test program and test specimens

	M-D-B	**M-D-B2**	**M-D-B4**	**M-D-B8**
test number	1	2	3	4
wall base b [mm]	1250	1250	1250	1250
wall height h [mm]	2500	2500	2500	2500
sheathing panel type	OSB/3	OSB/3	OSB/3	OSB/3
s. p. thickness [mm]	15	15	15	15
braced sides	1	1	1	1
nail type	2.8x80	2.8x80	2.8x80	r2.8x80
fastener spacing [mm]	1150	575	288	144

Table 4: Specimens mechanical and geometrical properties

Four light timber-frame walls were tested to asses their yielding point, ultimate displacement, maximum force as well as their ductility. The specimens (see Tab. 4), which had the same geometrical dimensions, were made of the same materials: OSB/3 for the sheathing panels and wood C24 for the frame (see [24] and [25] respectively). On the contrary, the fasteners spacing was different for each specimen; the fasteners used were annular-ringed nails 2.8×80.

Figure 20: Connecting-devices: hold-down and locking rectangolar tube

The specimens were tested under the same boundary conditions. The walls, in fact, were connected to the ground trough a heavy hold-down and a rectangular steel tube, see Figure 20. The hold-down, a prototype specifically developed for the test campaign, was made of steel S355 according to [26], it had flanges of thickness equal to 15 mm and it was designed for a strength of 250 kN. Whereas, the rectangular tube had a cross-section of $120 \times 80 \times 5$ mm and it was made of steel S255 according to [26].

In order to reproduce the fully-anchoring condition, according to section 4, both the connection devices were designed to be stronger than the sheathing-to-framing connection and to avoid both the rigid-body rotation and the rigid-body translation.

The specimens were tested in the The Materials and Structural Testing Laboratory of the University of Trento, applying the monotonic-test method under displacement control, with a displacement velocity of $0,1mm/sec$ (see [27]). The tests were performed using a MTS-244 hydraulic-actuator, see Figure 21.

5.2. Test set-up and instrumentation

The test set-up (see Figure 21) was composed by a heavy timber reaction frame on which a system of four lever-arms was connected (see [28]) and by a steel sole-plate anchoring the walls to the ground.

Figure 21: Global view of the set-up used for the tests

The reaction frame leverage system can be used to apply vertical dead load on the specimens; anyway, in the campaign-test described no vertical load was applied. The sole-plate was made by two UPN240 S235 welded together.

Each test was monitored by-means of five instruments placed as shown in Figure 22:

- the load-cell of the actuator to measure the applied-horizontal-force (1);
- a LVDT transducer incorporated in the actuator to control the applied-horizontal displacement (2);
- a wire potentiometer to measure the horizontal displacement (3) ;
- two LDVT to measure the uplifting (4) and the rigid-body translation (5) respectively.

5.3. Results from experimental tests and main observations

Despite the use of the heavy hold-down and the use of the lock-plate, the deformation contributions due to rigid-body-rotation and the rigid-body-

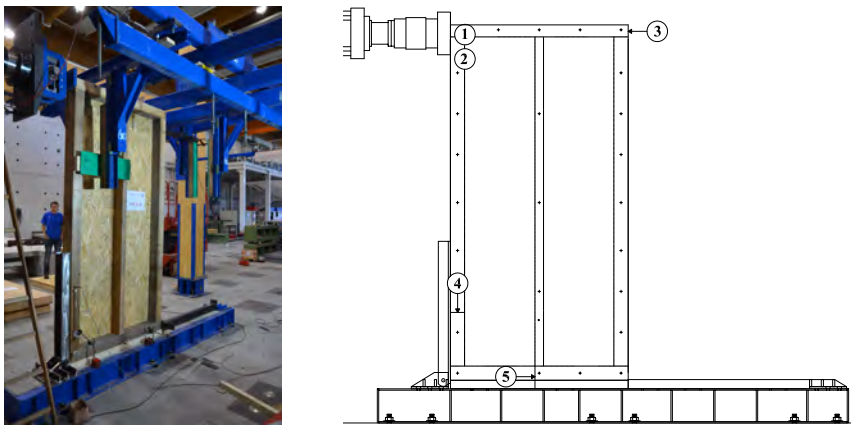

Figure 22: Test instrumentation set-up

translation have not been completely avoided. Anyway, these are considerably small compared to the total horizontal deformation and therefore they can be considered negligible, see Figure 23.

The Force-vs-Displacement Curves, see Figure 24 a), are the main result of the tests. Analyzing these curves, it is possible noting how the strength of the specimen, as well as their stiffness, increase with the decrease of the fasteners spacing. This confirms what stated in sec. 3.3, in which both the strength and the stiffness of the wall, see Eq. 14 and Eq. 15 respectively, are considered inversely-proportional to the fastener spacing. Using the equations 14 and 15 to evaluate the yielding-point, this can be shown to be not dependent on the fastener spacing:

$$\Delta_{Y,SH} = \frac{R_{SH}}{K_{SH}} = \frac{n_{bs} \cdot r_c \cdot \frac{\sum b_i \cdot c_i}{s}}{\frac{n_{bs} \cdot k_c}{s \cdot \sum \frac{\lambda_i(\alpha_i)}{b_i}}} = \frac{r_c \cdot \sum b_i \cdot c_i \cdot \sum \frac{\lambda_i(\alpha_i)}{b_i}}{k_c} \tag{46}$$

Consequently, both the ultimate displacement and the ductility does not change, as demonstrated in equations 45 and 43 respectively.

The results of the test campaign back this theory. The Figure 24 a) shows that yielding point and ultimate displacement can be considered constant for each test-specimen; the curves, therefore, confirm the hypothesis presented in

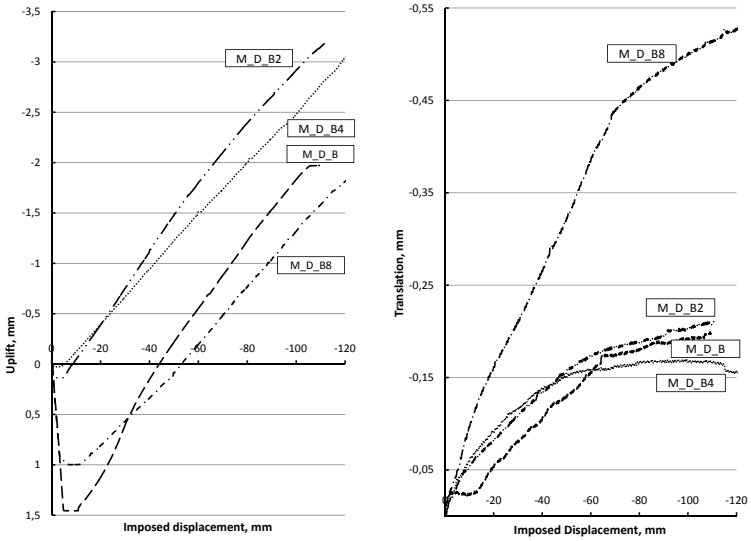

Figure 23: Test results: uplift, translation-vs-imposed displacement

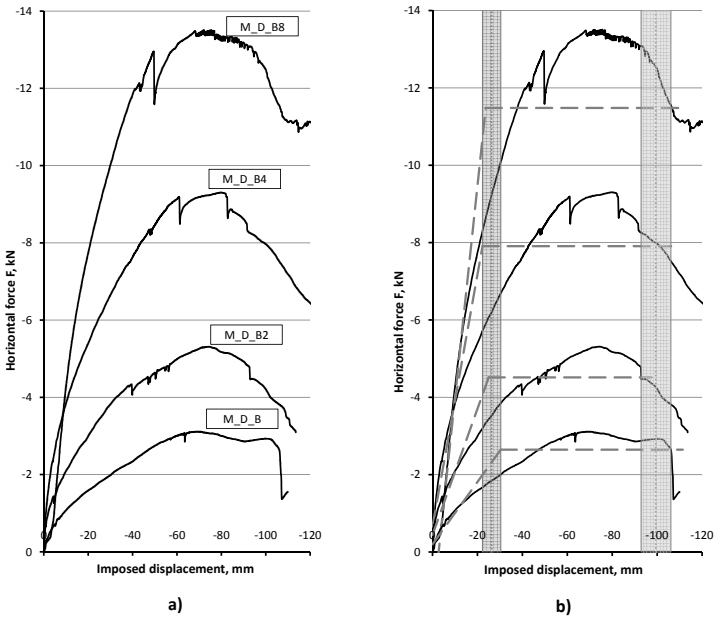

Figure 24: Test results: Force-vs-Displacement and Bi-linear curves

the paper that the behavior of a timber-frame wall due to the sheathing-to-framing connection in not influenced by the fastener spacing.

In particular, for the bi-linear curves obtained from the specifications of [27] see Figure 24 b), the yielding displacement is included in a gap of $\pm 4mm$ with respect to the mean value, whereas the ultimate displacement is included in a gap of $\pm 6mm$ with respect to the mean value. These gaps could be considered acceptable for timber and allow to consider yielding point, ultimate displacement and consequently ductility as constant parameters.

6. Concluding remarks

In the paper an analytical method, based on a simplified rheological model, was presented with the aim to describe the elasto-plastic behaviour of a light timber-frame wall under a horizontal force. The proposed expressions allow to define an analytical relationship between the mechanical properties of the structural elements (fasteners, angle brackets and hold-downs) and the mechanical properties of the entire wall. With particular reference to a seismic design, these expressions can be useful to relate the local ductility (i.e. fastener) to the global wall ductility and hence to define the ductility demand of the components (weak) where a energy dissipation is expected. The rheological model takes account of the deformation contributions of fasteners, hold-downs and angle-brackets but simply it can be modified adding other elastic or elasto-plastic springs positioned in series regarding other contributions (wood frame flexibility, sheathing panel shear deformation, compression perpendicular to the grain of the bottom plate, etc.).

Another innovative matter regards the relationship between the ductility of a fully anchored light timber-frame wall and the ductility of fasteners. By means of the mathematical model proposed in [18], assuming the timber-frame as rigid, several elasto-plastic analyses of different types of light timber-frame shear walls were carried out with EATW in MatLab, changing the geometrical properties of the wall and the fastener spacing. A simple linear equation was

proposed for the researched relationship, depending on the geometrical properties of the sheathing panels and the fastener ductility. As expected, the wall ductility results lower than the fastener ductility. It is not significantly influenced by fastener spacing whereas the geometrical shape of the panel is to be taken into account. This key aspect has been also investigated by means of four laboratory tests which have demonstrated that the yielding displacement and the ultimate displacement can be considered constant with the fasteners spacing. The proposed formula for the ductility, in combination with the expression for the strength and stiffness, allows to define the elasto-plastic behaviour of an equivalent horizontal spring representing the mechanical behaviour of all fasteners used to connect the wood-frame to the sheathing panel. The ability to represent the total force carried by all fasteners (allowing for their sequential yielding) in one non-linear spring is shown to be a key benefit especially when a non-linear analysis (e.g. pushover) of multi-storey multi-walls timber buildings is required, reducing hugely the number of degrees of freedom of the model. At each level for each wall only one elasto-plastic spring is sufficient to represent the elasto-plastic behaviour of the all fasteners. Otherwise each fastener should be represented by a suitable elasto-plastic spring, increasing a lot the complexity of the model.

Acknowledgments

The presented research has been carried out in the framework of the ReLUIS-DPC 2015 project. Support from the ReLUIS-DPC network, the Italian University Network of Seismic Engineering Laboratories and Italian Civil Protection Agency, is gratefully acknowledged. Authors would also to thanks Prof. M. Piazza for his precious technical suggestions, to Ph.D. Eng. Tiziano Sartori for his help during the laboratory test, to Eng. F. Vinante for his help during the paper writing and to technicians of the Material and Structural Testing Laboratory of the University of Trento for their support.

Nomenclature

α is the shape parameter of the sheathing-panel;

δ_c is the displacement of the nails;

Δ_{nail} is the displacement of the horizontal spring related to the sheathing-to-framing connection;

$\Delta_{pl,W}$ is the plastic displacement of the wall;

$\Delta_{q,W}$ is the displacement of the wall when the friction block yields;

$\Delta_{U,A}$ is the ultimate-displacement of the equivalent horizontal spring related to the angle-brackets;

$\delta_{u,a}$ is the ultimate-displacement of the angle-brackets;

$\delta_{u,c}$ is the ultimate-displacement of the nails;

$\Delta_{U,H}$ is the ultimate-displacement of the equivalent horizontal spring related to the hold-downs;

$\delta_{u,h}$ is the ultimate-displacement of the hold-downs;

$\Delta_{U,SH}$ is the ultimate-displacement of the equivalent horizontal spring related to the sheathing-to-framing connection;

$\Delta_{U,W}$ is the ultimate-displacement of the wall;

$\Delta_{Y,A}$ is the yielding-point of the equivalent horizontal spring related to the angle-brackets;

$\delta_{y,a}$ is the yielding-point of the angle-brackets;

$\delta_{y,c}$ is the yielding-point of the nails;

$\Delta_{Y,H}$ is the yielding-point of the equivalent horizontal spring related to the hold-downs;

$\delta_{y,h}$ is the yielding-point of the hold-downs;

$\Delta_{Y,SH}$ is the yielding-point of the equivalent horizontal spring related to the sheathing-to-framing connection;

$\Delta_{Y,W}$ is the yielding-point of the wall;

κ is the ratio between the stiffness of the wall and the stiffness of the weakest connection device;

λ_{swn} is the factor taking into account the geometrical properties of the sheathing panel;

μ_A is the displacement-ductility of the equivalent horizontal spring related to the angle-brackets;

μ_a is displacement-ductility of the angle-brackets;

μ_c is displacement-ductility of the nails;

μ_H is the displacement-ductility of the equivalent horizontal spring related to the hold-downs;

μ_h is displacement-ductility of the hold-downs;

μ_{SH} is the displacement-ductility of the equivalent horizontal spring related to the sheathing-to-framing connection;

τ is the internal level arm ratio of the hold-downs;

ξ is the ratio between the force activating the friction block and the strength of the wall;

b is the width of the sheathing-panels;

c is the factor taking into account the shape of the sheathing panel;

F is the external horizontal force;

F_q is the magnitude of the horizontal force which activates the friction block;

h is the height of the wall;

i_a is the angle-brackets spacing;

K_A is the stiffness of the equivalent horizontal spring related to the angle-brackets;

k_a is the stiffness of the angle-brackets;

k_c is the stiffness of the nails;

K_H is the stiffness of the equivalent horizontal spring related to the hold-downs;

k_h is the stiffness of the hold-downs;

K_P is the stiffness of the equivalent horizontal spring related to the sheathing panels;

K_{SH} is the stiffness of the equivalent horizontal spring related to the sheathing-to-framing connection;

K_{SP} is the equivalent horizontal stiffness accounting for both the sheathing-panel and the sheathing-to-framing connection contributions;

$K_{tot,nt}$ is the stiffness of the wall when the rigid rotation contribution is not considered;

K_{tot} is the stiffness of the wall when the rigid rotation contribution is considered;

K_W is the stiffness of the wall;

l is the length of the wall;

M_{ovt} is the overturning moment produced by the horizontal force;

M_{stb} is the stabilizing moment produced by the vertical distributed load;

n_a is the number of angle-brackets;

n_h is the number of hold-downs;

n_{bs} is the number of braced sides of the wall;

q is the vertical distributed load;

R_A is the strength of the equivalent horizontal spring related to the angle-brackets;

r_a is the strength of the angle-brackets;

r_c is the strength of the nails;

R_H is the strength of the equivalent horizontal spring related to the hold-downs;

r_h is the strength of the hold-downs;

R_{SH} is the strength of the equivalent horizontal spring related to the sheathing-to-framing connection;

R_W is the strength of the wall;

s is the spacing of the fasteners;

7. References

[1] Pauley, T., Priestley, M.. Seismic design of reinforced concrete and masonry structures, j. J Wiley & Sons, INC USA 1992;.

[2] UNI EN 1998-1:2013, . Eurocode 8: Design of structures for earthquake resistance part 1: General rules, seismic actions and rules for buildings. 2013. Brussels, Belgium: CEN, European Committee for Standardization.

[3] Building, C.C.O., Codes, F.. National building code of canada. canadian commission on building and fire codes national research council canada. 2010.

[4] Pozza, L., Scotta, R.. Influence of wall assembly on behaviour of cross-laminated timber buildings. Proceedings of the Institution of Civil Engineers journal Structures and Buildings 2014;.

[5] Winkel, M., Smith, I.. Structural behavior of wood light-frame wall segments subjected to in-plane and out-of-plane forces. Journal of structural engineering 2009;136(7):826–836.

[6] Blaß, H.J., für Holzforschung, D.G.. Erläuterungen zu DIN 1052: 2004-08: Entwurf, Berechnung und Bemessung von Holzbauwerken; inkl. Originaltext der Norm. Bruderverlag; 2005.

[7] Nzs 3603:1993: Timber structures standard. 1993.

[8] Association, C.S.. Engineering design in wood. Standard Council of Canada; 2005.

[9] Judd, J., Fonseca, F.. Analytical model for sheathing-to-framing connections in wood shear walls and diaphragms. Journal of Structural Engineering 2005;131(2):345–352.

[10] Judd, J.P., Fonseca, F.. Equivalent single degree of freedom model for wood shearwalls and diaphragms. In: Proceeding of the 9th World Conference on Timber Engineering. 2006, p. 6–10.

[11] Casagrande, D., Rossi, S., Sartori, T., Tomasi, R.. Proposal of an analytical procedure and a simplified numerical model for elastic response of single-storey timber shear-walls. Construction and Building Materials 2015;DOI:10.1016/j.conbuildmat.2014.12.114.

[12] Fragiacomo, M., Amadio, C., Rinaldin, G., Sancin, L.. Non-linear modelling of wooden light-frame and x-lam structures. Conference Proceeding: WCTE 2012 2012;.

[13] Rinaldin, G., Fragiacomo, M.. A component model for cyclic behaviour of wooden structures. In: Materials and Joints in Timber Structures. Springer; 2014, p. 519–530.

[14] Folz, B., Filiatrault, A.. Seismic analysis of woodframe structures. i: Model formulation. Journal of Structural Engineering 2004;130(9):1353–1360.

[15] Folz, B., Filiatrault, A.. Seismic analysis of woodframe structures. ii: Model implementation and verification. Journal of Structural Engineering 2004;130(9):1361–1370.

[16] Doudak, G., Smith, I., McClure, G., Mohammad, M., Lepper, P.. Tests and finite element models of wood light-frame shear walls with openings. Progress in Structural Engineering and Materials 2006;8(4):165–174.

[17] Källsner, B., Girhammar, U.A.. Plastic models for analysis of fully anchored light-frame timber shear walls. Engineering Structures 2009;31(9):2171 – 2181.

[18] Källsner, B., Girhammar, U.. Analysis of fully anchored light-frame timber shear walls-elastic model. Materials and Structures 2009;42:301–320.

[19] UNI EN 1995-1-1:2005, . Eurocode 5: Design of timber structures - part 1-1: General - common rules and rules for building. 2005.

[20] Sartori, T., Tomasi, R.. Experimental investigation on sheathing-to-framing connections in wood shear walls. Engineering Structures 2013;56:2197–2205. doi:10.1016/j.engstruct.2013.08.039.

[21] Källsner, B., Girhammar, U.A.. A plastic lower bound method for design of wood-framed shear walls. WCTE conference 2014 2004;:129–134.

[22] Casagrande, D.. Study of timber-frame building seismic behaviour by means of numerical modelling and full-scale shake table testing. Ph.D. thesis; DICAM Unitn; 2014.

[23] Conte, A., Piazza, M., Sartori, T., Tomasi, R.. Influence of sheathing to framing connections on mechanical properties of wood framed shear walls. Proceedings of Italian National Association of Earthquake Engineering, ANIDIS 2011;.

[24] de Normalisation, C.E.. En 300:2006 oriented strand boards (osb) definitions, classification and specifications. 2006.

[25] de Normalisation, C.E.. En 338:2009 structural timber - strength classes. 2009.

[26] 2004, C.. En 10025-2:2004; hot rolled products of structural steels - part 2: Technical delivery conditions for non-alloy structural steels. 2004.

[27] EN 12512: 2001, . Timber structures - test methods - cyclic testing of joints made with mechanical fasteners. 2001. CEN, European Committee for Standardization, Brussel, Belgium.

[28] Andreolli, M., Grossi, P., Sartori, T., Tomasl, R.. Design and production of a heavy timber reaction frame for a laboratory test setup. Conference Proceeding: ICSA 2013 2013;:199.

Chapter 5

Non-linear analysis and ductility evaluation of light timber-frame buildings

5.1 Introduction

The capacity of structures to resist to seismic forces in the non-linear range as well as because a purely linear-elastic design may not sustainable both from the economic and technical point of view, make inelastic structural analysis a common and normal procedure for the seismic design.

The attainment of the post-elastic capabilities implies that the structural system has to be able to distort sufficiently to achieve the level of deformation required (brittle failures shall be avoided), which in turns requires a deep knowledge of the relationships between the properties of the basic components of the system and the overall behavior of the structure.

This type of design should therefore be based on two key aspects. From one side, the identification of the base-component whose failure would give

the building a brittle behaviour in order to avoid them is fundamental. The basic idea is to force the building to fail in a ductile manner by making the capacity of the brittle elements greater compared to the capacity of other components whose failure assure a global ductile behaviour. This approach is generally known as *Capacity Design* and it can be effectively represented by Fig. 5.1 in which the failure of the fragile components shall be avoided favoring the rupture of the ductile ring.

Figure 5.1: *Capacity design approach.*

On the other hand, in order to avoid explicit inelastic analysis (which can be very demanding for timber structure) a simplified elastic procedure can be used by adopting a design response spectrum reduced by means of the *behaviour factor* (q), which tries to consider, in an approximate manner, the effects of the energy dissipation and cyclic deformation during an earthquakes that characterize a building.

Despite the use of the behaviour factor in the seismic design of building built with other materials such as reinforced concrete, masonry etc. is a widely established and validated procedure, with respect to timber structure and in particular to light timber-frame buildings, a procedure to apply the capacity design is still missing and also a direct relation between the base-components properties and the behaviour of the structure has not developed yet. So, the behaviour factor values given by European Standard do not match the real dissipative capacity of timber buildings and therefore using them can be potentially dangerous because they do not provide the structure the ductility hypothesized.

With the goal of evaluating the real capability to absorb energy associated with inelastic deformations and to assess how this capability changes by changing the base component involved in the failure; as well as to deter-

mine the real relationship between the global behaviour of the building and the ductility at subsystem levels in order to assess and propose a new set of reliable values of behaviour factor (q) to use in the seismic design, the present Chapter deals with the inelastic analysis of full-scale buildings.

This analysis is initially carried considering the post-elastic behaviour of two coupled one-storey walls, see Fig. 5.2. The study is performed from the analytical point of view in order to determine the influence of both the geometry, the strength and the applied loads on the ductility of the whole system. It is worth noting that this analysis is needed to highlight the essential features and qualitative aspects that characterize the different failure mechanisms and not to properly assess the dissipative capability of system of two walls.

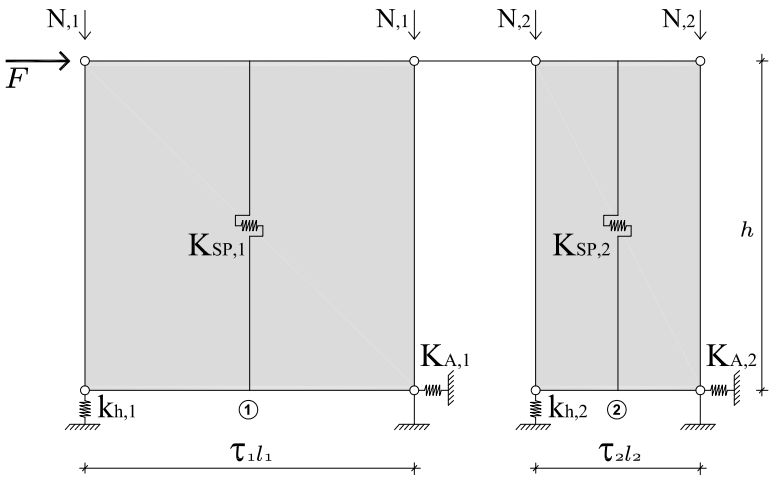

Figure 5.2: *A system of* 2×1 *coupled walls.*

It has to be remarked that two coupled walls have to be regarded as a hyperstatic system; in fact, they can be represented by means of two non-linear springs placed in parallel, see Fig. 5.3, and therefore they be loaded by a higher force than that of the yielding point.

The behaviour of coupled walls is quite different from that of single walls: single walls can be considered as systems governed by the forces, in fact the

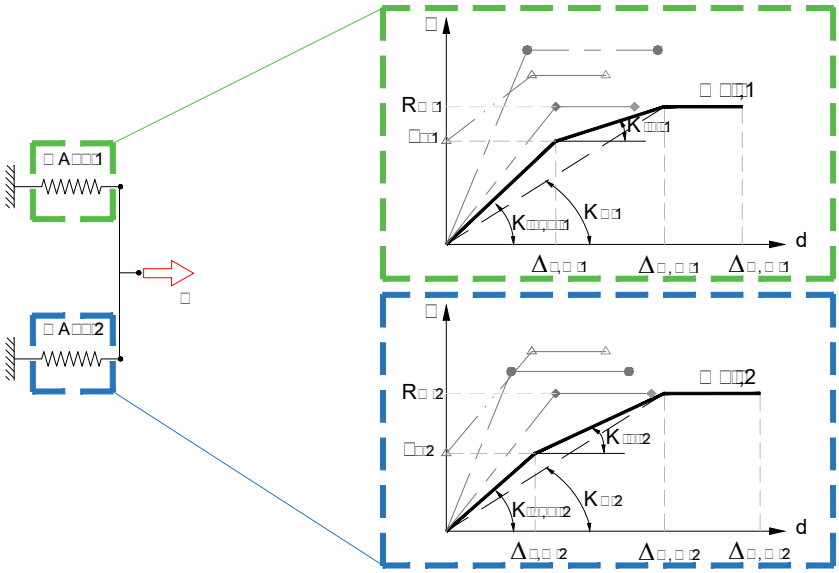

Figure 5.3: *Two coupled walls can be considered as a system of springs placed in parallel.*

strength of a wall is equal to the strength of the weakest base component, whereas coupled walls represent systems governed by the displacement. Indeed, the yielding displacement of the whole system match that of the wall with the lower yielding displacement, even if it is the stronger wall. That is why coupled walls can be loaded over the yielding: after the yielding of the first wall the second-one is still elastic and it can be loaded by more force. The ratio between the ultimate force and the yielding force is known as *Over Strength Ratio* [O.S.R].

The study of the inelastic behaviour of coupled walls is analytically performed and it allows to determine six different scenarios by varying the ratio between the walls in terms of strength and stiffness. These six cases can be identified through the following equations:

$$\Delta_{Y,A} < \Delta Y, B \rightarrow \begin{cases} \Delta Y, B < \Delta U, A < \Delta U, B \rightarrow \ case\ 1.1 \\ \Delta U, A > \Delta U, B \rightarrow \ case\ 1.2 \\ \Delta U, A < \Delta Y, B \rightarrow \ case\ 1.3 \end{cases} \tag{5.1}$$

$$\Delta_{Y,A} > \Delta Y, B \rightarrow \begin{cases} \Delta Y, A < \Delta U, B < \Delta U, A \rightarrow \ case\ 2.1 \\ \Delta U, B > \Delta U, A \rightarrow \ case\ 2.2 \\ \Delta U, B < \Delta Y, A \rightarrow \ case\ 2.3 \end{cases} \tag{5.2}$$

By analyzing the results it is possible to state that all the mechanical parameters of the base components, such as strength, stiffness as well as ductility, contribute to define the overall behaviour in terms of ductility and overstrength. These highlight that the analytical study of more complex systems, namely systems with more walls, is not possible.

In order to study larger systems, as well as to validate and prove the analyses presented, some numerical finite element models analyses were carried out using SAP2000. The analyses have been performed by means of a *complete numerical model*, where complete stands for the accuracy of the model. In fact, in order to get reliable results, the framing of the structure, the hold-downs, the angle-brackets as well as each single nails were modeled, see Fig. 5.4.

As an example in Fig. 5.5 is shown the capacity curve obtained with SAP2000 with respect to a system of two coupled walls whose properties are summarized in Tab. 5.1.

Despite the use of SAP2000 for the nonlinear analysis allows to get reliable and accurate results, the computational effort required to create and run the model, the need to analyse several different cases, together with the difficulty in identifying both of the yielding and ultimate displacements have highlighted the need to adopt a different procedure from the SAP2000 analysis. It was therefore decided to develop a Matlab program. This specifically developed program is composed by some sub-routines, each of which handles a specific phase of analysis, namely:

- data acquisition;
- design of connection devices;

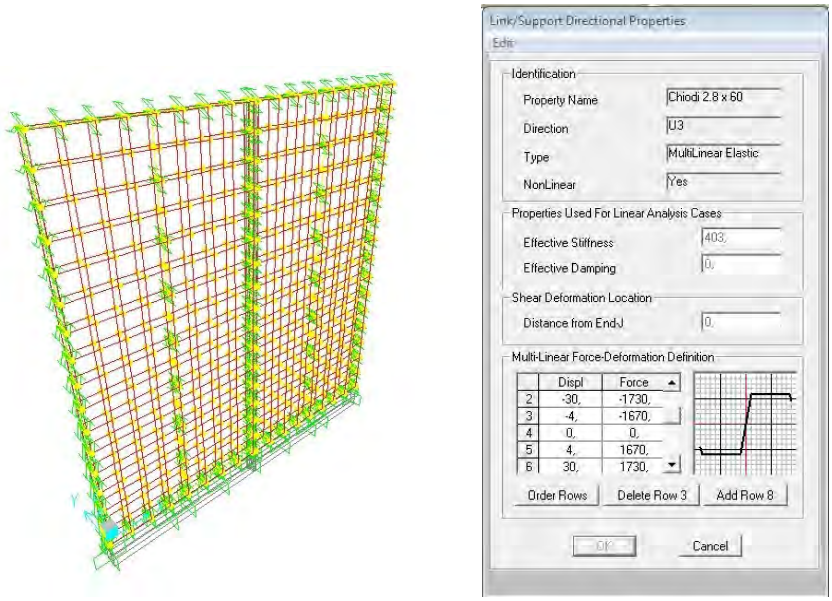

Figure 5.4: *Complete numerical model and definitions of properties nails.*

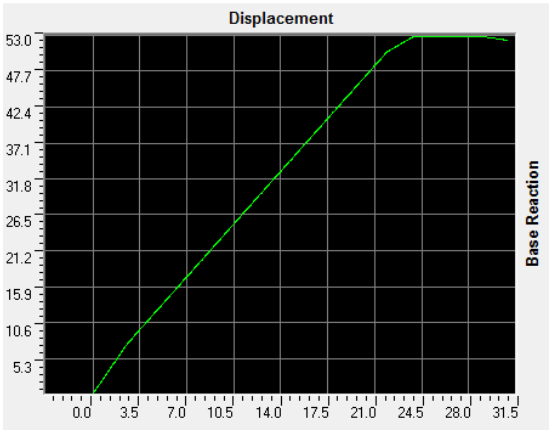

Figure 5.5: *Capacity curve of a system composed by two coupled walls (force in [kN], displacement in [mm]).*

- definition of the force-vs-displacement nonlinear curve of the walls;
- creation of the stiffness matrix of the building;
- evaluation of the force-vs-displacement curve of the building.

Wall 1							
Geometry		Nails		Angle-brackets		Hold-downs	
h	2500	f_c	1.2	f_a	12	f_{hd}	25
l	2500	δ_y	3.02	δ_y	11	δ_y	25
b_p	1250	δ_y	15.1	δ_u	16.5	δ_u	11.02
τ	1	k_c	397	k_a	1091	k_{hd}	4533.68
n_{bs}	1	μ_c	4.00	μ_a	1.50	μ_{hd}	2.00
n_{ang}	5	Δ_y	13.65	Δ_y	11.00	Δ_y	5.51
sp	100	Δ_u	45.74	Δ_u	16.50	Δ_y	11.03
n_{HD}	1	F_{SH}	30.00	F_A	60.00	F_{HD}	28.75
q_{ver}	3	K_{SH}	2197.7	K_A	5454.5	K_{HD}	4533.68
F_q	3.75	μ_{SH}	3.35	μ_A	1.50	μ_{HD}	2
Wall 2							
h	2500	f_c	1.2	f_a	12	f_{hd}	26
l	2500	δ_y	3.02	δ_y	11	δ_y	25
b_p	1250	δ_y	15.1	δ_u	16.5	δ_u	11.02
τ	1	k_c	397	k_a	1091	k_{hd}	4715.03
n_{bs}	1	μ_c	4.00	μ_a	1.50	μ_{hd}	2.00
n_{ang}	5	Δ_y	13.65	Δ_y	11.00	Δ_y	5.51
sp	125	Δ_u	45.74	Δ_u	16.50	Δ_u	11.03
n_{HD}	1	F_{SH}	24.00	F_A	60.00	F_{HD}	29.75
q_{ver}	3	K_{SH}	1758.2	K_A	5454.5	K_{HD}	4715.03
F_q	3.75	μ_{SH}	3.35	μ_A	1.50	μ_{HD}	2

Table 5.1: *Mechanical and geometric properties of the walls.*

The program creates the capacity curve of a building by means of an incremental static analysis by pushing the building up to the point of collapse by means of a stiffness adaptation procedure. Specifically, a starting load pattern is increased by means of a load multiplier and the stiffness of the whole building is updated at each step, in order to properly account for the real state of the connection as well as for the effects of the vertical load. The program evaluate the force carried by each walls, the total shear force at the base of the building as well as the displacement of the system at each step of the analysis. Therefore, the total shear force borne by the whole building at the

$i-th$ step can be determined by the following equation:

$$F_i = F_{i-1} + \boldsymbol{K}^T_{(i-1)} \cdot \boldsymbol{\Delta u} \tag{5.3}$$

where:

- F_i is the total force acting on the building at the $i-th$ step;
- F_{i-1} is the total force acting on the building at the $(i-1)-th$ step;
- $\boldsymbol{K_{i-1}}$ is the stiffness matrix of the whole system at the $(i-1)-th$ step;
- Δu is the incremental displacement imposed to the system;

The use of the developed Matlab program has several computational advantages compared to both the analytical and FEM analysis. Firstly, it has to be stressed the saving of time during the modeling phase as well as the running-analysis phase (the Matlab procedure do no need a explicit modeling); and then it is worth noting that the results given by the Matlab can be considered much more refined compared to those of SAP2000; in fact, the force-vs-displacement curve is determined by SAP2000 with a number of analysis step from 200 to 400, whereas it is created by Matlab with a number of steps from 10'000 to 100'000.

As an example, Fig. 5.6 shows the capacity curve determined by Matlab with respect to the system of two coupled walls previously presented (see Tab. 5.1). It can be noted that the result are matching those of SAP2000 (see Fig. 5.5).

On the basis of the considerations made above, it was decided to adopt only the Matlab procedure for the analyses made later. In detail, the program was further developed in order to allow it to analyse multi-storey buildings; it has also to be remarked that the program has been extensively tested and validated by comparing the results obtained with those obtained analytically and by other commercial software.

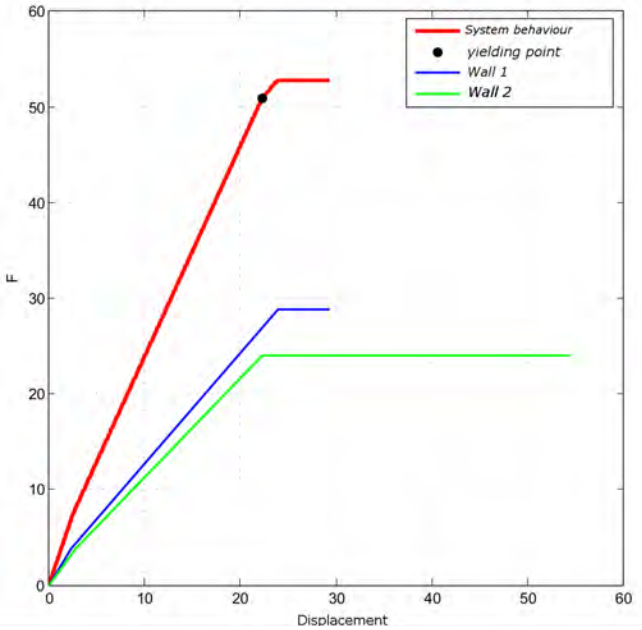

Figure 5.6: *Capacity curve determined by the Matlab Program (force in [kN], displacement in [mm]).*

The analysis was so extended to one-storey buildings in order to assess the ductility achievable and to evaluate the influence of the base components properties. Three real one-storey building were considered, whose geometrical properties are shown in Tab. 5.2 and their plans are shown in Fig. 5.7.

	Building 1	Building 2	Building 3
Dimension $[m^2]$	104	110	153
Mass $[ton]$	50	55	76
Shear walls X $[number]$	9	7	11
Shear walls Y $[number]$	6	6	9
Length Resisting system X $[m]$	19.2	19.5	17.5
Length Resisting system Y $[m]$	13.2	18.8	19.1

Table 5.2: *Mechanical and geometric properties of the Buildings.*

Several cases were analysed starting from the plans considered by varying the ductility of the nails, the ductility of the hold-down as well as the hold-down

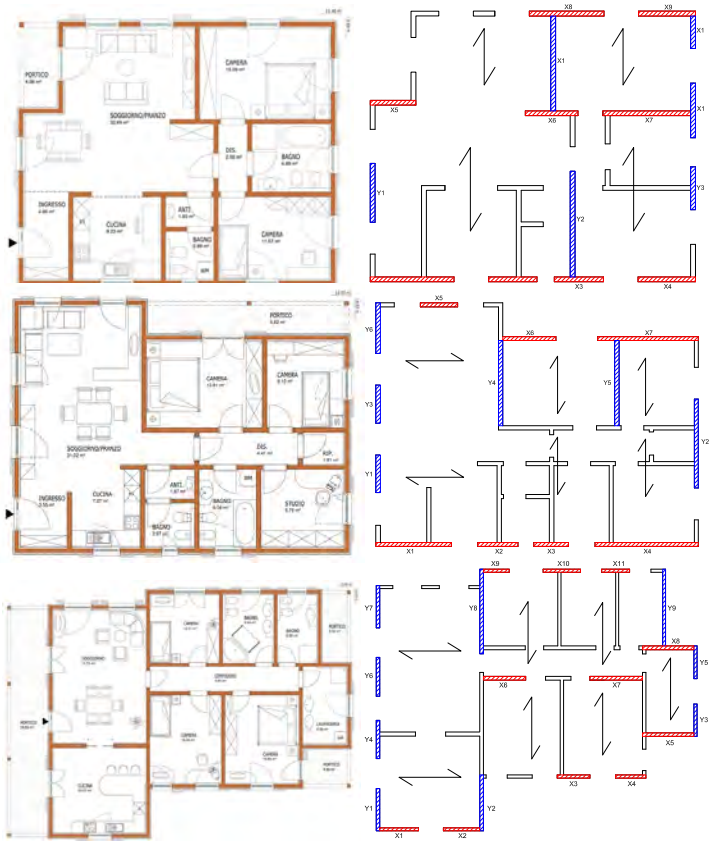

Figure 5.7: *Plans geometry and shear walls of the three one-storey buildings considered.*

strength in the following ranges (the spectral acceleration used in the design phase is equal to $S_d(T_0) = 0.55g$):

$$\mu_c \in [2.0 - 2.5 - 3.0 - 3.5 - 4.0 - 4.5 - 5.0 - 5.5 - 6.0] \tag{5.4}$$

$$\mu_{HD} \in [1.5 - 2.0 - 2.5 - 3.0] \tag{5.5}$$

(5.6) $$f_{HD}[kN] \in [10 - 18 - 26 - 34]$$

It is worth noting that possible failure mechanisms involving the angle brackets were not considered. This choice was made mainly for two reasons: on the basis on some preliminary analyses and also taking into consideration the results of several analyses performed by the *Timber Research Group* it was noted that angle-brackets are rarely stressed over the yielding; moreover the interface between the wall and the lower floor provide some friction that decreases the force in the angle-brackets.

Considering the results obtained, it is possible to make some considerations:

- two different group of failure mechanisms can be defined: failures that can be defined *pure*, namely the yielding and the rupture involve only one base components, and failures that can be defined *hybrid*, namely yielding and rupture happen in two different components;
- the involvement of the hold-downs in the failure-mechanism of the building implies the attainment of really low values of ductility. Moreover these kind of mechanism do not have any benefit in the increasing of the nails ductility;
- the most ductile mechanism iinvolves the nails and more precisely a *pure* mechanism has to be preferred;
- the variation of the hold-downs strength may cause a significant change in the overall behavior of the structure.

The fact that the failure mechanism is influenced by the hold-downs strength represents a very important aspect to consider. The ductility modification caused by the change in resistance of the hold-downs can effectively shown

Wall	Length [mm]	Vertical Load [kN]
W_1	2000	11,86
W_2	3300	19,56
W_3	1500	8,86

Table 5.3: *System properties.*

by the example of Fig. 5.8, which shows the ductility reached by the system to vary the strength of the hold-downs used. The system analysed is a case-study composed by three different walls whose properties are shown in Tab. 5.3

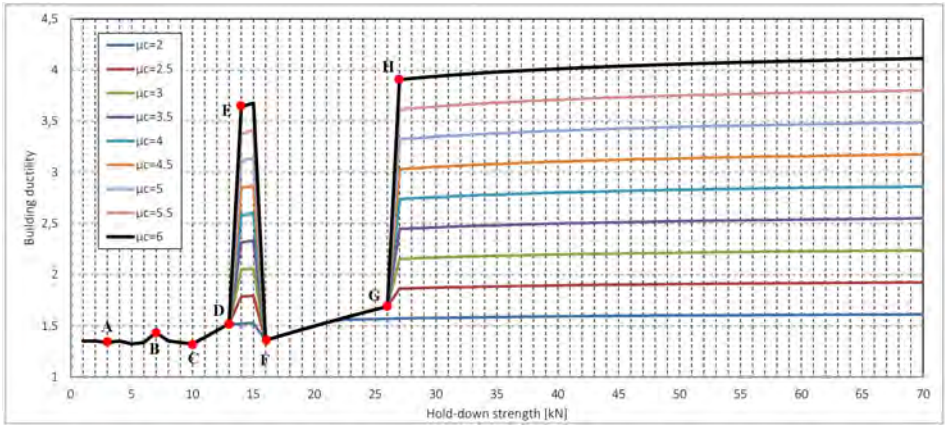

Figure 5.8: *System ductility vs hold-down resistance (resistance in [kN]).*

It is worth noting that the variation of the hold-downs resistance implies the change of the number of connecting devices to be used in order to avoid the rigid rotation of the walls. In the chart of Fig. 5.8, some relevant points which represent the variation of the system behaviour are highlighted: points A and C are characterized by low values of ductility; in fact, yielding and failure involve the hold-down of the $Wall_1$.

Point B shows a slight increase of ductility due to the fact that the failure

mechanism can be defined *hybrid*, namely the yielding involves the sheathing-to-framing connection of $Wall_3$, whereas the failure is due to the rupture of the hold-down of the $Wall_1$. The same failure happens also for values between points C and D, except for point D.

Point E shows a peak of ductility due to the occurrence of a ductile failure mechanism, which is related to the involvement of the sheathing-to-framing connection of $Wall_3$. Between points F and G the failures are characterized by the same hybrid mechanics of point B; it is worth noting that the ductility increases slightly moving from point E up to point G because the yielding displacements are gradually smaller due to the increase of the stiffness of the system which is caused by the use of stronger hold-downs.

Beyond point G the failure of the sheathing-to-framing assures a ductile behaviour for each value of hold-down resistance. It is possible to note a tiny increase of ductility for the same reason explained before.

It is possible to state that the change between a ductile and a brittle behaviour is due the change of the over-strength of the hold-downs, which in turns depends on the resistance considered for them. It has to be remark that different values of nails ductility (μ_c) provide different values of system ductility only when the failure mechanism of the whole system involves the nails.

In order to collect a large set of data, several random generated one-storey buildings were then analaysed. Specifically, 19200 different configurations were studied by varying the plan-area A, the length of the shear-walls L, the tributary area of the walls L_{inf}, the nails ductilty μ_c and hold-downs μ_{hd} ductility as well as the resistance of the hold downsf_{hd}:

$$L\,[m] = [1-1,25-2-2,5-3-3,5-3,75-4-4,5-5] \tag{5.7}$$

$$L_{inf}\,[m] = [0,5-1-1,5-2-2,5-3-3,5-4;4,5-5-5,5-6] \tag{5.8}$$

(5.9) $$A\,[mq] = [70 - 75 - 80 - 85 - 90 - 95 - 100 - 105 - 110 - 115]$$

(5.10) $$f_{hd}\,[kN] = [10 - 18 - 26 - 34]$$

Four different combinations of ductility were considered, see Tab. 5.4.

	μ_c	μ_{hd}
$Comb$ 1	1,5	2
$Comb$ 2	1,5	6
$Comb$ 3	3	2
$Comb$ 4	3	6

Table 5.4: *Combination of ductility cosidered.*

The main result of the analysis are the Chats of Fig. 5.9 whose show the ductility achievable by the buildings. It can be noted that for the $Comb$ 2 the results are grouped into two bands; the upper band is related to the failure of the nails whereas the lower band is related to the failure of the hold-downs. With respect to the $Comb$ 1 all the cases show a brittle behaviour.

It is therefore possible to state that in order to assure a ductile behaviour, the involvement of the hold-down in the failure mechanism should be avoided and nails with a quite high ductility are suggested to use.

The attainment of a specified failure mechanism, specifically the failure of the sheathing-to-framing connection, can be assured by the use of a capacity design approach. The capacity approach suggested to the design of light timber-frame walls consists of designing hold-downs and angle-brackets more resistant than the nailing using the following equations:

(5.11) $$V_{Ed,AB} \leq \alpha_r \cdot V_{Ed} \cdot \gamma_{rd}$$

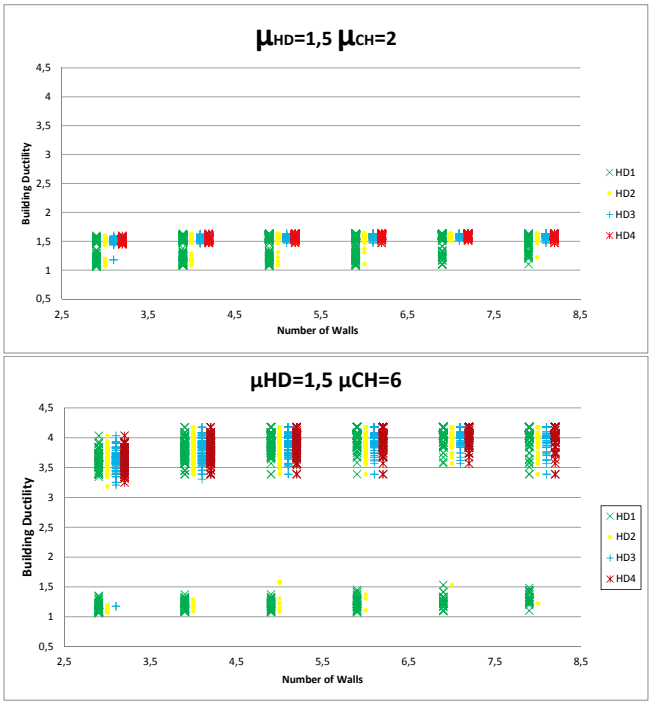

Figure 5.9: *Systems ductility for* $Comb$ *1 and* $Comb$ *2.*

$$T_{Ed,HD} \leq (\alpha_r \cdot V_{Ed} \cdot \gamma_{rd}) \cdot \frac{h}{\tau \cdot l} - \frac{q \cdot l}{2} \tag{5.12}$$

where α_r is equal to:

$$\alpha_r = \frac{V_{Rd,SH}}{V_{Ed}} \tag{5.13}$$

The same set of analysis is then preformed again but using the Capacity Design approach presented. The result is that all the buildings show a ductile behaviour, see Fig. 5.10, and that the relationship between the nails ductility and the building ductility can be considered linear, see Fig. 5.11.

The analysis of several one-storey buildings highlighted the need of a design capacity approach in order to avoid the involvement of the hold-downs in the failure mechanisms. It is also possible to state that the building geom-

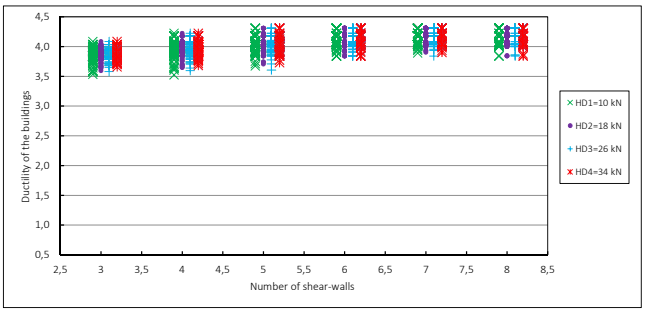

Figure 5.10: *Systems ductility obtained by the use of the capacity design.*

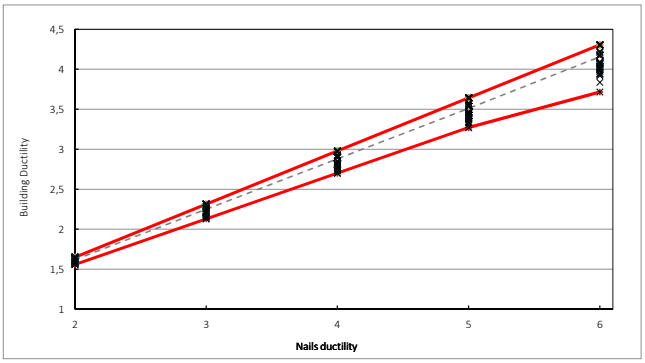

Figure 5.11: *Systems ductility vs. nails ductility.*

etry as well as the number of the shear walls do not influence the ductility achievable.

The non linear analysis was then extended to multi-storey buildings in order to evaluate the influence of the building dimensions as well as the number of storey on the ductility. The analyses were performed by the Matlab program previously mentioned; the case considered were 3456 and they were determined by varying the number of storey from 2 to 4, by changing the seismic level as well as the behaviour factor used in the design.

The main result of the analysis is the chart of Fig. 5.12 showing the ductility reached by the buildings. It is possible to note that the ductility decreases with the increase of the number of storey and that the values related to nails with a higher ductility are more scattered.

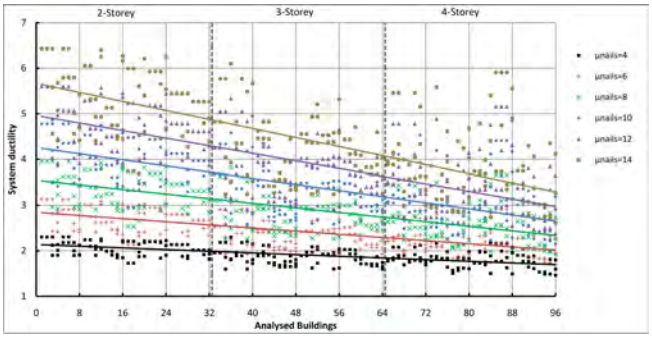

Figure 5.12: *Multi-storey building ductility.*

Buildings with a higher number of storey display a lower ductility because the failure mechanisms involves generally the firsts storey, namely the lasts storey remain in the elastic range. In fact, it is hard to guarantee the spread of the ductility in many storey. Moreover, the fact that the ductility values related to more ductile nails show an unfavorable deviation from the average is due to these nails allow a higher plastic-displacement and therefore allow the failure to involve a variable numbers of walls. It has to be remarked that the values of Fig. 5.12 were determined by the use of the Capacity Design; in fact, in the case it would not be used, the involvement of the hold-down in the failure mechanism would not be avoided and the ductility values displayed by the buildings would be those shown in the Chart of Fig.5.13.

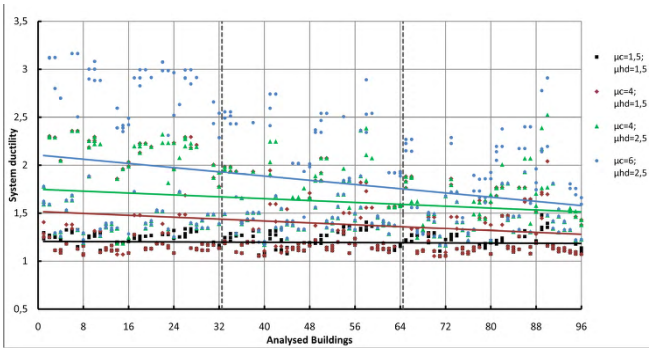

Figure 5.13: *Ductility achievable without Capacity Design.*

Specifically, the capacity design for multi-storey buildings consists in en-

suring that nails are yielded for the first, namely the hold-downs have to be over-resistant. This can be achieved by the use of the following equations due to the fact that a multi-storey wall can be considered as a system of springs placed in series, see Fig. 5.14, and so it can be considered as an isostatic system.

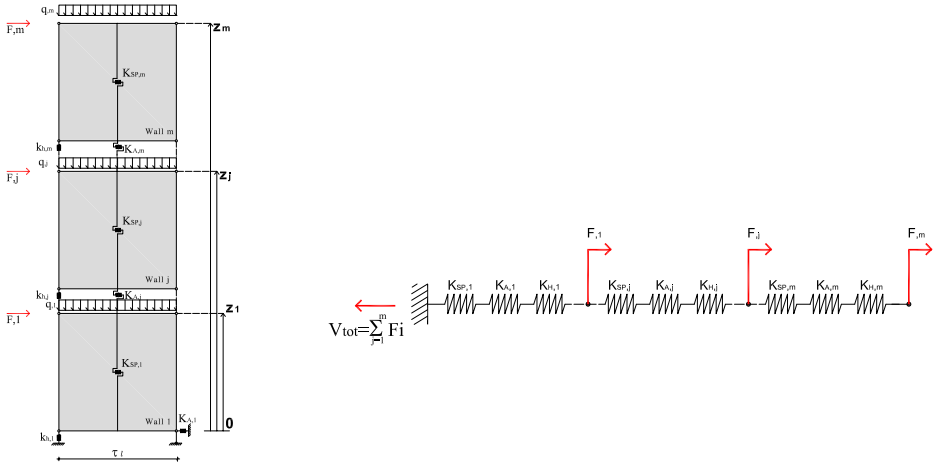

(a) Numerical $m \times 1$ model (b) Rheological model

Figure 5.14: *Multi-storey wall of m-storey.*

$$F_{Ed,HD,i} = \alpha_{min} \cdot \gamma_{rd} \cdot \left[\sum_{j=i}^{m} \left(V_{Ed,j} \cdot \frac{h_j - h_i}{\tau \cdot l} \right) - \sum_{j=i}^{m} \left(\frac{q_j \cdot l}{2} \right) \right] \tag{5.14}$$

where:

$$\alpha_{min} = min \left[\frac{V_{Rd,SH,j}}{V_{Ed,j}} \right] \; for j \in [i; m] \tag{5.15}$$

All the ductility values collected during the analysis are used to evaluate and propose a new set of value for the behaviour factor to be used in the seismic design of light timber-frame buildings.

Two different methods to evaluate the q factor were considered; the first method is known as *N2-method*, developed by Fajfar, which provide two different equations with respect to the fundamental period of the structure:

$$\begin{cases} q^* = (\mu_s - 1) \cdot \dfrac{T^*}{T_c} + 1 \quad \rightarrow if \quad T^* < T_C \\ q^* = \mu_s \quad \rightarrow if \quad T^* \geq T_C \end{cases} \tag{5.16}$$

whereas the second method, known as *Newmark method*, has the advantage to not correlate the q-factor with the dinamic properties of the buildings:

$$q^* = \sqrt{(2\mu_s - 1)} \tag{5.17}$$

Because of the Newark method is less accurate to the Fajfar-one, even because the values provided by it seem to be extremely conservative, it is suggested to take into account only those of the N2-method.

It is worth remarking that the behaviour factor is the ratio between the seismic force that a structure would experience if its response was completely elastic $[F_{el,max}]$ and the minimum seismic force that may be used in the design $[F_y]$, with a conventional elastic analysis model:

$$q = \frac{F_{el,max}}{F_{el}} = \frac{F_{el,max}}{F_y} \cdot \frac{F_y}{F_{el}} = q^* \cdot OSR \tag{5.18}$$

The behaviour factor q can be effectively represented by Fig. 5.15, which represent the capacity curve of an equivalent S-DOF system. The M-DOF system can be reduced into a S-DOF system by the evaluation of the period T^* of the idealized system:

$$T^* = 2\pi \sqrt{\frac{m^* \cdot d_y^*}{F_y^*}} \tag{5.19}$$

where the ratio $\frac{F_y^*}{d_y^*}$ is the elastic stiffness of the S-DOF idealized system and

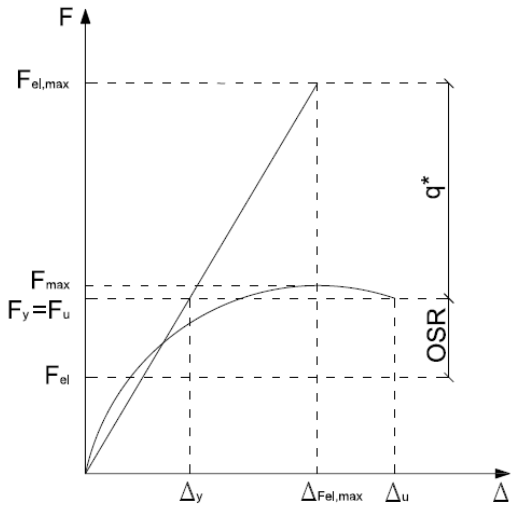

Figure 5.15: *Parameters for the definition of the behaviour factor.*

specifically it has been evaluated for each case as the slope of the curve obtained by the pushover analysis.

The mass of the idealized system is instead equal to:

$$m^* = \sum (m_i \cdot \Phi_i) \tag{5.20}$$

where m_i represents the mass of the $i-th$ storey whereas Φ_i is the dimensionless and normalized displacement at the same storey for the first mode of vibration.

For the cases considered, the values of T^* shown in Tab. 5.5 were determined.

	Buil.1X	Buil.1Y	Buil.2,	Build2Y	Buil.3X	Buil.3Y	Buil.4X	Buil.4Y
2-Stor.	0,555	0,546	0,520	0,540	0,522	0,532	0,532	0,544
3-Stor.	0,697	0,686	0,643	0,665	0,655	0,670	0,668	0,674
4-Stor.	0,765	0,753	0,772	0,800	0,777	0,797	0,769	0,776

Table 5.5: *Values of the period T^* in [sec] for the idealized structures.*

The values of the period T_c, namely the period corresponding to the point

starting from which the elastic response spectrum is with constant velocity, they are shown in Tab. 5.6.

Ground type	Tc [s]
A	0.4
B	0.5
C	0.6
D	0.8
E	0.5

Table 5.6: *Value of T_C period in function of the ground type.*

The base values of the behaviour factor q^* are shown in the Charts of Fig. 5.16.

With the aim to generalize the results, namely neglecting the variation given by the type of ground as well as by number of storey, a mean value for each nails ductility class was determined, see Tab. 5.7.

	μ_N=4		μ_N=6		μ_N=8		μ_N=10		μ_N=12		μ_N=14	
	DM	N2	DM	N2	DM	N2	DM	N2	DM	N2	DM	N2
M.V.	2,0	2,2	2,3	2,8	2,6	3,3	2,8	3,9	3,1	4,5	3,3	5,0
L.V.	1,6	1,7	1,7	1,8	1,8	2,1	2,0	2,3	2,1	2,6	2,2	2,8

Table 5.7: *Value of q for different values of the nails ductility.*

As conclusion, due to the fact that the nails currently on the market have an average ductility around 8 the values of behaviour factor q of Tab. 5.8, are suggested to use in the seismic design of light timber-frame buildings.

	D-Method	N2-Method
One - Storey	3,1	4,5
n - Storeys	2,6	3,3

Table 5.8: *Proposal of q values to use in seismic design.*

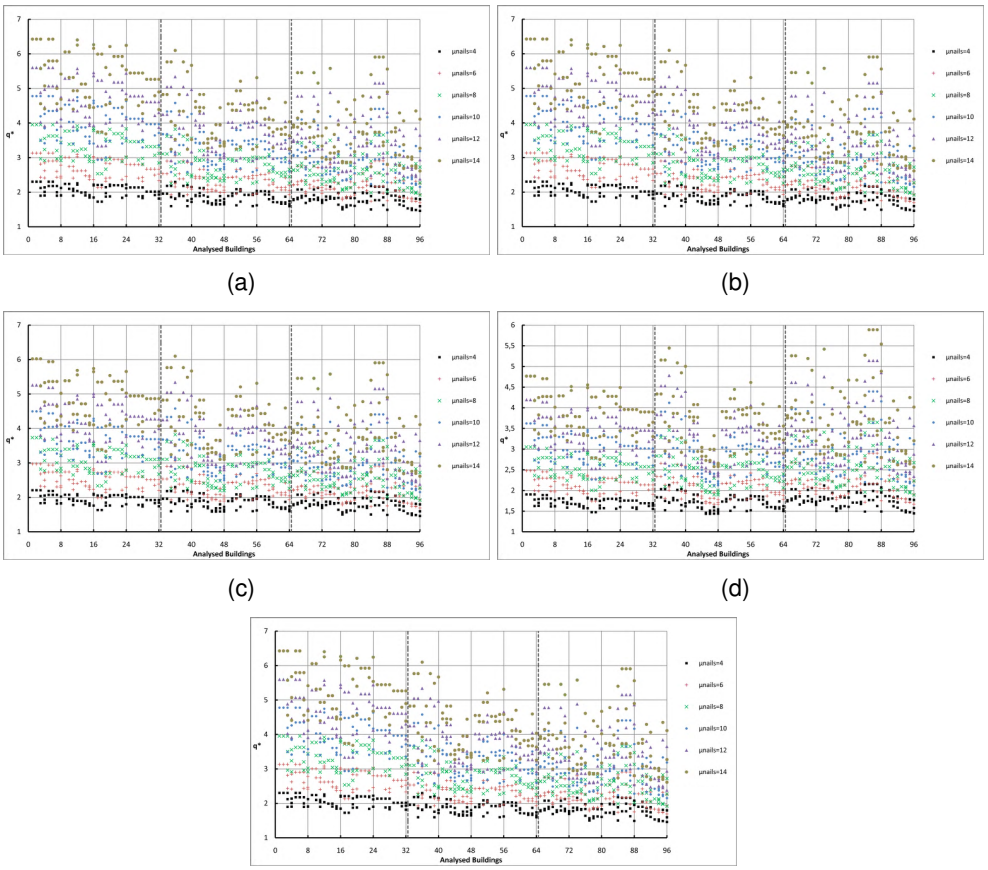

Figure 5.16: *Base values of the behaviour factor q^* give by N2-Method for: a) ground Type A, b) ground Type B, c) ground Type C, d) ground Type D, e) ground Type E.*

5.2 Appended Paper IV

Non-linear static analysis of light timber-frame buildings: determination of the displacement ductility, over-strength ratio and estimation of the reduction factor for the seismic design

Simone Rossi, Flavio Vinante, Maurizio Piazza, Daniele Casagrande

Submitted to Engineering Structures, Elsevier;

Non-linear static analysis of light timber-frame buildings: determination of the displacement ductility, over-strength ratio and estimation of the reduction factor for the seismic design

Simone Rossi[1,*], Flavio Vinante[2], Maurizio Piazza[3], Daniele Casagrande[4]

Department of Civil, Environmental and Mechanical Engineering, University of Trento, Italy, Tel. +39 0461 282529

Abstract

This paper deals with the non-linear static analysis of light timber-frame buildings in order to establish the relationship between the global ductility of the buildings and the local ductility of their components. Firstly, the study of single-storey buildings allowed to highlight different failure mechanisms and their influence on the building ductility; then the study was extended to multi-storey buildings in order to underline how the number of storey affects the ductility. In order to get general results, each analysis was performed varying the values of some mechanical-geometrical parameters as the seismic input and the ductility of the base components.

Keywords:
Light timber-frame buildings, Seismic analysis, Horizontal displacement, Response Spectrum Analysis, UniTn-Model, Behaviour Factor, Timber buildings

*Corresponding Author
Email address: simone.rossi1@unitn.it (Simone Rossi)
[1]Civil Engineer, Ph.D. Candidate
[2]Civil Engineer
[3]Civil Engineer, Professor
[4]Civil Engineer, Ph.D., Assistant Researcher

1. Introduction and objectives

Timber buildings were traditionally used in North Europe Countries as well as in North America, anyway they were mostly used for residential houses and small-size buildings and therefore they were not considered engineered-buildings but, primarily, a carpentry work based on the experience. Nowadays, instead, they are widely used also in earthquake prone regions such as Italy and other South-Europe countries and also mid and high-rise building are built.

The reason of this large diffusion is mainly due to the renewed sensitivity with respect to sustainability, low energy-consume and environment preservation ensured by these buildings, but also because timber buildings (in particular light timber-frame and cross laminated timber buildings) showed a quite safe and good behaviour during the last earthquakes. Recent researches, see [1]-[2]-[3] and [4], highlighted also the potentialities of this type of buildings and some other specialists studies have proposed a value of the behaviour factor q for some cases of study, see [5], [6] and [7].

Despite the diffusion of these buildings, and even though several research campaigns have been already performed, both in literature and in the standards a correlation between the *behaviour factor q* and the real dissipative capacity of timber building is missing. In fact, it is not clear how reduction factor values q for the seismic design were determined; in fact, some research pointed out that these values may have been over estimated, see [8] and [9].

The need of a clear correlation between the ductility of the base components and the ductility achievable by the buildings is a key aspect in the seismic design of structures, see [10] and [11]. Moreover the need to use the *Capacity Design* in order to force a favorable failure mechanism in spite of a brittle-one, see [12], is a concept not yet well-developed for timber buildings.

The present paper is the last part of a wide and structured research with the aim to develop some tools and methods suitable for the analysis and design of these type buildings, see [13]-[14] and [15], and in detail it deals with the post-elastic analysis of light timber-frame buildings. By means of some F.E.

analyses performed with SAP2000, but primarily, through a Matlab Program specifically developed (which performs a non-linear incremental static analysis based on a stiffness adaptation procedure) several different cases are analysed with the following goals to: establish and propose an analytical correlation between the ductility of the base-components and the ductility achievable by the buildings; to assess the most ductile failure mechanism (which ensure higher level of plasticization); and, on the basis of the ductility values collected, to propose a new set of values of the behaviour factor q to be used in the design, which are more realistic and more reliable than those currently given by standards.

2. Mechanical behaviour of a single-storey timber shear-wall

This section briefly exposes how the non-linear behaviour of a light timber-frame shear-wall can be described from the mechanical point of view through analytical expression and a numerical simplified model taking into account of the main deformation contributions, see [14] and [13].

2.1. Simplified and rheological model

According to [13] the behaviour of a light timber-frame shear-wall subjected to a horizontal force F and a uniform distributed vertical load q_v, can be represented by a simple pinned frame regarded as a mechanism, braced by a horizontal spring of stiffness equal to K_{SP} representing the sheathing panels and their connection, and connected to the ground by two other springs of stiffness equal to k_h and K_A representing the hold-down and the angle brackets (or screws) respectively, see Fig. 1.

The model proposed in [13] takes into account the four main deformation contributions, namely the sheeting to framing connection, the rigid body rotation, the rigid-body translation and the sheathing-boards; other contributions (as frame deformation, bending deflection, compression perpendicular to the grain ect.) could be taken into account, but for the most used wall typologies

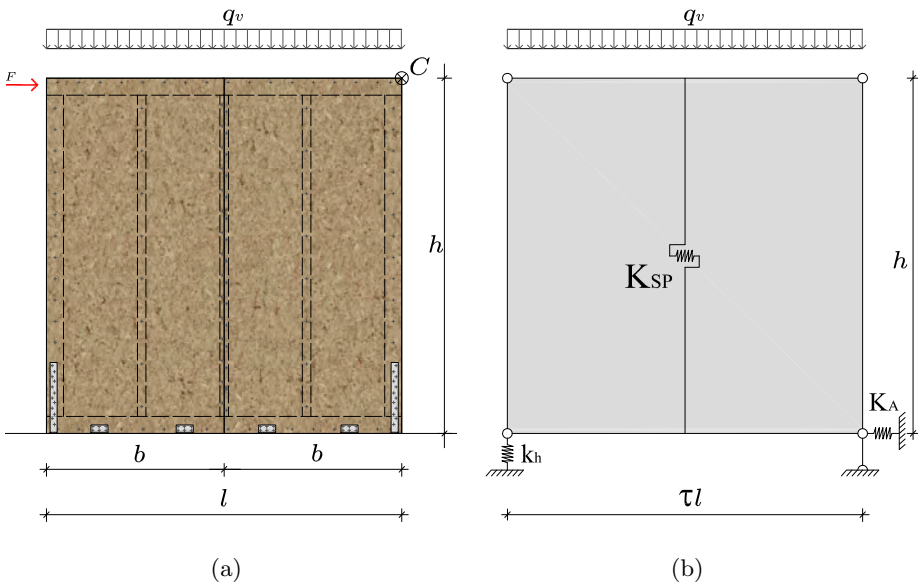

Fig. 1: Light timber-frame wall: (a) configuration and loads, (b) simplified numerical model.

in south Europe, these contributions are negligible compared to the others. For more details see [16], [17] and [18].

The simplified model, as deeply explained in [14] and [15], can be conveniently replaced by the rheological model of Fig. 2, where K_A is the horizontal stiffness of angle-brackets or screws; K_{SP} is the horizontal stiffness accounting for the sheathing-to-framing connection stiffness K_{SH} and the sheathing panel stiffness K_P ($K_{SP} = (\frac{1}{K_{SH}} + \frac{1}{K_P})^{-1}$); K_H is the horizontal stiffness of the hold-down and F_q is the activation force of the hold-down, which is represented by means of a block of friction.

The first model, namely the simplified model, can be conveniently used for elastic-analyses made by means of F.E. software, because describing the mechanical behaviour through three degrees of freedom, taking into account of the real geometrical properties directly. On the other hand, the rheological model, considering the geometrical properties of the wall in the constitutive laws of its springs, is more useful for analytical studies.

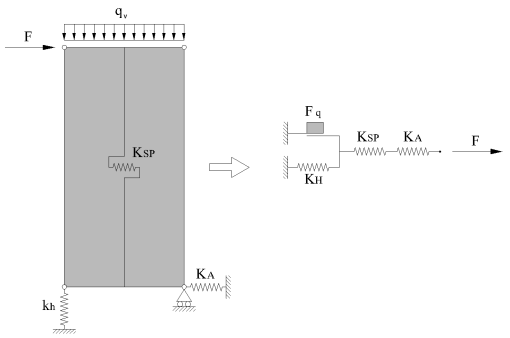

Fig. 2: Rheological model.

2.2. Implementation in the non-linear range

The implementation of the wall model in the non-linear range is quite simple and straightforward: assuming for each spring an elasto-perfectly plastic force vs displacement curve (characterised by proper stiffness, strength and ductility), the non-linear mechanical behaviour of the wall is therefore described by a bi-linear or tree-linear curve, depending on the magnitude of the vertical distributed load q_v (See Fig. 3). After defining the idealized elasto-perfectly plastic curve of each element of the rheological model, the elasto-plastic curve of the wall can be obtained adding each deformation contribution corresponding to a given force level. The mechanical properties defining the wall curve are: the friction block yield force F_q; the wall strength R_W; the wall stiffness $K_{tot,nt}$ when the rotation contribution is not considered; the wall stiffness K_{tot}, when the rotation contribution is considered; the wall secant stiffness K_W; the wall displacement $\Delta_{q,W}$ when the friction block yields; the wall yield displacement $\Delta_{Y,W}$ and the wall ultimate displacement $\Delta_{U,W}$.

It is important to highlight that the wall yield displacement $\Delta_{Y,W}$ can be determined as the ratio between the wall strength and the wall stiffness:

$$\Delta_{Y,W} = \frac{R_W}{K_W} \tag{1}$$

where the wall strength R_W corresponds to the minimum value of the strengths of the components (sheathing-to-framing, translation and rotation), since the

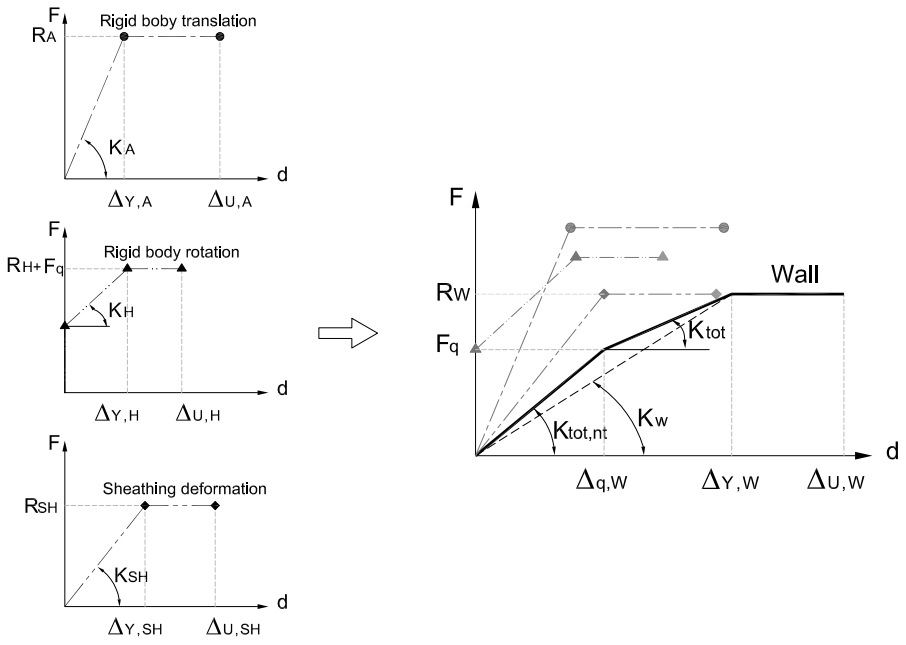

Fig. 3: Trilinear mechanical curve.

light-frame shear wall is an isostatic system (in fact it can be modelled by springs placed in series):

$$R_W = min(R_H + F_q; R_A; R_{SH}) \tag{2}$$

and wall secant stiffness K_W is given by:

$$K_W = \begin{cases} \left(\dfrac{1}{K_{SP}} + \dfrac{1}{K_A} + \dfrac{1}{K_H} - \dfrac{F_q}{K_H \cdot R_W}\right)^{-1} \rightarrow if\ R_W \geq F_q \\ \left(\dfrac{1}{K_{SH}} + \dfrac{1}{K_A}\right)^{-1} \rightarrow if\ R_W < F_q \end{cases} \tag{3}$$

It is important to note that if the strength of the wall R_W is lower than the activation force F_q the force vs. displacement curve of the wall becomes bi-linear and the secant stiffness K_W corresponds to the total stiffness K_{tot}.

The ultimate displacement of the wall $\Delta_{U,W}$ an be evaluated by means the following equation:

$$\Delta_{U,W} = \Delta_{Y,W} + \Delta_{pl,W} \tag{4}$$

where $\Delta_{pl,W}$ is the horizontal plastic displacement which coincides with the plastic displacement of the weakest (and hence yielded) component. The wall ductility μ_W can be defined as the ratio between the ultimate displacement and the yield displacement of the wall:

$$\mu_W = \frac{\Delta_{U,W}}{\Delta_{Y,W}} = \frac{\Delta_{Y,W} + \Delta_{pl,W}}{\Delta_{Y,W}} = 1 + \frac{\Delta_{pl,W}}{\Delta_{Y,W}} \tag{5}$$

As demonstrated before, the yield and plastic displacements of the wall correspond to those of the weakest component; therefore, identifying with the index i the weakest component, the wall ductility can be expressed trough the following relationship:

$$\mu_W = 1 + \frac{\frac{R_i}{K_i} \cdot (\mu_i - 1)}{\frac{R_W}{K_W}} \tag{6}$$

where: R_i, K_i and μ_i are the strength, the stiffness and the ductility of the weakest connections respectively.

2.3. Displacement ductility of the base components

As explained before, the wall displays different values of ductility according to the failure mechanism, namely the ductility depends on which connection devices yields and collapses. Specifically, three different cases can be defined: yielding and failure of the hold-down; yielding and failure of the angle-brackets (nails or screws) or yielding and failure of the sheathing-to-framing connection. It has to be remarked that more than one base-component may yield at the same time; anyway, the failure mechanism is associated to the least ductile one.

It is important to highlight that, according to several laboratory tests made by authors, see [19] and [20], and other research groups, see [21] and [22], the ductility of hold-downs and angle-brackets currently available on the market is sharply lower than the ductility of the nails or screws used for the sheating-to-framing connections. Consequently, the failure of the wall due to the failure of the sheathing-to-framing connections is the most ductile.

3. Non-linear analysis of single-storey buildings

This section deals with the non linear behaviour of systems made of several single-storey walls, namely single-storey buildings. Firstly, the behaviour of two-coupled walls is studied by means of a parametric approach in order to realize the way their interaction influences the behaviour of the whole system. In fact, if a single wall can be assumed as an isostatic system, two or more coupled walls constitute a hyper-static system, which behaviour is much more complex in analyzing and describing. In the second part of the chapter, full-scale single-storey building are analysed in order to detect the occurrence of some failure mechanisms, which are responsible of different ductility levels; due to the grate amount of mechanical and geometrical parameters, these mechanisms are difficult to foresee and to control. These analyses highlighted that the current design procedure, even if it ensures the proper strength, it does not allow to design the ductility of buildings.

In order to properly define the influence of the base components and of the building geometry on the global behaviour, a large set of buildings has been analysed. Consequently, due to the great amount of input data required, as well as the large number of different cases studied, a Matlab Code has been specifically developed by authors to perform incremental static analysis.

3.1. System of two coupled shear-walls

Two coupled shear walls, from the rheological point of view, can be regarded as a system of springs placed in parallel; consequently, as a single wall can be represented by three spring placed in series, a system of coupled walls, can be describer by means of a set of springs placed in series placed in parallel, see Fig. 4. As deeply explained in [15], the condition so that coupled walls can be modeled as springs placed in parallel is the presence of a rigid floor/diaphragm which imposes to the elements the same displacement. The action of the floor is taken into account in the model through a rigid link, or a pinned beam, between the walls, which remains unreformed and transits only horizontal force. It might

be stressed that this assumption is valid only in the case of blocked diaphragms, which are typically used in the seismic regions.

For a single wall the yielding component is the weakest one, therefore the behaviour depends on the strength of the base elements; on the other hand, for systems of coupled walls the yielding component is that characterized by the lower yielding displacement, even if it is not the weakest one. This occurs because the wall are forced to undergo the same displacement and so, the acting external force stresses them proportionally to their stiffness. As a consequence, despite the single wall can not carry any increase in force over the yielding point, a system of coupled wall is able to bear force over the yielding point; this force increase is called over-strength and it is greater for systems of walls that have yielding points distant from each-other.

3.1.1. Parametric analysis of the non-linear behaviour of two coupled walls

Systems of coupled walls can display several different yielding and failure mechanisms with the change of strength, stiffness and ductility of the walls.

Considering a system of two walls called $Wall_A$ e $Wall_B$, where the first one is stronger and stiffer, namely a system which can be defined by means the

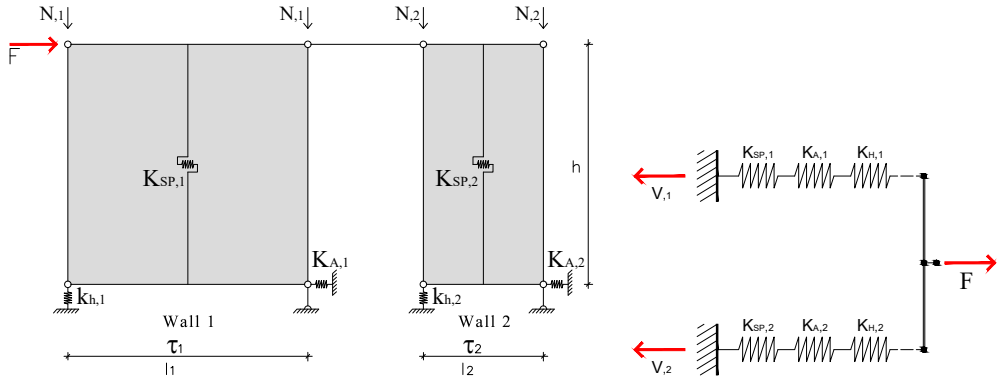

(a) Numerical $1 \times n$ model; (b) Rheological model;

Fig. 4: System of two coupled walls.

following equations:

$$\begin{cases} F_A > F_B \\ K_A > K_B \end{cases} \tag{7}$$

where, with the aim to simplify the mathematical treatment without compromising the correctness, K_A and K_B are assumed to be the secant stiffness.

On the base of these assumption it is possible to identify two cases: in the $Case$ 1 the yielding displacement of spring representing the $Wall_A$ is lower than that of spring representing the $Wall_B$, in the $Case$ 2 the yielding displacement spring representing the $Wall_A$ is higher than that of the $Wall_B$; each case allows to identify three sub-cases definable to vary the bi-linear curve of the walls.

The $Case$ 1 is described by the following equations:

$$\Delta_{Y,A} < \Delta Y, B \rightarrow \begin{cases} \Delta Y, B < \Delta U, A < \Delta U, B \rightarrow \ case\ 1.1 \\ \Delta U, A > \Delta U, B \rightarrow \ case\ 1.2 \\ \Delta U, A < \Delta Y, B \rightarrow \ case\ 1.3 \end{cases} \tag{8}$$

whereas the $Case$ 2 is described by the following equations:

$$\Delta_{Y,A} > \Delta Y, B \rightarrow \begin{cases} \Delta Y, A < \Delta U, B < \Delta U, A \rightarrow \ case\ 2.1 \\ \Delta U, B > \Delta U, A \rightarrow \ case\ 2.2 \\ \Delta U, B < \Delta Y, A \rightarrow \ case\ 2.3 \end{cases} \tag{9}$$

defining the following dimensionless parameters:

$$\tilde{f} = \frac{F_B}{F_A} \tag{10}$$

$$\tilde{k} = \frac{K_B}{K_A} \tag{11}$$

the six cases introduced before can be analysed in detail.

Case 1.1

In the $Case$ 1.1 the yielding and failure displacements of the spring A are lower

than the corresponding ones of the spring B, see Fig. 5. The inequalities describing this case are the following:

$$\frac{\tilde{f}}{\tilde{k}} \geq 1 \tag{12}$$

$$\frac{\tilde{f}}{\tilde{k}} \leq \mu_A \leq \frac{\tilde{f}}{\tilde{k}} \cdot \mu_B \tag{13}$$

In this case, it is evident that the ductility of the system matches the ductility of the $Wall_A$, because this is responsible for the yielding and failure of the whole system. The $Wall_B$ influences the system only in terms of over-strength (O.S.R.), namely the ratio between the ultimate force and the yielding force:

$$OSR = \frac{F_A + F_B}{F_A \cdot \frac{K_A + K_B}{K_A}} = \frac{1 + \frac{F_B}{F_A}}{1 + \frac{K_B}{K_A}} = \frac{1 + \tilde{f}}{1 + \tilde{k}} \tag{14}$$

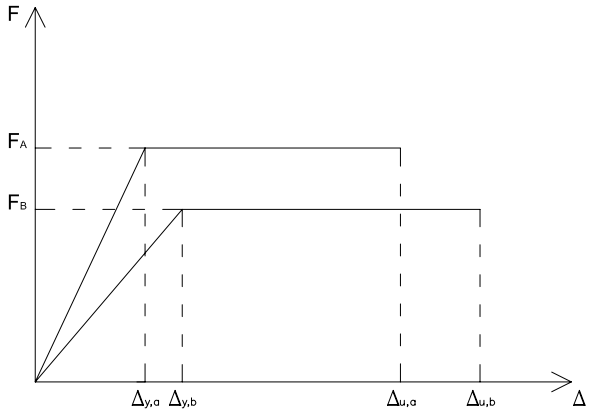

Fig. 5: Case 1.1.

Case 1.2

The *Case* 1.2 differs from the previous one for the fact that the ultimate displacement of spring A is higher than the corresponding one of spring B and therefore, the system collapses when this gets its ultimate displacement, see Fig. 6. The inequalities are the following:

$$1 \leq \frac{\tilde{f}}{\tilde{k}} \leq \frac{\mu_A}{\mu_B} \tag{15}$$

In this case the ductility of the whole system and of the less ductility spring do not match. In fact the system ductility depends on the mechanical parameters of both springs; this can be defined dimensionless by means of the following equation:

$$\mu_{SYS} = \mu_B \cdot \frac{\tilde{f}}{\tilde{k}} \tag{16}$$

The system over-strength is equal to that one of the previous case:

$$OSR = \frac{1+\tilde{f}}{1+\tilde{k}} \tag{17}$$

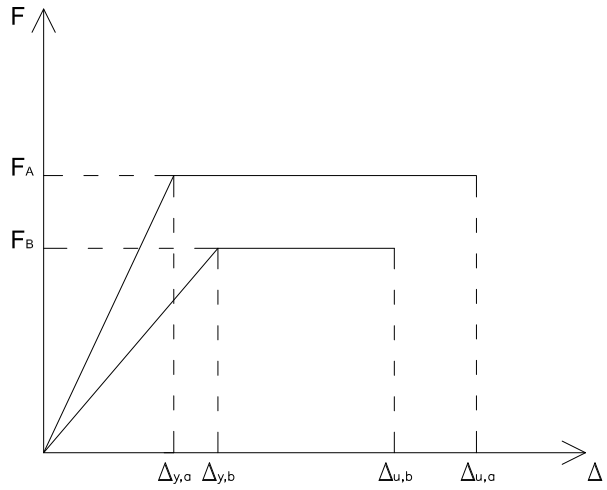

Fig. 6: Case 1.2.

Case 1.3

In the *Case* 1.3, the ultimate displacement of the spring A is lower than the yielding displacement of the spring B, see Fig. 7; therefore this can be defined by means just one inequality:

$$\frac{\tilde{f}}{\tilde{k}} \geq \mu_A \tag{18}$$

The system gets the ultimate displacement before the spring of the $Wall_B$ reaches the yielding point and so the system shows a strength lower than those of the previous cases, moreover, the ductility matches obviously the ductility

of the $Wall_A$. The over-strength is given by the following expression:

$$OSR = \frac{1 + \mu_A \cdot \tilde{k}}{1 + \tilde{k}} \tag{19}$$

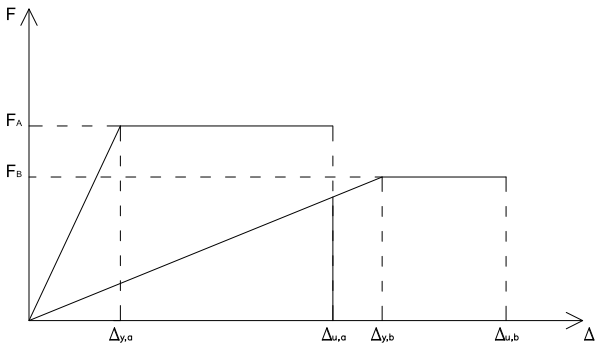

Fig. 7: Case 1.3.

Case 2.1

The inequalities describing the $Case$ 2.1 are the following:

$$\frac{\tilde{f}}{\tilde{k}} \leq 1 \tag{20}$$

$$1 \leq \mu_B \cdot \frac{\tilde{f}}{\tilde{k}} \leq \mu_A \tag{21}$$

From Fig. 8, it can be easily understood that the $Case$ 2.1 is equal to the $Case$ 1.1, but the walls have roles reversed. Therefore, the system ductility matches the ductility of the $Wall_B$ whereas the $Wall_A$ contributes to the system behaviour just in terms of over-strength, which is give by the following:

$$OSR = \frac{1 + \frac{1}{\tilde{f}}}{1 + \frac{1}{\tilde{k}}} \tag{22}$$

Case 2.2

In the $Case$ 2.2 the ultimate displacement of spring B is higher than that of spring A:

$$\frac{\mu_A}{\mu_B} < \frac{\tilde{f}}{\tilde{k}} \leq \mu_A \tag{23}$$

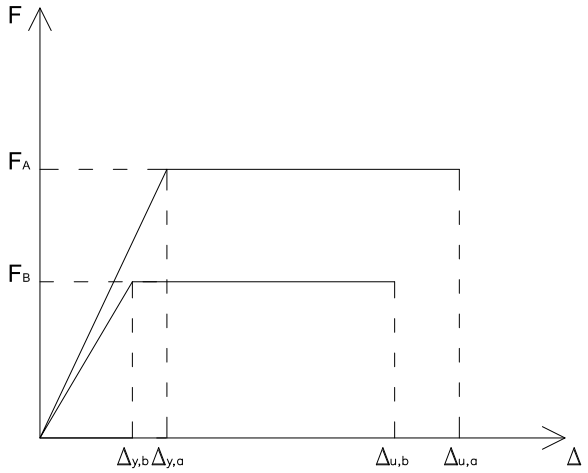

Fig. 8: Case 2.1.

In the same way as *Case* 1.2, both the springs contributes to define the system ductility:

$$\mu_{SYS} = \mu_A \cdot \frac{\tilde{f}}{\tilde{k}} \tag{24}$$

whereas the over-strength is the same of the previous case.

Case 2.3

In this case the ultimate displacement of spring B il lower than the yielding displacement of spring A:

$$\mu_B \cdot \frac{\tilde{f}}{\tilde{k}} \leq 1 \tag{25}$$

the system ductility matches the ductility of wall B, whereas the over-strength is given by:

$$OSR = \frac{1 + \frac{\mu_B}{\beta}}{1 + \frac{1}{\beta}} \tag{26}$$

3.2. Non-linear analysis of a real one-storey building

The previews section highlighted that all the mechanical parameters of the walls influence the non-linear behaviour of the system. For this reason, extending the analytical analysis to full-scale building would necessary bring to iden-

tify a really great amount of different cases (namely, several full scale buildings with different geometric and mechanical properties) has led to adopt a numerical approach. In detail, as explained before, a Matlab program specifically develop has been used to perform the incremental static analyses.

3.2.1. Geometry and design of the building

The building analysed is a real single-family one storey house characterized by structural simplicity as well as the uniformity in plan, which allows to neglect the torsional effects on the force distribution. As explained before, the floor of

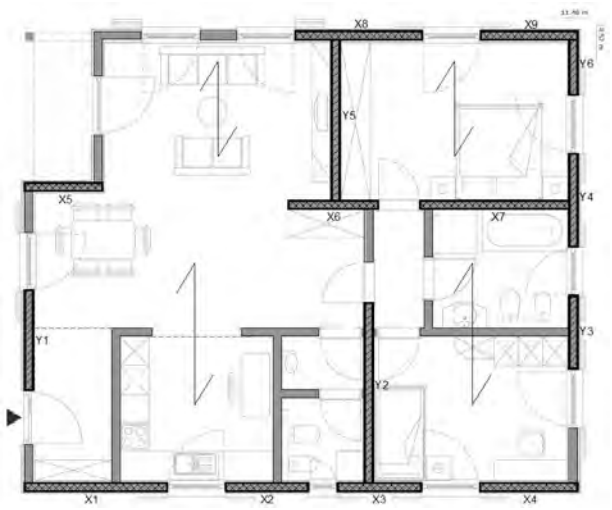

Fig. 9: Plant of the building.

the building has been regarded as an infinite rigid diaphragm.

The plant of the building is approximately squared with sides 11.46 by 9.52 meters. Fig. 9 shows the plant of the building in which the bearing shear-walls are highlighted; the other walls are secondary members, namely partition-walls not forming part of the seismic action resisting system. The shear-walls have been identified in terms of number and length in order to ensure a proper strength against the seismic force.

The buildings analysed were designed adopting average values of elastic response spectrum $S_E(T) = 0.55g$ and a behaviour factor $q = 3.5$. The shear-

walls were designed through the formulations of [23] and [24] using the common procedure according to which each base component is designed to resist to the seismic force.

3.2.2. Discussion of the results

The three-linear curve of each shear-wall of the building, according to 2.1, can be defined knowing its geometric and mechanical properties. From the three-linear curve of the walls it is possible to determine the capacity curve of the whole building, from which it is possible to get the values of ductility and over-strength.

As an example, Fig. 10 reports the capacity curve of the walls and of the whole buildings obtained analyses the building in the two main directions X and Y. For the sheathing-to-framing connection were used nails with a static ductility equal to 6 and hold-downs with a static ductility equal to 1.5.

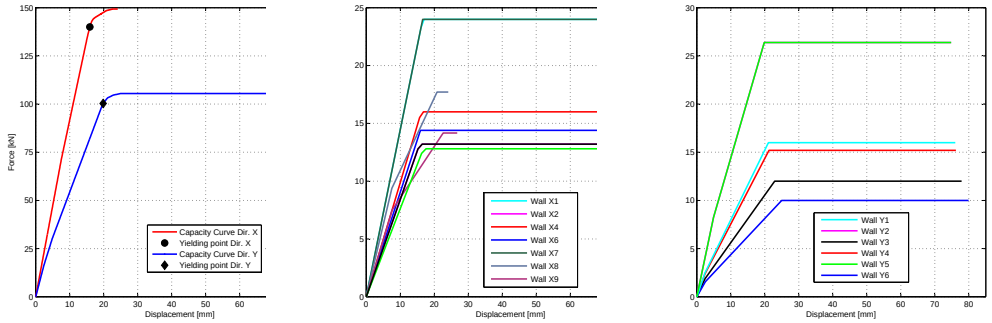

(a) (b) (c)

Fig. 10: (a) Capacity curves of the system, (b) Capacity curves of the walls along X direction, (c) Capacity curves of the walls along Y direction.

From the capacity curves of figure Fig. 10 (a), it is evident that the behaviour of the building in X direction displays a small level of ductility; in fact, it is conditioned by walls $X8$ and $X9$ the collapse of which is caused by the failure of the hold-downs. On the other hand, the behaviour of the building in Y direction is more ductile; indeed, the failure of each wall in this direction is caused by the failure of the sheathing-to-framing connection.

In order to determine the way the hold-down and nail ductility influence the global ductility, the building was analysed several times (36 different cases) assigning to nails the following values of ductility:

$$\mu_{nails} \in [2,\ 2.5,\ 3, 3.5,\ 4,\ 4.5,\ 5,\ 5.5,\ 6] \tag{27}$$

and to hold-down the following values of ductility and strength (in $[kN]$):

$$\mu_{HD} \in [1.5,\ 2, 2.5,\ 3] \tag{28}$$

$$R_{k,HD} \in [10,\ 18,\ 26,\ 34] \tag{29}$$

The values of the ductility used for the analyses are based on the results of several experimental tests ([19], [20] and see [22]); the nails commonly used for the sheathing-to-framing connection are characterized by a neglecting variation of strength, for this reason it has assumed as a constant (the characteristic resistance of the nails was assumed equal to $R_{nails} = 1\ kN$).

The most significant results of the analyses of the buildings in X direction are shown in the tables from Tab. 1 to Tab. 6; the results given are derived from the cases in which the hold-downs strength is equal to 10 and 18 kN. In detail, the results are collected in a table form and they are shown in terms of displacement ductility of the whole building and in terms of over-strength, it is also reported the failure mechanism.

The failure mechanism of the building is described by means of an abbreviation in which it is reported the base components responsible for the yielding y and the failure f; as an example the abbreviation $y : N2\ f : HD8$ specifies that the yielding and the failure are due to the nails of $Wall_2$ and to the hold-down of $Wall_8$ respectively.

From the results of Tab. 1 (related to hold-down of strength of 10 kN), it can be noted that for any cases, the behaviour is depending on the yielding of the sheathing-to-framing connection of $Wall_6$ and the collapse of the hold-down of $Wall_8$. These kind of failure mechanisms can be defined as *hybrid mechanisms* because involving two different base components.

μ_{hd}/μ_c	2.0	2.5	3.0	3.5	4.0	4.5	5.0	5.5	6.0
1.5	y:N6 f:HD8	y:N6 f:HD8	y:N6 f:HD8	y:N6 f:HD8	y:N6 f:HD8	y:N6 f:HD8	y:N6 f:HD8	y:N6 f:HD8	y:N6 f:HD8
2.0	y:N6 f:HD8	y:N 6 f:HD8	y:N6 f:HD8	y:N6 f:HD8	y:N6 f:HD8	y:N6 f:HD8	y:N6 f:HD8	y:N6 f:HD8	y:N6 f:HD8
2.5	y:N6 f:N6	y:N6 f:HD8	y:N6 f:HD8	y:N6 f:HD8	y:N6 f:HD8	y:N6 f:HD8	y:N6 f:HD8	y:N6 f:HD8	y:N6 f:HD8
3.0	y:N6 f:N6	y:N6 f:HD8	y:N6 f:HD8	y:N6 f:HD8	y:N6 f:HD8	y:N6 f:HD8	y:N6 f:HD8	y:N6 f:HD8	y:N6 f:HD8

Tab. 1: Failure mechanisms, Building 1, Dir. X ($R_{hd} = 10$ kN).

μ_{hd}/μ_c	2.0	2.5	3.0	3.5	4.0	4.5	5.0	5.5	6.0
1.5	1.35	1.35	1.35	1.35	1.35	1.35	1.35	1.35	1.35
2.0	1.50	1.50	1.50	1.50	1.50	1.50	1.50	1.50	1.50
2.5	1.57	1.65	1.65	1.65	1.65	1.65	1.65	1.65	1.65
3.0	1.57	1.80	1.80	1.80	1.80	1.80	1.80	1.80	1.80

Tab. 2: Ductility, Building 1, Dir. X ($R_{hd} = 10$ kN).

μ_{hd}/μ_c	2.0	2.5	3.0	3.5	4.0	4.5	5.0	5.5	6.0
1.5	1.07	1.07	1.07	1.07	1.07	1.07	1.07	1.07	1.07
2.0	1.07	1.07	1.07	1.07	1.07	1.07	1.07	1.07	1.07
2.5	1.07	1.07	1.07	1.07	1.07	1.07	1.07	1.07	1.07
3.0	1.07	1.07	1.07	1.07	1.07	1.07	1.07	1.07	1.07

Tab. 3: Over Strength Ratio, Building 1, Dir. X ($R_{hd} = 10$ kN).

The involvement of the hold-downs in the failure mechanism, as already explained, implies the attainment of small values of ductility, as it is reported in Tab. 2; moreover, for the failure mechanism caused by the hold-downs, it can be remarked that variation of the nails ductility does not influence the building

ductility.

μ_{hd}/μ_c	2.0	2.5	3.0	3.5	4.0	4.5	5.0	5.5	6.0
1.5	y:N2 r:N2	y:N2 r:N2	y:N2 r:N2	y:N2 r:N2	y:N2 r:N2	y:N2 r:N2	y:N2 r:N2	y:N2 r:N2	y:N2 r:N2
2.0	y:N2 r:N2	y:N2 r:N2	y:N2 r:N2	y:N2 r:N2	y:N2 r:N2	y:N2 r:N2	y:N2 r:N2	y:N2 r:N2	y:N2 r:N2
2.5	y:N2 r:N2	y:N2 r:N2	y:N2 r:N2	y:N2 r:N2	y:N2 r:N2	y:N2 r:N2	y:N2 r:N2	y:N2 r:N2	y:N2 r:N2
3.0	y:N2 r:N2	y:N2 r:N2	y:N2 r:N2	y:N2 r:N2	y:N2 r:N2	y:N2 r:N2	y:N2 r:N2	y:N2 r:N2	y:N2 r:N2

Tab. 4: Failure mechanisms, Building 1, Dir. X ($R_{hd} = 18$ kN).

μ_{hd}/μ_c	2.0	2.5	3.0	3.5	4.0	4.5	5.0	5.5	6.0
1.5	1.57	1.86	2.15	2.44	2.73	3.02	3.31	3.60	3.89
2.0	1.57	1.86	2.15	2.44	2.73	3.02	3.31	3.60	3.89
2.5	1.57	1.86	2.15	2.44	2.73	3.02	3.31	3.60	3.89
3.0	1.57	1.86	2.15	2.44	2.73	3.02	3.31	3.60	3.89

Tab. 5: Ductility, Building 1, Dir. X ($R_{hd} = 18$ kN).

μ_{hd}/μ_c	2.0	2.5	3.0	3.5	4.0	4.5	5.0	5.5	6.0
1.5	1.09	1.09	1.09	1.09	1.09	1.09	1.09	1.09	1.09
2.0	1.09	1.09	1.09	1.09	1.09	1.09	1.09	1.09	1.09
2.5	1.09	1.09	1.09	1.09	1.09	1.09	1.09	1.09	1.09
3.0	1.09	1.09	1.09	1.09	1.09	1.09	1.09	1.09	1.09

Tab. 6: Over Strength Ratio, Building 1, Dir. X ($R_{hd} = 18$ kN).

Differently, assuming for the hold-downs a strength of 18 kN, see Tab. 4,

it can be noted that the failure mechanisms change, implying the yielding and the failure of the sheathing-to-framing connection of $Wall_2$. In these case the building ductility increases significantly (see Tab. 5) becoming dependent only on the ductility of the nails. Further increasing the strength of the hold down the failure mechanisms do no change and in the same way the ductility of the building does not vary.

With respect to the over-strength, see Tab. 3 and Tab. 6, it assumes values not far from the unity because all the walls yield in a small range of displacement; this occurs because all the walls are characterized by the same mechanical properties and them length does not vary significantly.

The same set of analyses have been conducted on two other real full-scale building similar to the that presented. The results obtained have anyway omitted from this paper because of leading to the same considerations, namely they do not bring any other information.

The analyses exposed allow to make some consideration on the ductility of single storey building: firstly it can be remarked that the attitude of a building to display a ductile behaviour is strictly limited by the involvement of the hold-downs in the failure mechanism; moreover, it can be noted as the strength increase of the hold-down is related to the occurrence of different failure mechanisms, those are more ductile mechanisms.

3.3. Influence of the hold-down on the global ductility of the building

In order to completely clarify the rule of the hold-downs strength on the building ductility, a set of specific analyses were made on a case-study obtained from the previews building increasing the hold-down strength from 1 to 70 kN. The results obtained from this study (630 different cases) are shown in form of curves reported in Fig. 11.

From the curves it can be noted that for low values of hold-down strength, less than 13 kN (weak hold-downs), the global ductility of the building assumes small values and not dependent on the nails ductility; in fact the failure of the building is caused by the failure of the hold-downs. This happens because the

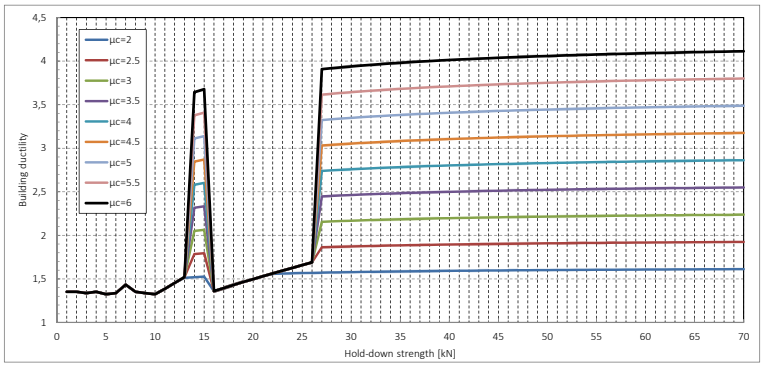

Fig. 11: Ductility of the building related to the hold-down strength.

use of hold-down characterized by small values of strength allows to obtain a resistance slightly greater than that required, but lower than that displayed by the sheathing-to-framing connection, and so the hold-down assumes the rule of the weakest base component which influences the failure mechanisms.

By contrast, for values of hold-downs strength higher than 26 kN the global ductility increases significantly because the failure of the building is caused by the failure of the nails. This occurs because the use of hold-downs characterized by a sufficiently high strength generates a remarkable over-design compared to that of the sheathing-to-framing connection, which so becomes the weakest base component. In detail, for the case analysed, for values of strength higher than 26 kN, one hold-down is enough to ensure the proper resistance.

It is worth noting that for hold-downs strength values between 14 and 15 kN, the failure mechanism of the building is determined by the nails failure, and so the building displays values of ductility comparable to those associated to higher values of hold-downs strength; this occurs because the over-strength of the hold-down connections is higher than that of the sheathing-to-framing one.

This set of analyses allowed to realize that trough the control of the over-strength of the base component it is possible to force a building to behave according to a ductile mechanism.

3.4. Non-linear analysis of a set of random generated buildings

With the aim to asses how the geometry of the building, in terms of dimensions and number of shear walls, influences the failure mechanism and so the global ductility assured by the building, a large set of randomly-generated buildings were studied (19200 different buildings). Specifically, in order to cover the largest range of cases and to detect the sensitivity of the building ductility from the mechanical parameters of the base components, the geometry of the building is defined randomly by the Matlab. For each case the geometry and the mechanical properties are defined by picking out in a random way the values of the parameter from those shown below:

$$Area\,[70-75-80-85-90-95-100-105-110-115]\ \left(m^2\right) \tag{30}$$

$$L_{walls}\,[1.00-1.25-2.00-2.50-3.00-3.50-3.75-4.00-4.50-5.00]\ (m) \tag{31}$$

$$\begin{aligned} L_{inf}[&0.50-1.00-1.50-2.00-2.50-3.00\\ &3.50-4.00-4.50-5.00-5.50-6.00]\ (m) \end{aligned} \tag{32}$$

$$R_{d,HD}\,[10-18-26-34]\ (kN) \tag{33}$$

Where:

- $Area$ is the plant dimension;
- L_{walls} is the length of the wall;
- L_{inf} is the tributary length;
- $R_{d,HD}$ is the strength of the hold-down.

It is worth to note that the chosen mechanical and geometrical values are representative for light-frame single-storey buildings.

The chart of Fig. 12 shows the values of ductility displayed by the buildings analyzed related to the number of shear walls of which they are composed and

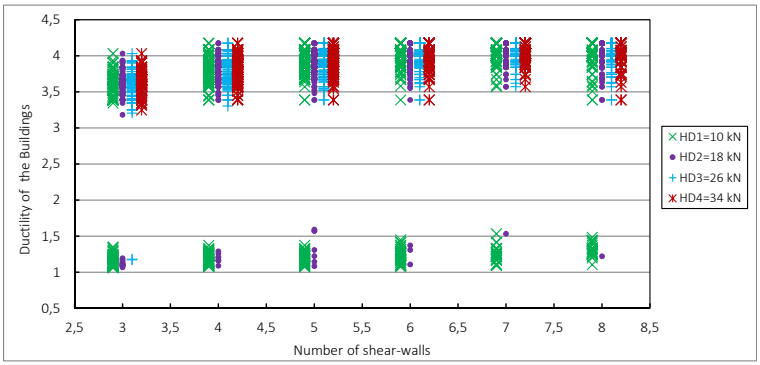

Fig. 12: Ductility of the random generated buildings related to the number of walls, $\mu_{nails} = 6$; $\mu_{HD} = 1.5$.

to the hold-down strength adopted. Specifically, the data are collected in four different series associated to four different strength of the hold-downs. The ductility chosen for the hold-downs and for the nails are equal to 1.5 and to 6.0 respectively. The graph points are grouped into two bands of ductility: a upper and a lower band. The point seated in the first one are related to the yielding and failure of the sheathing-to-framing connection (ductile failure), whereas the points of the lower one are related to the yielding and failure of the hold-downs or to hybrid mechanisms (brittle failure). It is necessary to highlight that the graph points located in the lower band are mainly associated to hold-downs characterized by low strength; this is in agreement with what was exposed in Sec.3.3.

The chart of Fig. 13, compared with that of Fig. 12, shows that the lower band moves slightly upwards changing the hold-downs ductility from 1.5 to 3. Anyway, the buildings characterized by the failure of the hold-downs as well as the ones characterized by hydride mechanisms still display low values of global ductility.

The analysis of the collected data makes it evident that the common design procedure does not allow to control the ductility that can be displayed by the designed buildings. It is worth also noting the limit values of ductility

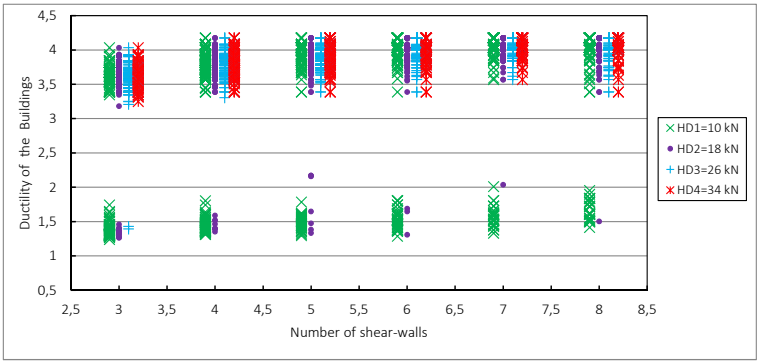

Fig. 13: Ductility of the random generated buildings related to the number of walls, $\mu_{nails} = 6$; $\mu_{HD} = 3$;.

(maximum and minimum) do not depend significantly on the dimension of the building, as well as on the number of shear-walls. However, it may be noted as the increase of the building area adversely influences the global ductility which slightly decreases (in both bands). On the contrary the increase of the number of shear-walls allows to decrease the number of brittle failure mechanisms. The parameter that exerts the greatest influence is the ductility of the base component involved in the failure mechanism.

3.5. Non-linear behaviour of buildings designed according to the capacity-design approach

From the previews sections it is evident the need to adopt a design approach that assures the occurrence of ductile failure mechanisms, namely failure mechanisms involving the sheathing-to-framing connection. This need can be met by the use of the *capacity design approach*, as, on the other hand, it is pointed out in the current version of the [25] which, anyway, does not provide any detailed application method.

From the general point of view the *capacity design approach* involves two key aspects: firstly, the identification of a mechanism with designated ductile connections or regions within the structure; secondly, the design of the other components (i.e. less ductile or brittle components) with a proper over-strength

to guarantee the activation of the selected ductile mechanism.

In view of the above , it is evident that for light-timber frame timber buildings, the ductile mechanism is that associated with the yielding and failure of the nails of the sheathing-to-framing connections. According to [12], for single storey buildings, the capacity design approach may be applied by means of the following expressions:

$$V_{Ed,AB} \leq \alpha_r \cdot V_{Ed} \cdot \gamma_{rd} \tag{34}$$

$$T_{Ed,HD} \leq (\alpha_r \cdot V_{Ed} \cdot \gamma_{rd}) \cdot \frac{h}{\tau \cdot l} - \frac{q \cdot l}{2} \tag{35}$$

where $V_{Ed,AB}$ is the design force acting in the angle-brackets, V_{Ed} is the shear-force that the wall bears and where α_r is the over-design ration between of the sheathing-to-framing connection:

$$\alpha_r = \frac{V_{Rd,SH}}{V_{Ed}} \tag{36}$$

The same set of analyses previously presented have been performed but designing the buildings according to the capacity design approach of [12]; differently from the previous cases, all the buildings, see Fig. 14, display a ductile failure mechanism. In fact, the graph points are grouped only in the upper ductility band, namely no brittle failure mechanisms happened.

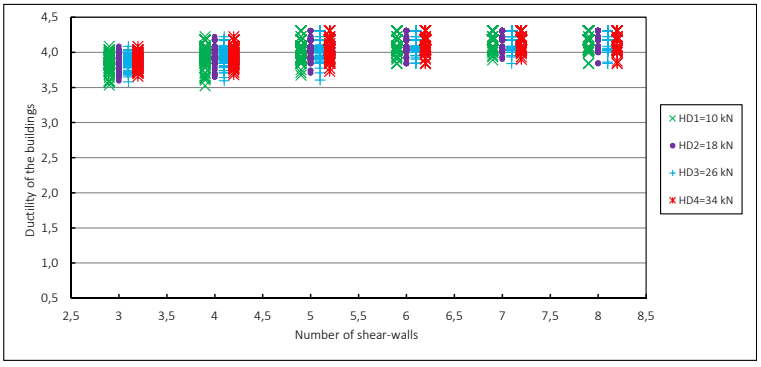

Fig. 14: Ductility of the random generated buildings related to the number of walls, $\mu_{nails} = 6$; $\mu_{HD} = 3$;.

3.6. Ductility of the building related to the nails ductility

From the chart of Fig. 15 it is worth to note that the variation of the building ductility related to the ductility of the nails used for the sheathing-to-framing connections can be considered linear; in fact, an increase of the nail ductility directly corresponds to an increases of the building ductility.

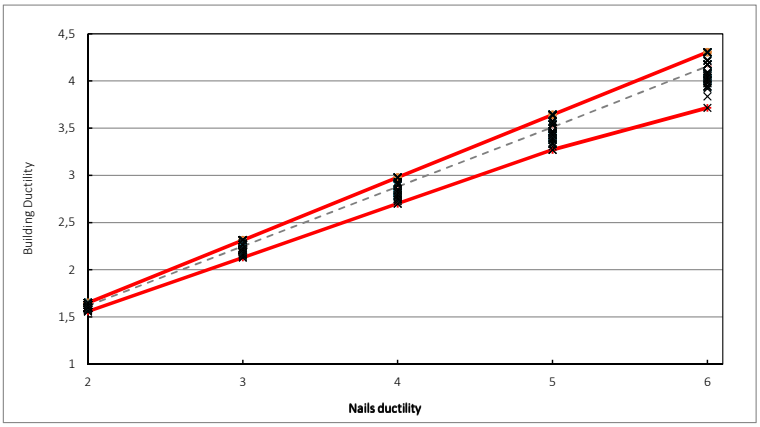

Fig. 15: Ductility of the building related to the nails ductility.

In detail, the chart points represent the results of all the analyses performed (ductility of all the buildings designed with the capacity approach) rearranged to show the variation of the system ductility of function of the nails one. The red lines represent the upper and lower limits whereas the gray dashed line is the mean value of the ductility.

The relation between the nails and the system ductility is well represent by following equation, which is the linear interpolation of the mean values of the results:

$$\mu_{system} = 0.63 \cdot \mu_{Nails} + 0.35 \tag{37}$$

4. Non-linear behaviour of a multi-storey shear-wall

The analysis of single-storey light-frame buildings highlighted two fundamental and correlated aspects: the need to force the buildings to collapse in-

volving the sheathing-to-framing connection, namely the nails; and the need to adopt the capacity design approach, which ensures the activation of the established collapse mechanism.

As stated by recent researches, see [4] and [2], if floors and diaphragms can be considered infinitely rigid, the Seismic Force Resisting System (SFRS) of multi-storey light-frame buildings is represented by the multi-storey shear-walls, see [15]. In other words, the seismic behaviour of this kind of buildings is determined by only the contribution of the multi-storey shear-walls continuous from the base to the top of the building, see Fig. 16. In fact, the contribution of the walls containing openings has not to be considered, according to [23]. From the constructive point of view, a multi-storey wall is erected by means of

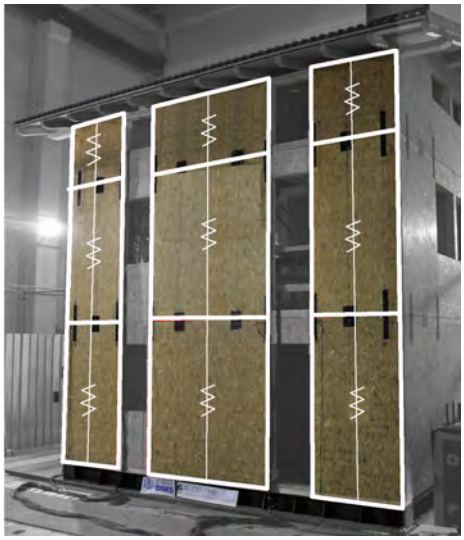

Fig. 16: Interpretation model of a full scale building.

the super imposition of single walls which are connected each other through tie-downs or nailing-plates, shear connections (screws, angle-brackets, etc), which ensures the continuity of the structural element, that is the forces transmission (shear, tension and compression) within the storey.

Therefore, to properly assess the behaviour of full-scale buildings, this section shows the analysis of the inelastic behaviour of a multi-storey shear-wall,

giving particular focus on the ductility achievable and on the way it is influenced by geometrical and mechanical properties.

4.1. Modelling of a multi-storey shear-wall

From the mechanical point of view a multi-storey single shear wall, as for the elastic behaviour see [15], can be modelled by means of m of macro-springs placed in series, where m is the number of storey. In the present case, see Sec. 2.2, each macro-spring displays a non-linear behaviour and it is obtained by the union of the three springs placed in parallel modelling the base components, see Fig. 17. It is worth noting that a multi-story shear wall is an isostatic system,

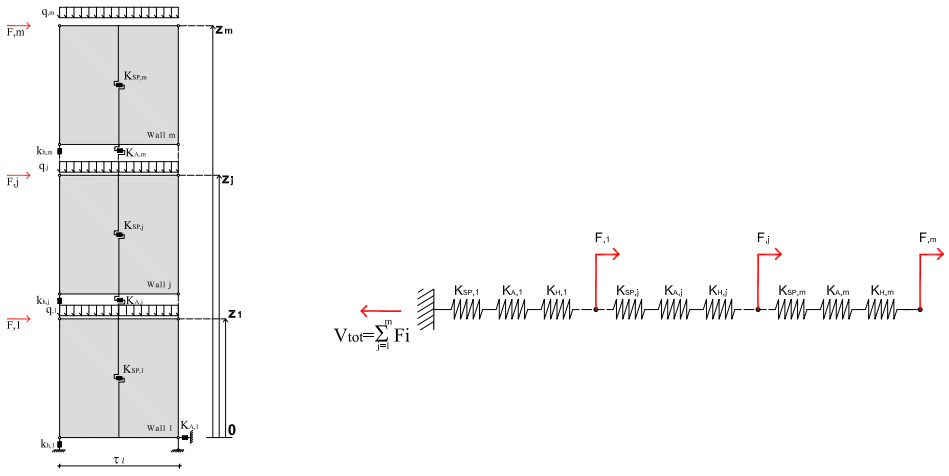

(a) Numerical $m \times 1$ model; (b) Rheological model;

Fig. 17: System of $m \times 1$ walls modelling a single-shear wall of m-storey .

whereas two or more coupled walls create an hyperstatic system; therefore a multi-storey shear-wall can not bear any horizontal-force increase beyond the collapse of any spring modelling the base components. Specifically, according to the elasto-perfectly plastic behaviour, the wall yielding is followed by a plastic displacement under a constant magnitude of horizontal-force.

Considering a force distribution $\boldsymbol{F}$ applied to a multi-story wall, the equilibrium condition can be expressed by the following equation (for a more detailed

discussion see [15]):

$$\boldsymbol{F} = \boldsymbol{K}\ \boldsymbol{\Delta} + \boldsymbol{F_N} \tag{38}$$

where $\boldsymbol{\Delta}$ is the array of the displacements and $\boldsymbol{F_N}$ is the array of the equivalent horizontal force due to the vertical load, which is equal to:

$$\boldsymbol{F_N} = \boldsymbol{K} \cdot \boldsymbol{\Delta_N} \tag{39}$$

where in turns $\boldsymbol{\Delta_N}$ is the array of the fictitious displacement related to the vertical load:

$$\Delta_{N,j} = \sum_{r=1}^{j} \left(\sum_{y=r}^{m} N_y \right) \cdot \frac{z_j - z_{r-1}}{k_{h,r} \cdot \tau \cdot l} \tag{40}$$

where N_y is the vertical load applied at the $y-th$ storey, z_j is the height of the $j-th$ storey and $k_{h,j}$ is the stiffness of the hold-down placed at the $j-th$ storey.

The stiffness matrix of the multi-storey wall $\boldsymbol{K}$ is obtained from the flexibility matrix $\tilde{\boldsymbol{U}}$:

$$\boldsymbol{K} = \tilde{\boldsymbol{U}}^{-1} \tag{41}$$

the elements of which are given from the sum of the deformation contributions of each base element:

$$\tilde{U}_{j,\xi} = \sum_{r=1}^{min(j,\xi)} \frac{1}{K_{SP,r}} + \frac{1}{K_{A,r}} + \frac{(z_\xi - z_{r-1}) \cdot (z_j - z_{r-1})}{k_{h,r} \cdot (\tau \cdot l)^2} \tag{42}$$

4.2. Ductility of multi-storey shear-walls

The analysis of the mechanisms influencing the ductility of a single multi-storey walls represents a generalization of the mechanisms highlighted in the previews section, in which the behaviour of a single shear wall was studied. In fact, because of a single multi-storey walls is a superimposition of several single walls, some consideration about its kinematics is required.

Let's consider a multi-storey shear wall loaded by a horizontal force F placed at the top floor. In the hypothetical case that only the sheathing-to-framing connections undergoes deformation (the other base components are considered

infinitely rigid), the inelastic displacement is not dependent on which storey the yielding occurs and moreover it is exactly equal to the inelastic displacement of the spring related to the sheathing-to-framing connection. On the contrary, if the only deformation contribution is that of the hold-down, the inelastic displacement changes if yielding story changes, see Fig. 18. Anyway, it is important to note that the global ductility, for both cases, is not dependent on which storey yields, but it is only related to the local ductility of the yielded base component.

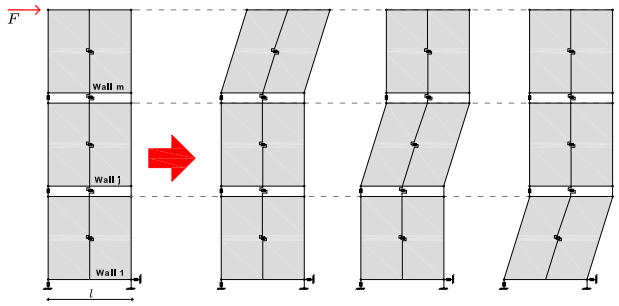

Fig. 18: Yielding patterns for multi-storey shear-walls.

After these preliminary considerations, it is possible to state that the ductility of a single multi-storey shear-wall decreases at the increasing of its height (that is the increase of the number of storey) and at the decreasing of its stiffness. This depends on two basic aspects: the fact that the displacement of the top floor is assumed as reference-displacement of the whole system; and the fact that the top floor displacement is produced by the deformation of all the base components, the number of which increases with the number of storey. Moreover the loss of ductility is related to the yielded storey; in fact, the yielding of the first storey does not allow the structural system to display all the available ductility; this can be easily demonstrated trough some mechanical consideration derived from [10]. It has to be reminded that when any base component reaches the yielding condition the external horizontal force con not be increased because a multi-storey shear-wall is an isostatic system.

To prove this, let's consider a single multi-storey shear wall composed by m walls with similar geometrical and mechanical properties, loaded by a force F placed at the top, see Fig. 19, which yields the sheathing-to-framing connections of the base wall: $\delta_1 = \delta_y$.

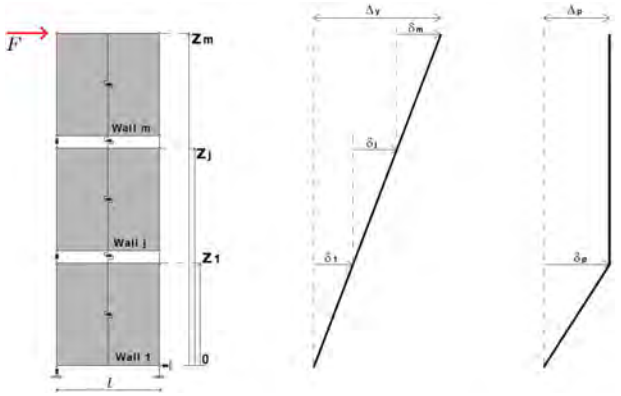

Fig. 19: Elastic and inelastic displacement of a single multi-storey shear wall.

The displacement of the reference point (top floor) at the yielding Δ_Y is given by the sum of the displacement contributions of the lower walls:

$$\Delta_Y = \sum_{j=1}^{m} \delta_j = \delta_1 + \delta_2 + ... + \delta_m = (1 + \frac{\delta_2}{\delta_y} + ... + \frac{\delta_m}{\delta_y}) \cdot \delta_y = (\rho \cdot m) \cdot \delta_y \quad (43)$$

where m is the number of storey and ρ is a parameter equal or less than 1, which accounts for the fact that the walls are not mechanically equal. In the same way the ultimate displacement Δ_U is equal to:

$$\Delta_U = \Delta_Y + \Delta_P \quad (44)$$

where Δ_P is the plastic displacement of the multi-storey wall, which is equal to the plastic displacement of the yielded wall:

$$\Delta_P = \delta_P \quad (45)$$

Known the yielding and ultimate displacements it is possible to evaluate the ductility:

$$\mu_{Pier} = \frac{\Delta_U}{\Delta_Y} = \frac{\Delta_Y + \Delta_P}{\Delta_Y} = 1 + \frac{\Delta_P}{\Delta_Y} \quad (46)$$

substituting Eq. 43- 44 and 45 in 46, it is possible to obtain:

$$\mu_{Pier} = 1 + \frac{\delta_p}{(\rho \cdot m) \cdot \delta_y} = 1 + \frac{\delta_u - \delta_y}{(\rho \cdot m) \cdot \delta_y} = 1 + \frac{\mu_{wall} - 1}{\rho \cdot m} \tag{47}$$

where μ_{wall} is the ductility of the single yielded wall. It is evident that, as stated before, the ductility of the wall-pier is inversely proportional to the number of storey.

What exposed previously allows to state that, in order to reduce the loss of ductility that occurs passing from the single wall to the multi-storey system, it is necessary to force the yielding of the largest number of storey. In fact, assuming that all the walls of a single multi-storey single wall yield at the same time (this means that all the walls have the same geometrical/mechanical properties, namely $\rho = 1$), see Fig. 20, the ductility of the whole system matches the ductility of a single walls without any loss. in fact, rewriting Eq. 46 it is

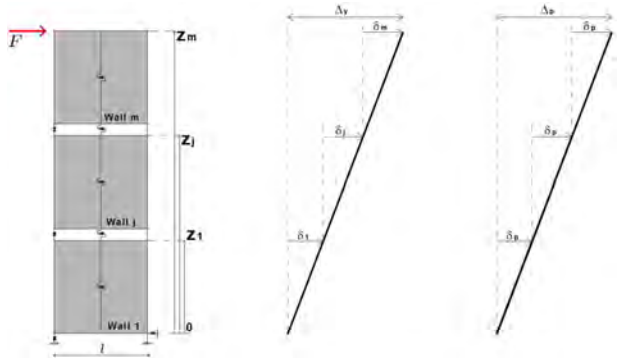

Fig. 20: Elastic and inelastic displacement of a single multi-storey shear wall.

possible to obtain:

$$\mu_{Pier} = 1 + \frac{\Delta_P}{\Delta_Y} = 1 + \frac{m \cdot \delta_p}{m \cdot \delta_y} = 1 + \mu_{wall} - 1 = \mu_{wall} \tag{48}$$

As an example, let's consider a four storey shear-wall made of walls which ductility is equal to 5, and for simplicity consider $\rho = 1$.

In the first case (concentrated yielding at the first storey), the ductility of the multi-storey shear-wall, according to Eq.47, is equal to:

$$\mu_{Pier} = 1 + \frac{\mu_{wall} - 1}{\rho \cdot m} = 1 + \frac{5 - 1}{1 \cdot 4} = 2 \tag{49}$$

whereas, the ductility of the multi-storey shear-wall in the second case (spread ductility), according to Eq.48, is equal to:

$$\mu_{Pier} = \mu_{wall} = 5(>> 2) \tag{50}$$

It is therefore evident that the use of the capacity design is not enough to ensure a good level of ductility, both for multi-storey walls and whole buildings, in fact it is also necessary to yield as many storey as possible.

4.3. Generalized study of multi-storey single shear walls ductility

With the aim to assess the ductility achievable by a multi-storey shear-wall and how it is influenced by the nails spacing as well as by the Over Strength Ratio γ_{Rd} to be used in the capacity design, a large set of cases was analysed. The analyses performed belong to the *Non linear Static Analysis* family and, in detail, they are incremental static analysis, and they are performed using the Matlab program previously mentioned.

	2 Storey		3 Storey		4 Storey	
μ_{nails}	Nailing A	Nailing B	Nailing A	Nailing B	Nailing A	Nailing B
4	1.9	1.9	1.9	1.9	1.4	1.3
6	2.5	2.5	2.5	2.4	1.6	1.5
8	3.1	3.0	3.1	3.0	1.9	1.7
10	3.7	3.6	3.7	3.6	2.1	1.9
12	4.3	4.2	4.3	4.1	2.3	2.1
14	4.9	4.8	4.9	4.7	2.6	2.3

Tab. 7: Ductility of the shear-wall for $\gamma_{Rd} = 1.3$.

On the base of what exposed in the previews section (see Sec. 4.2), with the goal to ensure the spread of the yielding within the storey, in the analyses reported below, an extremely small slope has been given to the plastic branch of the sheathing-to-framing force-vs-displacement curves. The assumption that a multi-storey shear-wall can not bear any force increase after the first yielding appears too conservative and not realistic, see [20] and [26]; in fact, it was observed in many analyses that several walls were under incipient yield at the

same time of the first wall yielded. Therefore, this *computational device* has been adopted to allow walls, that already are going to yield, to actually achieve this condition and undergo inelastic deformations.

	2 Storey		3 Storey		4 Storey	
μ_{nails}	Nailing A	Nailing B	Nailing A	Nailing B	Nailing A	Nailing B
4	2.0	1.9	2.0	1.9	1.4	1.4
6	2.7	2.5	2.6	2.5	1.7	1.6
8	3.3	3.1	3.2	3.0	2.0	1.8
10	4.0	3.7	3.8	3.6	2.2	2.0
12	4.6	4.3	4.5	4.2	2.5	2.2
14	5.3	4.9	5.1	4.8	2.7	2.4

Tab. 8: Ductility of the shear-wall for $\gamma_{Rd} = 1.6$.

Tables 7 and 8 show values of ductility displayed by multi-storey wall at the changing of the number of storey. Specifically, the ductility values of a 2.5 m long wall, under a horizontal load distribution proportional to the first mode of vibration, are reported. The values, referred to a specific number of storey, are grouped in two columns: *Nailing A* and *Nailing B*; in the first case the nail spacing is rounded with an accuracy of 1 cm (available spacing: from 5 to 15 cm with 1 cm of interval), whereas in the second one the spacing is rounded with an accuracy of 2.5 cm (available spacing: from 5 to 15 cm with 2.5 cm of interval). The ductility values of Table 7 are obtained with a $\gamma_{Rd} = 1.3$, whereas the values of Table 8 are obtained using $\gamma_{Rd} = 1.6$. The same set of analyses were done taking into account different wall lengths; for the results match those reported, they are omitted.

The results allow to state the following considerations:

- firstly, it can be observed that for $\gamma_{Rd} = 1.6$ the ductility values are greater, or at least equal, to those associated to $\gamma_{Rd} = 1.3$. This occurs because in the first case the system is stiffer than in the second one (connections become stronger and stiffer) and, as a consequence, the yielding displacement becomes smaller. However, to ensures adequate values of

ductility, it is not suggested the adoption of high values of O.S.R. but rather the use of connections as stiff as possible;

- as previously exposed, even if all the deformation contributions are taken in to account, it is evident how the global ductility decreases with the number of storey. Specifically, only for the case shown, it can be stressed the valuable loss of ductility from the case with four storey and the case with three storey, this occurs because the yielded storey changes.
- it is worth to note as, for the cases referring to *Nailing A*, the ductility is generally higher than in the cases referring to *Nailing B*. One potential reason for this is the different round precisions, which in the first case allows to limit the difference between the over-design ratios α_r, leading to spread the yielding within the storey. According to what exposed in 4.2, if all the walls would have the same value of α_r, the ductility of the system would display the maximum value achievable.

These considerations can be effectively summarized though the charts of Fig. 21, which show the ductility variation with the number of storey. Once again, it can be remarked that if the number of storey increases the global ductility exposed by the system decreases.

In addition, taking into account the charts of Fig. 22 which shows the system ductility-vs.-the nail ductility, a further consideration can be made, in fact, it can be easily assessed that the ductility of the multi-storey shear wall has a linear relation with that of the nails.

5. Non-linear behaviour of multi-storey buildings

The aims of the analyses presented in this section are the determination of the ductility-level achievable by light-frame timber full-scale buildings, as well as the Over Strength Ratio (O.S.R.) they can express. These two values have to be determined in order to assess and propose a new set of values for the behaviour factor q to be used in the seismic design of this Structural Type buildings.

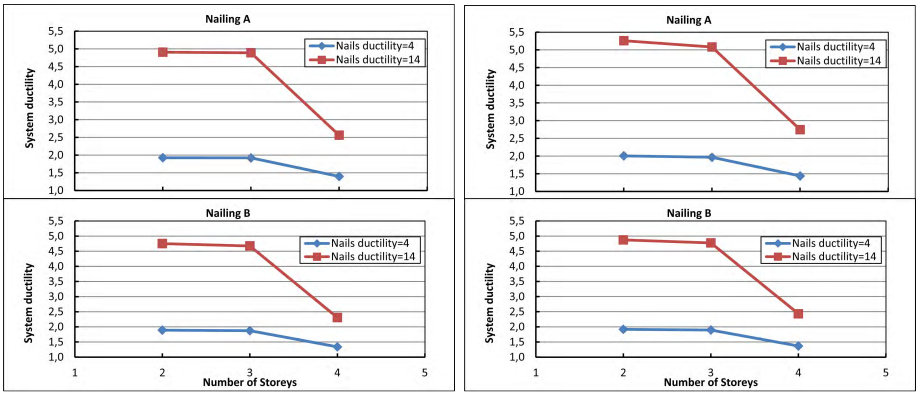

(a) (b)

Fig. 21: Ductility variation due to the increase in the storey number: (a) for $\gamma_{Rd} = 1.3$, (b) for $\gamma_{Rd} = 1.6$.

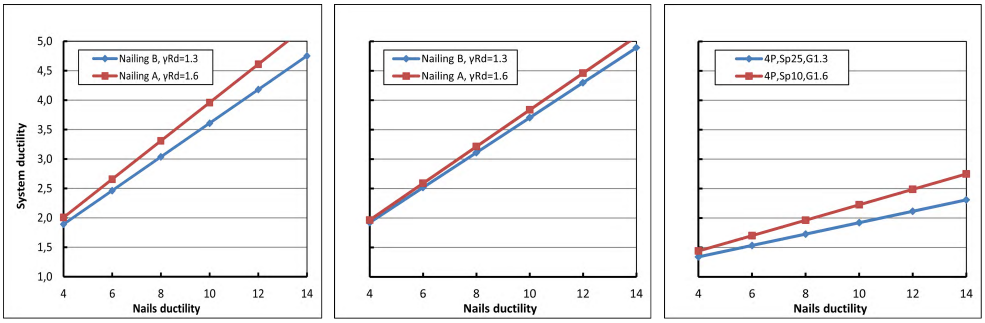

(a) (b) (c)

Fig. 22: Ductility variation due to the increase in the nails ductility: (a) 2 storey, (b) 3 storey, (c) 4 storey.

In order to get reliable results which can be generalized and extended, and to provide a good correlation between the base component properties and the system behaviour, a large set of full scale buildings (3456 different cases) has been analysed by varying the parameters that influences at most the seismic behaviour (geometry, storey number, design approach, etc.).

As previously exposed in Sec. 4.3, the used analysis procedure belongs to the NLSA-methods and it updates the stiffness matrix of the whole system at

each step. This represents one of the key aspect of the procedure because it allows to properly consider the effects both of the non-linear behaviour of the hold-down in the elastic range and the vertical load presence (see [13] and [15]).

5.1. Geometry of the buildings

(a) (b)

(c) (d)

Fig. 23: Plans analysed: (a) Building 1, (b) Building 4, (c) Building 2, (d) Building 3.

In accordance with what stated earlier, it is clear that many mechanical and geometric features of the building influence its ductility. With the goal to get results directly applicable and therefore of interest for both researchers and professional engineers, four different plans (see Fig. 23) were analysed by varying the number of storey from two to four (see Fig. 24), that is considering reasonable conditions for these kind of buildings.

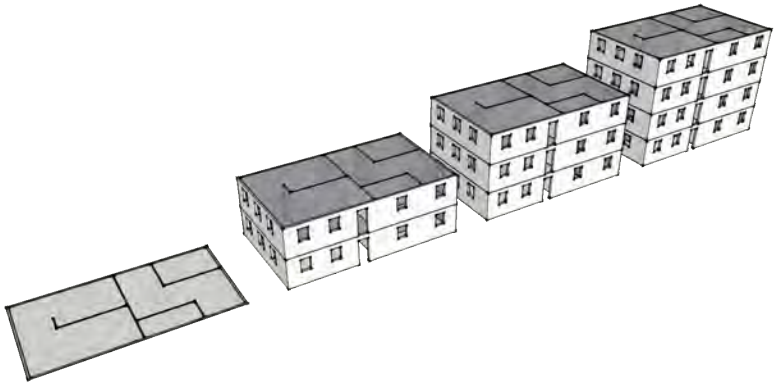

Fig. 24: Variation of Storey number.

	Area	Perimeter	S.W. X	S.W. Y	Leng. X	Leng. Y
Building 1	394	81	12	15	48.7	50.3
Building 2	491	100	14	16	50.3	47.0
Building 3	493	115	19	17	68.9	66.3
Building 4	265	82	21	11	46.3	46.3

Tab. 9: Properties of the analysed buildings, dimensions in meter.

The buildings were chosen because of their approximately symmetric plan in order to limit possible torsional effects. The building geometric features are synthetically shown in Tab. 9; the first two columns show the area and the perimeter of the plans respectively, whereas the remaining columns show the number of shear walls and their total length.

5.2. Analyses results

In order to make the results as general as possible, some input parameters have been vary. As said before four plan-geometries have been considered, each geometry was analysed along both the principal directions by varying the number of storey (2 to 4). In the design phase four seismic different levels ($a_g = 0.05g$; $0.15g$; $0.20g$; $0.25g$) and three values of behaviour factor $q = 2.0$; 3.0; 4.0) have been considered.

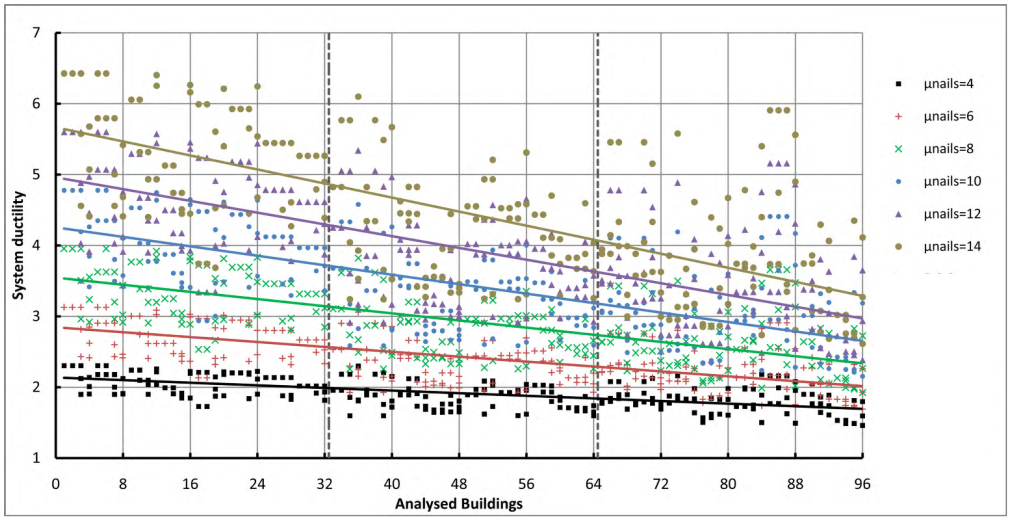

Fig. 25: Systems ductility VS Analysed cases.

Provided that the *Capacity Design* is adopted, it was observed that the variation of the values of acceleration and q factor in the design phase slightly influence the values of ductility reached by buildings. Moreover, this influence may be considered negligible compared to that exerted by other parameters. This occurs because both acceleration a_g and q factor collaborates to define the design seismic force, from which both the building strength and stiffness are dependent but not the ductility.

The most important achievement of the set of analysis carried out is represented by the chart of Fig. 25: the x-axis is related to the analysed cases whereas the y-axis is associated to the global ductility of the building which varies significantly as function of the nails ductility. It is worth noting that the 96-cases displayed along the x-axis are obtained by varying all the parameter except nails ductility as well as q factor used in the design. On the chart three bands are pointed out (cases 0 to 32, cases 32 to 64, cases 64 to 96), in which the results related to 2-Storey, 3-Storey and 4-Storey buildings are grouped respectively.

It is evident that the global ductility diminishes with the increase of the

	$\mu Nails$=4			$\mu Nails$=6			$\mu Nails$=8		
Storey	2	3	4	2	3	4	2	3	4
Lower Value	1.73	1.60	1.46	2.13	1.93	1.69	2.53	2.26	1.92
Mean value	2.08	1.87	1.79	2.75	2.34	2.19	3.41	2.81	2.59
Higher Value	2.30	2.30	2.18	3.13	3.06	2.91	3.95	3.82	3.66
Variance	0.023	0.026	0.032	0.066	0.066	0.088	0.130	0.127	0.181

	$\mu Nails$=10			$\mu Nails$=12			$\mu Nails$=14		
Lower Value	2.94	2.58	2.15	3.34	2.91	2.38	3.69	3.24	2.61
Mean value	4.07	3.28	2.98	4.74	3.75	3.38	5.40	4.22	3.77
Higher Value	4.78	4.58	4.41	5.60	5.34	5.16	6.43	6.10	5.91
Variance	0.225	0.211	0.309	0.341	0.316	0.475	0.481	0.442	0.677

Tab. 10: Lower, mean, higher and variance values of the buildings ductility.

number of storey; moreover, the higher the nails ductility the more pronounced this tendency. It can also be noted that the results related to high nails ductility values are more scattered.

The influence of the number of storey on the ductility level achieved, as well as the increase of the results dispersion due to the increase of the nails ductility are well resumed in Tab. 10. The table shows the higher, lower and mean values achieved by the ductility as well as the variance. This two aspects are once again highlighted in the charts of Fig. 26 where the higher, the lower and the mean values are shown by means of red lines.

The charts of Fig. 27 show the frequency distributions of the ductility values of the analysed buildings related to the values of nails ductility considered. The solid, dashed and dotted black curves are associated to buildings with 2, 3 and 4 storey respectively, whereas the red curves are obtained considered all the results, namely without dependence on the number of storey. From the black curves is evident that the ductility value associated to the higher frequency, decreases with the number of storey. In Tab. 11 the mean, mode and median values of ductility related to the analysis of all the cases are shown.

Because of the estimation of the q factor is based both on the ductility

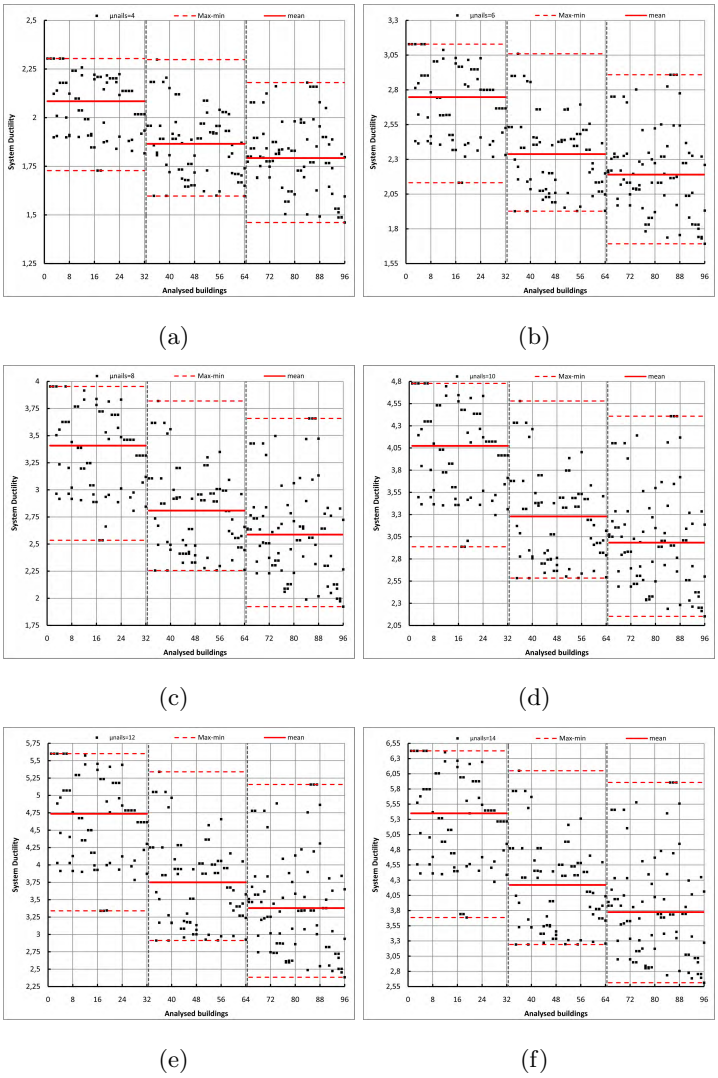

Fig. 26: System ductility for different nails ductility: (a) $\mu_N = 4$, (b) Building $\mu_N = 6$, (c) $\mu_N = 8$, (d) $\mu_N = 10$, (e) $\mu_N = 12$, (f) $\mu_N = 14$.

and the O.S.R., for each analysed case the O.S.R. has been evaluated. From the chart of Fig. 28 it is evident that the values of O.S.R. are less scattered than those of the ductility already presented; moreover, these values generally increase with the number of storey. It is also worth noting that the O.S.R. values do not depend on the nails ductility, but they only change by changing

	$\mu Nails$=4	$\mu Nails$=6	$\mu Nails$=8
mean	1.91	2.43	2.93
mode	2.00	2.50	2.7
median	1.90	2.41	2.92
	$\mu Nails$=10	$\mu Nails$=12	$\mu Nails$=14
mean	3.45	3.96	4.47
mode	3.9	3.7	5.00
median	3.42	3.93	4.43

Tab. 11: Mean, mode, median.

the analysed geometry. As for the chart of Fig. 25, the results are grouped in three bands associated to the number of storey. The higher, lower and mean values O.S.R. are shown in Tab. 12.

	Over Strength Ratio
Lower	1.07
Mean	1.17
Higher	1.39

Tab. 12: Values of $O.S.R.$

6. Estimation of the reduction factor for the seismic design

This section presents the values of the reduction factor q associated to the analysed cases previously presented and then a new set of values to be adopted in the seismic design of light timber-frame buildings is proposed.

6.1. Methods for the evaluation of the behaviour factor

The behaviour factor values are evaluated by means of two different procedures. The first method, known in literature as *N2-Method*, developed by Fajfar (see [27] and [28]) and introduced in the European seismic code [24], is based on the reduction of the capacity curve of the M-DOF system into

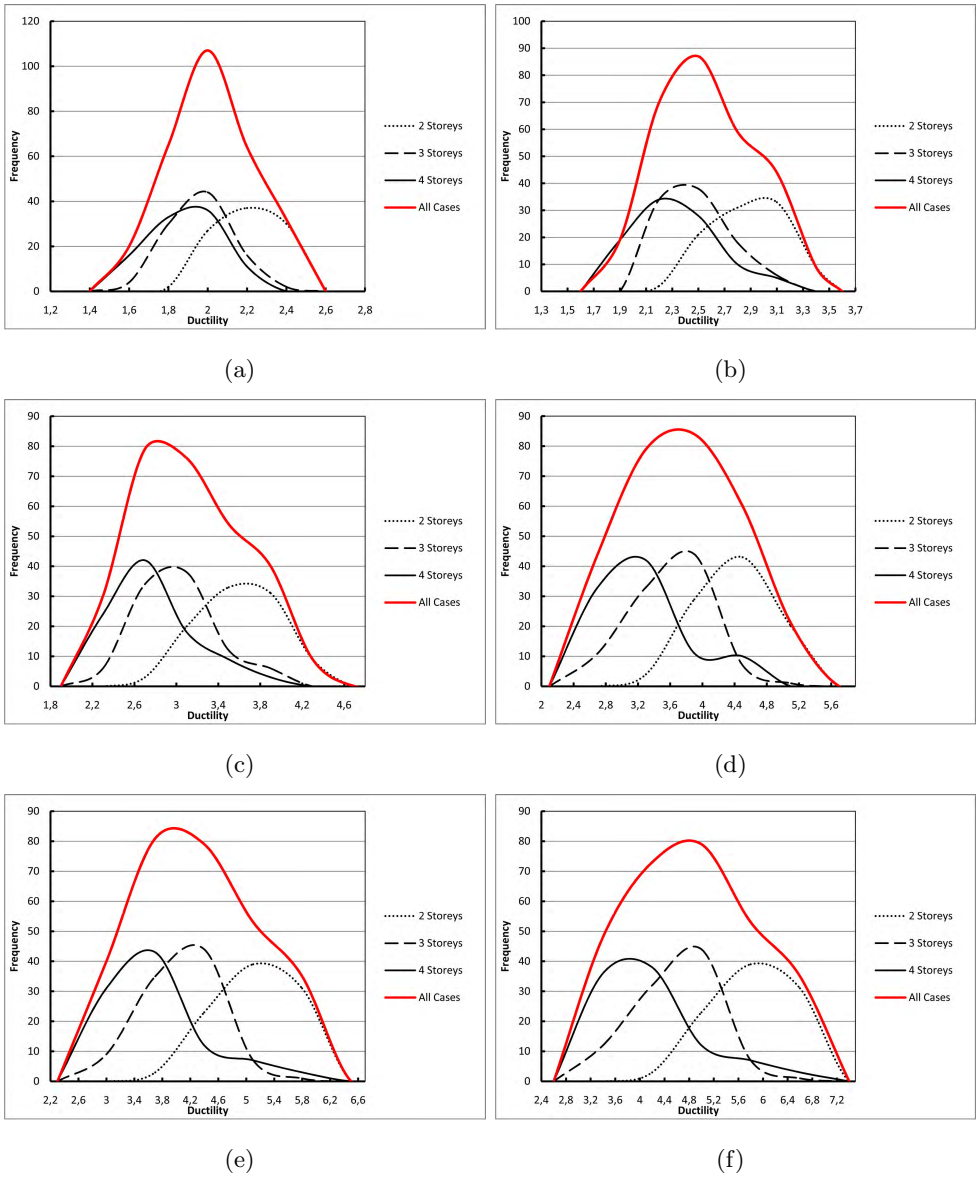

Fig. 27: Frequency distribution for different nails ductility: (a) $\mu_N = 4$, (b) Building $\mu_N = 6$, (c) $\mu_N = 8$, (d) $\mu_N = 10$, (e) $\mu_N = 12$, (f) $\mu_N = 14$.

an equivalent S-DOF curve. The behaviour factor evaluated by means of this method depends both on the dynamic properties of the building and on the

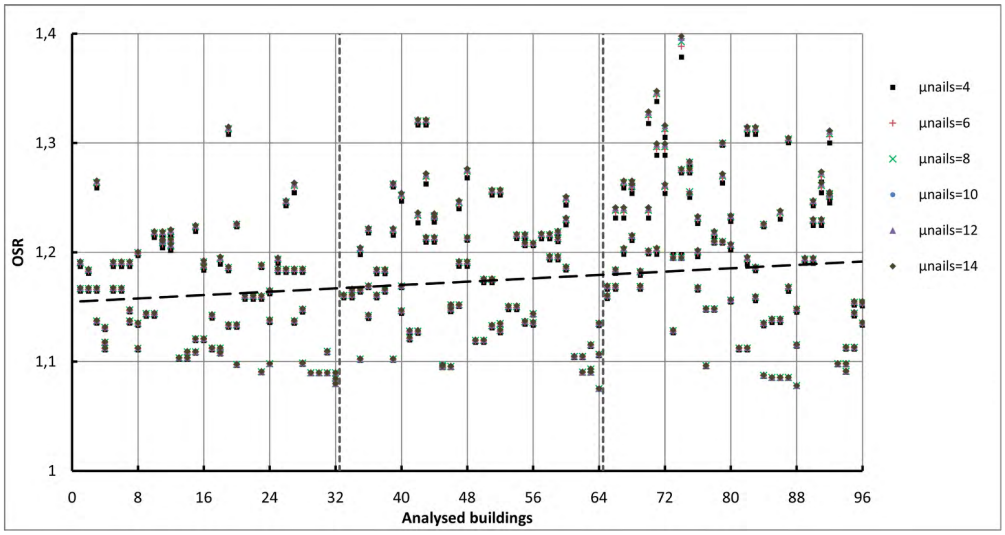

Fig. 28: O.S.R VS Analysed cases.

ground type.

The second method, developed earlier than the N2-method, is known as the *Newmark-method* (see [29]) and although less accurate has the advantage to makes the behaviour factor depending only on the building ductility. For simplicity in the following, reference to this method are made by means of Ne-Method (NeM).

The basic value of the behaviour factor q^*, according to N2-Method, is evaluated as follows:

$$\begin{cases} q^* = (\mu_s - 1) \cdot \dfrac{T^*}{T_c} + 1 \quad \rightarrow if \quad T^* < T_C \\ q^* = \mu_s \quad \rightarrow if \quad T^* \geq T_C \end{cases} \tag{51}$$

Where:

- μ_s is the displacement ductility of the structure;
- T^* is the period of the equivalent system;
- T_C is the transition period between the constant acceleration and constant velocity segments of the elastic response spectrum.

The Ne-Method provides instead the following equation:

$$q^* = \sqrt{(2\mu_s - 1)} \tag{52}$$

For both the procedures, the global value of the behaviour factor to be used in the design is determined by means of the following relation:

$$q = q^* \cdot OSR \tag{53}$$

According to what stated in [24], for a Type 2 spectrum, the values of the T_C period change by varying the ground type; these values are shown in Tab. 13.

Ground type	Tc [s]
A	0.4
B	0.5
C	0.6
D	0.8
E	0.5

Tab. 13: Value of T_C period in function of the ground type.

6.2. Behaviour factor values

The charts of Fig. 29 and Fig. 30 show the basic value of the behaviour factor q^* according to the N2-Method for a ground Type A and according to Ne-Method. It is possible to note that, as for the ductility , for both the procedures, the values of q^* diminish by incrementing the number of storey. It also worth remarking that the values, particularly those computed with the Ne-Method, are less scattered compared with the ductility values.

The Tab. 14 shows the values of $q*$ evaluated according to both the methods. It reports the values related to *Nails Ductility* [μ_N] and *Ground Types* [G.T.] considered. With the aim to propose a single global value of the behaviour factor for buildings with more than one storey, only the *Mean Values* [M.V.] and the *Lower Values* [L.V.] are resumed.

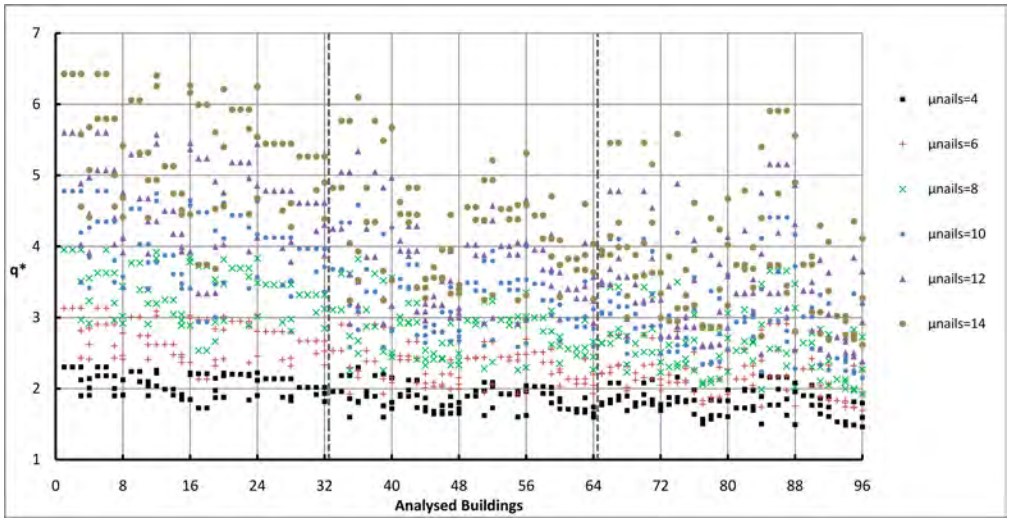

Fig. 29: q^* according to N2-Method and ground type A.

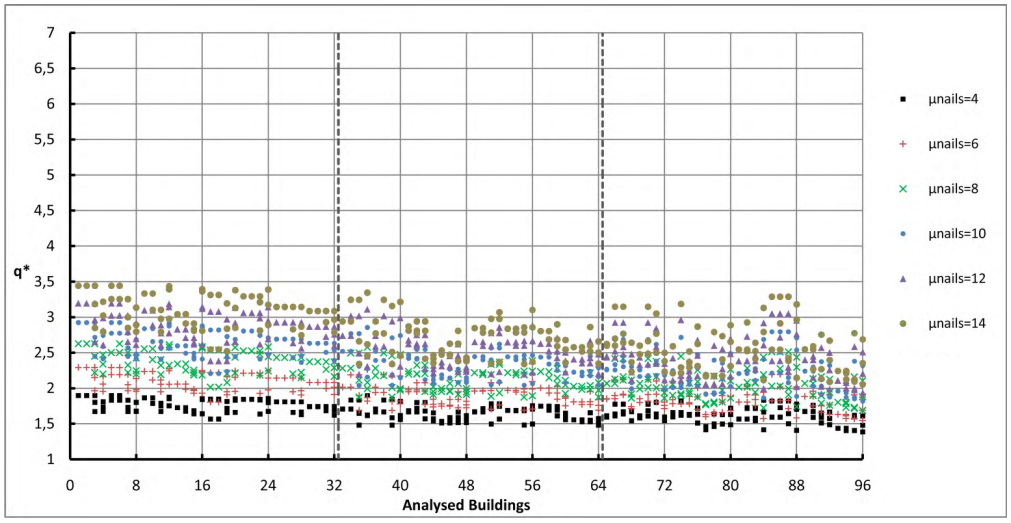

Fig. 30: q^* according to Ne-Method.

The values evaluated with the Ne-Method do not depend on the ground type, whereas the values determined with the N2-Method show a slight dependence from it. Therefore, in order to propose a single value of q, the average values of Tab. 15 are proposed. The values display a linear correlation with

		μ_N=4		μ_N=6		μ_N=8		μ_N=10		μ_N=12		μ_N=14	
		NeM	N2	NeM	N2	NeM	N2	NeM	N2	NeM	N2	NeM	N2
G.T. A	M.V.	1.7	1.9	1.9	2.4	2.2	2.9	2.4	3.4	2.6	4.0	2.8	4.5
	L.V.	1.4	1.5	1.5	1.7	1.7	1.9	1.8	2.1	1.9	2.4	2.1	2.6
G.T. B	M.V.	1.7	1.9	1.9	2.4	2.2	2.9	2.4	3.4	2.6	4.0	2.8	4.5
	L.V.	1.4	1.5	1.5	1.7	1.7	1.9	1.8	2.1	1.9	2.4	2.1	2.6
G.T. C	M.V.	1.7	1.9	1.9	2.4	2.2	2.8	2.4	3.3	2.6	3.9	2.8	4.3
	L.V.	1.4	1.5	1.5	1.7	1.7	1.9	1.8	2.1	1.9	2.4	2.1	2.6
G.T. D	M.V.	1.7	1.8	1.9	2.1	2.2	2.5	2.4	2.9	2.6	3.4	2.8	3.8
	L.V.	1.4	1.5	1.5	1.7	1.7	1.9	1.8	2.1	1.9	2.3	2.1	2.6
G.T. E	M.V.	1.7	1.9	1.9	2.4	2.2	2.9	2.4	3.4	2.6	4.0	2.8	4.5
	L.V.	1.4	1.5	1.5	1.7	1.7	1.9	1.8	2.1	1.9	2.4	2.1	2.6

Tab. 14: Value of q^* for different values of the nails ductility.

the nails ductility, which is shown in the charts of Fig. 31 and is analytically represented by Eq. 54 and Eq. 55, which are the interpolation of the *Mean Values* obtained using the N2-Method and Ne-Method respectively.

	μ_N=4		μ_N=6		μ_N=8		μ_N=10		μ_N=12		μ_N=14	
	NeM	N2	NeM	N2	NeM	N2	NeM	N2	NeM	N2	NeM	N2
M.V.	2,0	2,2	2,3	2,8	2,6	3,3	2,8	3,9	3,1	4,5	3,3	5,0
L.V.	1,6	1,7	1,7	1,8	1,8	2,1	2,0	2,3	2,1	2,6	2,2	2,8

Tab. 15: Value of q for different values of the nails ductility.

$$q = 0.28 \cdot \mu_{Nails} + 1.05 \tag{54}$$

$$q = 0.13 \cdot \mu_{Nails} + 1.49 \tag{55}$$

Tab. 16 shows the values of q that may be adopted in the seismic design. The values determined according to a nails ductility equal to 8 which is a representative value of the ductility of the nails currently present on the market, [20]. The values assessed according to the Ne-Method are much lower to those assessed with the N2-Method. Anyway it has to be stressed that the Ne-Method is less accurate and refined, leading to q-values that may be considered too conservative. For this reason the values related to the N2-Method may appear more realistic and representative of the behaviour of light timber-frame

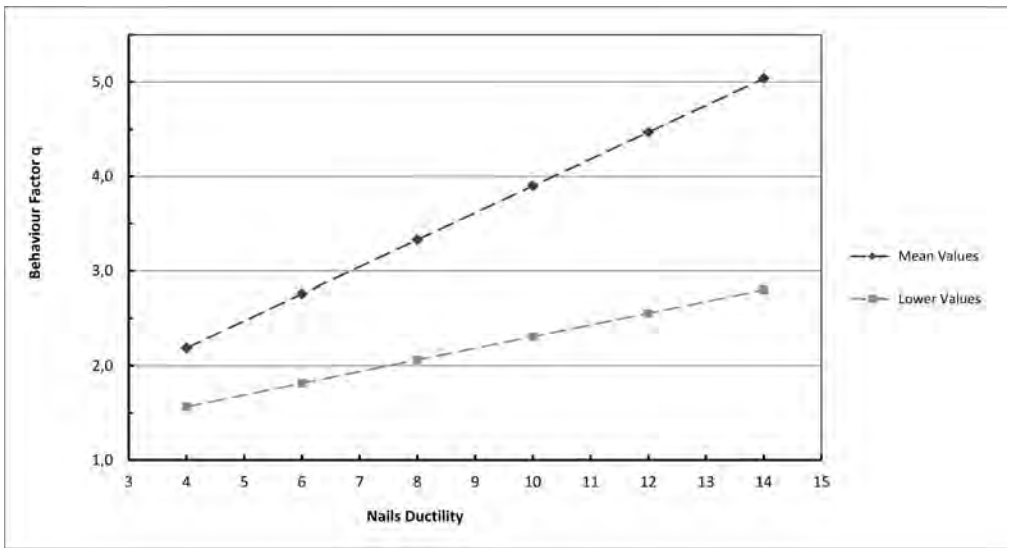

Fig. 31: q factor VS nails ductility according to N2-Method.

buildings. Specifically the proposed values are referred to one-storey (according to Eq. 37) and n-storey buildings (according to Eq. 54 and Eq. 55).

	Ne-Method	N2-Method
One - Storey	3,1	4,5
n - Storey	2,6	3,3

Tab. 16: Proposal of q values to use in seismic design.

7. Concluding remarks

In the present paper the non-linear static analysis of light timber-frame buildings was presented, with the aims to evaluate the ductility achievable by these type of buildings by varying the base components properties, as well as to assess and propose a new set of values for the behaviour factor q to be used in the seismic design.

In the first part of the paper, the analytical study of system composed by coupled-walls was performed. This analysis demonstrated that the post elastic

behaviour is determined by the strength and the stiffness of the base components; moreover, the unpredictability of the problem was also highlighted, namely the fact that the failure mechanism can no be controlled using a traditional design.

The post-elastic study was then extended to one-storey buildings. The analysis of a large set of randomly generated buildings has demonstrated the need to use a capacity design approach in order to control the failure mechanism and therefore the ductility of the building. In fact, it was possible to show that failure mechanisms involving the hold-down yielding and/or failure should be avoided because these can be considered brittle. According to the results collected, it is shown that influence of the geometry of the building on the displacement capacity can be considered negligible.

The non-linear analysis of multi-storey building has required the study of multi-storey shear-walls. In fact, the light timber-frame buildings can be considered as cantilever systems in which the global behaviour is determined by the coupled action of the multi-storey shear-walls that compose the building itself. It was demonstrated both from the numerical point of view and from the numerical point of view that the ductility displayed by the multi-storey wall decreases with the increasing of the number of storey.

The study was then completed by means of the analysis of several multi-storey buildings by varying the main parameters which influence the seismic behaviour such as the geometry-plan, the number of storey, the seismic level the ductility of the base components. Two main considerations were done: the ductility achieved by the cases decreases with the number of storey and the values of ductility are more scattered with reference to more ductile nails compared to those with a lower level of ductility.

All the ductility values collected were used in order to assess and propose a new set of values for the behaviour factor q. Two methods were considered: the *Fajfar method*, which is inserted in the [24], and the *Newmark method*, which has the advantage to not correlate the $q - factor$ with the dynamic

properties of the buildings. In order to propose general results which can be used for different geometric configurations, the average of the mean values and the average of the lower values were evaluated. Because of the *Newmark method* appeared too conservative and because, according to literature, this method can be considered less accurate than the other method, it is suggested to use only the values evaluated according to the *Fajfar procedure*. It was also possible to highlight that the behaviour factor q can be considered linearly proportional to the ductility of the nails and therefore, considering that the average value of ductility for the nails currently on the market is equal to 8, a value of $q_{one-storey} = 4.5$ and a value of $q_{one-storey} = 3.3$ are proposed.

Acknowledgments

The presented research has been carried out in the framework of the ReLUIS-DPC 2015 project. Support from the ReLUIS-DPC network, the Italian University Network of Seismic Engineering Laboratories and Italian Civil Protection Agency, is gratefully acknowledged.

Nomenclature

α is the shape parameter of the sheathing-panel;

$\mathbf{\Delta}$ is the array of the displacement provoked by the external force;

$\mathbf{F_N}$ is the array of equivalent horizontal force due to the vertical load;

$\mathbf{F}$ is the array of the external horizontal force;

$\mathbf{K}$ is the stiffness matrix of a multi-storey shear wall;

Δ_{nail} is the displacement of the horizontal spring related to the sheathing-to-framing connection;

$\Delta_{pl,W}$ is the plastic displacement of the wall;

$\Delta_{q,W}$ is the displacement of the wall when the friction block yields;

$\Delta_{U,A}$ is the ultimate-displacement of the equivalent horizontal spring related to the angle-brackets;

$\Delta_{U,H}$ is the ultimate-displacement of the equivalent horizontal spring related to the hold-downs;

$\Delta_{U,SH}$ is the ultimate-displacement of the equivalent horizontal spring related to the sheathing-to-framing connection;

$\Delta_{U,W}$ is the ultimate-displacement of the wall;

$\Delta_{Y,A}$ is the yielding-point of the equivalent horizontal spring related to the angle-brackets;

$\Delta_{Y,H}$ is the yielding-point of the equivalent horizontal spring related to the hold-downs;

$\Delta_{Y,SH}$ is the yielding-point of the equivalent horizontal spring related to the sheathing-to-framing connection;

$\Delta_{Y,W}$ is the yielding-point of the wall;

γ_{rd} is the overs strength design factor;

κ is the ratio between the stiffness of the wall and the stiffness of the weakest connection device;

μ_A is the displacement-ductility of the equivalent horizontal spring related to the angle-brackets;

μ_A is the displacement-ductility of the wall A;

μ_B is the displacement-ductility of the wall B;

μ_H is the displacement-ductility of the equivalent horizontal spring related to the hold-downs;

μ_{SH} is the displacement-ductility of the equivalent horizontal spring related to the sheathing-to-framing connection;

μ_{sys} is displacement-ductility of the system considered;

μ_W is displacement-ductility of the wall;

τ is the hold-downs dimensionless internal lever arm;

τ is the internal level arm ratio of the hold-downs;

$\tilde{f}$ is a dimensionless parameter related to the resistance;

$\tilde{k}$ is a dimensionless parameter related to the stiffness;

ξ is the ratio between the force activating the friction block and the strength of the wall;

b is the width of the sheathing-panels;

F is the horizontal external force applied to a wall;

F_q is the magnitude of the horizontal force which activates the friction block;

F_N is the equivalent horizontal force due to the vertical load;

i_a is the angle-brackets spacing;

K_A is the stiffness of the equivalent horizontal spring related to the angle-brackets;

k_a is the stiffness of the angle-brackets;

k_c is the stiffness of the nails;

K_H is the stiffness of the equivalent horizontal spring related to the hold-downs;

k_h is the stiffness of the hold-downs;

K_P is the sheathing panel shear stiffness;

K_{SH} is the stiffness of the equivalent horizontal spring related to the sheathing-to-framing connection;

K_{SP} is the stiffness of the equivalent horizontal spring related to the sheathing panel and the sheathing-to-framing connection;

$K_{tot,nt}$ is the stiffness of the wall when the rigid rotation contribution is not considered;

K_{tot} is the stiffness of the wall when the rigid rotation contribution is considered;

K_W is the stiffness of the wall;

l is the length of the wall;

n_a is the number of angle-brackets;

n_h is the number of hold-downs;

OSR is the Over Strength Ratio;

q is the behaviour factor for the seismic design;

q^* is the base value of behaviour factor for the seismic design;

q_v is the vertical distributed load acting on the wall;

R_A is the strength of the equivalent horizontal spring related to the angle-brackets;

r_a is the strength of the angle-brackets;

R_H is the strength of the equivalent horizontal spring related to the hold-downs;

r_h is the strength of the hold-downs;

R_{SH} is the strength of the equivalent horizontal spring related to the sheathing-to-framing connection;

R_W is the strength of the wall;

T^* is the period of the equivalent system;

T_c is the transition period between the constant acceleration and the constant velocity branch of the elastic response spectrum;

$T_{Ed,HD}$ is the tensile design force acting in the Hold-down;

$V_{Ed,AB}$ is the design force acting in the wall;

$V_{Ed,AB}$ is the shear design force acting in the angle-brackets;

8. References

[1] Ceccotti, A., Sandhaas, C., Okabe, M., Yasumura, M., Minowa, C., Kawai, N.. Sofie project–3d shaking table test on a seven-storey full-scale cross-laminated timber building. Earthquake Engineering & Structural Dynamics 2013;42(13):2003–2021.

[2] Leung, T., Asiz, A., Chui, Y.H., Hu, L., Mohammad, M.. Predicting lateral deflection and fundamental natural period of multi-storey wood frame buildings. In: Proceedings of World conference timber engineering. 2010,.

[3] Polastri, A., Pozza, L., Trutalli, D., Scotta, R., Smith, I.. Structural characterization of multi-storey buildings with clt cores. In: WCTE 2014. 2014,.

[4] Tomasi, R., Sartori, T., Casagrande, D., Piazza, M.. Shaking table testing of a full scale prefabricated three-story timber framed building. Journal of Earthquake Engineering 2014;19(3):505–534.

[5] Pozza, L., Scotta, R., Trutalli, D., Polastri, A.. Behaviour factor for innovative massive timber shear walls. Bulletin of Earthquake Engineering 2015;:1–21.

[6] Fragiacomo, M., Amadio, C., Rinaldin, G., Sancin, L.. Non-linear modelling of wooden light-frame and x-lam structures. Conference Proceeding: WCTE 2012 2012;.

[7] Chen, Z., Chui, Y.H., Doudak, G., Ni, C., Mohammad, M.. An approach for estimating seismic force modification factor of hybrid building systems. World Conference of Timber Engineering WCTE 2014 2014;.

[8] Zhu, X., Ni, Y.. Strength reduction factor spectra based on structural damage performance. In: Proceedings of the China-US Millennium Sym-

posium of Earthquake Engineering: Earthquake Engineering Frontiers in the New Millennium, Beijing, China. 2000,.

[9] Follesa, M., Fragiacomo, M., Vassallo, D., Piazza, M., Tomasi, R., Rossi, S., et al. A proposal for a new background document of chapter 8 of eurocode 8;. In: International Network on Timber Engineering Research - 2nd meeting of INTER;. 2015,.

[10] Pauley, T., Priestley, M.. Seismic design of reinforced concrete and masonry structures, j. J Wiley & Sons, INC USA 1992;.

[11] Frumento, S.. Interpretation of experimental shear tests on clay brick masonry walls and evaluation of q-factors for seismic design. IUSS Press; 2009.

[12] Casagrande, D., Sartori, T., Tomasi, R.. Capacity design approach for multy-storey timber-frame buildings. INTER Conference, Bath 2014 2014;.

[13] Casagrande, D., Rossi, S., Sartori, T., Tomasi, R.. Proposal of an analytical procedure and a simplified numerical model for elastic response of single-storey timber shear-walls. Construction and Building Materials 2014;DOI:10.1016/j.conbuildmat.2014.12.114.

[14] Casagrande, D., Rossi, S., Tomasi, R., Mischi, G.. A predictive analytical model for the elasto-plastic behaviour of a light timber-frame shear-wall. Construction and Building Materials 2015;doi: 10.1016/j.conbuildmat.2014.12.114.

[15] Rossi, S., Casagrande, D., Tomasi, R., Piazza, M.. Seismic elastic analysis of light timber-frame multi-storey buildings: proposal of an iterative approach. Construction and Building Materials 2015;.

[16] Grossi, P., Sartori, T., Tomasi, R.. Tests on timber frame walls under in-plane forces: Part 1. Proceedings of the Institution of Civil Engineers-

Structures and Buildings 2014;Special Issue on Seismic Test on Timber Buildings:xx.

[17] Grossi, P., Sartori, T., Tomasi, R.. Tests on timber frame walls under in-plane forces: Part 2. Proceedings of the Institution of Civil Engineers-Structures and Buildings 2014;Special Issue on Seismic Test on Timber Buildings:xx.

[18] Conte, A., Piazza, M., Sartori, T., Tomasi, R.. Influence of sheathing to framing connections on mechanical properties of wood framed shear walls. Proceedings of Italian National Association of Earthquake Engineering, ANIDIS 2011;.

[19] Tomasi, R., Sartori, T.. Mechanical behaviour of connections between wood framed shear walls and foundations under monotonic and cyclic load. Construction and Building Materials 2013;44:682–690. doi: 10.1016/j.conbuildmat.2013.02.055.

[20] Sartori, T., Tomasi, R.. Experimental investigation on sheathing-to-framing connections in wood shear walls. Engineering Structures 2013;56:2197–2205. doi:10.1016/j.engstruct.2013.08.039.

[21] Seim, W., Hummel, J., Vogt, T.. Earthquake design of timber structures - remarks on force-based design procedures for different wall systems. Engineering Structures 2014;76:124–137. doi:10.1016/j.engstruct.2014.06.037. Cited By 0.

[22] Seim, W., Kramar, M., Pazlar, T., Vogt, T.. Osb and gfb as sheathing materials for timber-framed shear walls: Comparative study of seismic resistance. Journal of Structural Engineering 2015;.

[23] EN1995-1-1, . Design of timber structures part 1-1: General-common rules and rules for building. 2014. CEN, European Committee for Standardization, Brussel, Belgium.

[24] UNI EN 1998-1:2013, . Eurocode 8: Design of structures for earthquake resistance part 1: General rules, seismic actions and rules for buildings. 2013. Brussels, Belgium: CEN, European Committee for Standardization.

[25] Design of structure for earthquke resistance, part 1-1: General rules, seicmic actions and rules for buildings. 2005. CEN, European Committee for Standardization, Brussel, Belgium.

[26] Verdret, Y., Faye, C., Elachachi, S., Le Magorou, L., Garcia, P.. Experimental investigation on stapled and nailed connections in light timber frame walls. Construction and Building Materials 2015;91:260–273.

[27] Fajfar, P.. Capacity spectrum method based on inelastic demand spectra. Earthquake Engineering & Structural Dynamics 1999;28(9):979–993.

[28] Fajfar, P.. A nonlinear analysis method for performance-based seismic design. Earthquake spectra 2000;16(3):573–592.

[29] Newmark, N.M., Hall, W.J.. Earthquake spectra and design. Earth System Dynamics 1982;1.

Chapter 6

Conclusions and future developments

6.1 Conclusions

In the first part of the thesis, an equation suitable to describe the elastic behavior of a single storey timber shear-wall by adding the four main deformation contributions is given; in the case of CLT walls, sheathing-to-framing connections are absent, so that the sheathing-to-framing connection deformation is zero. The study of the walls stiffness highlighted that two different regimes can occur, namely the walls expose a non-linear behaviour even in the elastic range due to the ON-OFF behaviour of hold-downs, which may lead to the adoption of an iterative procedure of analysis. On the basis of the displacement equation as well as on the stiffness equation, a numerical simplified model, called UNITN Model, is proposed. The model is called simplified because it reproduces the wall behaviour by means of only three elastic springs whose stiffness is related to a specific deformation contribution. The use of only three springs is the main feature of the Model because of it reduces the time needed to create and to run the analysis without loosing precision.

The second part of the thesis has dealt with the static and dynamic seismic elastic analysis of light timber-frame multi-storey buildings performed by means of the use of the UniTn-model and assuming a cantilever-behaviour for the shear-walls. An iterative procedure that evaluate how a horizontal force is spreader to the shear-walls is presented; the iterations are needed to determine the horizontal-forces distribution in a proportional manner to the walls stiffness and it can be conveniently used for applying the seismic lateral force method. The procedure involves two level of iteration: the first iteration is required to evaluate the correct position of the hold-downs, which have to be placed in the tension corner of the walls, whereas the second-one is needed to update the stiffness matrix of the system in the case that the boundary condition used are not in accordance with the results obtained. Three iterative approaches for the application of the RSA are also proposed, in fact the modal analysis can not be directly applied to light timber-frame building due to the non-linearity introduced by the hold-down and the vertical load. The three iterative methods are characterized by different levels of accuracy from the analytical point of view; in fact, they differ in the way in which the vertical load effects are considered. The method provide similar results in terms of shear-forces, bending moments and tensile forces in the hold down; the results changes by increasing the dimension of the model analysed. Due to the fat that VTM-method (Vertical Load to the Main mode) represents a compromise between computational expensiveness and accuracy, it should be considered the reference method for the application of the RSA.

In the third part of the thesis an analytical method, based on the extension of the UniTn-model in the post-elastic range, was presented. The proposed expressions are a key aspect in the non-linear analysis of light timber-frame buildings because it allows to define an analytical relationship between the mechanical properties of the base components and the mechanical properties of a shear-wall. In fact, these expressions can be useful to relate the local ductility to the global wall ductility and hence to define the ductility demand

of the component where the energy dissipation is expected in order to get a global ductile behaviour. The analysis of the relationship between the ductility of the nails and the sheathing-to-framing connection ductility highlight that the wall post-elastic behaviour is not dependent on the nails spacing but it is only related to the geometrical properties of the sheathing panels and the fastener ductility. This aspect has been also investigated by means of four laboratory tests which have demonstrated that the yielding displacement and the ultimate displacement can be considered constant with the fasteners spacing that validate the proposed model. In order to fully prove the theory some non-linear staged F.E.M. analysis have been also performed. The ability to represent the total force carried by the fasteners in one non-linear spring is shown to be a key benefit reducing significantly the number of degrees of freedom of the model.

In the fourth part, the non-linear analysis of multi-storey light timber-frame buildings was presented. The study of coupled-walls was firstly shown in order to highlight that both strength and stiffness of the walls influence the failure mechanism and therefore the ductility displayed by the system. It was also demonstrated the need to develop a numerical procedure to analyse more complex system. The non-linear analysis was then extended to one-storey building; the result of the analyses have shown that failure mechanism involving the failure of the hold-downs have to be considered brittle failures and therefore have to be avoided. The same set of analysis have therefore performed again, but adopting a capacity design approach which has assured the attainment of a ductile failure mechanism for each case. It is worth to remarking that a linear correlation between the nails ductility and that of the whole building has been shown. The analysis of full-scale multi-storey buildings was then presented; a large set of cases, obtained by varying the main important parameters such as number of storey, plan-geometry as well as seismic intensity, have been considered. The results obtained allow to make two considerations: the ductility displayed by a building diminishes by the increases

of the number of storey due to difficulty of yielding the upper storey (in other words, taller buildings come to collapse before they have used all the available reserves of ductility); results related to nails with high ductility are more scattered compared to those related to less ductile nails. All the ductility values collected were then used to assess a proper set of values for the behaviour factor q. Two method to the evaluation of q were considered; the Fajfar method (known as N2-method), that relates the behaviour factor of a buildings to its dynamic properties, and the holder method of Newmark that has the benefit to provide results regardless the seismic response of the building. Because of the second method seems to be too precautionary and also less accurate, only the results of the N2-method are suggested to use. In order to propose a general value of the behaviour factor q to be used in the design, and because the nails currently available on the market have an average ductility equal to 8, a behaviour factor $q = 4.5$ for one-storey building and $q = 3.3$ for multi-storey buildings were proposed.

6.2 Future Developments

The research project can be further developed from different points of view:

- the displacement equation proposed in the first part can be improved by considering other deformation contribution related to much slender walls, but also by some mathematical quantity that allow to considered the effect of concentrated vertical loads, as well as horizontal forces applied not at the top;
- the presented iteration methods for the response spectrum analysis can be improved from the computational point of view to increase the their stability and also in order to make these procedures faster;
- the non-linear analysis, as well as the evaluation of the behaviour factor q can be preformed with regard to cross laminated timber buildings.

Publications

I **Analytical and numerical analysis of timber framed shear wall**;
Casagrande D.; Rossi S.; Sartori T.; Tomasi R.;
World Conference on timber Engineering - WCTE 2012, Auckland.

II **Proposal of an analytical and a simplified numerical model for the elastic response of single-storey timber shear walls**;
Casagrande D.; Rossi S.; Sartori T.; Tomasi R.;
Construction and building Material, 2014;
DOI: 10.1016/j.conbuildmat.2014.12.114.

III **A predictive analytical model for the elasto-plastic behaviour of a light timber-frame shear-wall**;
Casagrande D.; Rossi S.; Sartori T.; Tomasi R.;
Construction and building Material, 2015;
DOI: 10.1016/j.conbuildmat.2015.06.025.

IV **Seismic elastic analysis of light timber-frame multi-storey buildings: proposal of an iterative approach**;
Rossi S.; Casagrande D.; Tomasi R.; Piazza M.;
Construction and building Material, 2015;
DOI: 10.1016/j.conbuildmat.2015.09.037

V **Non-linear analysis of light timber-frame buildings: determination of the displacement ductility, over-strength ratio and estimation of the**

reduction factor for the seismic design;
Rossi S.; Casagrande D.; Vinante F.; Tomasi R.;
Engineering and structure, Submitted;

VI **A proposal for a new Background Document of Chapter 8 of Eurocode 8**;
Follesa M.; Fragiacomo M.; Vassallo D.; Piazza M.; Tomasi R.; Rossi S.; Casagrande D.;
International Network on Timber Engineering Research - 2nd meeting of INTER 2015;

VII **Una proposta di revisione del Capitolo 8 sulle strutture in di legno dell'Eurocodice 8**;
Follesa M.; Fragiacomo M.; Vassallo D.; Christovasilis I.; Piazza M.; Tomasi R.; Rossi S.; Casagrande D.;
Conference proceeding XVI Convegno ANIDIS (Associazione Nazionale Italiana di Ingegneria Sismica), L'Aquila 2015;

Bibliography

[1] Mauro Andreolli, Paolo Grossi, Tiziano Sartori, and Roberto Tomasi. Design and production of an heavy timber reaction frame for a laboratory test set-up. In *ICSA 2013*, 2013.

[2] Gian Michele Calvi, Stefano Pampanin, Peter Fajfar, and Matjaz Dolsek. New methods for assessment and design of structures in seismic zones: present state and research needs. *NZSEE Conference*, 2000.

[3] Giuseppe Caprolu. Experimental testing of anchoring devices for bottom rail in partially anchored timber trame shear walls with two-sided sheathing. Technical report, Luleå University of Technology Department of Civil, Environmental and Natural resources engineering Division of Structural and Construction Engineering, 2012.

[4] Ugo Carusi, Fabiana Riparbelli, and Ginevra Salerno. Open scientific problems about the platform frame constructive system. *Energy and Buildings*, 83:209–216, 2014.

[5] Daniele Casagrande, Paolo Grossi, Tiziano Sartori, and Roberto Tomasi. Shaking table test on 3-storey light-frame timber building with osb and gypsum fiber sheathing panels: outcomes and results. *Proceedings of the Institution of Civil Engineers-Structures and Buildings*, special issue on seismic test on timber buildings:xx, 2014.

[6] Daniele Casagrande, Simone Rossi, Tiziano Sartori, and Roberto Tomasi. Proposal of an analytical procedure and a simplified numerical model for elastic response of single-storey timber shear-walls. *Construction and Building Materials*, 2015. DOI:10.1016/j.conbuildmat.2014.12.114.

[7] Daniele Casagrande, Simone Rossi, Tiziano Sartori, and Roberto Tomasi. Analytical and numerical analysis of timber framed shear walls. In *World Conference on Timber Engineering 2012, WCTE 2012*, volume 5, pages 497–503, 2012.

[8] Daniele Casagrande, Simone Rossi, Tiziano Sartori, and Roberto Tomasi. Analytical and numerical analysis of timber framed shear walls. *WCTE conference*, 2012.

[9] Daniele Casagrande, Simone Rossi, Roberto Tomasi, and Gianluca Mischi. Apredictive analytical model for the elasto-plastic behaviour of a light timber-frame shear-wall. *Construction and Building Materials -IN PRESS-*, 2015.

[10] Daniele Casagrande, Tiziano Sartori, and Roberto Tomasi. Capacity design approach for multy-storey timber-frame buildings. *INTER Conference, Bath 2014*, 2014.

[11] Ario Ceccotti, Maurizio Follesa, and Marco Pio Lauriola. Le strutture di legno in zona sismica. *CLUT: Torino, Italy*, 2005.

[12] Ario Ceccotti, M Lauriola, Mario Pinna, and Carmen Sandhaas. Sofie project–cyclic tests on cross-laminated wooden panels. In *proceedings of the 9th world conference on timber engineering, Portland, Oregon, USA*, 2006.

[13] Zhiyong Chen, Ying H Chui, Ghasan Doudak, Chun Ni, and Mohammad Mohammad. Simulation of the lateral drift of multi-storey light wood

frame buildings based on a modified macro-element model. In *13th World Conference on Timber Engineering*, 2014.

[14] Zhiyong Chen, Ying H Chui, Ghasan Doudak, Chun Ni, and Mohammad Mohammad. An approach for estimating seismic force modification factor of hybrid building systems. *World Conference of Timber Engineering WCTE 2014*, 2014.

[15] Zhiyong Chen, Ying H Chui, Mohammad Mohammad, Ghasan Doudak, and Chun Ni. Load distribution in lateral load resisting elements of timber structures. In *13th World Conference on Timber Engineering*, 2014.

[16] Zhiyong Chen, Ying H Chui, Chun Ni, Ghasan Doudak, and Mohammad Mohammad. Load distribution in timber structures consisting of multiple lateral load resisting elements with different stiffnesses. *Journal of Performance of Constructed Facilities*, 28(6):A4014011, 2014.

[17] Anil K Chopra. *Dynamics of structures*, volume 3. Prentice Hall New Jersey, 1995.

[18] Ioannis Periklis Christovasilis. *Numerical and experimental investigations of the seismic response of light-frame wood structures*. State University of New York at Buffalo, 2011.

[19] Andrea Conte, Maurizio Piazza, Tiziano Sartori, and Roberto Tomasi. Influence of sheathing to framing connections on mechanical properties of wood framed shear walls. In *Congresso Ingegneria Sismica Anidis*, 2011.

[20] Andrea Conte, Maurizio Piazza, Roberto Tomasi, and Tiziano Sartori. Experimental investigation on connections between wood framed shear walls and foundations. In *Structural Engineering World Congress, Villa Erba, Como, Italy, 2011*, 2011.

[21] CSA 086-01:2005. Engineering design in wood, 2005. CSA, Canadian Standard Association, Toronto, Canada.

[22] Ian De la Roche, J OŠConner, and P Tetu. Wood products and sustainable construction. *New Zealand Timber Design Journal*, 12(1):5, 2003.

[23] BL Deam and PJ Moss. Modelling the seismic response of light-timber-framed buildings. *NZSEE 2001 Conference*, 2001.

[24] G Doudak, I Smith, G McClure, M Mohammad, and P Lepper. Tests and finite element models of wood light-frame shear walls with openings. *Progress in Structural Engineering and Materials*, 8(4):165–174, 2006.

[25] Jürgen Ehlbeck, Heinrich Kreuzinger, Günter Steck, and Hans Joachim Blaß. *DIN 1052 Erläuterungen*. Bruderverlag, 4 2005.

[26] Massimiliano Ferraioli, Angelo Lavino, and Alberto Mandara. Behaviour factor of code-designed steel moment-resisting frames. *International Journal of Steel Structures*, 14(2):243–254, 2014.

[27] M Ferraioli, A Lavino, and A Mandara. Behaviour factor for seismic design of moment-resisting steel frames. In *15th World Conference on Earthquake Engineering. Lisbon, Portugal*, 2012.

[28] Andre Filiatrault, Mary Epperson, and Bryan Folz. Equivalent elastic modeling for the direct-displacement-based seismic design of wood structures. *ISET J. Earthquake Technol*, 41:75–99, 2004.

[29] A. Filiatrault and B. Folz. Performance-based seismic design of wood framed buildings. *Journal of Structural Engineering*, 128(1):39–47, 2002.

[30] A. Filiatrault, H. Isoda, and B. Folz. Hysteretic damping of wood framed buildings. *Engineering Structures*, 25(4):461 – 471, 2003.

[31] Bryan Folz and Andre Filiatrault. Seismic analysis of woodframe structures. ii: Model implementation and verification. *Journal of Structural Engineering*, 130(9):1361–1370, 2004.

[32] Bryan Folz and Andre Filiatrault. Seismic analysis of woodframe structures. i: Model formulation. *Journal of Structural Engineering*, 130(9):1353–1360, 2004.

[33] Bryan Folz and Andre Filiatrault. Seismic analysis of woodframe structures. i: Model formulation. *Journal of Structural Engineering*, 130(9):1353–1360, 2004.

[34] Bryan Folz and Andre Filiatrault. Seismic analysis of woodframe structures. ii: Model implementation and verification. *Journal of Structural Engineering*, 130(9):1361–1370, 2004.

[35] Fernando S. Fonseca, Sterling K. Rose, and Scott H. Campbell. *Nail, Wood Screw, and Staple Fastener Connections W-16*. Caltech Woodframe Project, 2002.

[36] Ricardo O. Foschi. Analysis of wood diaphragms and trusses. part i: Diaphragms. *Canadian Journal of Civil Engineering*, 4(3):345–352, 1977.

[37] Massimo Fragiacomo, Claudio Amadio, Giovanni Rinaldin, and Ljuba Sancin. Non-linear modelling of wooden light-frame and x-lam structures. *Conference Proceeding: WCTE 2012*, 2012.

[38] Sara Frumento. *Interpretation of experimental shear tests on clay brick masonry walls and evaluation of q-factors for seismic design*. IUSS Press, 2009.

[39] Natalino Gattesco and Ingrid Boem. Seismic performances and behavior factor of post-and-beam timber buildings braced with nailed shear walls. *Engineering Structures*, 100:674–685, 2015.

[40] Federica Germano, Giovanni Metelli, and Ezio Giuriani. Experimental results on the role of sheathing-to-frame and base connections of a european timber framed shear wall. *Construction and Building Materials*, 80:315–328, 2015.

[41] Ulf Arne Girhammar and Bo Källsner. Elasto-plastic model for analysis of influence of imperfections on stiffness of fully anchored light-frame timber shear walls. *Engineering Structures*, 31(9):2182 – 2193, 2009.

[42] UlfArne Girhammar and Bo Källsner. Analysis of influence of imperfections on stiffness of fully anchored light-frame timber shear wallsâĂŤelastic model. *Materials and Structures*, 42:321–337, 2009.

[43] Paolo Grossi, Tiziano Sartori, and Roberto Tomasi. Tests on timber frame walls under in-plane forces: Part 1. *Proceedings of the Institution of Civil Engineers-Structures and Buildings*, Special Issue on Seismic Test on Timber Buildings:xx, 2014.

[44] Paolo Grossi, Tiziano Sartori, and Roberto Tomasi. Tests on timber frame walls under in-plane forces: Part 2. *Proceedings of the Institution of Civil Engineers-Structures and Buildings*, Special Issue on Seismic Test on Timber Buildings:xx, 2014.

[45] RA Joebstl, T Bogensperger, and G Schickhofer. In-plane shear strength of cross laminated timber. In *41st CIB-Meeting, St. Andrews, Canada (August 2008)*, 2008.

[46] Scott N. Jones and Fernando Fonseca. Strength of osb shear walls with over-driven sheathing nails. In *Proceedings of World conference timber engineering*, 2000.

[47] J. Judd and F. Fonseca. Analytical model for sheathing-to-framing connections in wood shear walls and diaphragms. *Journal of Structural Engineering*, 131(2):345–352, 2005.

[48] Johnn P Judd and FS Fonseca. Equivalent single degree of freedom model for wood shearwalls and diaphragms. In *Proceeding of the 9th World Conference on Timber Engineering*, pages 6–10, 2006.

[49] Bo Källsner and Ulf Arne Girhammar. Plastic models for analysis of fully anchored light-frame timber shear walls. *Engineering Structures*, 31(9):2171 – 2181, 2009.

[50] Andreas Kappos and GG Penelis. *Earthquake resistant concrete structures*. CRC Press, 2010.

[51] William J Kirkham, Rakesh Gupta, and Thomas H Miller. State of the art: Seismic behavior of wood-frame residential structures. *Journal of Structural Engineering*, 140(4):04013097, 2013.

[52] R Langenbach. Better than steel!? the use of timber for large and tall buildings from ancient times until the present. *Structures & Architecture*, page 103, 2010.

[53] Randolph Langenbach. Resisting earth's forces: typologies of timber buildings in history. *Structural Engineering International*, 18(2):137–140, 2008.

[54] Thomas Leung, Andi Asiz, Ying Hei Chui, Lin Hu, and Mohammad Mohammad. Predicting lateral deflection and fundamental natural period of multi-storey wood frame buildings. In *Proceedings of World conference timber engineering*, 2010.

[55] J. van de Lindt. Evolution of wood shear wall testing, modeling, and reliability analysis: Bibliography. *Practice Periodical on Structural Design and Construction*, 9(1):44–53, 2004.

[56] John W. van de Lindt, Shiling Pei, Weichiang Pang, and Seyed Masood Hassanzadeh Shirazi. Collapse testing and analysis of a light-

frame wood garage wall. *Journal of Structural Engineering*, 138(4):492–501, 2012.

[57] G Magenes and A Penna. Seismic design and assessment of masonry buildings in europe: recent research and code development issues. In *Proceedings of the 9th Australasian masonry conference*, 2011.

[58] KA Malo, J Siem, and P Ellingsbø. Quantifying ductility in timber structures. *Engineering Structures*, 33(11):2998–3006, 2011.

[59] Nathan M' Newmark and William J Hall. Seismic design criteria for nuclear reactor facilities. In *Proceedings 4th World conference on earthquake engineering, Santiago, Chile*, volume 4, pages 37–50, 1969.

[60] Nathan Mortimore Newmark and Emilio Rosenblueth. Fundamentals of earthquake engineering. *Civil engineering and engineering mechanics series*, 12, 1971.

[61] NZS 3603. Timber Structures Standard, 1993. NZS, Wellington, New Zealand.

[62] A Palermo, S Pampanin, A Buchanan, and M Newcombe. Seismic design of multi-storey buildings using laminated veneer lumber (lvl). *NZSEE Conference*, 2005.

[63] Gerard C Pardoen. *Testing and analysis of one-story and two-story shear walls under cyclic loading*. Consortium of Universities for Research in Earthquake Engineering, 2003.

[64] T Pauley and MJN Priestley. Seismic design of reinforced concrete and masonry structures, j. *J. Wiley & Sons, INC USA*, 1992.

[65] L. Petrini, R. Pinho, and G. M. Calvi. *Criteri di progettazione antisismica degli edifici*. IUSS Press, 2004.

[66] Maurizio Piazza, Roberto Tomasi, and Roberto Modena. *Strutture in legno. Materiale, calcolo e progetto secondo le nuove normative europee*. HOEPLI EDITORE, 2005.

[67] A. Polastri, L. Pozza, D. Trutalli, R. Scotta, and I. Smith. Structural characterization of multi-storey buildings with clt cores. In *WCTE 2014*, 2014.

[68] Jack Porteous and Abdy Kermani. *Structural timber design to Eurocode 5*. John Wiley & Sons, 2013.

[69] Luca Pozza and Roberto Scotta. Influence of wall assembly on behaviour of cross-laminated timber buildings. *Proceedings of the Institution of Civil Engineers journal Structures and Buildings*, 2014.

[70] L Pozza, R Scotta, D Trutalli, A Ceccotti, and A Polastri. Analytical formulation based on extensive numerical simulations of behavior factor q for clt buildings. In *Proceedings of the 46th meeting of the working commission W18-timber structures, CIB, Vancouver, Canada, paper CIB-W18/46-15-5*, 2013.

[71] Luca Pozza, Roberto Scotta, Davide Trutalli, and Andrea Polastri. Behaviour factor for innovative massive timber shear walls. *Bulletin of Earthquake Engineering*, pages 1–21, 2015.

[72] T. Reynolds, ÃĚ. Bolmsvik, J. Vessby, W.-S. Chang, R. Harris, J. Bawcombe, and J. Bregulla. Ambient vibration testing and modal analysis of multi-storey cross-laminated timber buildings. In *WCTE 2014 - World Conference on Timber Engineering, Proceedings*, 2014.

[73] Giovanni Rinaldin, Claudio Amadio, and Massimo Fragiacomo. A component approach for the hysteretic behaviour of connections in cross-laminated wooden structures. *Earthquake Engineering & Structural Dynamics*, 42(13):2023–2042, 2013.

[74] Giovanni Rinaldin and Massimo Fragiacomo. A component model for cyclic behaviour of wooden structures. In *Materials and Joints in Timber Structures*, pages 519–530. Springer, 2014.

[75] Alexander J. Salenikovich. *The racking performance of lightframe shear walls.* PhD thesis, Wood Science and Forest Products, Virginia Polytechnic Institute and State University, VA, 2000.

[76] Francesco Sarti, Alessandro Palermo, and Stefano Pampanin. Development and testing of an alternative dissipative posttensioned rocking timber wall with boundary columns. *Journal of Structural Engineering*, page E4015011, 2015.

[77] Tiziano Sartori, Maurizio Piazza, Roberto Tomasi, and Paolo Grossi. Characterization of the mechanical behaviour of light-frame timber shear walls through full-scale tests. In *World conference on timber engineering*, pages 180–8, 2012.

[78] Tiziano Sartori, Maurizio Piazza, Roberto Tomasi, and Paolo Grossi. Characterization of the mechanical behaviour of light-frame timber shear walls through full-scale tests. In *World Conference on Timber Engineering 2012, WCTE 2012*, volume 3, pages 180–188, 2012.

[79] Tiziano Sartori and Roberto Tomasi. Experimental investigation on sheathing-to-framing connections in wood shear walls. *Engineering Structures*, 56:2197Ű2205, 2013.

[80] W. Seim, J. Hummel, and T. Vogt. Earthquake design of timber structures - remarks on force-based design procedures for different wall systems. *Engineering Structures*, 76:124–137, 2014. cited By 0.

[81] Werner Seim, Miha Kramar, Tomaž Pazlar, and Tobias Vogt. Osb and gfb as sheathing materials for timber-framed shear walls: Comparative study of seismic resistance. *Journal of Structural Engineering*, 2015.

[82] Ian Smith and Andrea Frangi. Overview of design issues for tall timber buildings. *Structural Engineering International*, 18(2):141–147, 2008.

[83] Ian Smith, Andrea Frangi, and Greg C Foliente. *Use of Timber in Tall Multi-Storey Buildings*. IABSE c/o ETH Zürich, 2014.

[84] Iztok Sustersic and Bruno Dujic. Simplified cross-laminated timber wall modelling for linear-elastic seismic analysis. In *CIB-W18 Timber Structures*, August 2012.

[85] R. Tomasi. Seismic behavior of connections for buildings in clt. In *Proceeding CLT conference Graz*, 2013.

[86] Roberto Tomasi and Maurizio Piazza. Investigation of seismic performance of multi-storey timber buildings within the frame of the series project. In *ICSA 2013*, 2013.

[87] Roberto Tomasi and Tiziano Sartori. Mechanical behaviour of connections between wood framed shear walls and foundations under monotonic and cyclic load. *Construction and Building Materials*, 44:682–690, 2013.

[88] Roberto Tomasi, Tiziano Sartori, Daniele Casagrande, and Maurizio Piazza. Shaking table testing of a full scale prefabricated three-story timber framed building. *Journal of Earthquake Engineering*, 2014.

[89] Chia-Ming Uang and Kip Gatto. Effects of finish materials and dynamic loading on the cyclic response of woodframe shearwalls. *Journal of Structural Engineering*, 129(10):1394–1402, 2003.

[90] UNI EN 12512:2003. Strutture di legno - metodi di prova - prove cicliche di giunti realizzati con elementi meccanici di collegamento, 2003.

[91] UNI EN 1990:2004. Criteri generali di progetttazione strutturale. par. 4.1.2: Valori caratteristici delle azioni, 2004.

[92] UNI EN 1995-1-1:2005. Eurocode 5: Design of timber structures - part 1-1: General - common rules and rules for building, 2005.

[93] UNI EN 1995-1-1:2005. Progettazione delle strutture in legno. parte 1-1: Regole generali - regole comuni e regole per gli edifici, 2005.

[94] UNI EN 1998-1:2005. Progettazione delle strutture per la resistenza sismica. parte 1: Regole generali, azioni sismiche e regole per gli edifici, 2005.

[95] UNI EN 1998-1:2013. Eurocode 8: Design of structures for earthquake resistance Ű part 1: General rules, seismic actions and rules for buildings, 2013. Brussels, Belgium: CEN, European Committee for Standardization.

[96] UNI EN 26891:1991. Strutture di legno. assemblaggi realizzati tramite elementi meccanici di collegamento. principi generali per la determinazione delle caratteristiche di resistenza e deformabilità, 1991.

[97] John W Van De Lindt. Evolution of wood shear wall testing, modeling, and reliability analysis: Bibliography. *Practice Periodical on Structural Design and Construction*, 9(1):44–53, 2004.

[98] Johan Vessby. Shear walls for multi-storey timber buildings. *WCTE 2008*, 2008.

[99] Tobias Vogt, Johannes Hummel, and Werner Seim. Timber framed wall elements under cyclic loading. In *12th World conference on timber engineering, Auckland*, 2012.

[100] Michael Winkel and Ian Smith. Structural behavior of wood light-frame wall segments subjected to in-plane and out-of-plane forces. *Journal of structural engineering*, 136(7):826–836, 2009.

[101] Xi Zhu and Yongjun Ni. Strength reduction factor spectra based on structural damage performance. In *Proceedings of the China-US Millennium Symposium of Earthquake Engineering: Earthquake Engineering Frontiers in the New Millennium, Beijing, China*, 2000.